Winter 3-21-2018

Hydrodynamic and Water Quality Modeling of the Tigris River System in Iraq Using CE-QUAL-W2

Muhanned Al Murib
Portland State University

Hydrodynamic and Water Quality Modeling of the Tigris River System in Iraq Using CE-QUAL-W2

by

Muhanned Al Murib

A dissertation submitted in partial fulfillment of the
requirements for the degree of

Doctor of Philosophy
in
Civil and Environmental Engineering

Dissertation Committee:
Scott Wells, Chair
Chris Berger
Mark Sytsma
Stefan Talke

Portland State University
2018

Abstract

The Tigris River is one of two primary rivers in Iraq and is, along with the Euphrates, the main source for drinking and irrigation water in the country. The Tigris River originates in the Taurus Mountains in Turkey, and is 1850 km long. The majority of the river, 1418 km lie within Iraq. The river passes through, and is the primary drinking water source for, major cities such as Mosul, Baeji, Samarra, Baghdad (the capital), and Kut. The Tigris River joints the Euphrates River in Qurna city within Basra province to form the Shatt Al-Arab River which eventually discharges into the Persian Gulf.

As a result of fluctuations in flow rate along the Tigris River that cause both potential flooding and drought, Mosul Dam was built on the mainstem of the Tigris River upstream of the city of Mosul and was operated starting in July1986 to control the river flow and to generate hydroelectricity. Some canals were also constructed to divert excess fresh water from the mainstem of the river at Samarra Barrage located 125 km north (upstream) of Baghdad to Tharthar Lake, an artificial lake located 100 km northwest Baghdad city. The Tigris-Tharthar canal, 75 km long, was constructed in 1956 to divert excess water from Samarra Barrage to Tharthar Lake and to prevent potential flooding in Baghdad. During dry seasons, high total dissolved solids (TDS) water is diverted from Tharthar Lake into the mainstem of the Tigris River through the 65 km long Tharthar-Tigris canal, which is located 25 km upstream Baghdad.

Due to rapid population growth and increasing industrial activates, the Tigris River is also facing many water quality challenges from inflows of contaminated wastewater from treatment plant stations. A water quality model that simulates the Tigris River system is therefore needed to study the effects of these discharges and how water quality of the Tigris River could be managed. To address this issue, I used CE-QUAL-W2 to develop a 2-D (longitudinal and vertical) hydrodynamic and water quality model of the mainstem Tigris River from Mosul Dam (Rkm 0) to Kut Barrage (Rkm 880). In addition, Tharthar Lake and its canals were modeled.

A full suite of hydrodynamic and water quality variables were simulated for the year 2009, including flowrates, water level, and water temperature. Additionally, water quality constituents such as total dissolved solids (TDS), phosphate (PO4), ammonium (NH4), nitrate (NO3), biochemical oxygen demand (BOD), chlorophyll-a (Chl-a), and dissolved oxygen (DO) were also simulated. Bathymetry of the Tigris River and field data such as flowrate, water level, TDS, NO3 were obtained from the Ministry of Water Resources in Iraq, while surface water temperatures of the Tigris River were estimated remotely using Landsat satellites. These satellites provided a continuous observation record of remote sites. Other water quality field data, such as PO4, NH4, BOD, and DO, were estimated from literature values.

Meteorological data, including, wind speed, wind direction, air and dew point temperatures, cloud cover, and solar radiation were obtained from the Iraqi Ministry of Transportation, the General Organization for Meteorology and Seismic Monitoring.

Model predictions of flow and water level were compared to field data at three stations along the mainstem of the Tigris River, including Baeji, downstream of Samarra Barrage, and Baghdad. The absolute mean error in the flow varied from 12.6 to 3.4 m^3/s and the water level absolute mean error varied from 0.036 to 0.018 m. The percentage error of the overall flowrate at Baeji, downstream Samarra Barrage and Baghdad was 1.9%, 0.8%, and 0.8% respectively. Injecting a conservative tracer at Mosul Dam showed that a parcel of water reaches to Baeji, Samarra Barrage, Baghdad, and Kut Barrage after approximately 3 days, 5 days, 10 days, and 19 days, respectively.

Water temperature field data in Iraq are limited and there was no archive of existing field data. Therefore, I obtained estimates of surface water temperature on the Tigris River using the thermal band of the Landsat satellite, one of a series of satellites launched by the National Aeronautics and Space Administration (NASA). The calibration between satellite data and water temperature was validated using sparse field data from 2004, and the calibration then applied to 82 Landsat images from the year 2009. Landsat estimates showed a bias of -2 ° C compared to model results in winter months, possibly due to uncertainty in Landsat estimations. The absolute mean errors of the CE-QUAL-W2 model predictions of water temperature compared to Landsat estimated temperatures were 0.9 and 1.0 ° C at Baeji and Baghdad respectively. Temperature calibration in the Tigris River system was highly sensitive to meteorological input data. Landsat Images were also used to estimate longitudinal variation in surface water temperature of Tharthar Lake. It was

found that surface water temperature in Tharthar Lake varied longitudinally along the North-South axis with warmer temperatures in the lower part compared with the upper part of the lake.

Total dissolved solids concentrations in the Tigris River significantly increased from Mosul Dam to Kut Barrage with peak concentrations of 900 mg/l and 1050 mg/l at Baghdad and Kut, respectively, due to high TDS water diverted from Tharthar Lake, irrigation return flow, urban runoff, and uncontrolled discharge of wastewater effluents. NO3 concentrations did not significantly increase between Samarra Barrage and Baghdad city. BOD concentrations within Baghdad were extremely high due to direct discharge of industrial wastewater into the mainstem of the Tigris River from outlets located within the city.

Management scenarios were simulated with the model of the Tigris River system and were compared with the base model. The main scenarios implemented on the Tigris River system were altering upstream hydrology, increasing air temperature due to the effect of climate change, disconnecting Tharthar Lake from the Tigris River system, and simulating long-term effects on Tharthar Lake. Increasing upstream inflows caused a decrease in TDS concentrations from 495 mg/l to 470 mg/l over all the mainstem of the river. In addition, CBOD concentrations decreased somewhat from 5.9 mg/l to 5.74 mg/l. On the other hand, decreasing upstream flows caused a significant increase in average TDS concentrations over the entire Tigris mainstem from 495 mg/l to 527 mg/l. Also, an increase in CBOD concentrations from 5.9 mg/l to 6.2 mg/l was predicted over all the mainstem of the river. Implementing the climate change scenario on the base model of the Tigris River system showed a 5% increase in annually averaged water temperature from 20.7 ^{0}C to 21.68 ^{0}C

over the mainstem river. Climate change scenarios produced no significant impacts on TDS and CBOD concentrations in the mainstem, while DO concentrations decreased from 8.15 mg/l to 7.98 mg/l with a slight increase in Chl-a concentration from 1.97 µg/l to 2 µg/l in the mainstem. Disconnecting Tharthar Lake from the system showed a remarkable 25% decrease in TDS concentrations, with an average concentration changed from 495 mg/l to 397 mg/l in the mainstem due to an extra 36% increase in flow discharged downstream of Samarra Barrage. Also, Chl-a concentration significantly decreased by 40% with an average concentration changed from 2 µg/l to 1.2 µg/l.

Additionally, a 6-year model simulation of the Tigris River system was performed to evaluate the long-term effects on Tharthar Lake. No significant impact was observed in the average temperature of the lake. TDS concentrations in the lake decreased from 1239 mg/l to 1041 mg/l. PO4, NH4 and NO3 concentrations decreased by 2%, 66% and 26%, respectively. Chl-a concentration in Tharthar Lake decreased from 2.0 µg/l to 1.61 µg/l. After decreasing BOD concentrations of the Tigris River by 50%, BOD concentrations in the mainstem decreased by 24%, while DO concentrations increased by 2.8%. There were no significant impacts on Chl-a concentrations in the mainstem of the river. Finally, for a scenario where extremely low dissolved oxygen release from Mosul Dam in the summer, it was found that approximately 50 km below Mosul Dam was affected before DO concentrations reached an equilibrium concentration.

For further work on the Tigris River system, it is recommended to model the Tigris River from Kut Barrage to the confluence with the Euphrates River, about 400 km long, and connect it with the current model to have a complete model of the Tigris River system from Mosul Dam to the confluence with the Euphrates River. This is necessary to manage water the entire system of the Tigris River and also to provide enough water with good quality in Basra.

Acknowledgments

A huge thank you to Dr. Scott Wells for his continued teaching, assistance, kindness, and availability throughout my PhD program. Without him, this work wouldn't be possible.

Thanks and appreciation to Dr. Stefan Talke for his assistance with remote sensing techniques.

Thanks to Dr. Chris Berger and Dr. Mark Sytsma for serving in my PhD committee.

Thanks and appreciations to the Civil and Environmental Department of Portland State University for having me succeed through this journey.

Thanks and appreciations to my parents, my wife (Mawj) and kids (Abdullah and Taim), and my friends for their continuous support and encouragement.

Thanks to the Iraqi Ministry of Water Resources and the Iraqi Ministry of Communication for providing field data of the Tigris River system.

Table of Contents

List of Tables

List of Figures

Chapter One: Introduction

The Tigris River is one of the largest rivers in the Middle East and is one of two primary rivers in Iraq (Figure 1). The Tigris River is the main source for drinking and irrigation water for Baghdad which is the largest city in the country and the second largest city in the Arab world with a population estimated to be 7.5 million (Burnham et al., 2006). The Tigris is 1850 km long of which 1418 km are within Iraq. It rises in the Taurus Mountains of eastern Turkey about 25 km southeast of the city of Elazig and about 30 km from the headwaters of the Euphrates. The Tigris River then flows for about 400 km through Turkey before entering Iraq, and then passes through major cities in Iraq such as Mosul city, Samarra city, Baghdad city and Kut city. Hence, Iraq, with a population of about 31.5 million according to 2009 estimates (CSO, 2010), depends heavily on the Tigris River to supply water for drinking, municipal use, irrigation, industries, power generation, navigation, and recreation. However, the seasonal pattern of flow and the river discharge has decreased over time, primarily due to the many storage reservoirs have been built along the Tigris in both Turkey and Iraq. Altered flow has led to changes in the elevation of the river, with implications for water resource management. As an example, intakes for water treatment plants and power generation plants have been affected (Al-Obaidy, 1996; Al-Jubori, 1998). Figure 1 shows the two main rivers, the Tigris and the Euphrates, from their headwaters in Turkey to the confluence in Iraq, where they form Shatt Al-Arab River. The continued Shatt Al-Arab River, which is 200 km long, discharges into the Persian Gulf.

Figure 1: The official map of Iraq showing the Tigris and the Euphrates Rivers (Arc GIS).

The Tigris and Euphrates Rivers form the main water sources in Iraq and represent together 98% of the water resources in the country. Both these rivers originate in the highlands of Turkey and share similar physical, climatic, hydrologic and geomorphologic characteristics. The Ministry of Water Resources (MWR) in Iraq estimated that the annual flow from both rivers dropped from 30 billion cubic meter (BCM) to only 11 BCM over the last seven years (USAID 2007). Figure 2 shows the origin of water sources for both the Tigris and the Euphrates Rivers.

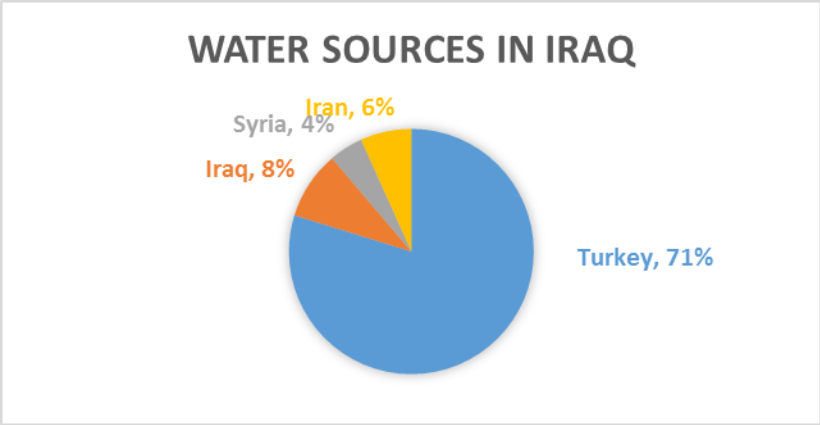

Figure 2: Sources of water for the Tigris and the Euphrates Rivers in Iraq (MWR 2005).

Figure 3 shows water uses in Iraq in 2009. More than 85% of all water resources in Iraq are allocated for irrigation, while only 3% of the water is allocated for domestic uses. Since agriculture in Iraq plays a crucial role for increasing Iraq's revenue, water quality of the Tigris River such as total dissolved solids (TDS) and nutrients is critical for meeting irrigation standards. Central Statistical Organization (CSO) (2010) reported the Iraqi land characteristics for the year 2009 as shown in Figure 4. About 27% of the land is classified as agricultural areas.

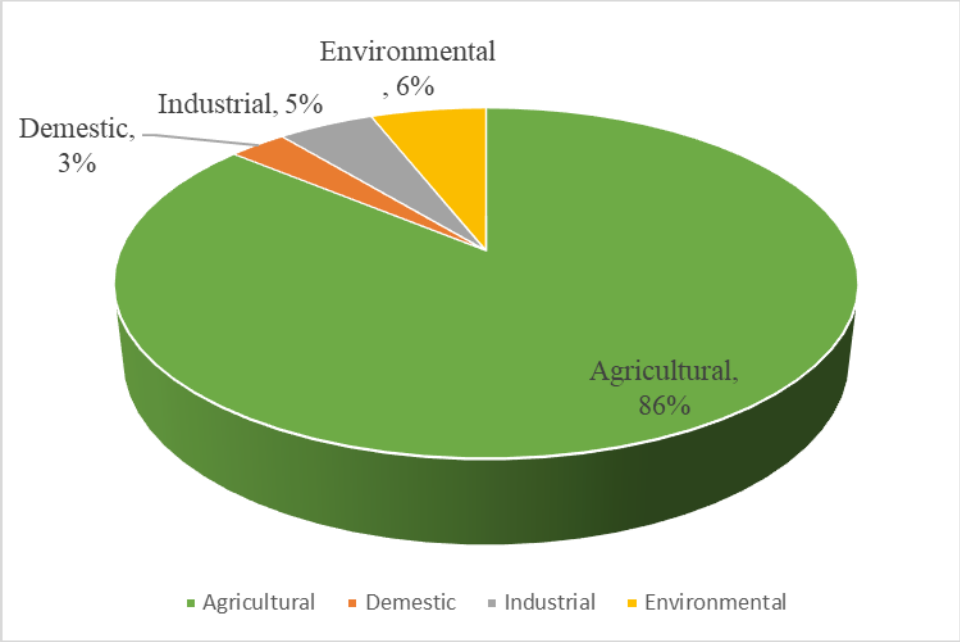

Figure 3: Water uses in Iraq in 2009 (CSO, 2010).

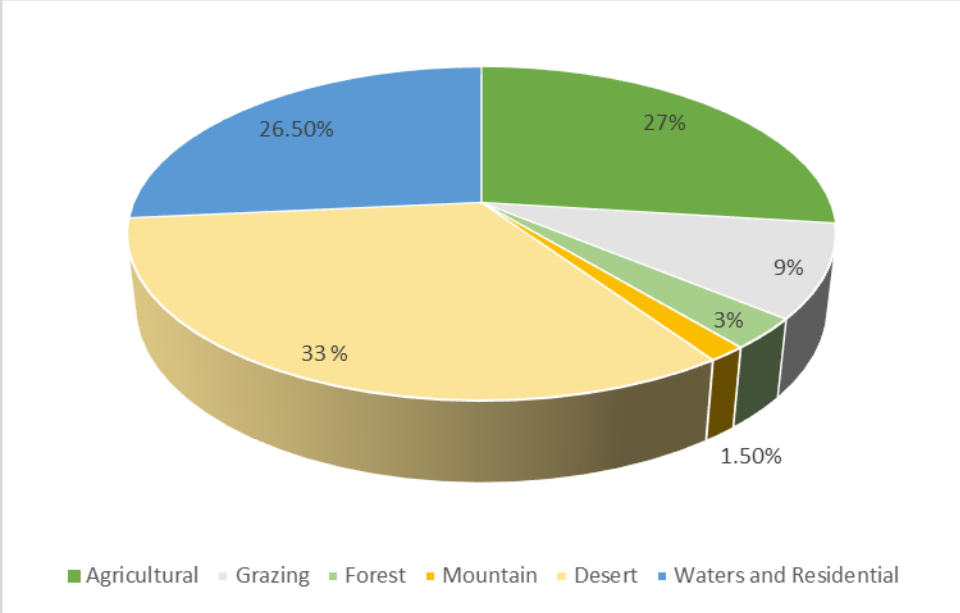

Figure 4: Land characteristics in Iraq in 2009 (CSO, 2010).

A water quality model that simulates the Tigris River system is needed to study the effects of how changes in water quality affect the Tigris River. Besides modeling changes in water

level and flow and velocity, important water quality state variables include temperature, total dissolved solids (TDS), organic matter, nutrients, dissolved oxygen, and algae. TDS is an important variable for the Tigris River since agricultural areas downstream of Baghdad city are heavily dependent on the Tigris River for irrigation.

Field data required to set-up and evaluate a water quality model are very limited in Iraq. Using conventional monitoring techniques are often prohibitive because of the current social and political upheavals in the country. Since there is a lack of water quality data, satellite imagery is potentially a useful source for obtaining the field data required for developing a water quality model.

Study Objectives and Hypotheses

The primary objective of this research is to develop a systematic hydrodynamic and water quality model of the Tigris River and use it to evaluate changes in water quality as a result of changes in flow management in the Tigris basin. Specifically, this objective will be met by

- Developing a 2-D water quality model of the Tigris River system and Tharthar Lake using the water quality and hydrodynamics model CE-QUAL-W2 (Cole and Wells, 2017). This includes compiling historical water quality, meteorological, and stream channel morphology data for the Tigris River System.
- Estimating surface water temperature of the Tigris River from remotely sensed data using thermal bands of both Landsat 5 TM and Landsat 7 ETM+ to obtain upstream boundary conditions and downstream water temperatures for the model calibration.
- Estimating water quality constituents such as total dissolved solids (TDS), biological oxygen demand (BOD), nutrients (NO_3) and (PO_4), and algae of the Tigris River using limited field data obtained from Water Resources Ministry in Iraq (WRM) and other field data extracted from previous studies of the Tigris River.
- Using the Tigris model system to evaluate some management scenarios for improving water quality in the Tigris River such as altering river flow due to upstream flow control by Turkey and disconnecting Tharthar Lake from the Tigris River system to enhance the river quality in Baghdad and downstream cities.
- Estimating the potential impact of climate change on the river system.

The hypotheses to be investigated by this dissertation are:

- Increasing upstream river flow at Mosul Dam will decrease total dissolved solids (TDS) concentrations in both Tharthar Lake and the Tigris River through dilution and reduction in both residence time and evaporation rates.
- Estimating surface water temperature from remote sensing is a feasible method for defining the model's upstream boundary conditions and calibrating downstream areas.
- Disconnecting Tharthar Lake from the Tigris River system will enhance water quality in Baghdad and downstream cities by passing more waters from Samarra Barrage.
- Increasing air temperature due to the impact of climate change will increase water temperature in the Tigris River system and negatively impact DO concentrations.

Chapter Two: The Tigris River and Tharthar Lake Study Area

The study area in this dissertation includes the mainstem of the Tigris River, from Mosul Dam (Rkm 0) and ending at Kut Barrage (Rkm 880) (Figure 5). Mosul Dam, which began operations in 1986, is the largest dam in Iraq with a total length of 3.65 km and crest elevation of 341 m above sea level; the storage capacity at normal operation level (330 m above sea level) is 11.11 km^3 (Al-Ansari, 2015). Samarra Barrage and Kut Barrage are crucial flow control structures located on the mainstem of the Tigris River and regulate the river flow upstream and downstream Baghdad city, respectively, as shown in Figure 6 and Figure 7. Four major tributaries join the eastern bank of the Tigris River. These tributaries are (upstream to downstream): (a) the Upper Zab, located about 50 km downstream of Mosul, (b) the Lower Zab, located about 220 km upstream of Baghdad, (c) the Adhaim River, located 50 km upstream of Baghdad, and (d) the Diyala River, located 10 km downstream of Baghdad city (Al-Samak et al., 1985). Table 1 lists a description of the main tributaries of the Tigris River in Iraq.

Figure 5: The Tigris River and Tharthar Lake study area from Mosul Dam to Kut Barrage.

Figure 6: Samarra Barrage (Google Earth).

Figure 7: Kut Barrage (Google Earth).

Table 1: Lower tributaries of the Tigris River (ESCWA-BGR, 2013)

Tributary	Description
Feesh Khabour	This tributary is shared between Iraq and Turkey. It originates in Sırnak, Turkey, and flows through Zakho, Iraq, before its confluence with the Tigris at the Iraqi-Turkish border. The Feesh Khabour delineates the international border between Iraq and Turkey. Its mean annual flow volume at the confluence with the Tigris is approximately 2 BCM.
Greater Zab	This river, which is shared by Iraq and Turkey, originates in Turkey and is the largest Tigris tributary. It supplies the Tigris River with an average annual flow volume of 12.7 BCM. 62% of the total area of the river's basin of 25 810 km^2 is in Iraq
Lesser Zab	The Lesser Zab is shared by Iran and Iraq. It originates in Iran, not far from the Iraqi border. The total river basin is 21 475 km^2, of which 74% is in Iraq. The average annual flow volume of the Lesser Zab is about 7.8 BCM, contributing an average of 249 m3/s to the Tigris.
Adhaim	While not a shared tributary, Adhaim is an intermittent stream that drains an area of about 13,000 km^2 in Iraq. The river generates about 0.79 KCM annually at its confluence with the Tigris and is subject to flash flooding.
Diyala	Shared by Iran and Iraq, this tributary forms the border between the two countries. It drains about 31 896 km^2, of which 75% in Iraqi territory. The Diyala has a mean annual flow volume of 5.74 KCM.

In addition, Tharthar Lake and its canals are also included in the study area (Figure 8). The Tharthar reservoir was originally a natural depression with a floor at -3m below sea level. It serves as a discharge area for the ground water in the vicinity of the depression and as storage for the runoff of wadi Tharthar. After the diversion channel from the Tigris River was constructed in 1956, Tharthar Lake became a large flood storage reservoir to protect Baghdad from flooding and a potential source of water for irrigation. The lake has a maximum length of 120 km, a width of 48 km, and an average depth of 40-65 m. The main purpose of Tharthar Lake is to collect the excess or flood waters from the Tigris River during flood seasons and to recharge the waters of both the Tigris and Euphrates Rivers

during dry seasons. Evaporation and leakage through soil beds are the main causes of water losses in the lake.

In 1969, the water level in the lake reached its maximum permissible level of 60 m, and the ministry of irrigation investigated other options to store the excess water from Tigris River. As result was the construction of the Tharthar-Euphrates canal, with a total length of 37.5 km. Additionally, the Tharthar-Tigris canal with a total length of 65 km was constructed and began to operate in 1988. Water from this canal is being diverted to the Tigris River, upstream of Baghdad, to compensate for the water deficit in Baghdad and downstream cities (Jasim, 1988).

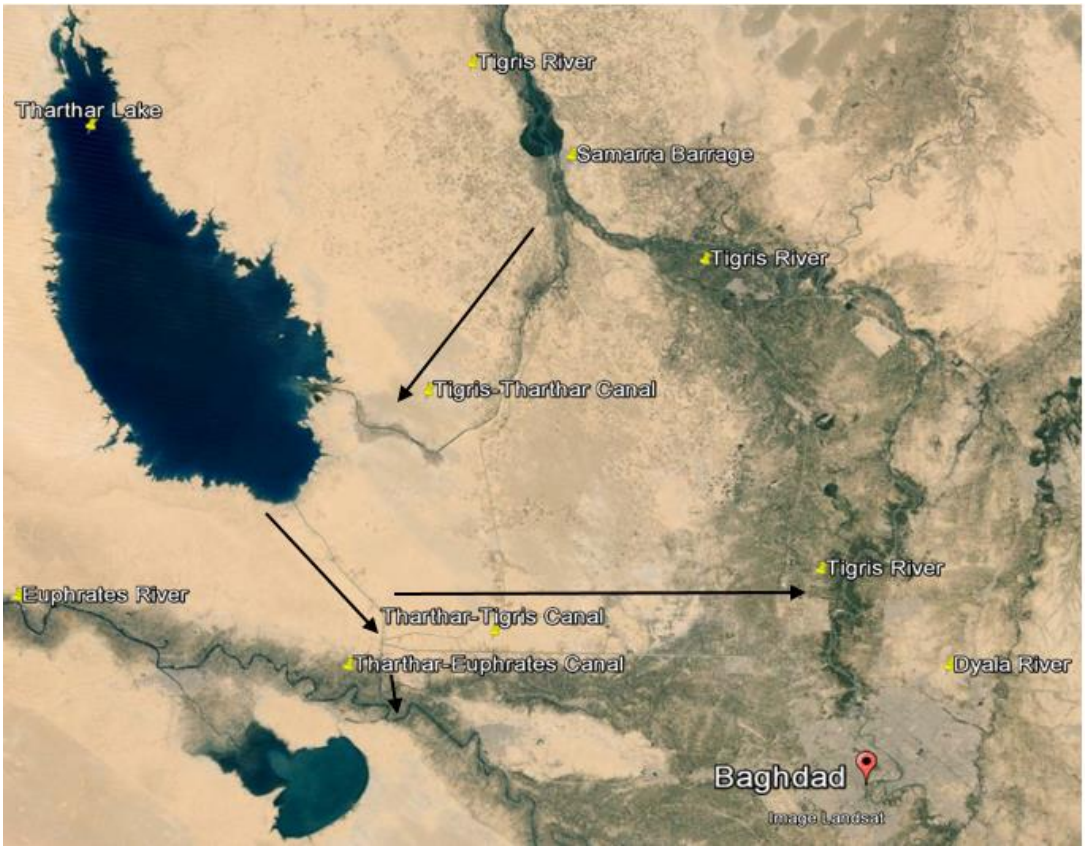

Figure 8: Tharthar Lake and its canals (Google Earth).

Point Sources in the Study area within Baghdad City

Water Treatment Plants (WTPs)

Eight water treatment plants (WTPs) are located along the main stream of the Tigris River within Baghdad city that draw water from the river. These water treatment plants (see Figure 9) from upstream to downstream area: Karkh, Sharq Dijlah (or East Tigris), Karama, Wathba, Qadisiya, Dora, and Rasheed water treatment plants. The annual amount of treated water produced by these plants in the year 2009 was about 797.5E6 m^3. Relative to the average flow of the Tigris River within Baghdad city, the water treatment plants mentioned above withdrew about 6% of the average water flow in the Tigris River.

Table 2: Designed and Produced capacity of WTPs in Baghdad city in 2009 (CSO, 2010).

Water TreatmentPlant	**Designed Capacity (1000 m^3/year)**	**Produced Capacity (1000 m^3/year)**
Kharkh	491400	415160
East Dijla	269700	225387
Karama	79200	54837
Wathba	48900	28250
Qadisiya	74640	31721
Dora	41400	26328
Wihda	5920	19480
Rasheed	24480	15780
Total	1055640	816943

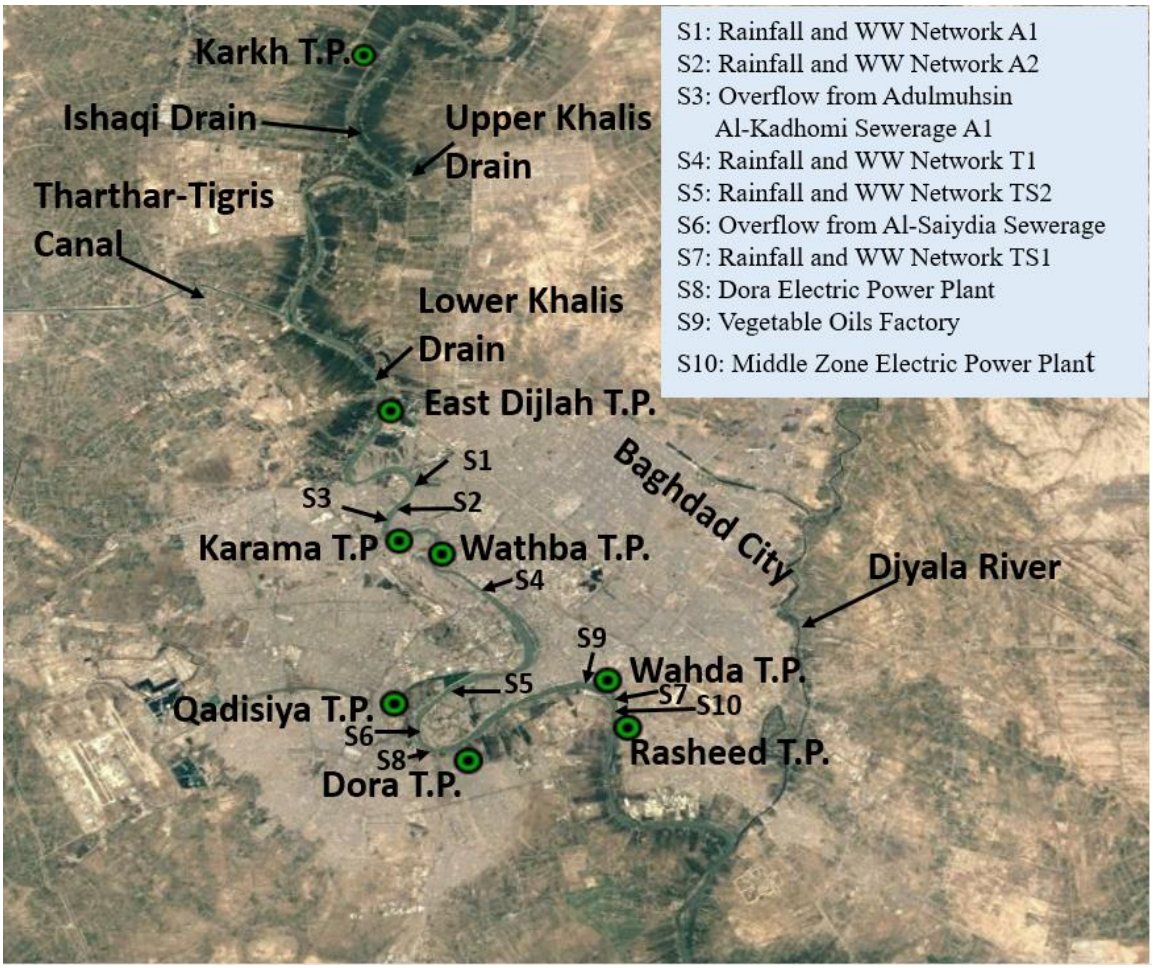

Figure 9: Point and non-point sources in Baghdad city.

Wastewater Treatment Plants (WWTPs)

Baghdad city has only three sewage treatment plants (WWTPs) that serve Baghdad's residents. These three plants together contribute three-quarters of the entire nation's sewage treatment capacity. Currently, some raw waste from residential areas in Baghdad city flows untreated directly into the Tigris River (USAID 2003). WWTPs face many problems related to improper design, population growth, power shortages, lack of maintenance, and lack of experienced operators. In Iraq, 13 municipal sewage treatment plants are located across the country, however, several are not in service, three of which are in Baghdad city (USAID 2003). The amount of generated and treated wastewater

through central and small wastewater plants (WWTPs) in Mosul, Tikrit, and Baghdad cities in the year 2009 is listed in Table 3. According to CSO (2010), 100% of treated wastewater in Mosul city was discharged into natural Wadies (Valleys), while 25% and 75% of treated wastewater in Tikrit city was discharged into the mainstem of the Tigris River and irrigational canals, respectively. In Baghdad city, 100% of treated sewage in Baghdad is directed from treatment plants to the Diyala River, a tributary of the Tigris River, and eventually to the Tigris River through additional treatment (Aziz and Aws, 2012).

Table 3: Designed and Produced capacity of WWTPs in Mosul, Tikrit, and Baghdad cities in 2009 (CSO, 2010).

Province	Population	Population served by WWTPs	% Population served by WWTPs	Number of Central WWTPs	Number of Small WWTPs	WW generated (m3/d)	WW treated (m3/d)	Type of treatment
Mosul	2994979	263558	8.8	0	2	8400	8400	Biological
Tikrit	1351150	337788	25	4	0	35000	34900	Biological
Baghdad	7455849	4337991	58	3	0	1225000	540000	Physical/ Biological

Non-Point Sources of the Tigris River

Non-point source pollution generally results from land runoff, precipitation, atmospheric deposition, drainage, seepage or hydrologic modification. Non-point source pollution could include excess fertilizer such as herbicides and insecticides from agricultural lands and residential areas, oil, grease and toxic chemicals from urban runoff and energy production, salt from irrigation practices and acid drainage from abandoned mines, bacteria and nutrients from livestock, pet wastes and faulty septic systems. Unfortunately, no information was available about these non-point sources.

The Tigris River Flow Regime

Due to large annual and interannual fluctuations in both the Tigris and the Euphrates Rivers, the average annual flow in both rivers is difficult to estimate (FAO, 2008). Baghdad city is occasionally exposed to flooding due to high flows in the Tigris River. The last big flood happened in 1950 as shown in Figure 10 with minor ones occurred later. Therefore, the Iraqi Government started to construct a series of dams and projects to control the flow and to prevent major cities from flooding. According to Al-Shahrabaly (2008), monthly average discharge of the Tigris River within Baghdad city at Sarai Baghdad station has fallen sharply from 927 m^3/s during the 1960-1999 period to 531 m^3/s during the 2000-2010 period. Since water is highly regulated by Turkey and there has been a huge increase of water demand, the Iraqi Government realized that a plan of building dams along both rivers and all tributaries should be investigated and considered seriously.

Figure 10: A famous Iraqi street in Bagdad City under flooding in 1950 (Mix Max, 2009).

Issa et al. (2014) studied the expected future of water resources within Tigris-Euphrates Rivers Basins in Iraq. In this study, 15 flow gage stations within both basins were used to evaluate and compare current and future challenges of water availability and demand in Iraq. The results showed that Iraq receives annually 70.92 km^3 of water with 45.4 and 25.52 km^3 coming from Tigris and Euphrates Rivers, respectively. Table 4 lists the drainage area of the Tigris River basin, divided between countries. An amount of 18.04 km^3 of the Tigris water comes from Turkey while its tributaries inside Iraq supply 27.36 km^3. It was found that the annual decrease in the Tigris water inflow is 0.1335 km^3/yr due to upstream decrease in water sources, while water demand increases annually by 1.002 km^3.

Table 4: Drainage area of the Tigris River basin (Al-Ansari and Knutsson, 2011).

Country	**Catchment Area (km^2)**	**Catchment Area (%)**
Iraq	253,000	58
Turkey	57,614	12.2
Syria	834	0.2
Iran	140180	29.6
Total	473103	100

Al-Anbari et al. (2006) studied the hydraulic geometry for a stretch of 202.5 km on the Tigris River from Mosul at km 177.5 in the north, downstream to km 380 near Baeji at the Al-Fathaa Bridge using Leopold's method of maximum, minimum, and average discharges. They defined and estimated Manning friction values for the entire 202.5 km study area. The results show that there are different hydraulic geometry characteristics along the river reach with high width to depth ratio. At Al-Fathaa gauging station, the width (W) and depth (D) of Tigris River was correlated to its flowrate (Q) according to the following equations:

$W=136Q^{0.05}$
$D=0.0748Q^{0.61}$

Ali et al. (2012) used surveyed data of the bed of Tigris River to predict the maximum flood capacity for the river using the HEC-RAS (U.S. army Corps of Engineers, 2010) one-dimensional hydraulic model for steady flow. This study used bathymetry data from MWR (2008) and extended from north of Baghdad to the confluence with the Diyala River south of Baghdad. Calibration of the model was carried out using field measurements for water level. The model showed a significant predicted reduction in the current river capacity below that which the river had carried during the floods of 1971 and 1988.

Hydraulic Structures on The Tigris River in Iraq

The Ministry of Water Resources in Iraq has undertaken the task of dam construction in Iraq (Table 5) since 1962 when the first concrete dam, Dokan Dam, was constructed on the Lower Zab tributary of the Tigris River. Water shortage and drought are fundamental motivations for the construction of dams. Therefore, the Ministry of Water Resources in Iraq planned a strategy to construct numerous dams across the country to save and control water.

Table 5: Dams in the Tigris River Basin, Iraq; BCM: billion cubic meters; I: Irrigation; F: Flood control.

Dam	River	Year	Height (m)	Length (m)	Capacity (BCM)	Main Use
Dokan	Lower Zab	1962	116	360	6.8	I
Mosul	Tigris	1983	131	3650	12.5	I
Dibis	Lower Zab	1965	15		3	I
Samarra	Tigris	1954	-		72.8	F
Adhaim	Adhaim River	1999	-	3800	-	-
Himrin	Diyalah River	1980	40	3500	4	I
Derbendi Khan	Diyalah River	1962	128	445	3	I

Irrigation in Iraq

Although treated wastewater, rich in nutrients, has been used for irrigation of grasslands and pastures and some vegetables, some raw wastewater has also been used by some farmers. This has caused serious problems such as crop contamination with pathogens and heavy metals, and salinity accumulation in soils (Aziz and Aws, 2012). The reuse of drainage irrigation flow can lead to salt accumulation in soils. Irrigation return flows are large and are approximately 20-25% of the original supplied water, or about 7 billion cubic meters (BCM) (Aziz and Aws, 2012). This implies that about 14% of the water contribution to the Tigris and the Euphrates Rivers is from irrigation return flows.

Due to numerous wars during the 1980s, 1991, and 2003, lack of maintenance and irrigation development plans have adversely affected agriculture and consequently reduced the percentage of irrigable lands. To a substantial extent, the irrigation infrastructure has broken down in Iraq (The World Bank, 2006). On the other hand, the combination of over-irrigation, poor drainage, and high evaporation rates are the main factors that significantly affect the quality of irrigation water. Currently, unregulated water has been withdrawn from the main stream of the Tigris River through pumps, while saline return flow is being directly discharged into the river causing a significant degradation in its quality.

Water Quality in The Tigris River System

Due to the rapid population growth from about 11.5 million in 1975 to 31 million in 2010 (Worldometers, 2017) and increasing industrial development, the Tigris River is facing many water quality challenges such as inflows of contaminated water from wastewater treatment plants and saline irrigation return flows (Baban, 1977). Several provinces including Baghdad have suffered from fatal outbreaks of cholera due to poor drinking water quality (Aenab and Singh 2012). Also, sewage is often discharged directly into the river because some areas do not have sewage treatment plants. In central Baghdad, the water supply and sewerage network system are broken in many places and therefore there is cross-contamination of the drinking water supply (Aenab and Singh 2012). According to the UN factsheet (2013), water quality of the water used for drinking and irrigation is poor and violates both Iraqi National Standards and World Health Organization guidelines. As reported by IOM (2012), high pollution and salinity had devastating effects on livestock, agriculture, and fishing in the southern part of Iraq.

Many researchers have studied water quality of the Tigris River. A summary of several of these studies is listed below.

Ismail and Abed (2013) conducted a BOD and DO modeling study of the Tigris River within Baghdad city using the QUAL2K model. The study area was 50 km long and extended from Fahama region at which the river enters Baghdad city into the south of Baghdad at Zuforaniyah where the river exits Baghdad city. Field DO concentrations at multiple locations within the study area were 5, 7.2, 1, 5.5, 7.6, and 0 mg/l at river km 0, 17.7, 20, 38, 43.4, and 48.5 respectively, while field BOD concentrations at these river kms were 2, 2, 120, 5.2, 220, and 160 mg/l respectively. The high concentrations of BOD were

found at locations where industrial and oil effluents were discharged directly to the Tigris River. Remote sensing and GIS applications were used in this study to provide input data for the QUAL2K model. It was found that the simulation results agreed with the measured concentrations. DO concentrations in the entire study area were found above 4 mg/l. CBOD in the Tigris River within Baghdad city from Fahama region to Al-Dora district was between 2-4 mg/l. Due to the industrial discharge of pollutants to the river, the most polluted zone in the Tigris River study area was located downstream of Al-Dora refinery and extended to the end of the study area. To control the level of CBOD in the river, it was suggested that CBOD of the discharged effluents from industries should not exceed 50 mg/l to keep the CBOD in the study area no more than 4 mg/l.

Al-Jebouri and Edham (2012) conducted a study in 2004 utilizing selected sectors of the Tigris River and the Lower Zab tributary in Kirkuk and Salahaldeen cities. The study area was divided into eight stations starting at the confluence of the Lower Zab and the Tigris River passing through downstream of the river at Samarra. Water quality analyzed in this study were BOD, turbidity, electrical conductivity (EC), and water temperature. It was found that BOD concentrations at the end of the Lower Zab before the confluence with the Tigris River were in the range of 1.4-3.8 mg/l in August and January, the mean water turbidity was 35 NTU, while EC was about 354 µS/cm. A wide variation in the water quality was found in this study. BOD data provided in this study were used in our study for boundary conditions of the Upper Zab and the Lower Zab Rivers in the Tigris River model.

Alobaidy et al. (2010) evaluated both raw and treated water quality of the Tigris River within Baghdad city by means of a water quality index (WQI). WQI was a single value indicator of the water quality determined through summarizing multiple parameters of water test results into simple terms for management and decision makers. In this study, 7 sampling stations and 13 water quality parameters were considered. These parameters were pH (7.63), alkalinity (139.88 mg/l), turbidity (5.5 NTU), total dissolved solids, hardness, calcium, magnesium, chloride, sulphate, ammonia, fluoride, iron, and aluminum. The data used in this study were provided from Baghdad Mayoralty and covered the period from February 2002 to December 2008. According to the WQI, it was concluded that the Tigris water never reached an excellent nor an unsuitable condition.

Abdul Razzak et al. (2009) developed a model to simulate the distribution of total dissolved solids (TDS) and biochemical oxygen demand (BOD_5) in a stretch of 9 km of the Tigris River extended from Al-A'imma Bridge to Al-Jumhuria Bridge within Baghdad city. Field data were collected from twelve stations along the river twice a month from November 2005 to April 2006. It was found that the concentration of BOD_5 varied in the range of 140-170 mg/l, while TDS concentrations were at the acceptable range 500 mg/l with exception of a high value of 1100 mg/l was measured 1 km downstream Al-Sarafiya Bridge. During the days of field sampling, the water level (Z) m and flowrate (Q) m^3/s of the Tigris River were measured at Sarai gauging station (6.8 km from Al'Aimma Bridge). The rating curve was estimated using the following correlation

$$Q=32.014\ (Z-24.01)^{1.89}$$

Odemis et al. (2010) studied the quantifying long-term changes in water quality and quantity of the Euphrates and the Tigris Rivers in Turkey. Both watersheds originate in Turkey and are "one of the most import transboundary watersheds in the Middle East." In this study, data from 1971 to 2002 from 14 stations on the Euphrates River and seven stations on the Tigris River were analyzed. It was found that the upper west part of the Tigris River had higher electrical conductivity (EC), Ca, Mg, and SO_4 and lower flow rate, Na, and sodium adsorption ratio (SAR) than the lower parts of the Tigris River. The upper east parts of the river had higher HCO_3 and Boron (B) and lower flowrate and water temperature than the lower Tigris River.

Mutlak et al. (1980), studied the effect of Baghdad on the water quality of the Tigris River from April 1977 to March 1978. Typical chemical and physical characteristics of the water that were necessary in judging the quality of water for irrigation were studied. The study area was divided into four sampling sites with a total length of 50 km and extended from Fahama region at which the river enters Baghdad City into the south of Baghdad at Zuforaniyah region at which Baghdad City ends. Water temperature, pH, turbidity, flow rate and the stream level were recorded once a month at each sampling site. Other water quality parameters measured in this study were dissolved oxygen (DO), biochemical oxygen demand (BOD), nitrate (NO_3^-), nitrite (NO_2^-), and ammonium (NH_4^+) ions. It was found that Baghdad City was responsible for increasing the water salinity from 390 to 443 mg/l. On the other hand, total hardness and turbidity were increased in the Tigris River when it passed through Baghdad City. It was concluded that the increase in the total hardness was mostly due to the increase in Mg concentration. Heavy metals have no direct impact on the water used for irrigation. Table 6 shows changes in temperature, water level,

discharge, and turbidity of the Tigris River passing through Baghdad City from April 1977 to March 1978.

Table 6: Water characteristics of the Tigris River within Baghdad City (Mutlak et al., 1980)

Month	Temp °C	Water Level (m)	Discharge (m^3/s)	Turbidity (NTU)
April-1977	15	31.74	1920	149.35
May	18	32.72	1960	256.77
June	22	29.83	1060	73.35
July	25.5	28.83	507	54.52
August	27.5	28.68	379	45.82
September	25.2	28.40	321	35.60
October	19.7	28.35	384	32.50
November	14.3	28.66	470	34.90
December	12	-	898	37.91
January-1978	9.8	30.83	989	81.92
February	10	30.52	1370	312.5
March	18	32.43	1960	408

Al-Rawi (2005) studied the contribution of man-made activities to the pollution of the Tigris River within Mosul city. In his study, Al-Rawi presented an overall view of major sources that may lead to the pollution of the Tigris River within Mosul city. The study area was a river stretch of about 20 km in length. Samples from 40 sources sites were taken for quality analyses. It was found that domestic discharges were among the most important sources of pollution. In addition, untreated sanitary wastes were often discharged directly into the Tigris River. Other illegal practices such as in-house slaughtering add to the

pollution as well. Industrial wastewater was discharged to the Tigris River with low treatment efficiency. These wastes contain lead, chrome, and other heavy metals that may pose health risks. On the other hand, eutrophication which is a characteristic problem of lakes was found to occur in the Tigris River because of the intensive use of detergents rich in nutrients (P&N compounds). Textile industries discharged effluents with pH (7.7), PO4 (1.01 mg/l), NO3 (1.22 mg/l), and BOD (135 mg/l).

The Tigris River system has suffered from high water salinity for decades. Total dissolved solids (TDS) refer to any minerals, salts, metals, cations (positive ions) or anions (negative ions) dissolved in water. TDS represent the total amount of mobile charged ions and expressed in units of mg/unit volume of water mg/l or sometimes referred to as parts per million (ppm). In general, TDS concentration is the sum of both cations and anions. Some principal constituents of TDS in water are calcium, carbonate, nitrate, phosphate, sodium, potassium, chloride, iron, manganese, magnesium, and aluminum. Potential sources of TDS are leaves, industrial waste, wastewater or sewage, silt, fertilizers, pesticides, mining, and runoff from urban areas. The current EPA secondary maximum contaminant level (MCL) for TDS in drinking water is 500 mg/l (Water research foundation, 2015).

The Iraqi standards of TDS concentrations in drinking water is 500 mg/l (Ministry of Environment, 1998). Many researchers have studied the effect of salinity on the water quality of both the Tigris River and Tharthar Lake. It was found that the salinity in the Tigris river increased from 390 to 443 mg/l in Baghdad city as the river passes through the city from April 1977 to March 1978 (Mutlak et al., 1980). The main cations causing hardness in the water of the Tigris River are calcium and magnesium, while the predominant anions are bicarbonates, sulphate, chlorides, and carbonate of calcium and

magnesium. It was also found that hardness in the Tigris River increases in the middle and southern regions of Iraq due to existing irrigation return flow drainage canals (Baban, 1977). In general, the concentration of total dissolved solids in the Tigris River is governed by urban runoff, irrigation return flow through multiple canals along both banks of the Tigris River, wastewater flow into the river through Diyala River, and high salinity intrusion through both Tharthar-Tigris canal and Audaim River tributary. On the other hand, salinity in Tharthar Lake is of high concern in Iraq since the lake is the largest reservoir in the country and the main water supply to Baghdad city and downstream areas during dry seasons. The water in Tharthar Lake is unsuitable for both drinking and irrigation purposes due to high concentrations of sulphate and salinity (Albadry, 1972). Tharthar Lake's water is classified as C4S1 (C4: waters with electrical conductivity > 2.25 dS/m; S1: very high sodium adsorption ratio) class according to the U.S. salinity laboratory classificatory (Jehad, 1983). According to Swiss consultants (1979), salinity in Wadi Al-Tharthar was estimated as 5000 mg/l. It was found that there was only a 1-3% change in the vertical gradient in salinity from the surface of the lake to the bottom (Al-Badry and Artin, 1972), while the horizontal gradient in salinity along the North-South axis of the lake was in the range of 4500-2500 mg/l (Swiss consultants, 1979). This indicates that water salinity highly corresponds to the inflow from local catchment areas in the northern parts of the lake. According to the salinity classifications listed in Table 7, irrigation water in the Tigris River at Baghdad and downstream areas is classified as high salinity water.

Table 7: USDA Salinity Laboratory's classification of saline irrigation water based on salinity level, potential injury to plants, and management necessary for satisfactory utilization (Camberato, 2001).

Salinity Class	TDS mg/l	Potential injury and necessary management for use as irrigation water
Low	<150	Low salinity hazard; generally, not a problem; additional management is not needed
Medium	150-500	Damage to salt sensitive plants may occur. Occasional flushing with low salinity water may be necessary.
High	500-1500	Damage to plants with low tolerance to salinity will likely occur. Plant growth and quality will be improved with excess irrigation for leaching, and/or periodic use of low salinity water and good drainage provided.
Very High	>1500	Damage to plants with high tolerance to salinity may occur. Successful use as an irrigation source requires salt tolerant plants, good soil drainage, excess irrigation for leaching, and/or periodic utilization of low salinity water

Rahi and Halihan (2010) studied water salinity in the Euphrates River as it enters Iraq. It was found that the concentration of total dissolved solids (TDS) in the river was more than doubled compared with that in 1973. Also, it was showed that TDS concentration in Tharthar Lake was 1500 mg/l in 2003 causing high TDS concentration in the mainstem of the Euphrates River as water diverted from the lake to the river through Tharthar-Euphrates canal. Other causes of high TDS in the river were attributed to irrigation back flow and a decrease in upstream river flow.

Kadhem (2013) compared water quality data of the Tigris River using a geographic information system (GIS). In his study, 96 water samples were collected from eight locations along the Tigris River. The locations were chosen to cover all the distance of the Tigris River within Baghdad city during Jun-Dec 2008. The chemical analysis shows the mean concentration of 700 mg/l for total dissolved solid (TDS), 28 NTU for turbidity, and 0.77 mg/l for Iron (Fe). Field data compiled by Kadhem (2013) were compared to the World Health Organization (WHO) and Iraqi drinking water quality standards. These standards were 500 mg/l for TDS, 5 NTU for turbidity, and 0.3 mg/l for Fe. Other water quality variables included in this study that were compared with the Iraqi drinking water quality standards were pH, total hardness (TH), Magnesium (Mg), Chlorine (Cl), Nitrate (NO_2), Nitrate (NO_3), and Phosphate (PO_4). The average values for pH, NO_3, PO_4 were 8.02, 0.53, and 0.07 mg/l, respectively.

Al-Marsoumi et al. (2006) investigated the ionic concentrations of the Tigris and Euphrates Rivers. A significant increase in the total dissolved solids (TDS) concentrations was found downstream of Baghdad city (557 mg/l) at Amara city compared to 260 mg/l at Mosul city which is located about 560 km north of Baghdad. As total hardness was measured in the study, the Euphrates could be divided into two groups from upstream to downstream as hard to very hard, respectively, while Tigris water is considered hard.

Al-Layla and Al-Rizzo (1989) developed and calibrated a mathematical model that numerically solved a 1-D advection-dispersion equation for water quality parameters of interest in the Tigris River downstream of Sadam Dam. The studied study area was 75 km long extending from Sadam Dam to Mosul city. Fieldwork was conducted in the period

from July to September 1986. Water samples were collected twice a month. Water quality parameters of interest were DO with a range of 7.0-9.0 mg/l, BOD with a range of 0.7-1.0 mg/l, ammonia-N with a range of 0.02-0.24, nitrate-N with a range of 1.0-0.7, nitrite-N with a range of 0.01-0.06, phosphate with a range of 0.4-0.55, chloride with a range of 35-48, sulphate with a range of 0.02-0.24, hardness with a range of 210-260, and TDS with a range of 234-260. Good agreement was found between modeled and in-situ measurements. It was found that DO concentrations increased downstream of the dam due to re-aeration by turbulence.

Jehad (1983) conducted a study to develop a mathematical model to decrease sulphate (SO4) concentrations in Tharthar Lake. He tested the scenario of diverting different quantities of fresh water through Tigris- Tharthar canal and releasing the same quantities through Tharthar canal to the Euphrates River. SO4 concentration could be reduced to the maximum allowable concentration of 400 mg/l after 11 years if 10 cubic km water diverted through the Tigris River and released through the lake.

Al-Dabbas and Al-Juburi (1985) evaluated the hydrochemical and sediment transport in Tharthar Lake and its canals. They confirmed that salinity in the lake was mostly increasing in the northern parts of the lake and the lake's water contains Ca, Mg, Na, K, and a combination of sulphate and chloride, while very low concentrations of Br, Cr, Cd, Fe, Cu, Zn, and Mn were determined.

The following conclusions can be reached:

- Most studies on the Tigris River were conducted for the river reaches within Baghdad, and focused on water quality and river discharge.
- Iraq heavily depends on the Tigris River for its water resources, including irrigation and drinking water.
- High concentrations of BOD were found in Baghdad at locations where industrial and oil effluents were discharged directly to the Tigris River.
- The Tigris River water never reached a quality of excellent nor of unsuitable.
- The increase in the total hardness in the Tigris River within Baghdad was mostly due to the increase in Mg concentration
- There is an increase in the annual water demand by 1 km^3, while there is an annual decrease in the Tigris water by 0.133 km^3 due to upstream decrease in water quantity.
- Field data in the Tigris River within Baghdad were compared with the Iraqi and the World Health Organization (WHO) water quality standards and showed that TDS concentrations exceeded both water quality standards.
- TDS in the Tigris River does not meet the Iraqi drinking water standards and does not reach the excellent level according to a water quality index. The Tigris River is considered medium to highly saline.
- Untreated domestic and industrial effluents were directly discharged to the Tigris River and are a main major source of pollution in the river.

- Eutrophication, which is a characteristic problem of lakes, was found to occur in the Tigris River because of the intensive use of detergents rich in nutrients (P and N compounds).
- The average Total dissolved solids (TDS) concentration in Tharthar Lake was 1500 mg/l in 2003, and salinity in the lake was mostly increasing in the northern parts of the lake.
- TDS concentrations were significantly increased in the Tigris River between Mosul Dam and Baghdad city as a result of irrigation return flow, saline water diverted through Tharthar-Tigris canal, and urban runoff.
- Typical BOD concentrations in the Lower Zab tributary were in the range of 1.4-3.8 mg/l in 2004, while seasonal BOD concentrations in the mainstem of the Tigris River within Baghdad city were in the range of 2-4 mg/l in 2009.

Chapter Three: Surface Water Temperature Estimation from Remote Sensing

In this chapter, the process of utilizing remote sensing to estimate the surface water temperature of the Tigris River is described. A statistical model of water temperature based on air temperature and flow rate is developed from these surface water temperature estimates, and is used to infill temporal gaps in the satellite record. The resulting daily water temperature data is used to define the upstream boundary conditions for water temperature and to calibrate/validate the model within the domain.

Introduction

Monitoring the temperature distribution in water is fundamental for modeling and interpreting the water quality of waterbodies. Water temperature is a key factor of chemical and biochemical processes in aquatic ecosystems and controls the thermodynamics of waterbodies. Conventional monitoring of water surface temperature requires in-situ measurements, which can be expensive, time consuming and limited in spatial extent. In Iraq, the evaporation rate during the summer is large and both water temperature and evaporation in off-river storage lakes such as Tharthar Lake (see Figure 8) is significant. Other factors influence water temperature, including effluents from water and wastewater treatment plants, agricultural return flow, and industrial wastewater discharged to the Tigris River. In addition, short wave solar radiation, long wave atmospheric radiation, back radiation, and conduction are significantly influence water temperature.

Unfortunately, surface water temperature field data in Iraq is limited, and there is no publically available archive of in-situ data. Therefore, remote sensing from satellites is

potentially an effective method of estimating surface water temperature over a range of temporal and spatial scales.

In remote sensing, satellites such as Landsat, TRMM, MODIS, MERIS, SPOT, Quickeye, Worldview, Aqua, Terra, and Quickbird have been continuously acquiring earth observations. Since publically available, Landsat satellite is adequate for estimating water temperature of the Tigris River. Landsat satellites have been continuously acquiring earth observations since 1972. Eight Landsat satellites have been built, and seven have been successfully launched and operated in orbit. The Landsat 5 thematic mapper (TM) was operational from 1984 to 2012, and the Landsat 7 enhanced thematic mapper plus (ETM+) launched on April 15, 1999 and is still operating. The thematic mapper sensor installed on the Landsat satellite has been the most widely used sensor to monitor inland waters (Ritchie et al. 1990). Due to good time coverage and good spatial and temporal resolution, remote sensing is a convenient alternative to estimate water quality variables of water waterbodies. However, weather conditions such as cloud cover might adversely influence quality of satellite images.

Remote Sensing

Remote sensing is the science of gathering object information on earth's surface, land and ocean, by sensors installed on aircrafts or on satellites. Satellites observe earth's surface and acquire images at different temporal (< 24 hours - > 16 days) and spatial (0.41m - >1000 m) resolutions. Reflective radiance from an object or a phenomenon is detected within a wide range of wavelengths. Reflective radiance can be converted to Top Of Atmosphere (TOA) reflectance where subsequent atmospheric correction is needed. Compared with conventional and traditional methods, data acquired from satellites could be a reliable alternative to provide information on earth's and water's surface such as surface water temperature, land use and cover.

Landsat 7 ETM+

Landsat is one of a series of satellites launched by the National Aeronautics and Space Administration (NASA) to acquire satellite imageries of earth. Landsat program began in 1972 with Landsat 1. Landsat 5 Thematic Mapper (TM) was launched on March 1, 1984 and decommissioned on January 2013. Landsat 7 enhanced thematic mapper plus (ETM+) was launched on April 15, 1999 and is still operating. Landsat satellites provide continuous earth observation information that are important for monitoring global changes (Fuller at al., 1994; Wulder at al., 2008). Figure 11 shows a schematic of Landsat 7 ETM+. Landsat imageries have been archived and available from the United States and Geological Surveys (USGS).

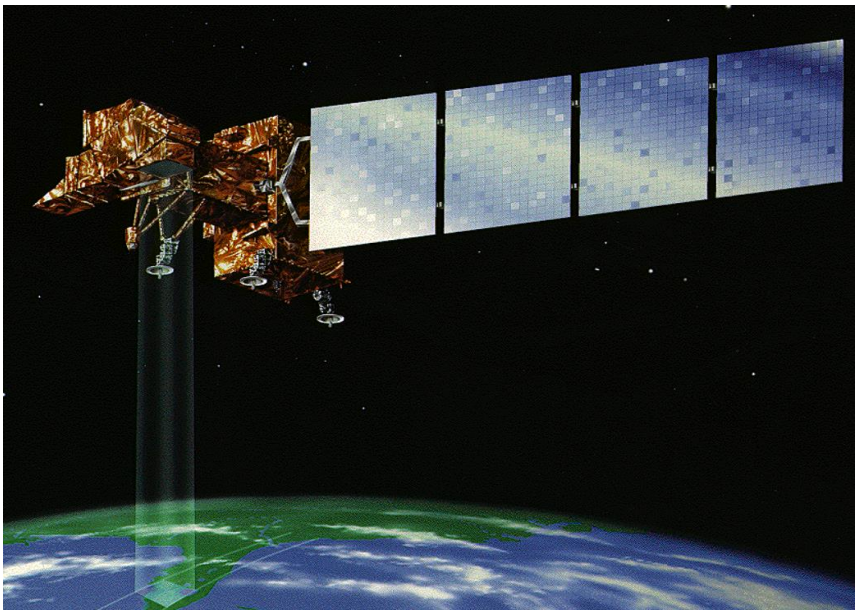

Figure 11: Schematic of Landsat 7 ETM+ satellite (NASA, 2014).

Previous Research Studies Using Remote Sensing Data

Nas et al. (2010) have investigated spatial patterns in water quality in Lake Beysehir, the largest fresh water reservoir in Turkey, using Landsat 5 Thematic Mapper (TM) data and ground data. Water quality variables of interest were suspended sediments (SS), turbidity, secchi disk depth (SDD), and chlorophyll-a (chl-a). Multiple regression (MR) and bivariate (2 band independents) were used to estimate spatial patterns based on both remote sensed and ground data. It was found that band 3 (TM3) provided a significant relationship with SS concentration, while band 1 (TM1), band 2 (TM2), and band 4 (TM4) were strongly correlated with Ch-a concentrations. Turbidity was shown to be significantly correlated with TM1, TM2, and TM3, while SDD was correlated with the ratio TM1/TM3 and TM1.

In Kabbara et al. (2008), Landsat 7 ETM+ was used to assess water quality in the coastal area of Tripoli (Lebanon). Empirical algorithms for chlorophyll-a concentration, secchi disk depth, and turbidity were derived. Maps of the distribution of selected water quality

parameters were generated for the entire area of interest. Moderate eutrophication conditions were indicated by the water quality in the coastal area.

Wang et al. (2006) investigated water quality in the Reelfoot Lake, Tennessee using Landsat5 TM imagery. Empirical algorithms were developed for water quality parameters such as turbidity, chlorophyll-a (Chl-a), and Secchi disk depth as listed in Table 8. They concluded that remote sensing was a useful tool to map Chl-a distribution in Reelfoot Lake.

Khattab and Merkel (2014) derived simple and accurate algorithms for the retrieval of water quality variables for Mosul Dam Lake, Iraq. Landsat 5 TM and Landsat 7 ETM+ were used in this study. Water quality variables of interest included temperature, turbidity, Secchi disk, chlorophyll-a, nitrate, nitrite, phosphate, total inorganic carbon, dissolved organic carbon, total dissolved solids, and pH. Image enhancement was used to evaluate the values of reflectance bands properly. A significant correlation between developed models and water quality variables was concluded in this study. Normalized difference water index (NDWI) was used to delineate the surface water of the lake. It was concluded that "ETM+ algorithms were more precise" and that algorithms based on surface reflectance for Landsat7 ETM+ were more quantitative and accurate than those based on Landsat 5TM.

Using Landsat Thematic Mapper (TM), Giardino et al. (2001) modeled and mapped water quality parameters including temperature in the sub-alpine Lake Iseo, Italy. A Landsat imagery-independent procedure was used to derive the surface temperature of the lake from the TM data. A window of 3×3-pixel array was used in the study. The temperature model was not based on a correlation between satellite and in-situ data such as other water quality

variables used in the study. It was based on an image independent procedure using the inverted Plank's law of temperature.

Lamaro et al. (2013) utilized the thermal bands of Landsat7 ETM+ to estimate surface water temperature in Embalse del Rio Tercero reservoir, Argentina. "The single-channel generalized method (SCGM) developed by Jimenez-Munoz and Sobrino (2003)" was used in this study. A constant water emissivity value of 0.9885 was used. Significant correlation coefficients R^2 of 0.9498 for SCGM method and R^2 of 0.9584 for RTM method were achieved.

Fan et al. (2014) predicted the chlorophyll a concentration in Xiangxi Bay in the Three Gorges Reservoir using Hj-1 satellite imagery. Several models were established based on a correlation analysis between in situ measurements of the chlorophyll a concentration and the values obtained from satellite images of the study area from January 2010 to December 2011. The results show that the maximum correlation is between the reflectance of the band combination of B4/(B2+B3) and in situ measurements of chlorophyll a concentration (see Table 8). The results provided a reference for water bloom prediction in typical tributaries of the Three Gorges Reservoir and was deemed useful for water quality management.

Table 8: Water quality correlations of some research studies. B1, B2, B3, B4, B5, B6, B61, and B62 are blue, green, red, near infrared, shortwave infrared, thermal, thermal Low Gain, and thermal High Gain bands respectively.

Water Quality Variable	Correlation	R^2	Reference
Ln(Turbidity)	10.6-5.6Ln(B1) +3.5Ln(B2)	0.57	
Ln(SDD)	-7.27+4.84Ln(B1)-2.95Ln(B2)	0.57	Kabbara et al. (2008)
Ln(Chl-a)	1.67-3.9Ln(B1) +3.8Ln(B2)	0.72	
Turbidity	-0.22-.46×B1+0.72×B2+0.84×B3	0.6	
SDD	-16.89+93.84×(B1/B3)-2.162×B1	0.71	Nas et al. (2010)
Chl-a	7.4-0.38×B1+0.54×B2+0.73×B4	0.6	
Turbidity	19+144×B2-118.7×B3	0.537	Wang et al. (2006)
SDD	33.6-133×B2+97.94×B3	0.588	
Chl-a	48.4+1142.22×B2-876.368×B3	0.705	
Temperature	No Correlation	0.95	Lamaro et al. (2013)
Turbidity	35.121−14.489(B2/B3) −0.911B4	0.99	
SDD	3119.27 e−0.233B3	0.88	
Chl-a	−15.16+0.449B1−1.252(B3/B1)	0.88	
TDS	−0.920−0.002B2+0.01$B6_2$+0.001B4	0.96	Khattab et al. (2014)
NO_3	1.782+75.469 ln($B6_2$/$B6_1$)	0.6	
PO_4	−0.081−0.008B3+0.018B4	0.96	
Temperature	-7.4+0.119B6+0.066$B6_2$-0.017B5	0.97	
SDD	8.01(B1/B2)-8.27	0.99	Giardino et al. (2001)
Chl-a	11.18B1-8.96B2-3.28	0.85	

Satellite Data Acquisition

Landsat imageries of interest that are used in this study were accessed from the US Geological Survey (USGS) database at http://glovis.usgs.gov/ and http://www.earthexplorer.usgs.gov/. Landsat images can be inquired over any portion in the world by specifying a nominal image center referred as Path/Row numbers. Figure 12, Figure 13, and Figure 14 show three satellite imageries cover the study area and their Path/Row from upstream to downstream are (170/35) at Mosul Dam, (169/36) at Samarra City, and (168/37) at Baghdad City respectively. All imageries of interest are available in both the Landsat 7 ETM+ and Landsat 5 TM archive. Level 1-T and atmospherically-corrected level 2 surface reflectance have been used in this study. All remotely sensed imageries used in this study are a combination of both Landsat7 ETM+ and Landsat 5 TM. The dimensions of each imagery are about 7000×8000 pixels which is equivalent to 210×240 km. All Landsat scenes were acquired at 10:30 AM local time. Table 9 lists Landsat 5 (LT5) and Landsat 7 (LE7) images used in this study.

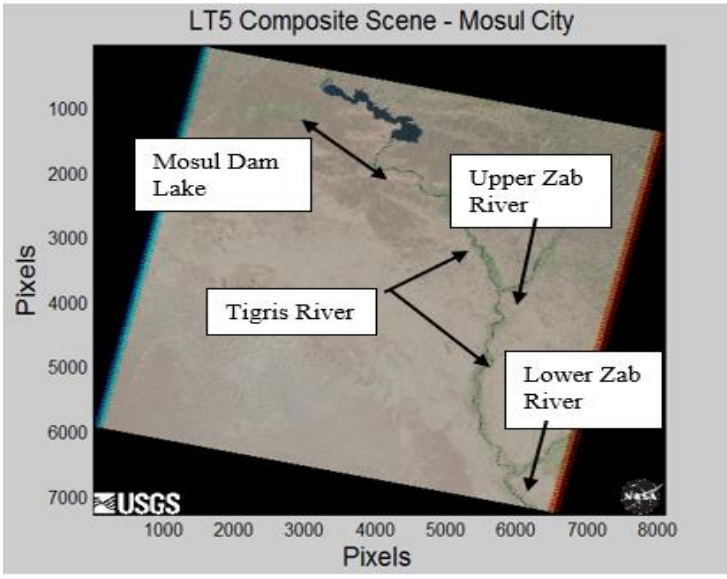

Figure 12: Landsat TM5 covers the Tigris River at Mosul Dam.

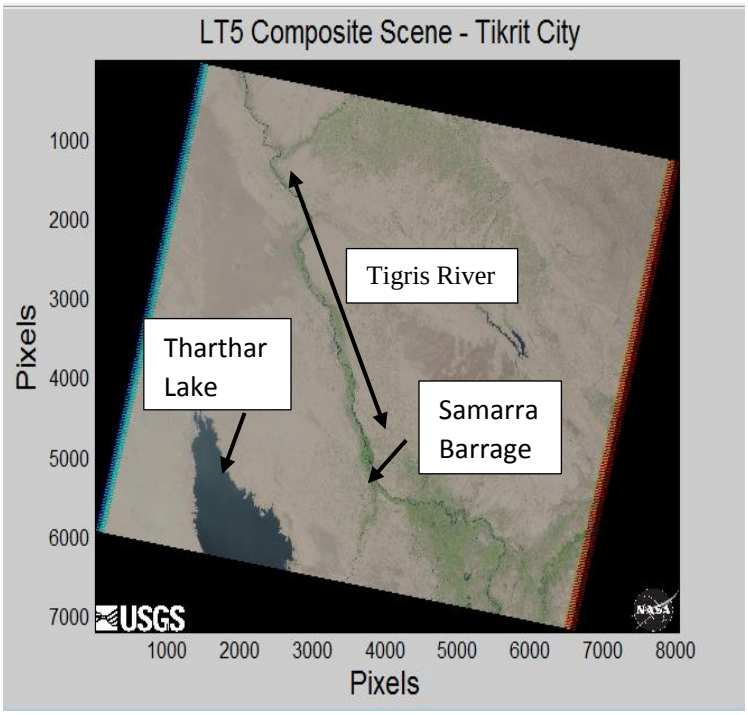

Figure 13: Landsat TM5 covers the Tigris River at Samarra Barrage and Tharthar Lake.

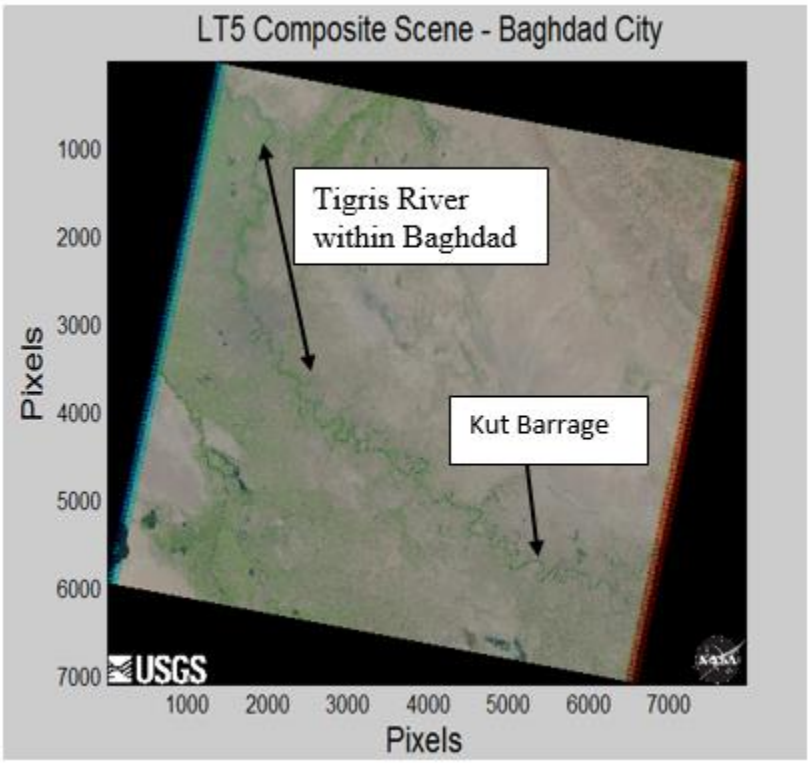

Figure 14: Landsat TM5 covers the Tigris River at Baghdad and Kut.

Table 9: Landsat 5 (LT5) and Landsat 7 (LE7) images used in this study.

Mosul City				Baeji City				Baghdad City			
Path/Row 170/35	Date	JDAY 2009	Cloud Cover %	Path/Row 169/36	Date	JDAY 2009	Cloud Cover %	Path/Row 168/37	Date	JDAY 2009	Cloud Cover %
LE7	2/11/2009	42	8	LE7	2/4/2009	35	3	LE7	1/12/2009	12	14
	5/2/2009	122	0		3/8/2009	67	4		1/28/2009	28	2
	5/18/2009	138	0		5/27/2009	147	0		2/13/2009	44	7
	6/3/2009	154	0		7/30/2009	211	2		3/17/2009	76	0
	7/5/2009	186	0		8/15/2009	227	0		4/18/2009	108	1
	12/28/2009	362	12		9/16/2009	259	4		5/20/2009	140	6
LT5	5/26/2009	146	1		10/2/2009	275	0		6/5/2009	156	0
	7/13/2009	194	0		10/18/2009	291	0		6/21/2009	172	0
	7/29/2009	210	0	LT5	5/3/2009	123	16		7/7/2009	188	0
	8/30/2009	242	0		5/19/2009	139	0		7/23/2009	204	0
	9/15/2009	258	0		6/4/2009	155	0		9/25/2009	268	0
	10/1/2009	274	0		6/20/2009	171	0		10/11/2009	284	2
	10/17/2009	290	0		7/22/2009	203	3		10/27/2009	300	4
Path/Row 169/35					8/7/2009	219	1		11/12/2009	316	0
LE7	2/4/2009	35	3		8/23/2009	235	0		12/14/2009	348	14
	5/27/2009	147	6		9/8/2009	251	0	Path/Row 169/37			
	6/28/2009	179	0		9/24/2009	267	0	LE7	1/19/2009	19	14
	7/14/2009	195	0		10/10/2009	283	2		2/4/2009	35	1
	7/30/2009	211	0		10/26/2009	299	3		2/20/2009	51	9
	8/15/2009	227	0		11/11/2009	315	0		3/8/2009	67	11
	8/31/2009	243	0						5/27/2009	147	8
	9/16/2009	259	14						7/14/2009	195	3
	10/2/2009	275	0						7/30/2009	211	1
	10/18/2009	291	0						8/15/2009	227	0
LT5	5/3/2009	123	1						9/16/2009	259	3
	5/19/2009	139	2						10/2/2009	275	0
	6/4/2009	155	0						10/18/2009	291	1
	6/20/2009	171	5								
	7/6/2009	187	5								
	7/22/2009	203	1								
	8/7/2009	219	1								
	8/23/2009	235	0								
	9/8/2009	251	0								
	9/24/2009	267	5								
	10/10/2009	283	0								
	10/26/2009	299	1								
	11/11/2009	315	0								
Total Images	36			Total Images	20			Total Images	26		

Image Processing

Remotely sensed data acquired from Landsat7 ETM+ is processed to convert the digital numbers (DNs) to reflectance and to minimize atmospheric effects (Lu et al. 2002). Image processing includes:

- Geometric Correction using ground control points (GCPs)
- Radiometric correction (Conversion of DNs to spectral radiance) using Equation 1 proposed by Chander and Markham (2003).

Equation 1. Radiometric correction equation

$$L = (\text{Gain} * \text{DN}) + \text{Bias}$$

where:

L: Radiance at satellite level of a specific band (W m^{-2} sr^{-1} u^{-1}).
DN: Value of the digital number.
Gain: Gain value for a specific band.
Bias: Bias value for a specific band.

- Conversion from spectral radiance to TOA planetary reflectance. This step is used to make the satellite data comparable with the spectral in-situ measurements. Equation 2 is used for this purpose.

Equation 2. Conversion from spectral radiance to TOA planetary reflectance

$$R = \frac{\pi L d2}{Esun\ Cos\theta}$$

where:
R= Planetary TOA reflectance [unit less]
π= Mathematical constant equal to ~3.14159 [unit less]
L= Spectral radiance at the sensor's aperture [W/(m^2 sr μm)]
d= Earth–Sun distance [astronomical units]
ESUN= Mean exoatmospheric solar irradiance [W/ (m^2 μm)]
θ= Solar zenith angle [degrees]

Atmospheric correction is needed because electromagnetic radiation travels through the atmosphere along its two paths from the sun to the earth surface and from there to the sensor, undergoing alterations to the radiometric signal.

- Waterline Extraction

According to Liu et al., (2011) and Ryu et al., (2002), the waterline is defined as a spatially continuous boundary between water and an exposed land mass. It is important to extract the water line for all Landsat imageries used to estimate surface water temperature of the Tigris River. For each individual scene, surface temperatures were estimated for the water pixels only, and land pixels were ignored. In this research, the surface reflectance land-water mask which is processed and provided by USGS as level 2 processed data, is used to extract the water line of the main stream of the Tigris River over the study area. The land-water mask is one of the successful methods used to extract the waterline from satellite images. Figure 15 shows an example of land-water mask of Landsat TM5 image that covered the Tigris River at Mosul Dam lake and the main stream of the Tigris river.

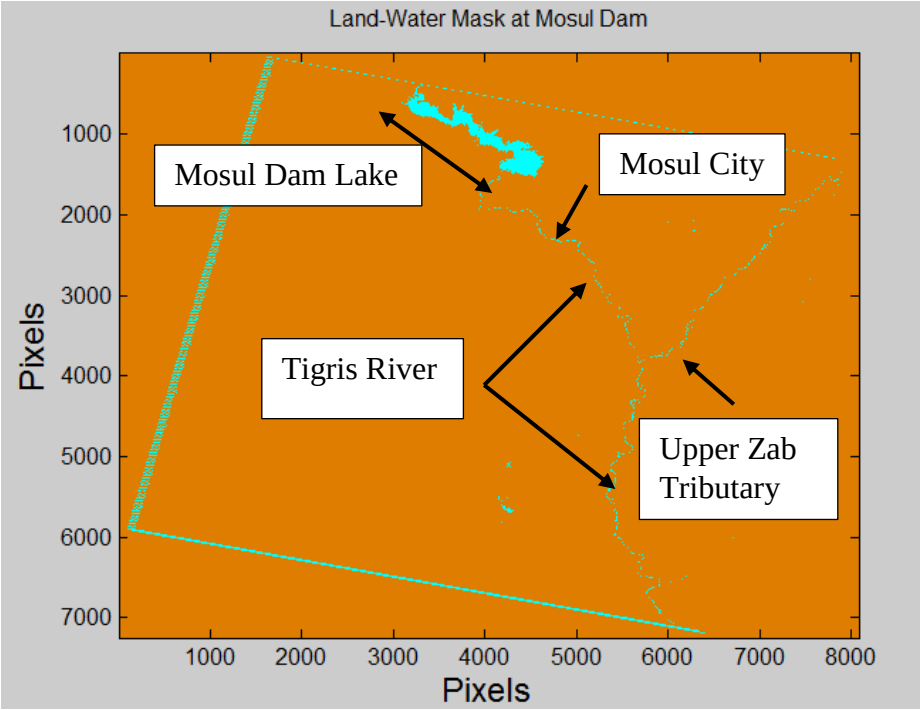

Figure 15: Land-water mask of the Tigris River at Mosul Dam and Mosul City.

Converting Landsat Thermal Bands to Surface Temperature

Landsat 5TM and Landsat 7 ETM+ sensors provide the spectral radiance that is stored at the sensor as digital numbers (DNs). It is possible to convert DNs to temperature values in degrees Kelvin using a two-step processes utilizing MATLAB for image processing, as described below (Coll et al. 2010):

- Conversion of DNs to Radiance, using Equation 1 "Gain and Bias Method"
- Conversion of Radiance to Kelvin, using the inverse of the Planck function as described in Equation 3 which determines at sensor temperature (this equation should be applied if no atmospheric correction is done on the band). Planck function is described in Equation 4.

Equation 3. Estimation of Pixel's temperature

$$T_w = \frac{K2}{\ln\left(\left(K1 * \frac{\varepsilon}{L}\right)+1\right)}$$

where:
T_w: At sensor brightness temperature in Degrees Kelvin
L: Radiance, estimated from Equation 1
ε: Emissivity (0.975)
K1: Constant (666.09 for ETM+), (607.76 for TM)
K2: Constant (1282.71 for ETM+), (1260.56 for TM)

Equation 4: Planck function

$$L = \frac{a}{\lambda^5\left(e^{b/\lambda t} - 1\right)}$$

where:
L: Radiance
a: 1.191042E8 (w/m^2 sr μm^{-4})
b: 1.4387752E4 (k μm)
λ : Wavelength (μm)
t: Blackbody temperature (k)

Emissivity is the ratio of the thermal radiation from a surface to the radiation from an ideal black surface. This ratio varies between 0 (gray bodies) and 1 (ideal blackbodies). Some factors affect emissivity such as temperature, emission angle, and wavelength. In this study, emissivity in Equation 3 was assumed constant with a value of 0.975 during the year 2009. This could introduce uncertainty in estimating of surface water temperature.

Estimation of Surface Water Temperature of the Tigris River

Thermal bands of Landsat images were utilized to estimate surface water temperature at Mosul Dam, Baeji city, and Baghdad city. For the year 2009, a total of 82 Landsat 5 TM and Landsat 7 ETM+ images with 20% or less image cloud cover condition were used to estimate surface water temperature in the mainstem the Tigris River. Unfortunately, most of Landsat images were unavailable in USGS archive for March and April of 2009. Figure 16 shows an example of surface water temperature at Mosul Dam and the main stream of the Tigris River downstream of Mosul City estimated in January 2009. A box filter of 2×2 km was used to estimate T_w. After defining the box filter, the median value was used to estimate T_w in that box. Although a land-water mask was used to differentiate between land and water pixels, some errors could be introduced by any remaining land pixels that have larger surface temperature than water pixels. Similarly, surface water temperatures at both Baeji and Baghdad cities were estimated from a combination of Landsat 5 TM and Landsat 7ETM+. Figure 17 and Figure 18 show surface water temperatures of the Tigris River at Baeji, Baghdad cities, and downstream areas along the main stream of the Tigris River estimated in January 2009. It can be seen that T_w at the northern ends of both Mosul Dam Lake and Tharthar Lake is very low (potentially spurious).

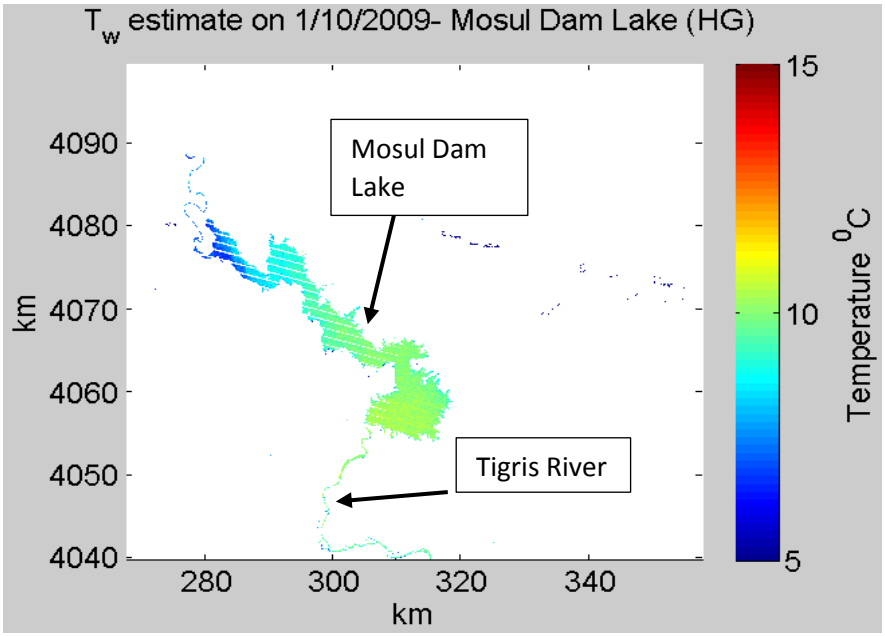

Figure 16: Surface water temperature of the Tigris River at Mosul Dam Lake.

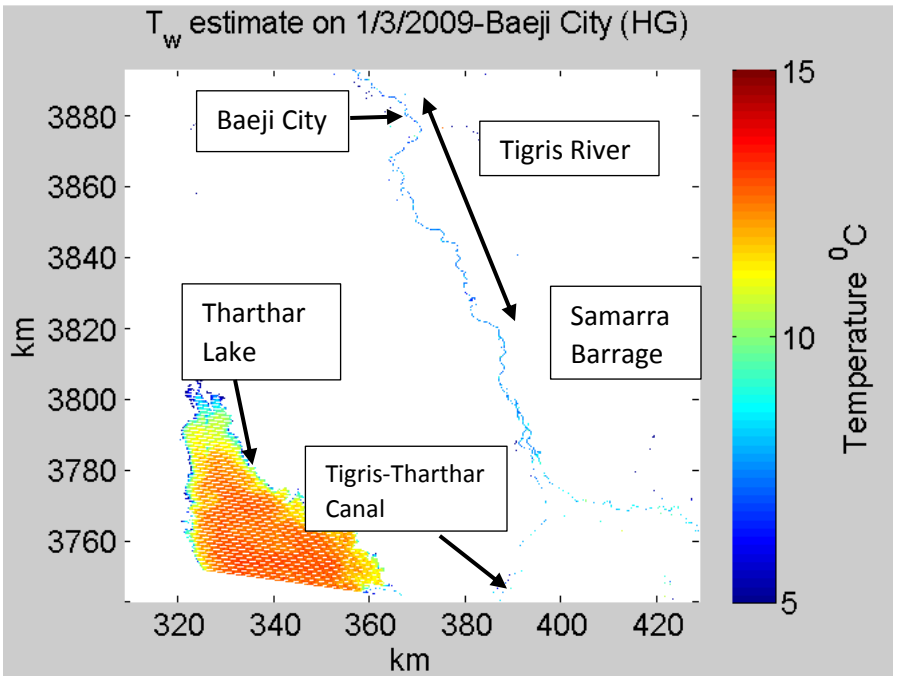

Figure 17: Surface water temperature of the Tigris River at Samarra Barrage.

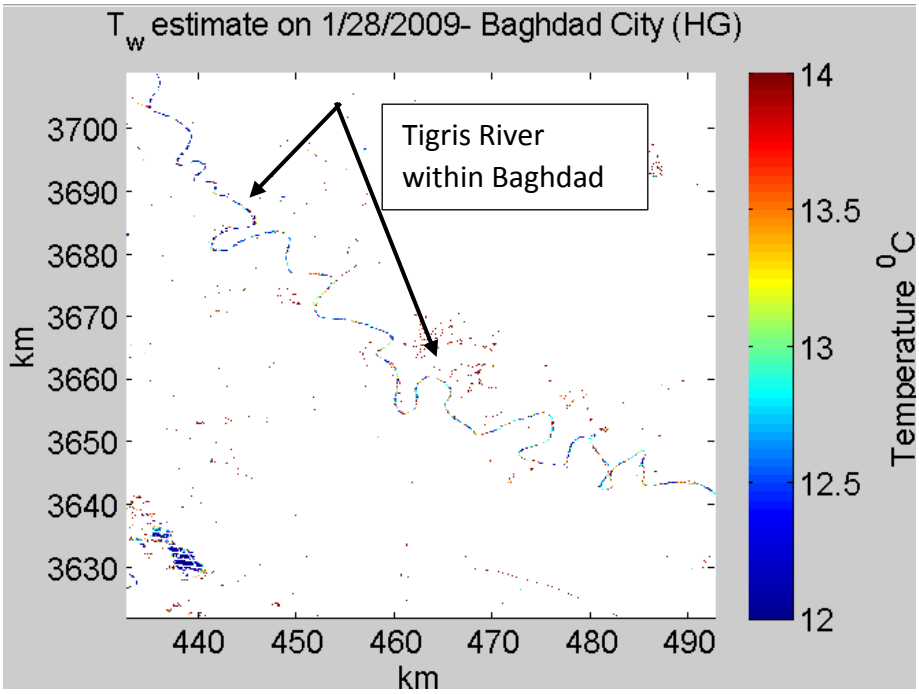

Figure 18: Surface water temperature of the Tigris River within Baghdad City.

Validation of Surface Water Temperature

Limited surface water temperature data of the Tigris River in Baghdad were obtained from a Master's thesis by Hikmat (2005). In 2004, Hikmat measured surface water temperature of the main stream of the Tigris River at a station located 3 km upstream of the confluence of the Tharthar-Tigris canal. Eleven point measurements of temperature were obtained that were used for validation. Landsat 7 ETM+ images were obtained within an acceptable range of ±5 days to the actual measured date. The median temperature of a 2x2 km box around the measurement site was estimated and regressed against in-situ data. Figure 19 shows the regression line, which shows a correlation coefficient of 0.915 and a root mean square error (RMSE) of 2.45 ° C.

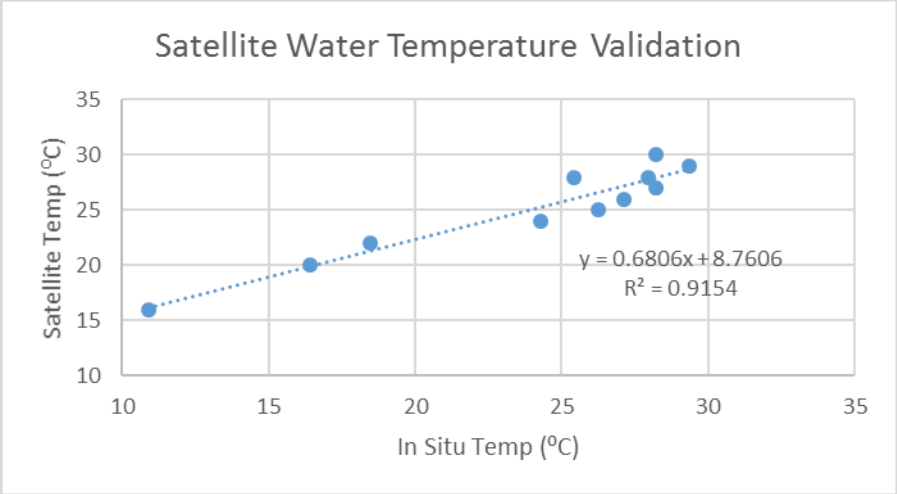

Figure 19: Validation of satellite water temperature.

Surface Water Temperature Statistical Model

A statistical model for surface water temperature of the Tigris River at Mosul, Baeiji, and Baghdad was next developed by correlating T_w estimated from Landsat against air temperature and river flow. Air temperature data (Figure 20) at Mosul, Baeji, and Baghdad cities were provided from the Iraqi Ministry of Transportation, the General Organization for Meteorology and Seismic Monitoring (MOT-IMOAS 2014) with a frequency of four hours for the year 2009. A weighted air temperature, with a five day response time was developed using an exponential filter to Equation 5 as below (Adams and Wells, 1984):

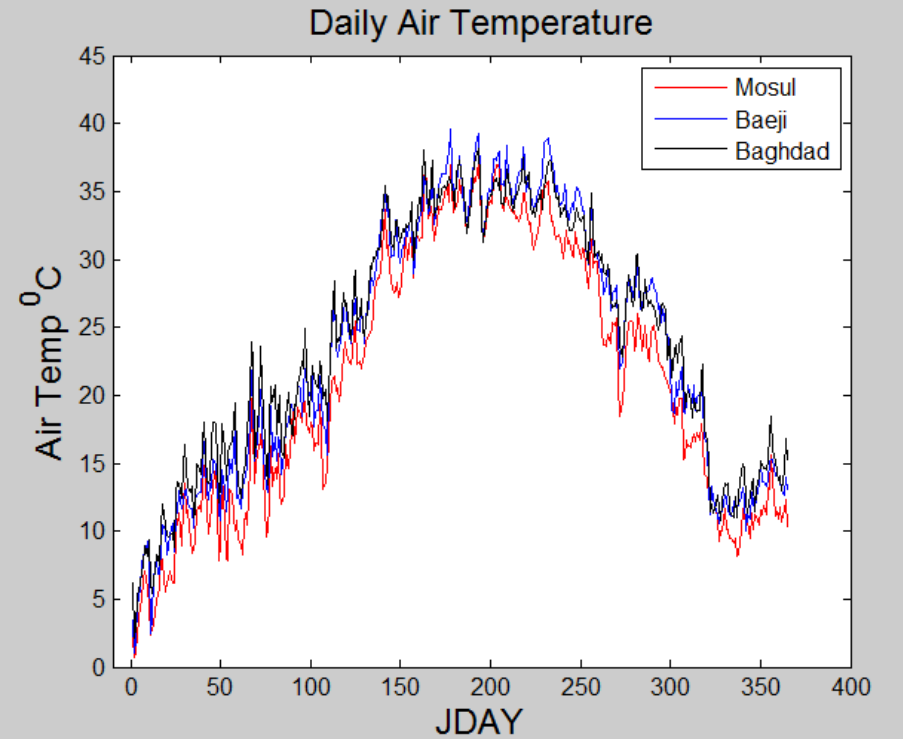

Figure 20: Daily air temperature at Mosul, Baeji, and Baghdad cities (2009).

Equation 5: Five days weighted air temperature

$$T_a = \frac{\Sigma_{n=1}^{tres/\Delta t} T_a(t-n\Delta t)\exp[-(n-1)k\Delta t]}{\Sigma_{n=1}^{tres/\Delta t}\exp[-(n-1)k\Delta t]}$$

where:

T_a: 5 days averaged air temperature in °C
t_{res}: Response time (5 days)
Δt: time step (1 day)
k: $\frac{Average\ depth\ (m)}{Response\ Time\ (s)}$ (Generally $k=10^{-5}$ m/s)

The time frame and the constants were selected based on the average river's depth of 4.5-5 m. Together, the weighted average in Equation 5 can be written more specifically as below:

$$T_a = \frac{T_a(n-1)*w1+T_a(n-2)*w2+T_a(n-3)*w3+T_a(n-4)*w4+T_a(n-5)*w5}{\Sigma_{n=1}^{5} w_n}$$

where:

W: Weight assigned to each day (the closer day to T_n the higher weight value assigned)

The last step after developing a weighted air temperature was to regress it, along with daily average flowrate, to the entire year of surface water temperatures estimated from Landsat images. The following statistical correlation (Equation 6) was solved using least-squares regression.

Equation 6: The statistical equation

$$T_w = a + bT_a + cQ$$

Flowrate was found to be a statistically insignificant predictor of surface water temperature, and was subsequently eliminated from all regression models (Equation 7, Equation 8, and Equation 9). Table 10 shows regression statistics. It can be seen that all coefficients (a1 and a2) are significant with a P-value much less than 0.05 for a confidence interval of 95%.

Equation 7: Statistical Model of water temperature at Mosul Dam

$$T_{w(Mosul)} = 4.3022 + 0.7294 * T_a$$

Equation 8: Statistical Model of water temperature at Baeji city

$$T_{w(Baeji)} = 4.7764 + 0.7010 * T_a$$

Equation 9: Statistical Model of water temperature at Baghdad city

$$T_{w(Baghdad)} = 3.4249 + 0.7594 * T_a$$

Table 10: Statistical values of the surface water models.

Parameter	**Mosul Dam Model**	**Baeji City Model**	**Baghdad City Model**
Intercept (a1)	4.3022	4.7764	3.4249
Slope (a2)	0.7294	0.7010	0.7594
P-value (a1)	0.0035	0.0046	1.725E-5
P-value (a2)	9.4E-17	3.33E-11	8.411E-21
R^2	0.864	0.9177	0.9753
Standard Error	2.160	1.537	1.148
Observations	36	20	26

Figure 21 shows estimated daily surface water temperature at Mosul Dam, Baeji, and Baghdad cities. The data show that water temperature typically increases by 25 ° C (range 6-31 ° C) over a year, with the largest along-channel gradients observed in spring/autumn and the smallest gradients observed in the summer. Also, the statistical model used to estimate T_w based on Landsat well captures the seasonal cycle of T_w. The standard error of statistical models was in the range of 1-2 ° C and was small relative to the amount of seasonal variation. Contamination of river pixels by land reflection could affect estimated water temperatures and causes uncertainty in the measurements. Temporal variation in water temperature of the Tigris River might be affected by the seasonal variations of both flow and solar radiation and other meteorological forcing data such as wind speed and direction, cloud cover, precipitation air temperature, and dew point temperature or relative humidity. These factors may not be captured by a regression model. On the other hand, spatial variation in water temperature of the Tigris River is mostly affected by the physical structure of the stream itself such as channel bathymetry (slope, width, and depth) and channel substrate (flow regime and sediment sources). Daily surface water temperatures

obtaining using Equation 7 were used to develop flow temperature input files as boundary conditions of the Tigris River model at Mosul Dam, while daily surface water temperatures at both Baeji and Baghdad (Equation 8 and Equation 9) were used for the model calibration.

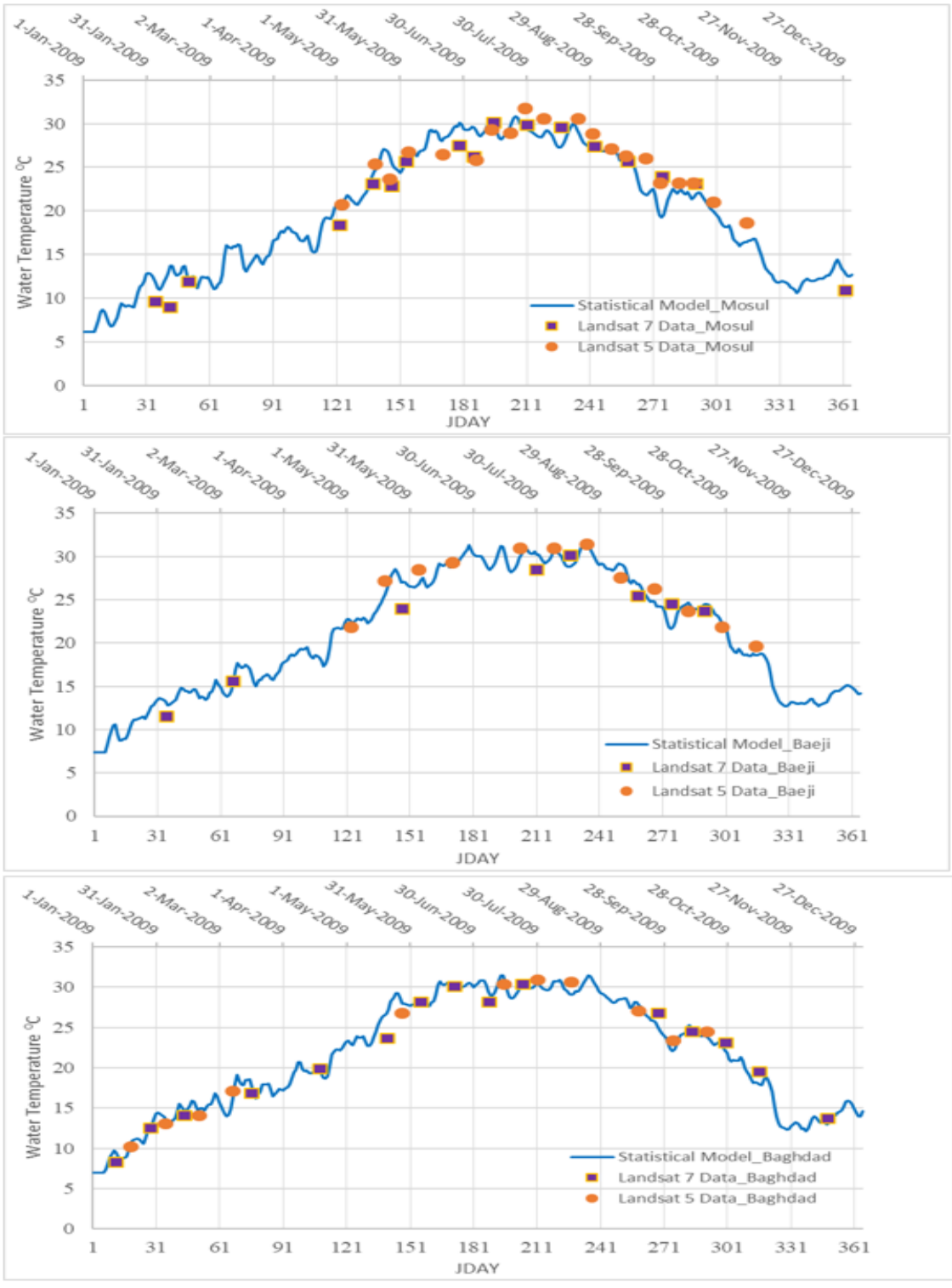

Figure 21: Satellite data (Landsat 5 and Landsat 7) and daily surface water temperature of the Tigris River estimated by regression models at Mosul Dam, Baeji city, and Baghdad city for the simulated year 2009.

Estimation of Surface water Temperature in Tharthar Lake

Thermal bands of Landsat 5TM and Landsat 7ETM+ images were utilized to estimate surface water temperature in Tharthar Lake. Two Landsat images cover the entire lake; Landsat image with path/row of 169/36 covers the upper part of the lake, while Landsat image with path/row of 169/37 cover the lower part of the lake. The Landsat images used to estimate surface water temperature in Tharthar Lake are listed in Table 11. Figure 22 and Figure 23 show surface water temperature in Tharthar Lake extracted from Landsat images taken at the same day during different months of 2009. A box filter 5×5 km was used to estimate T_w in the lake. After defining the box filter, the median value was used to estimate T_w in that box.

Table 11: Landsat images cover Tharthar Lake

Landsat	Date	Julian Day
LE7 169/36 & LT5 169/37	1/3/2009	3
	2/4/2009	35
	3/8/2009	67
	5/27/2009	147
	7/30/2009	211
	8/15/2009	227
	9/16/2009	259
	10/18/2009	291

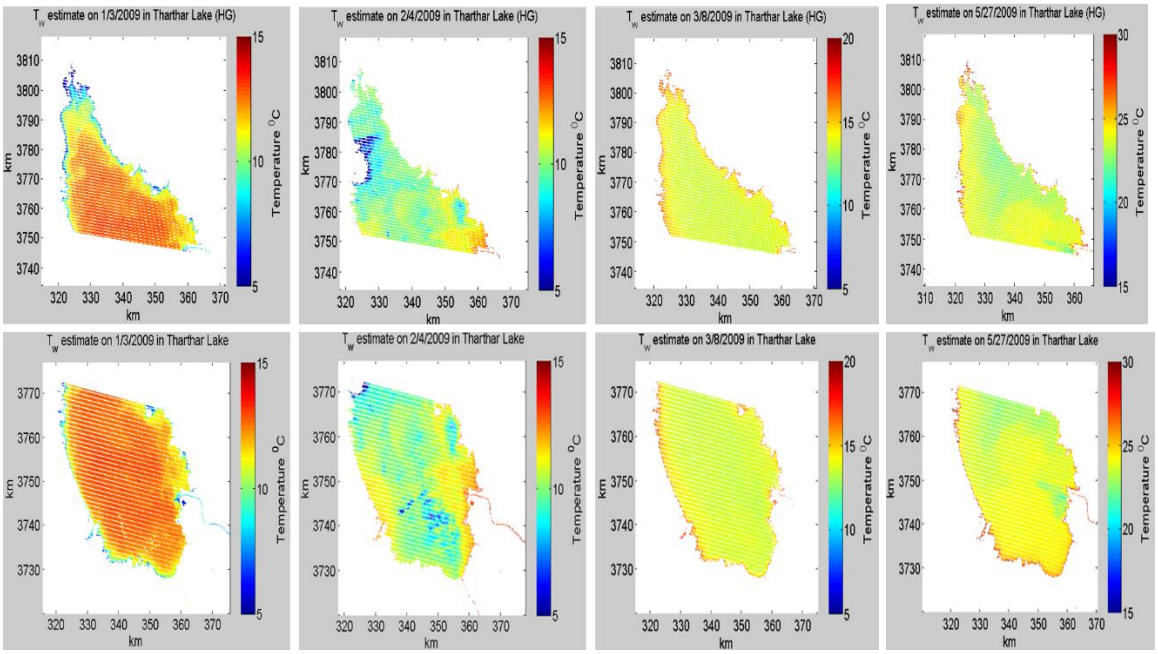

Figure 22: Surface water temperature in the upper and the lower parts of Tharthar Lake (part 1); the top row represents the upper part of the lake, while the bottom row represents the lower part of the lake.

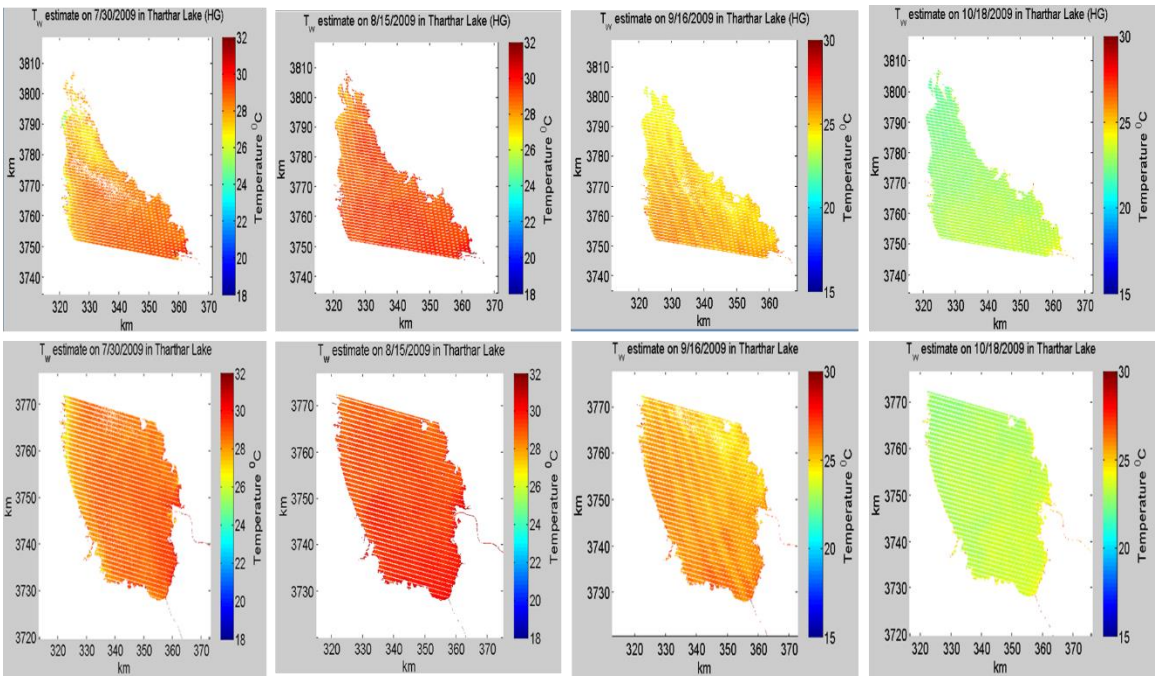

Figure 23: Surface water temperature in the upper and the lower parts of Tharthar Lake (part 2); the top row represents the upper part of the lake, while the bottom row represents the lower part of the lake.

Figure 24 shows longitudinal profile of seasonal variation in surface water temperature in Tharthar Lake, while Figure 25 shows longitudinal profile of surface water temperature in Tharthar Lake during winter and summer of 2009. The spatial gradient of surface water temperatures along the North-South axis of Tharthar Lake varied throughout the year. A larger gradient over a distance of 90 km can be observed in winter months with a temperature difference of 2.56 ºC in January and 2.27 ºC in February compared with summer months with a temperature difference of 1.40 ºC in July and 1.92 ºC in August. Longitudinal gradient in water temperature of Tharthar Lake is highly attributed to the lake's bathymetry and to meteorological forcing data that control evaporation in the lake. Some errors in estimation of surface water temperature in Tharthar Lake in winter could be attributed to cloud cover percentage on the day Landsat images were taken.

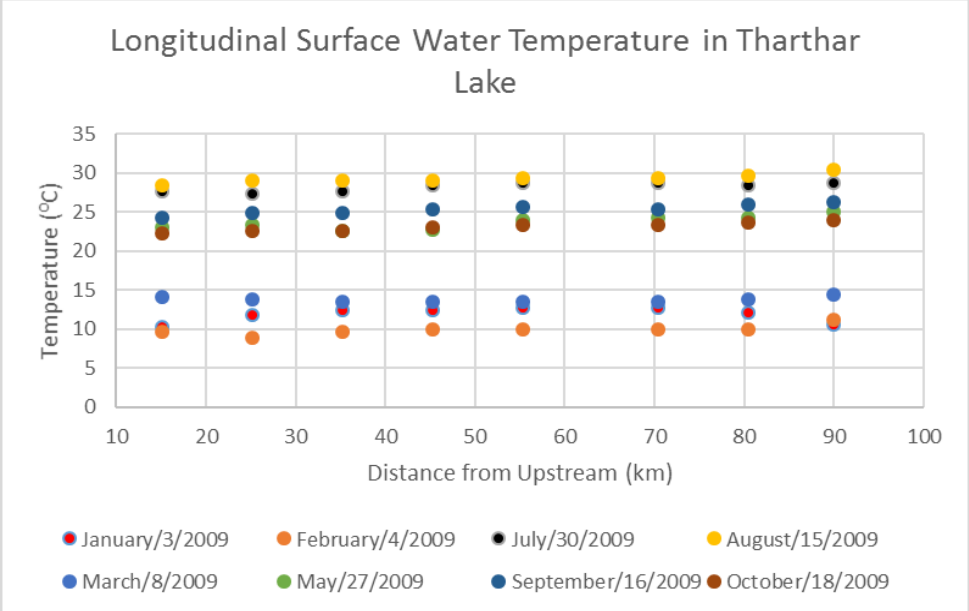

Figure 24: Seasonal variation in longitudinal surface water temperature in Tharthar Lake in 2009.

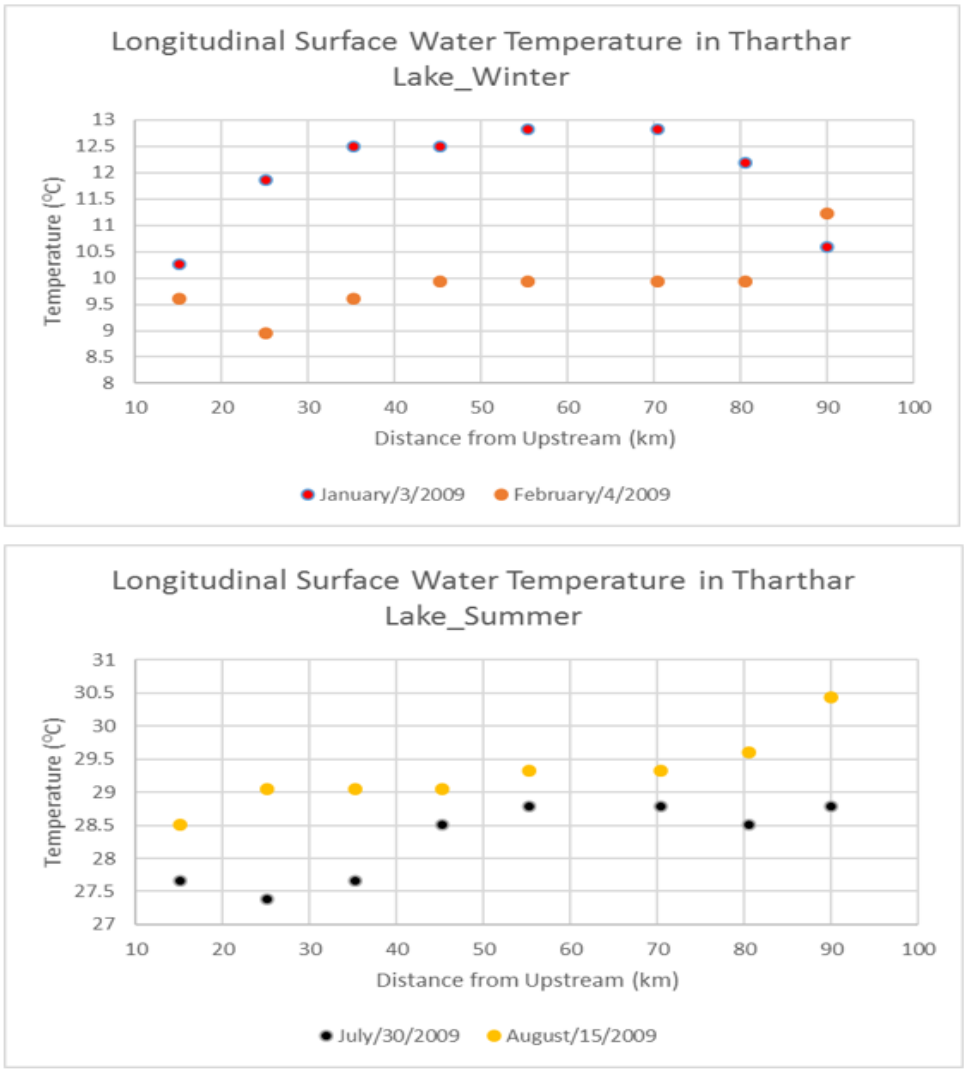

Figure 25: Longitudinal surface water temperature in Tharthar Lake in winter and summer of 2009.

Chapter Four: CE-QUAL-W2 Model Overview

This chapter reviews the governing equations of the hydrodynamic and water quality model, CE-QUAL-W2, Version 4. For more detailed discussion, refer to the user manual by Cole and Wells (2017).

Hydraulic Model Selection for the Tigris River System

1-D, 2-D, and 3-D models are general applications to simulate hydrodynamics and water quality of surface waterbodies. The choice of the proper model is based on the application of the model to evaluate management strategies, model calibration, model sensitivity analysis, computational representation, and the physical characteristics of each system component such as river, reservoir. Table 12 lists the main advantages and disadvantages of 1-D, 2-D, and 3-D hydraulic models.

Table 12: Comparison of 1-D, 2-D, and 3-D hydraulic models

Hydraulic Model	Advantage	Disadvantage
1-D	Fast to run Easy to set up	Need to identify major flow routes to set up the model No stratification Cross-sectionally averaged
2-D (x-z)	Solves 2-D flow equations Utilizes channel shape Easy to set up Velocity distribution can be calculated in 2-D vertical Applies to stratified flows	Relatively slow to run compared to 1D
2-D (x-y)	Solves 2-D flow equations Utilizes channel shape Easy to set up Velocity distribution can be calculated in 2-D horizontal	Relatively slow to run compared to 1D No stratification
3-D	Solves 3-D flow equations Good representation of complex riverine systems Good for systems with depth varied velocity Good representation of flow around structures	Complexity of model formulations and application Long model run times

Most studies on the Tigris River assumed one dimensional, steady state, and well-mixed in the cross-section conditions. These 1-D models are not adequate to compute stratification dynamics in deeper pools. Based on the depth of Tharthar Lake, a one-dimensional model would not be adequate because of possible vertical, as well as longitudinal gradients in water quality. Therefore, the model chosen for the Tigris River system is the 2-D Corps of Engineers model CE-QUAL-W2 (W2) (Cole and Wells, 2017). W2 is a dynamic 2-D (x-z) model that can simulate stratification in Tharthar Lake. W2 can handle a branched and/or looped system with flow and/or head boundary conditions. W2 model is efficient and

allows the user to use the ultimate quickest numerical scheme for improved numerical accuracy.

Model Introduction

CE-QUAL-W2 is a physically based, two-dimensional (longitudinal and vertical), laterally averaged, finite difference hydrodynamic and water quality model. The Version 3 model to Version 3.5 model was developed by a collaboration between the U.S. Army Corps of Engineers and the Water Quality Research Group at Portland State University. After Version 3.5, the model has been maintained by the water quality research group at Portland State University. The model applies spatial and temporal averaging to the Navier-Stokes and continuity equations to model surface water hydrodynamics. In addition, the advection diffusion equation is used for the transport of heat and water quality constituents. Because the model assumes lateral homogeneity, it is best suited for relatively long and narrow waterbodies exhibiting longitudinal and vertical water quality gradients. W2 simulates river/reservoir, lake stage, vertical and horizontal velocities, water temperature, and a user-defined number of water quality constituents including nutrients, algae, dissolved oxygen, and suspended sediment. W2 has been applied to hundreds of reservoirs, lakes, estuaries, and river systems all over the world (Cole and Wells 2017). W2 model has been used in many countries outside the United States such as Columbia, Brazil, Venezuela, Panama, United Kingdom, Spain, Thailand, Italy, New Zealand, China, South Korea, Taiwan, South Africa, Iran, Peru, Costa Rica, Israel, Canada, and Norway.

CE-QUAL-W2 State Variables

The hydrodynamic capabilities of the model include predictions of flow, water surface elevation, velocities, and temperature. The water quality state variables include (Cole and Wells, 2017):

1. any number of generic constituents defined by a 0 and/or a 1st order decay rate and/or a settling velocity and/or an Arrhenius temperature rate multiplier that can be used to define any number of the following:
    a. conservative tracer(s)
    b. water age or hydraulic residence time
    c. N2 gas and %Total Dissolved Gas
    d. coliform bacteria(s)
    e. contaminant(s)
2. any number of inorganic suspended solids groups
3. any number of phytoplankton groups
4. any number of periphyton/epiphyton groups
5. any number of CBOD groups
6. any number of submerged macrophyte groups
7. ammonium
8. nitrate and nitrite
9. bioavailable phosphorus (commonly represented by orthophosphate or soluble reactive phosphorus)
10. silica (dissolved and particulate)
11. labile dissolved organic matter
12. refractory dissolved organic matter
13. labile particulate organic matter
14. refractory particulate organic matter
15. total inorganic carbon
16. alkalinity

17. iron and manganese
18. dissolved oxygen
19. organic sediments
20. gas entrainment
21. any number of macrophyte groups
22. any number of zooplankton groups
23. labile dissolved organic matter-P
24. refractory dissolved organic matter-P
25. labile particulate organic matter-P
26. refractory particulate organic matter-P
27. labile dissolved organic matter-N
28. refractory dissolved organic matter-N
29. labile particulate organic matter-N
30. refractory particulate organic matter-N
31. Sediment and water column CH_4
32. Sediment and water column H_2S
33. Sediment and water column SO_4
34. Sediment and water column Sulfide
35. Sediment and water column $FeOOH(s)$
36. Sediment and water column Fe^{+2}
37. Sediment and water column $MnO_2(s)$
38. Sediment and water column Mn^{+2}
39. Sediment organic P, sediment PO_4
40. Sediment organic N, sediment NO_3, sediment NH_4
41. Sediment Temperature
42. Sediment pH
43. Sediment alkalinity
44. Sediment Total Inorganic C
45. Sediment organic C

46. Turbidity correlation to Suspended solids

Input Data Preparation

The follow input files were developed to run W2 model. Detailes about input data preparations are discussed in chapter five "The Tigris River Model Set Up"

- Bathymetry
- Meteorological data
- Shade file
- Wind Sheltering
- Initial conditions
- Boundary conditions, such as inputs from point or non-point sources, outflows or withdrawals from the system
- In-river water quality, water level, flow for calibration

Hydrodynamics Governing Equations

Governing equations for hydrodynamics are listed below. The assumptions made are (Cole and Wells, 2017):

- Incompressible fluid.
- Centripetal acceleration correction to the gravity term is negligible
- Boussinesq approximation
- Coriolis forces are not important in an x-z model
- Within a grid cell, density variation can be taken to be negligible for purposes of temporal averaging
- Each cell or control volume is vertically and laterally averaged
- The coordinate system is transformed so that the +z direction is vertical downward and perpendicular to the channel slope (thus, for a slope channel, there is a small difference in the +z direction and vertically downward).

- Scaling analysis showed that horizontal velocities are much larger than vertical velocities and was used to simplify the vertical momentum equation which becomes the hydrostatic condition.
- The state equation can be selected to represent freshwater (low salinity) or marine conditions.

In addition, the model allows the user to include the following physical processes:

- Channel bottom shear
- Wind driven surface shear
- Flow control structures such as weirs, gates, intakes, and pumps as well as selective withdrawal.
- Surface heat exchange
- Sediment-water heat exchange
- Vegetative and topographic shading
- Ice cover formation
- Light attenuation with depth
- Oxygen exchange at the air-water interface (reaeration, degassing)

Below are descriptions of x-momentum equation, z-momentum equation, continuity equation, and the equation of state:

x-Momentum

$$\frac{\partial UB}{\partial t} + \frac{\partial UUB}{\partial x} + \frac{\partial WUB}{\partial z} = -\frac{1}{\rho}\frac{\partial BP}{\partial x} + \frac{\partial \left(BA_x \frac{\partial U}{\partial x}\right)}{\partial x} + \frac{\partial B\tau_x}{\partial z}$$

Where

U = longitudinal, laterally averaged velocity, m/s
B = water body width, m
t = time, s
x = longitudinal Cartesian coordinate
z = vertical Cartesian coordinate

W = vertical, laterally averaged velocity, m/s
ρ = density, kg/m^3
P = pressure, N/m^2
A_x = longitudinal momentum dispersion coefficient, m^2/s^2
τ_x = shear stress per unit mass, m^2/s^2

z-Momentum

$$0 = g - \frac{1}{\rho}\frac{\partial P}{\partial z}$$

Where

g = acceleration due to gravity, m/s^2

Continuity

$$\frac{\partial UB}{\partial x} + \frac{\partial WB}{\partial z} = qB$$

Where

q = lateral boundary inflow or outflow, m^3/s

Free-Surface

$$\frac{\partial B_\eta \eta}{\partial t} = \frac{\partial}{\partial x}\int_\eta^h UBdz - \int_\eta^h qBdz$$

Where

B_η = spatially and temporally varying surface width, m

η = free water surface location, m

h = total depth, m

Constituent Transport

"The constituent transport relationships compute the transport of constituents with their kinetic reaction rates expressed in source and sink terms" (Cole and Wells, 2017).

$$\frac{\partial B\varphi}{\partial t} + \frac{\partial UB\varphi}{\partial x} + \frac{\partial WB\varphi}{\partial z} - \frac{\partial \left(BD_x \frac{\partial \varphi}{\partial x}\right)}{\partial x} - \frac{\partial \left(BD_z \frac{\partial \varphi}{\partial z}\right)}{\partial z} = q_\varphi B + S_k B$$

Where

φ = laterally averaged constituent concentration, mg/L

D_x = longitudinal temperature and constituent dispersion coefficient, m^2/s

D_z = vertical temperature and constituent dispersion coefficient, m^2/s

q_φ = lateral inflow or outflow mass flow rate of constituent per unit volume, mg/L/s

S_k =kinetics source/sink term for constituent

Equation of State

$$\rho = f(T, \varphi_{TDS}, \varphi_{SS})$$

Where

T = temperature, ^oC

φ_{TDS} = total dissolved solids concentration, mg/L

φ_{SS} = suspended solids concentration, mg/L

For a detailed description of the assumptions and processes in the derivation of these equations, and for other equations used in CE-QUAL-W2, see the user manual (Cole and Wells, 2017).

Chapter Five: The Tigris River Model Set Up

The mainstem of the Tigris River was modeled from Mosul Dam (river km 0) to Kut Barrage (river km 880). The mainstem of the Tigris River was discretized into four waterbodies. A waterbody is defined in the model by specifying the waterbody latitude and longitude, bottom elevation of the grid, starting and ending branches of the waterbody. Due to varying channel slope, the mainstem of the river was divided into four branches, a branch is a collection of model segments with variable model slope. The physical characteristics of the river varied widely, and multiple branches allowed for separate characteristics such as branch slope to be implemented in the model. In addition, Tigris-Tharthar Canal, Tharthar Arm, Tharthar-Tigris Canal, Tharthar Lake, and Erwaeiya canal were discretized into five waterbodies and were also modeled in this study. All model branches were connected based on specified upstream and downstream external/internal flow, internal head, or dam flow boundary condition. a schematic diagram of the Tigris River system is shown in Figure 26. Gates, spillways, and hydraulic structures were defined to convey water through the system.

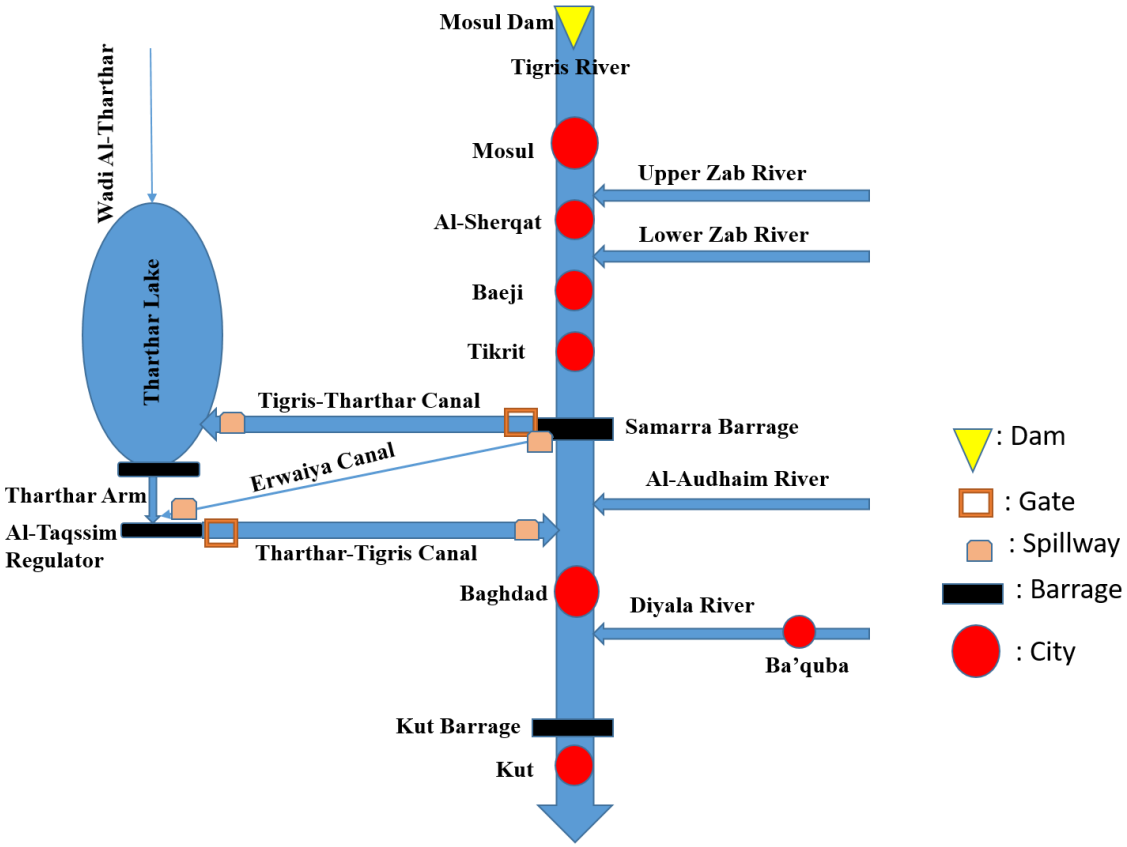

Figure 26: Schematic diagram of the Tigris River system.

Bathymetry and Grid Development of the Tigris River System

The Tigris River, Tharthar Lake, and canal system is divided into Waterbodies (a collection of model branches that have similar turbulence closure and water quality parameter values and meteorological forcing for a river or a reservoir), branches (a collection of model segments with variable model slope; a river with different slopes or a reservoir with multiple side arms), segments (a longitudinal segment of length DX), and layers (a vertical layer of height DZ).

The Tigris River Grid

The model grid of the mainstem of the Tigris River was developed based on the river cross section data provided by the Iraqi Ministry of Water Resources for 880 km along the main stream of the Tigris River from Mosul Dam to Kut Barrage. Data were provided in the form of x,y,z cross-sections with 5 km increments as shown in Figure 27 and were used to develop the river grid for the CE-QUAL-W2 model (Al-Murib, 2014). Geographical Information system (GIS) was implemented to visualize river morphology and project all cross sections with a projection UTM 1984 Zone 38N (North) and a datum GCS WGS 1984. Linear regression was used to fill gaps of some missing cross sections.

The first waterbody in the mainstem of the Tigris River (350 km in length) starts at Mosul Dam (River km 0) and ends 15 km downstream of Tikrit city (River km 350). The second waterbody starts from there to Samarra Barrage (a length of 40 km). The third waterbody (a length of 256.5 km) starts at Samarra Barrage and ends at 70 km downstream of Baghdad city, while the fourth waterbody (a length of 233.5 km) starts from there to Kut Barrage (at River km 880). Four main tributaries flow from the right bank of the main stream of the Tigris River between Mosul Dam to Kut Barrage.

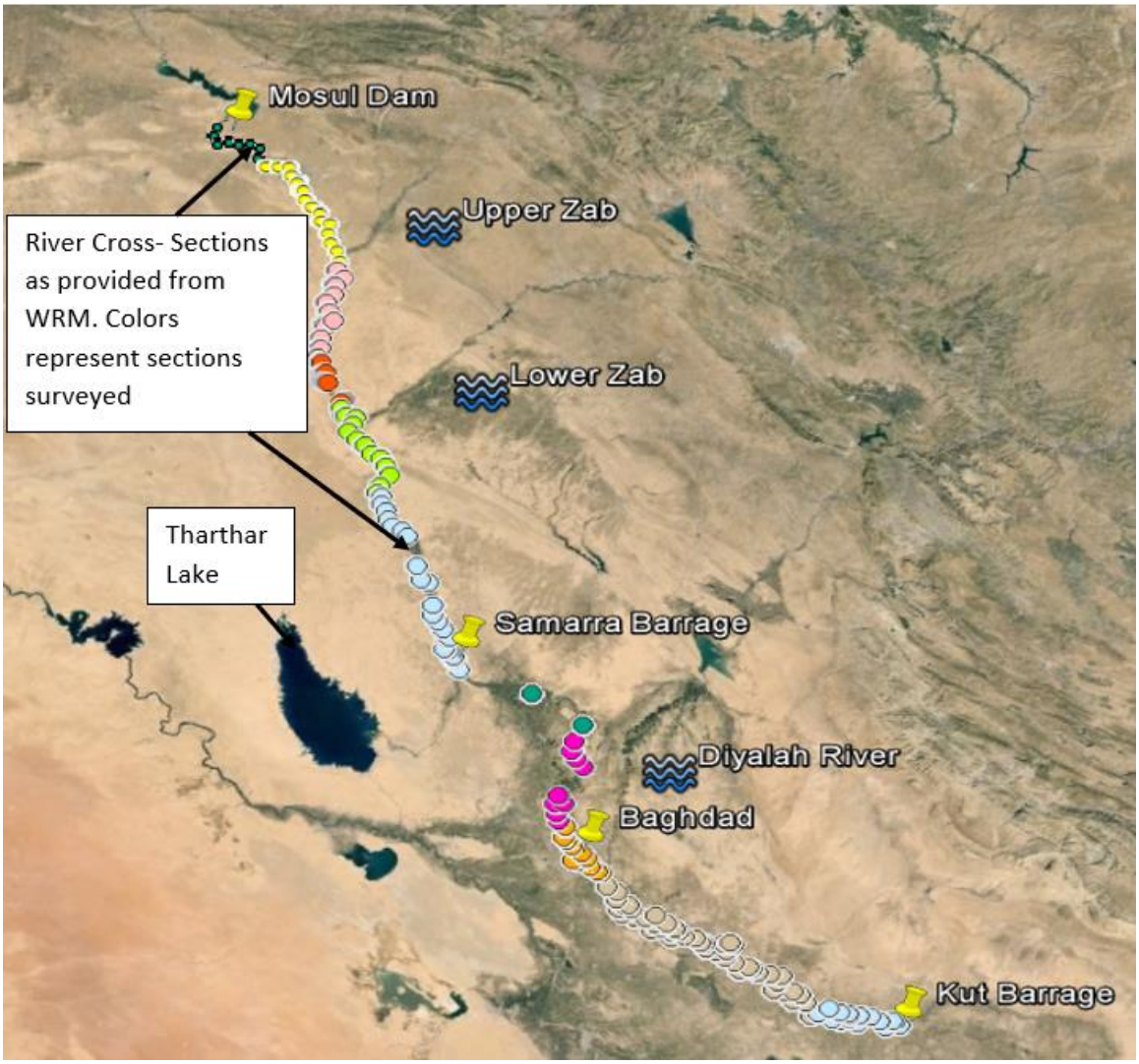

Figure 27: Cross sections of the Tigris River from Mosul Dam to Kut Barrage with the river cross-sections as provided from the Iraqi Water Resources Ministry (WRM), colors represent river cross-section files as received from WRM.

The model grid of the Tigris River system consisted of 343 longitudinal segments. Each of the model segments had 1 m thickness. 84 vertical layers (82 active layers and 2 inactive layers) were used in the model to represent the vertical elevation of the deepest point in Tharthar Lake. Field cross section data were interpolated to determine layer widths in each model segment. As an example, Figure 28 shows the river cross section at river km 490, while Figure 29 shows the bottom elevation of the mainstem of the Tigris River from Mosul

Dam to Kut Barrage estimated from bathymetric data. Figure 30 shows segment 123 section with 82 active vertical layers as constructed by the W2 model. Although the average water depth in the model segment is 6.3 m, 82 active layers were used in order to have the same number of layers as in Tharthar Lake. Figure 31 through Figure 34 show the longitudinal profile of the mainstem of the Tigris River for waterbody 1 (branch 1), waterbody 2 (branch 2), waterbody 3 (branch 3), and waterbody 4 (branch 4), respectively. The x-axis and y-axis represent segments and layers, respectively.

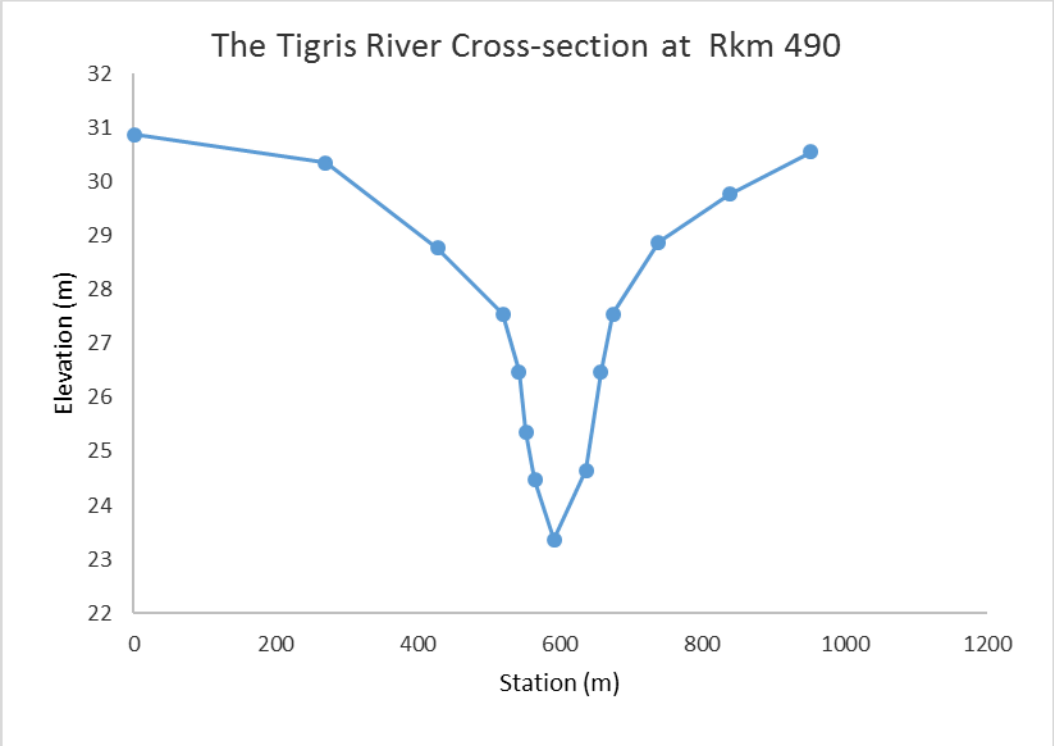

Figure 28: The Tigris River cross-section at river km 490 km.

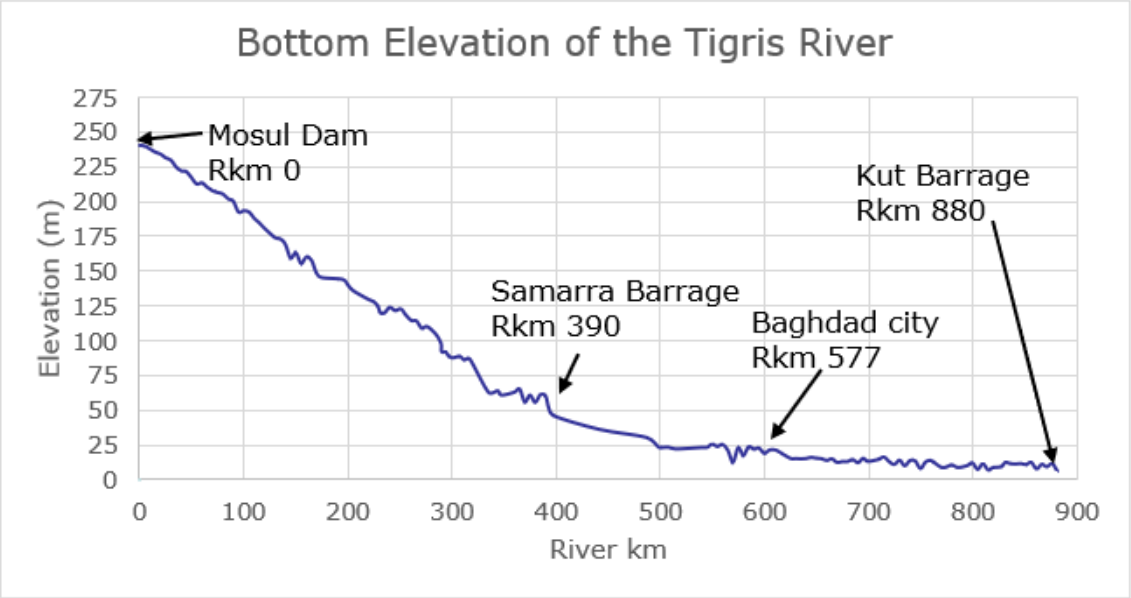

Figure 29: Bottom elevation of the mainstem of the Tigris River study area from Mosul Dam to Kut Barrage.

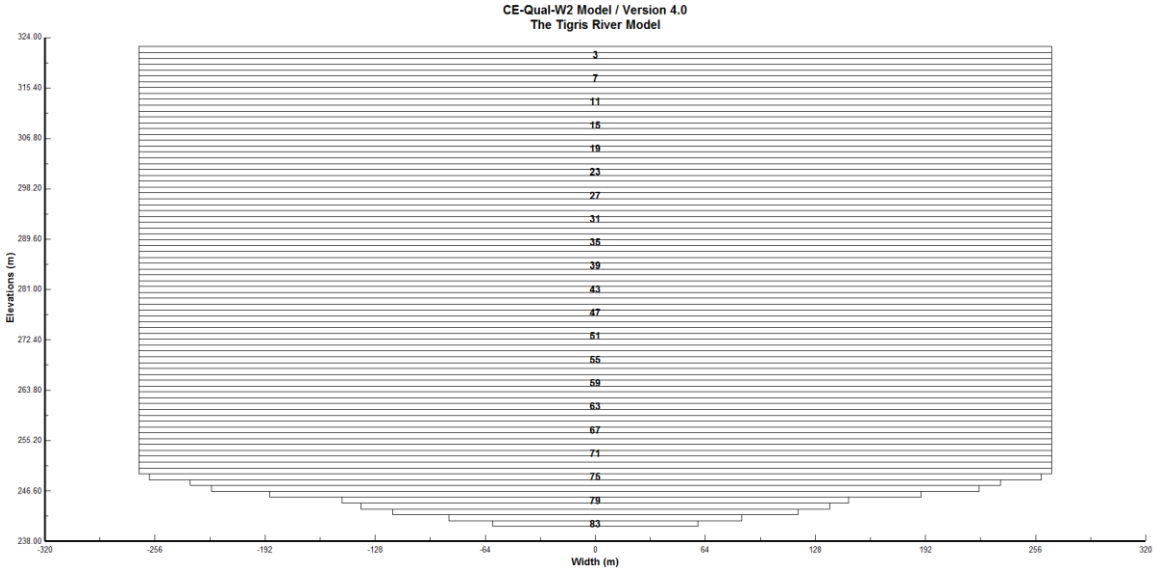

Figure 30: Segment section # 123 (Baghdad city) with 82 active layers (1 m each) constructed by the W2 model.

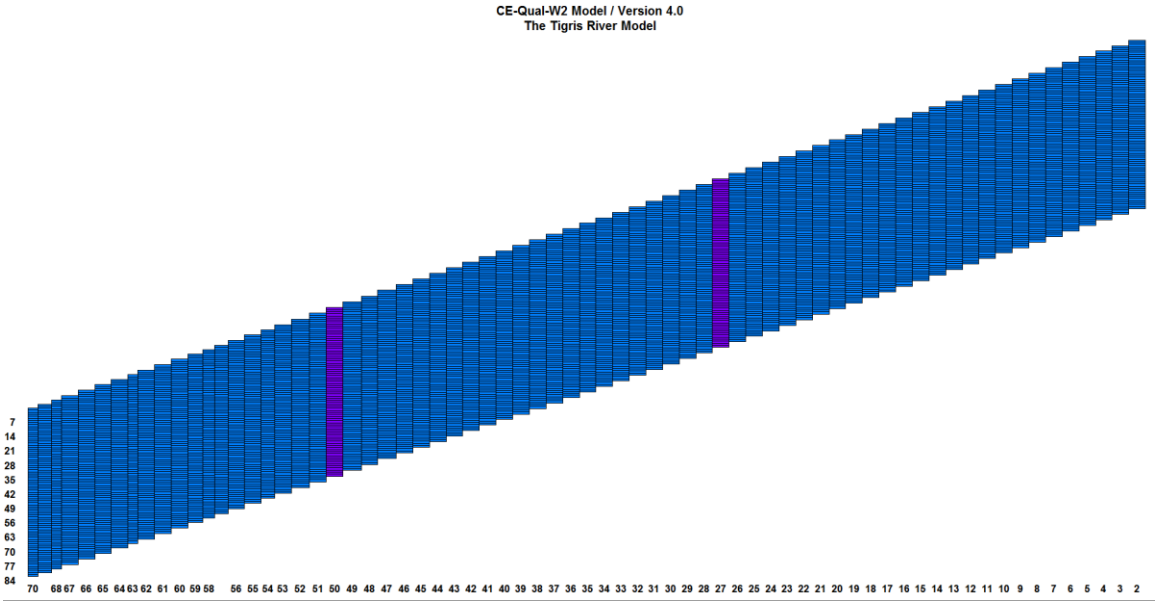

Figure 31: Longitudinal profile for waterbody 1, branch 1 of the Tigris River model constructed by the W2 model, Upper Zab and lower Zab at model segment 27 and 50 respectively with purple colors.

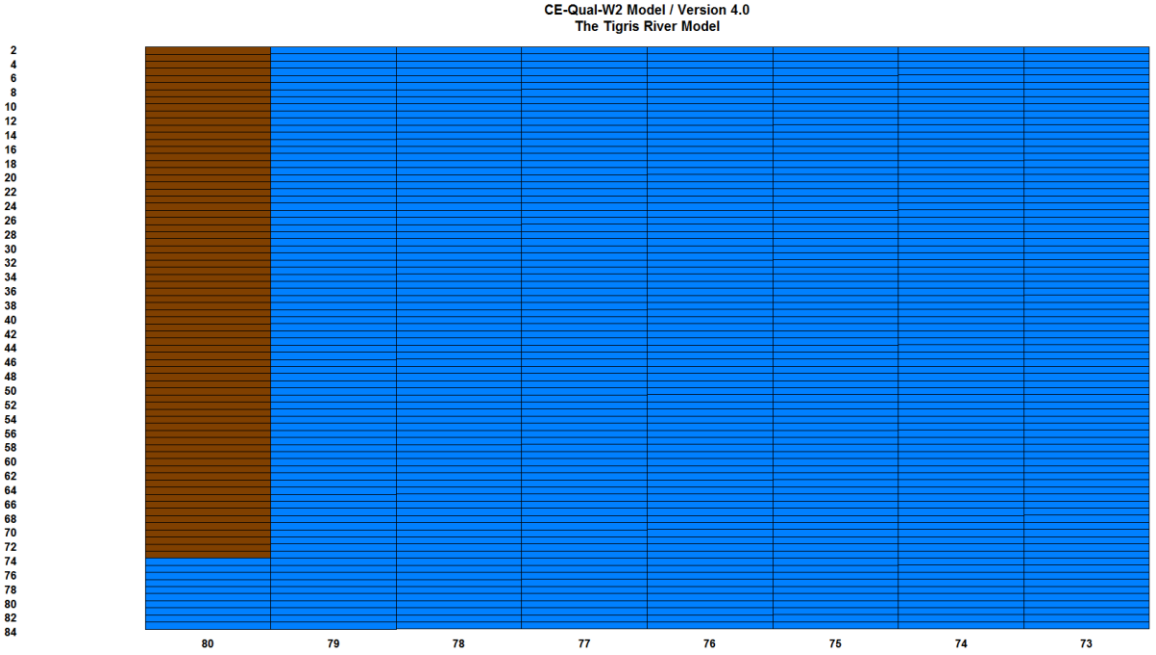

Figure 32: Longitudinal profile for waterbody 2, branch 2 of the Tigris River model constructed by the W2 model, Samarra Barrage at model segment 80 with a brown color.

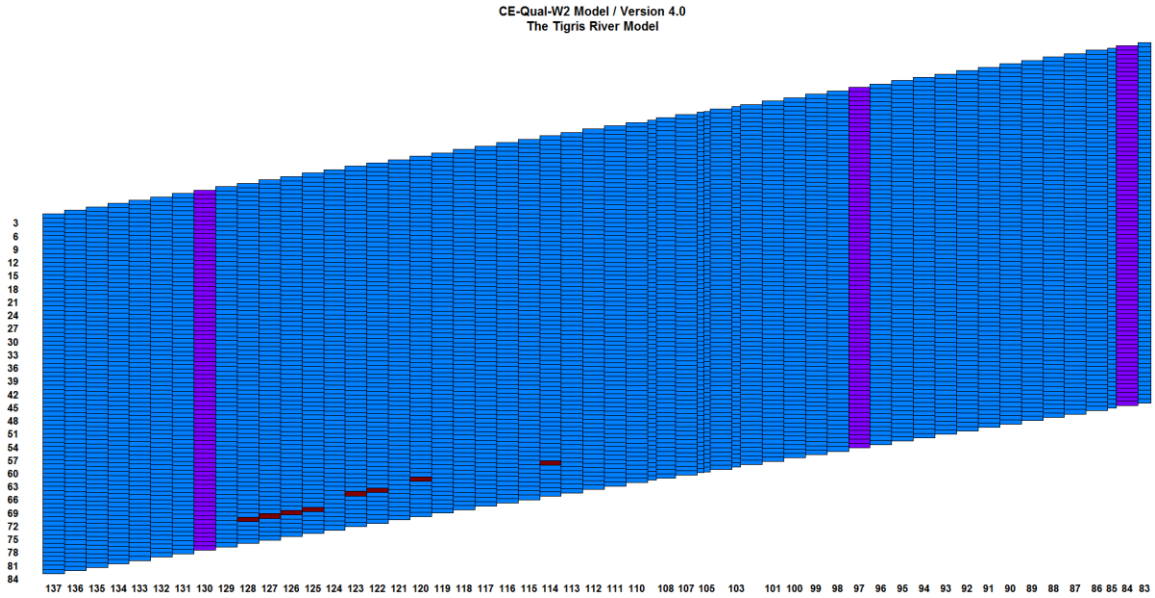

Figure 33: Longitudinal profile for waterbody 3, branch 3 of the Tigris River model constructed by the W2 model. Extra tributary at model segment 84. Audaim and Diyala Rivers at model segments 97 and 130 respectively with purple colors. Withdrawals represented in red colors.

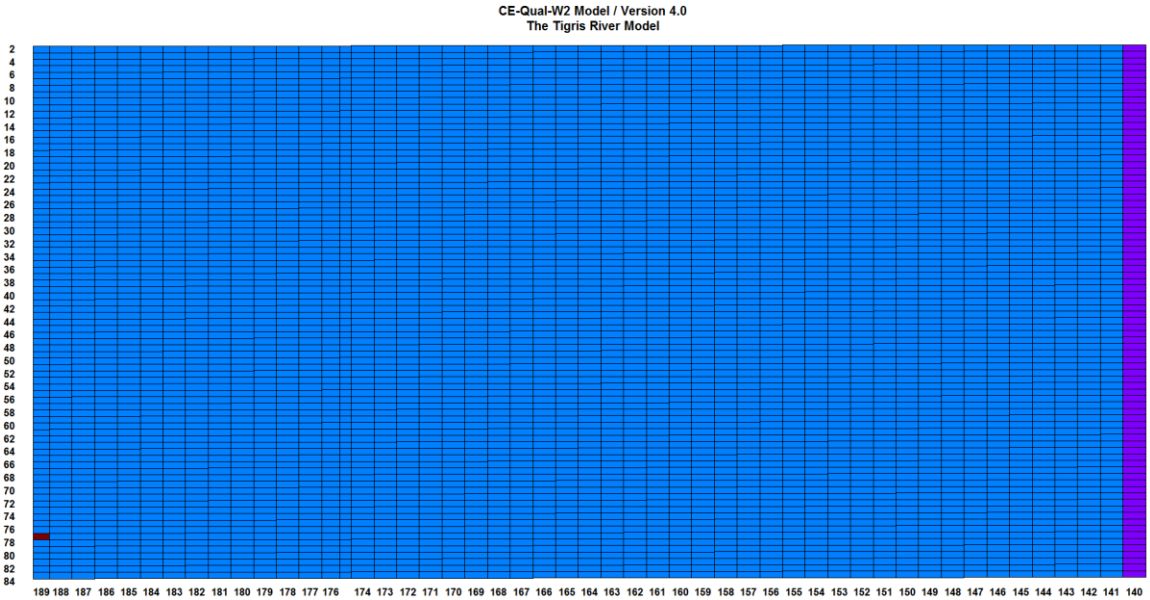

Figure 34: Longitudinal profile for waterbody 4, branch 4 of the Tigris River model constructed by the W2 model, an extra tributary at model segment 140 with a purple color.

Tharthar Lake Grid

The topographic map of Tharthar Lake showing the floor morphology was provided from Sissakian (2011) and shown in Figure 35. Arc map (GIS) was used to georeference this photo map with a base map and utilized to digitize and extract x and y coordinates of all contour lines at elevations 10 m, 25m, and 50 m. UTM 1984 Zone and datum GCS WGS 1984 was used to project Tharthar Lake's map in GIS. Digitized contour lines, shown in Figure 36, were used to develop the grid for Tharthar Lake. Surfer Version 8 (Golden Software) was used construct the lake's contour lines with minimum and maximum elevations of -5 m and 80 m, respectively, as shown in Figure 37. In addition, Surfer was used to create a set of polygons (Figure 38) to produce volume/area elevation curves. All polygons were adjusted to cover the entire lake's boundary. Figure 40 shows the side view of Tharthar Lake grid with its segments and layers constructed by the W2 model.

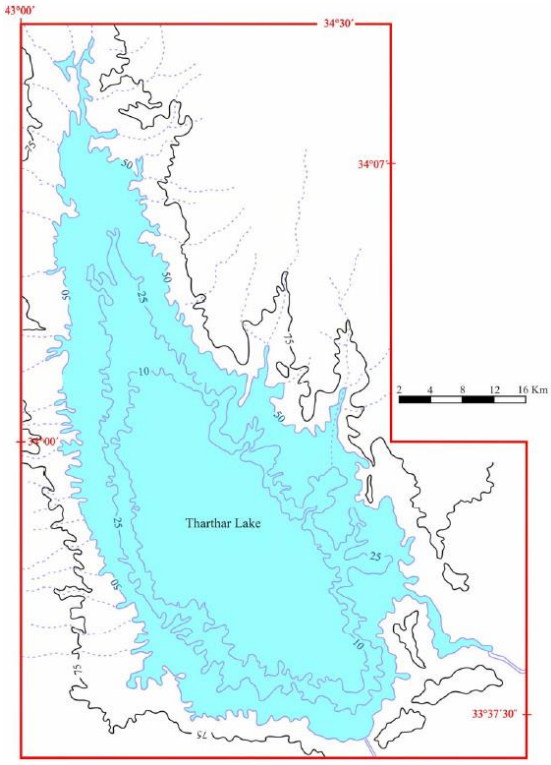

Figure 35: Topographic map of Tharthar Lake (Sissakian 2011).

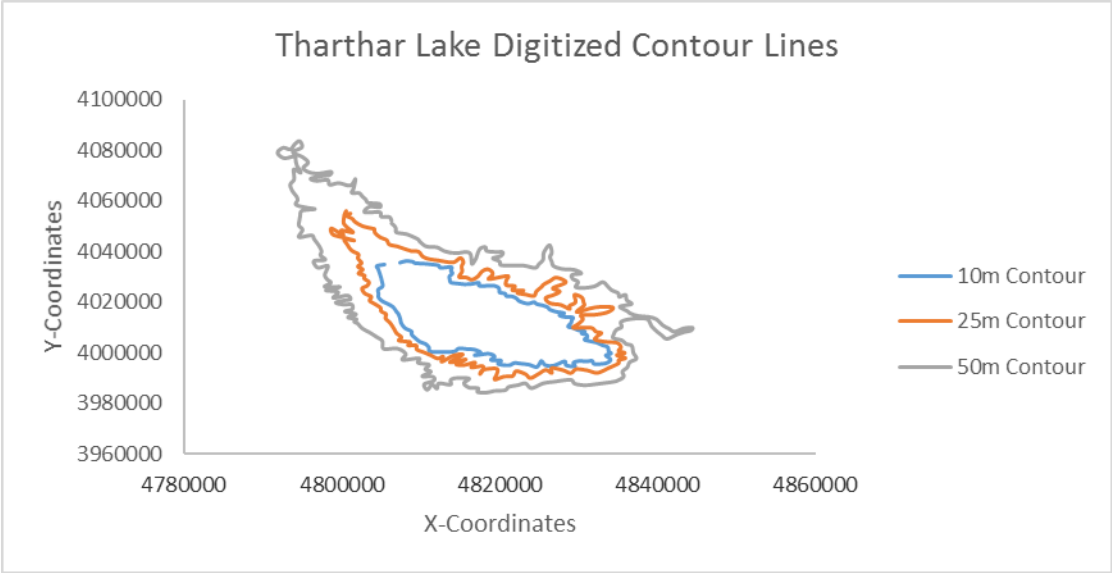

Figure 36: Tharthar Lake digitized contour lines.

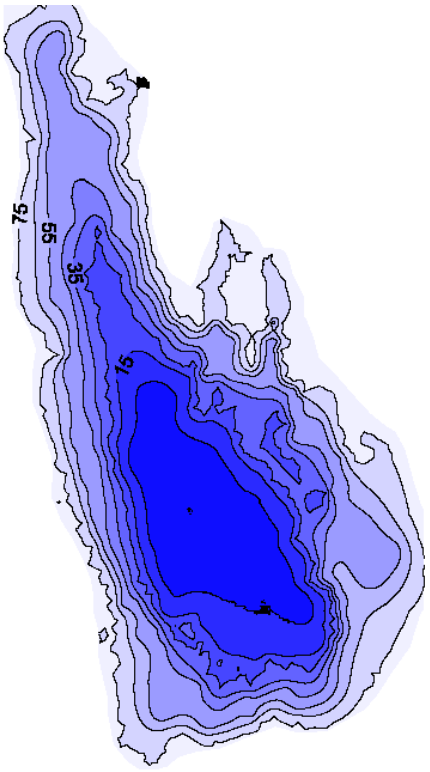

Figure 37: Constructing of contour lines in meters of Tharthar Lake constructed by Surfer.

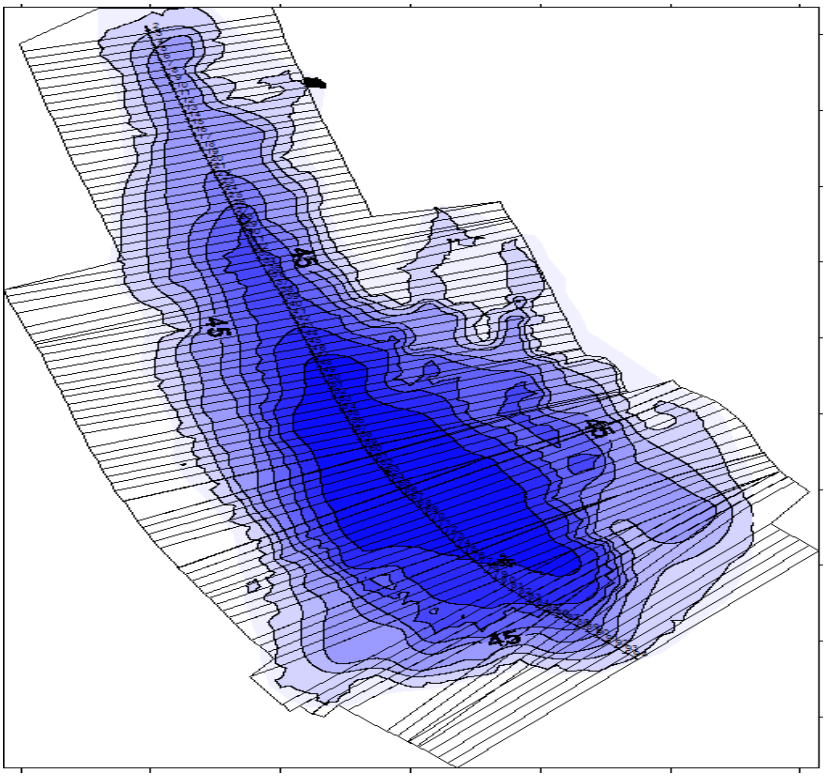

Figure 38: Model segments of Tharthar Lake created by Surfer.

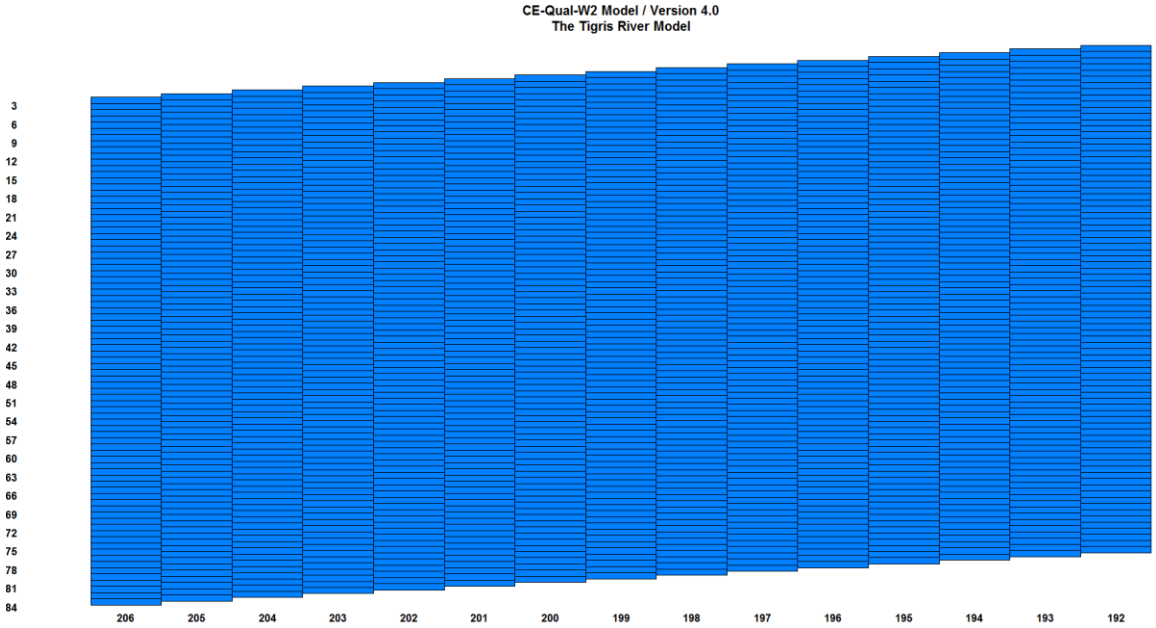

Figure 39: Longitudinal profile for waterbody 5, branch 5 (Tigris-Tharthar Canal) of the Tigris River model constructed by the W2 model (Cole and Wells, 2017).

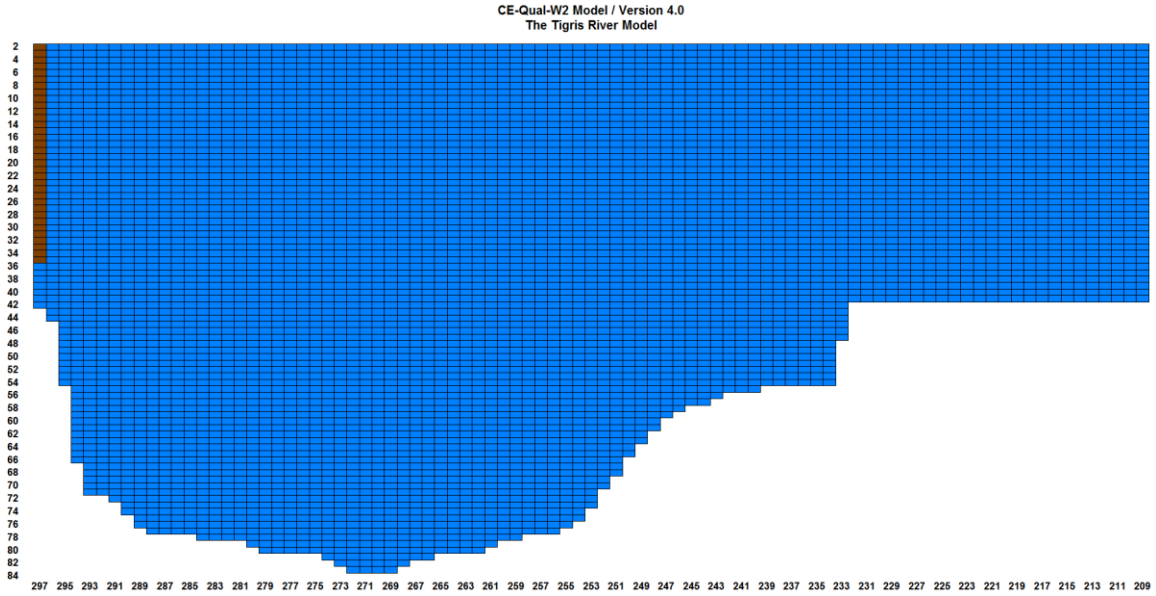

Figure 40: Model longitudinal profile of water body 6, branch 6 Tharthar Lake, including all segments and layers constructed by W2 model (Cole and Wells, 2017), the outlet of the lake at segment 297 with a brown color.

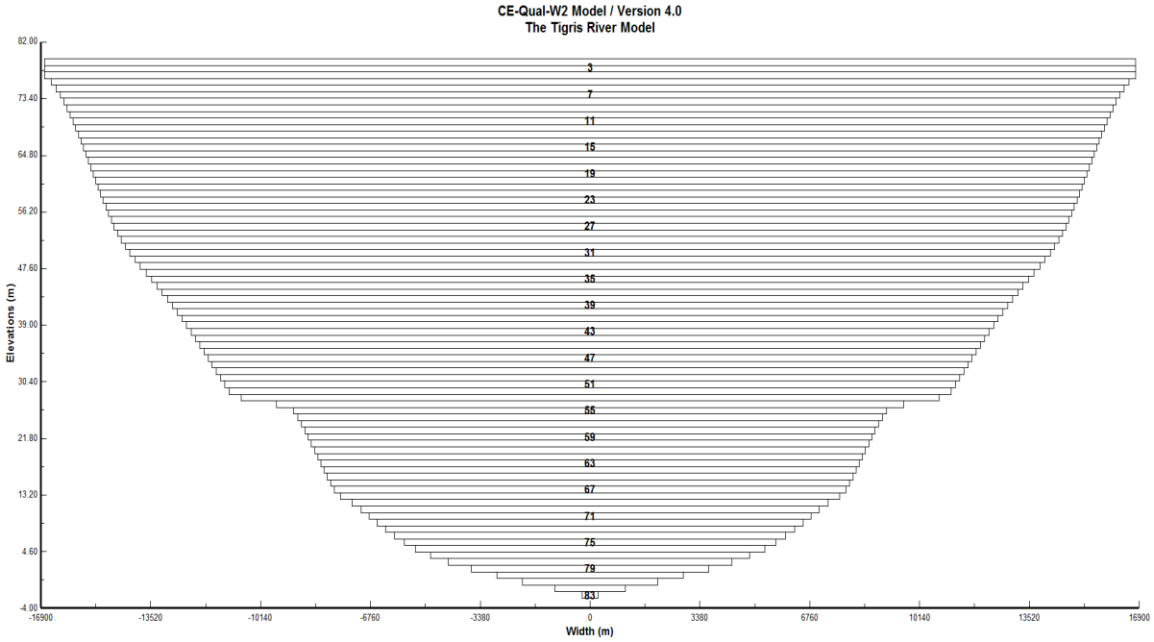

Figure 41: Model segment #270 section (Tharthar Lake) with 82 active layers (1 m each) constructed by the W2 model (Cole and Wells, 2017).

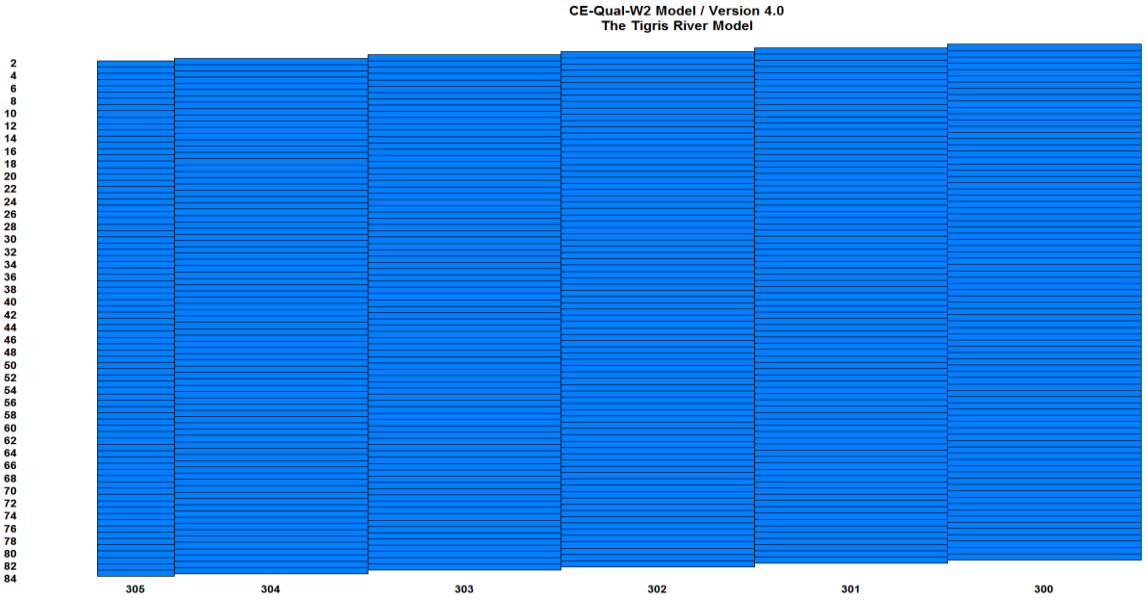

Figure 42: Longitudinal profile for waterbody 7, branch 7 (Tharthar Canal) of the Tigris River model constructed by the W2 model (Cole and Wells, 2017).

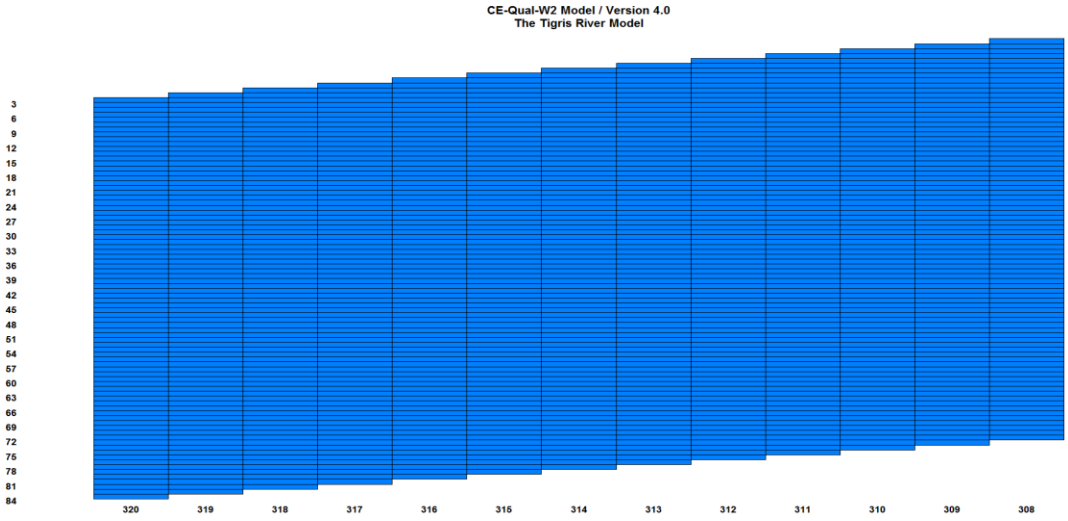

Figure 43: Longitudinal profile for waterbody 8, branch 8 (Tharthar-Tigris Canal) of the Tigris River model constructed by the W2 model (Cole and Wells, 2017).

In summary, Table 13 summarizes the model dimensions of all waterbodies and branches within the study area.

Table 13: Dimensions of all waterbodies and branches of the Tigris River System, DS: Downstream, B: Barrage

Water Body (Wb)	Branch (Br)	Starting Active Segment	Ending Active Segment	Branch Length (km)	Number of Segments	Number of Vertical layers	Details
Wb1	Br1	2	70	350	69	82	From Mosul Dam to 15 km DS Tikrit city
Wb2	Br2	73	80	40	8	82	From 15 km DS Tikrit city to Samarra B.
Wb3	Br3	83	137	256.5	55	82	From Samarra B. to 70 km DS Baghdad city
Wb4	Br4	140	189	233.5	50	82	From 70 km DS Baghdad city to Kut B.
Wb5	Br5	192	206	75	15	82	Tigris-Tharthar Canal
Wb6	Br6	209	297	90	89	82	Tharthar Lake
Wb7	Br7	300	305	27	6	82	Tharthar Arm
Wb8	Br8	308	320	65	13	82	Tharthar-Tigris Canal
Wb9	Br9	323	342	97	20	82	From Samarra B. to Tharthar Regulator

Meteorological Inputs

Meteorological data for the CE-QUAL-W2 model were obtained from the Iraqi Ministry of Transportation, the General Organization for Meteorology and Seismic Monitoring (MOT-IMOAS 2014). Data were provided in a frequency of four hours for the year 2009 at three main cities along the main stream of the Tigris River, more specifically at Mosul, Baeji, and Baghdad cities. The W2 model utilizes air and dew point temperature, wind speed and direction, and cloud cover or solar radiation. CE-QUAL-W2 has the capability to internally calculate solar radiation based on cloud cover data and latitude and longitude. Daily air temperature collected at Mosul, Samarra, and Baghdad cities was shown earlier in Figure 20 in chapter three. Daily dew-point temperature collected at Mosul, Samarra, and Baghdad cities is shown in Figure 44. Wind speed and direction data are also provided for the year 2009. Figure 45 shows daily wind speed, while Figure 46 show wind rose representations of wind direction at Baghdad city. Wind is mostly blowing from the North-West direction. Daily averaged cloud cover is plotted in Figure 47. Cloud cover is measured from zero (no cloud cover) to 10 (maximum cloud cover).

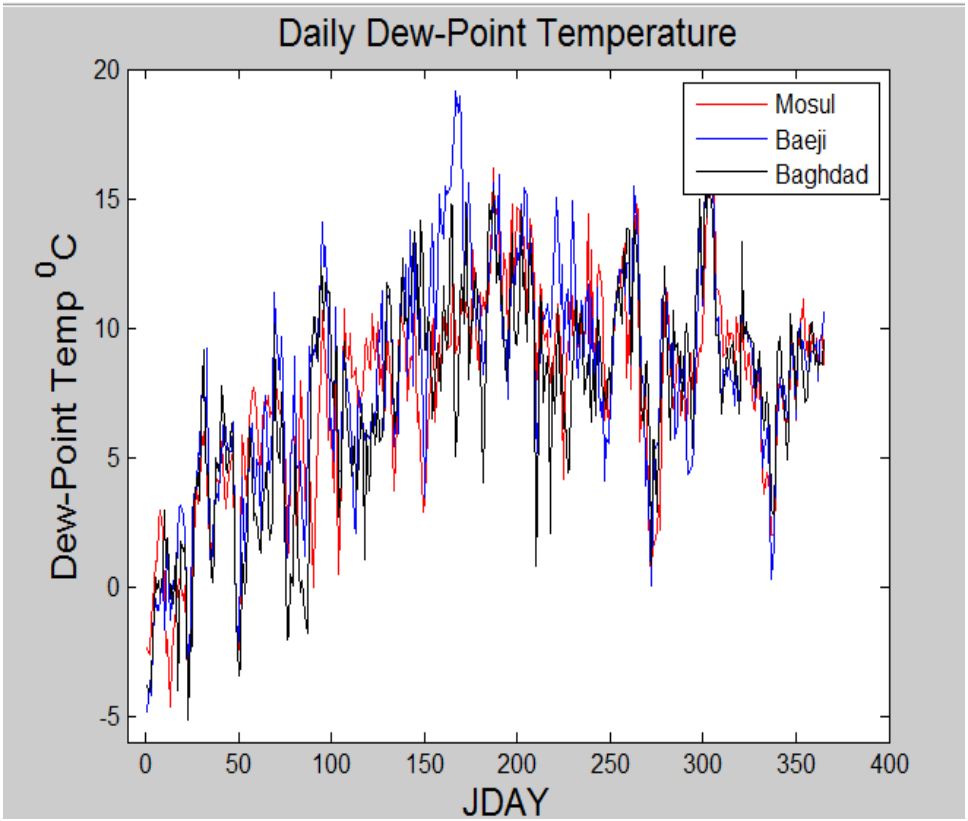

Figure 44: Daily dew-point temperature at Mosul, Baeji, and Baghdad cities (2009).

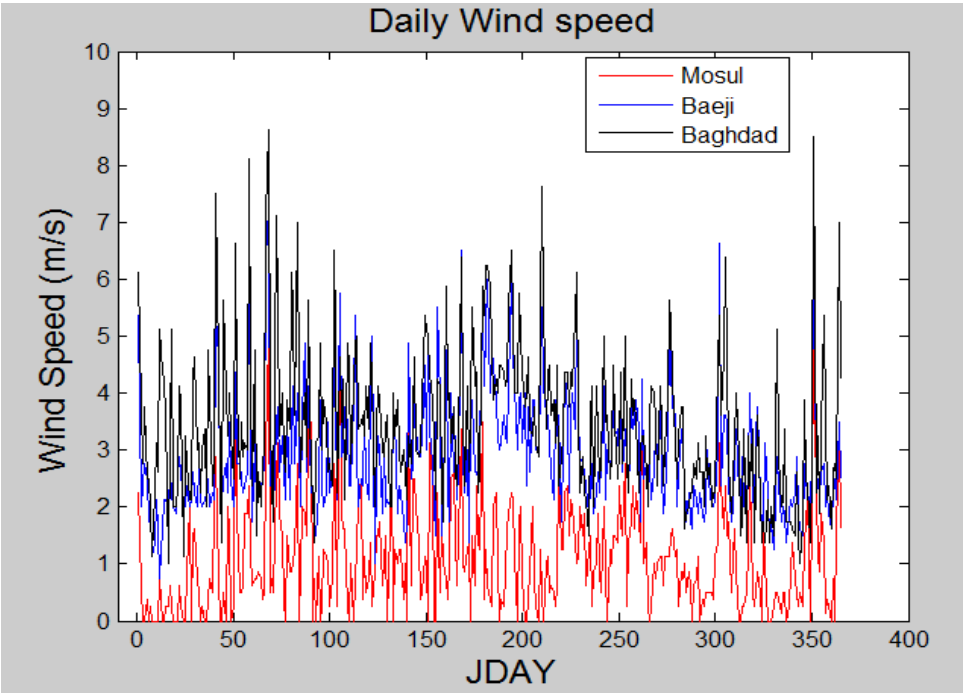

Figure 45: Daily wind speed at Mosul, Baeji, and Baghdad cities (2009).

Figure 46: Wind direction at Baghdad City (2009).

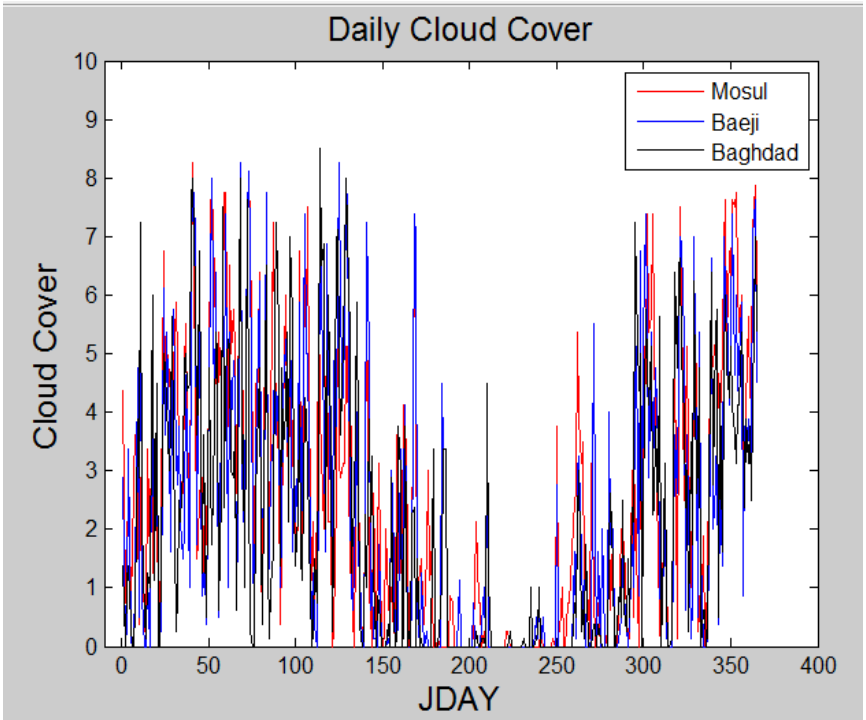

Figure 47: Daily cloud cover at Mosul, Baeji, and Baghdad cities (2009).

Flow Inputs

Daily flowrate and water level data were required for the entire model time period from January 1, 2009 to December 31, 2009 for upstream boundary conditions and calibration of the mainstem of the Tigris River model. These data were obtained at multiple monitoring stations from the Ministry of Water Resources (MWR) in Iraq for the year of 2009. Flowrate data were provided at Mosul Dam (Rkm 0), Beije city (Rkm 290), outflow from Samarra Barrage (Rkm 390), Baghdad City (Rkm 576.5), outflow from Kut Barrage (Rkm 880), and Tharthar-Euphrates canal. Water level data were provided at Baeji city, Samarra Barrage, and Baghdad city. Figure 48 shows daily flowrates of the mainstem of the Tigris River in 2009 at Mosul Dam, Baeji city, Samarra Barrage, Baghdad city, and Kut Barrage. Unfortunately, flowrate data for the Tigris River main tributaries, Upper Zab and Lower Zab Rivers, were unavailable at the Ministry of Water Resources (MWR) in Iraq for the

modeled year. However, flowrates at theses tributaries were estimated by computing the flow difference between Mosul Dam station and Baeji city station since these tributaries are located between these two stations. 80% of this flow difference was from the Upper Zab River and 20% from the Lower Zab River according to CSO (2010) as shown in Figure 49. Monthly average flowrates of Diyala River were constructed from the Environment statistical report (CSO, 2010). In addition, daily flowrate of Audaim River, located 68 km downstream Samarra Barrage, was also obtained from the Ministry of Water Resources (MWR) in Iraq for the year of 2009.

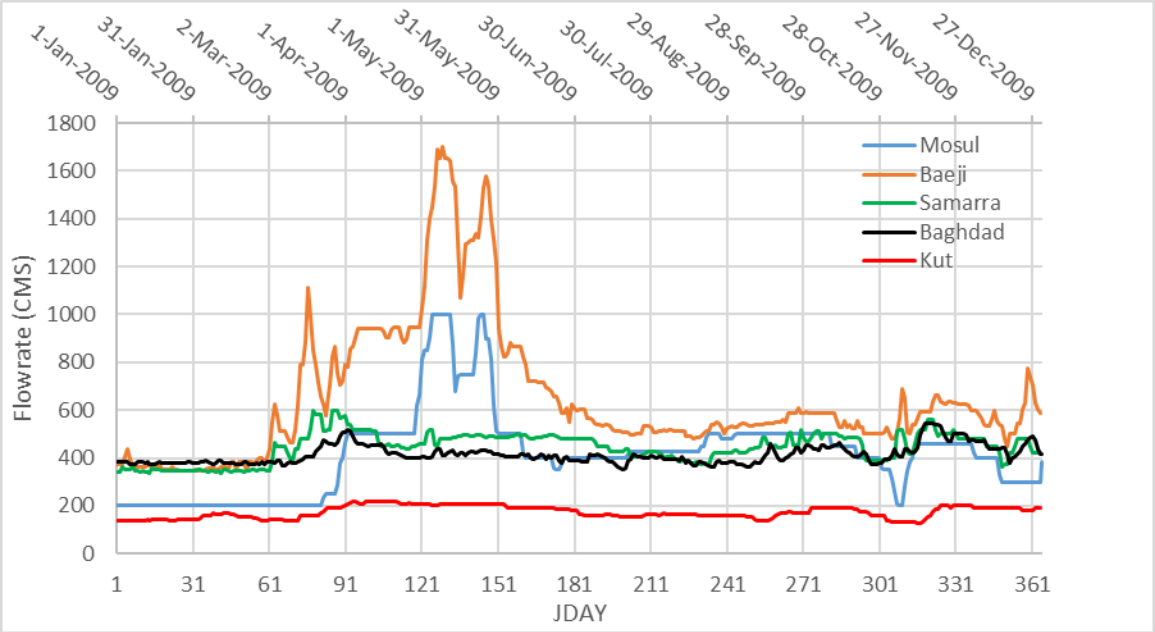

Figure 48: Daily flowrates of the Tigris River in 2009 at Mosul Dam, Baeji city, Samarra Barrage, Baghdad city, and Kut Barrage.

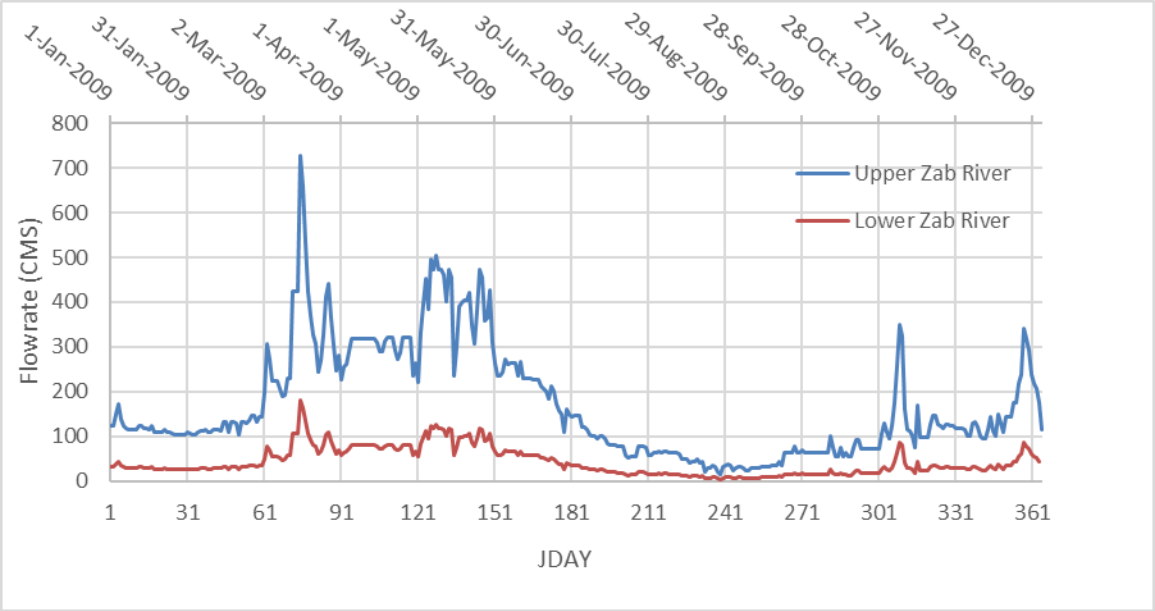

Figure 49: Daily flowrates of the Upper and Lower Zab Rivers in 2009.

Figure 50 shows the main sources of waters that feed the Tigris River in Iraq for the year 2009 (CSO, 2010). The Upper Zab River is the biggest contributor compared with all tributaries of the Tigris River, while Audaim River has no significant impact on the Tigris River flow. With no dams, the Upper Zab River is an uncontrolled tributary. The Ministry of Water Resources had planned to build Bekhme Dam on the Upper Zab tributary, but this project has not been implemented due to wars.

Water is withdrawn from the mainstem of the Tigris River to supply eight water treatment plants located on both banks along the mainstem of the Tigris River within Baghdad city. These withdrawals were specified in the model according to the produced capacity of each treatment plant in the year 2009 as listed previously in Table 2. Other inflows, such as precipitation, flowrate from wastewater treatment plants (WWTPs), agricultural return

flows, and flowrate of groundwater, were unavailable but were accounted for within the distributed tributary for each waterbody in the Tigris River model.

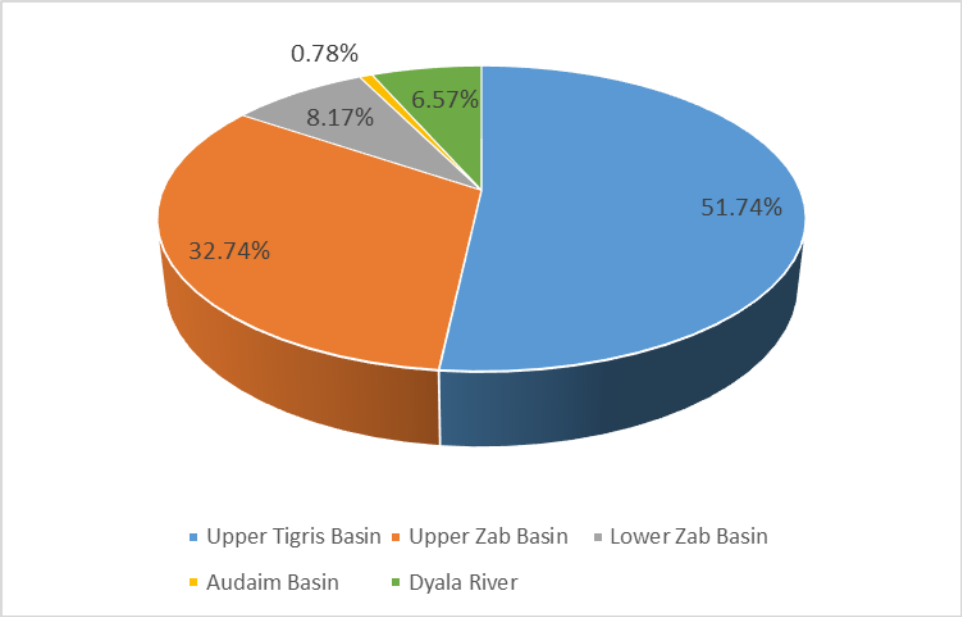

Figure 50: Water sources of the Tigris River in Iraq for the year 2009 (CSO, 2010).

Spillways

Spillways were added at the end of some branches in the Tigris River model to ensure smooth transition of water between branches. Crest elevations and other used-defined parameters affected the way water moved over the spillway. Generally, most spillways were set so that a spillway's crest was located on the bottom elevation of the channel. Spillways follow power functions for both free flowing and submerged conditions as described in Equation 10 and Equation 11, respectively (Cole and Wells, 2017):

Equation 10: Free flow conditions

$$Q = \alpha_1 \Delta h^{\beta_1}$$

Equation 11: submerged conditions

$$Q = \alpha_2 \Delta h^{\beta_2}$$

where:

α1 and β1 are empirical coefficients

α2 and β2 are empirical coefficients

Δh is the difference between the upstream head and spillway crest elevation (Free flow).

Δh is the difference between the upstream head and downstream head (Submerged flow).

α_1 was calculated by using the equation for a broad crested weir as described in Equation 12 (Cole and Wells, 2017):

Equation 12: Broad crested weir

$$\alpha_1 = C_D C_v \frac{2}{3}\sqrt{2g}W$$

where:

C_D: A discharge coefficient (0.84 to 1.06)

C_v: A velocity coefficient (1.0 to 1.2)

g: gravitational acceleration

W: channel width

α_2 could be calculated from α_1 and following the mathematics outlined in the CE-QUAL-W2 user manual (Cole and Wells, 2017), at a given flow value Q, Equation 10 and Equation 11 can be combined to solve for α_2 as described in Equation *13*:

Equation 13:

$$\alpha_2 = \frac{\alpha_1 (H_1 - H_{weir})^{\beta_1 - \beta_2}}{0.33^{\beta_2}}$$

Assuming an equal value for both β1 and β2, α_2 could be rewritten as:

$$\alpha_2 = \frac{\alpha_1}{0.33^{\beta_2}}$$

All spillway coefficients were defined based on above detailed analysis. Figure 51 shows a schematic diagram for water and spillway elevations used in spillway equations. Both C_D and C_v coefficients were assumed 1, while W, channel width, was estimated based on the average width of the bottom three layers of the segment where spillways were located. Table 14 lists the location of all spillways in the Tigris River system with weir coefficients.

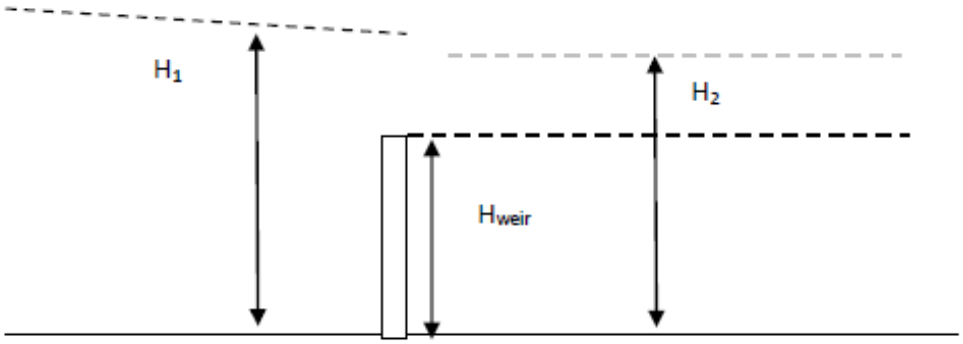

Figure 51: Schematic diagram of water and spillway elevations for free flowing and submerged weir used in spillway analysis (Cole and Wells, 2017).

Table 14: Spillway specifications in the Tigris River System.

Spillway #	Branch (Br)	US Segment	DS Segment	Spill Elevation (m)	α1	β1=β2	α2	Description
1	5	206	278	46	81	1.5	427.18	From Tigris-Tharthar canal to Tharthar lake
2	9	342	0	45.5	68.2	1.5	359.7	From Erwaeiya canal to the Euphrates River
3	8	320	119	31	36.14	1.5	190.65	From Tharthar-Tigris canal to the Tigris River upstream Baghdad city
4	7	305	0	42	68.2	1.5	359.7	From Tharthar Arm to the Euphrates River
5	4	189	0	17	627.4	1.5	3309.54	From Kut Barrage to downstream of the Tigris River below Kut city
6	2	80	323	68.5	2045.78	1.5	10791.9	From Samarra Barrage to Erwaeiya canal

Temperature Inputs

Temperature data were required for the entire model time period for all input flows. Daily water temperature data were estimated remotely from Landsat for the boundary conditions at Mosul Dam (Rkm 0). The Landsat data were used to provide in-river temperatures that were used for calibration at both Baeji city and Baghdad city. For Upper and Lower Zab tributaries where no data were available, the input temperature files were developed based on the statistical model developed to estimate water temperatures at Baeji city, while water temperatures for both Audaim and Diyala tributaries were estimated based on the statistical model developed to estimate water temperature at Baghdad city.

A 95% confidence interval, Equation 14, was estimated for remotely sensed water temperatures at both Baeji and Baghdad cities as shown in Figure 52 and Figure 53, respectively. Since there were no field data of water temperature for the year 2009 to compare with the modeled temperature data, the goal of model calibration will be to ensure that the model predictions of water temperature lie within the upper and lower limits of the confidence interval.

Equation 14: Estimation of 95% confidence interval

$$95\%\ CI = T_w \pm t_{n-2} * S_y \sqrt{\frac{1}{n} + \frac{(T_a - \mu)^2}{(n-1){S_x}^2}}$$

where:

T_w: Water temperature estimated from statistical models
T_a: 5 days weighed air temperature
S_y: Standard error
S_x: Variance (square of standard deviation)
n: Sample's number
μ: Average air temperature of the sample
t: tabulated values based on degree of freedom (n-2)

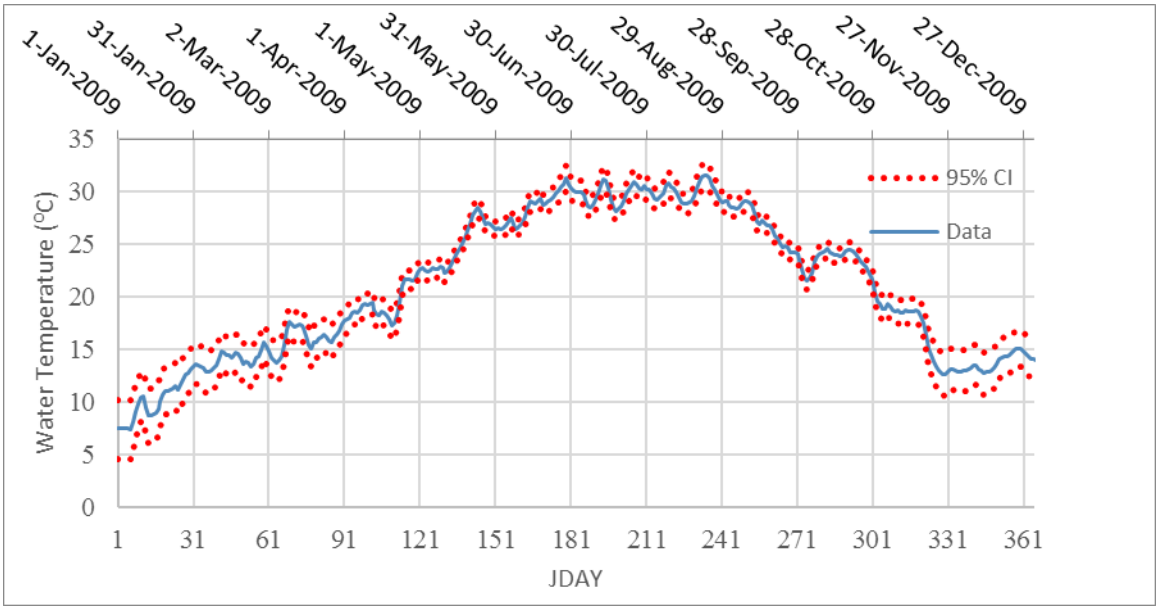

Figure 52: Daily surface water temperature of the Tigris River at Baeji City with 95% CI.

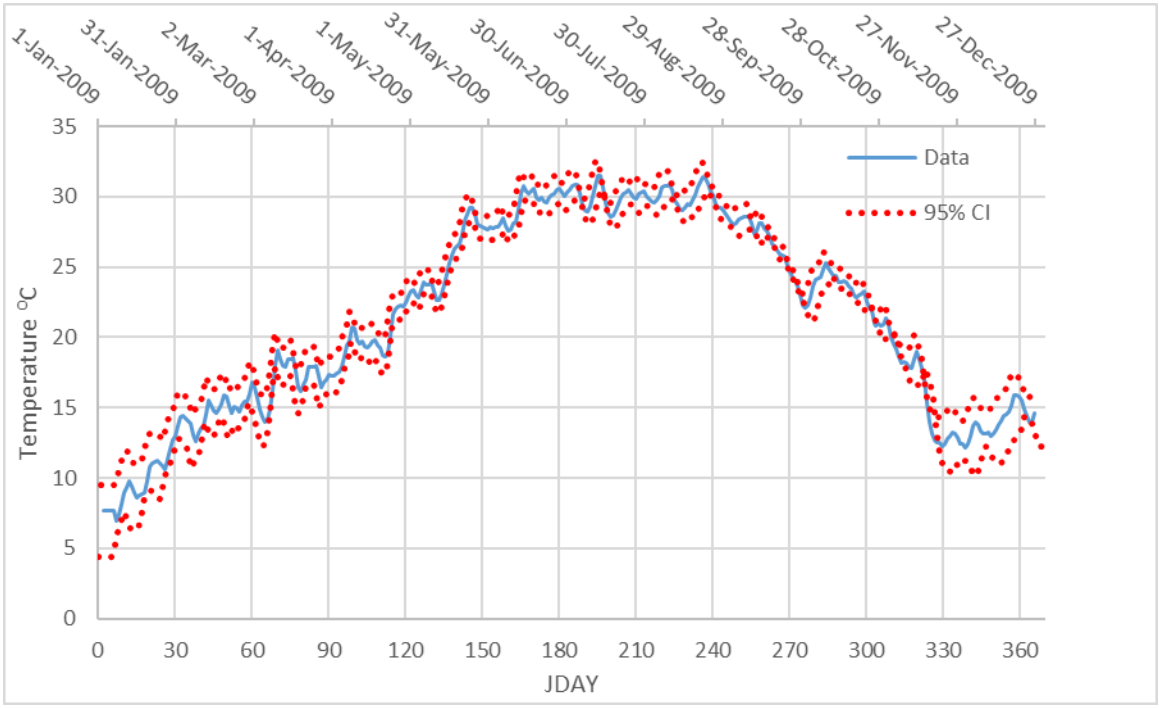

Figure 53: Daily surface water temperature of the Tigris River at Baghdad City with 95% CI.

Constituents Inputs

Water quality state variables modeled were:

- Total dissolved solids (TDS)
- Phosphate (PO4)
- Ammonia (NH3)
- Nitrates (NO3)
- Labile dissolved organic matter (LDOM)
- Refractory dissolved organic matter (RDOM)
- Labile particulate organic matter (LPOM)
- Refractory particulate organic matter (RPOM)
- Biochemical oxygen demand (BOD)
- Biochemical oxygen demand as phosphorus (BOD-P)
- Biochemical oxygen demand as nitrogen (BOD-N)
- Algae
- Dissolved oxygen (DO)

Data were needed for the entire simulation time for all input concentrations, but unfortunately only monthly averaged data of total dissolved solids (TDS) and nitrate (NO3) were available from the Iraqi Water Resources Ministry for the mainstem of the Tigris River. Monthly averaged field data of TDS were provided for Audaim and Diyala tributaries and for four stations along the mainstem of the Tigris River at Mosul Dam, Samarra Barrage, Baghdad City, and Kut Barrage. TDS concentrations for the Upper Zab and the Lower Zab tributaries were assumed as the same TDS concentrations as in Samarra city. Rahi & Halihan (2010), showed that TDS concentration in Tharthar Lake was 1500 mg/l in the year 2003. The initial condition of TDS in Tharthar Lake was assumed 1300 mg/l.

Field data of NO3 were provided at two stations along the mainstem of the Tigris River at Samarra Barrage and Baghdad City. Field data for NO3 at Mosul Dam were estimated from literature values measured in previous years.

Other modeled water quality constituents were phosphate (PO4), ammonia (NH3), biochemical oxygen demand (BOD), algae, and dissolved oxygen (DO). Field data of these constituents were estimated from literature values. Table 15 lists field data of water quality constituents extracted from literature studies.

Table 15: Water Quality field data extracted from literatures and used for boundary conditions at Mosul Dam and downstream model calibration at Baghdad City; WWTPs: Wastewater treatment plants.

Location	**Data Available**	**Data year**	**Reference**
Mosul Dam	DO, PO4, NO3	Aug 1986-Aug1987	Al-Layla et al., 1990
Lower Zab / Tikrit City	BOD	Jan-Sep 2004	Al-Jebouri and Edham (2012)
Lower Zab	DO, PO4, NO3	Nov2001-Oct2002	Abdul Jabar et al., (2008)
Diyal River	BOD	Oct (2002)-March (2003)	Husain Amal (2009)
Baghdad City	BOD	Feb, May, Aug, Oct (2009)	Rabee et al., (2011)
Baghdad City	PO4	Feb, May, Aug, Oct (2009)	Rabee et al., (2011)
WWTPs in Tikrit and Baghdad cities	PO4, NH4	Iraqi wastewater standards for effluents	Aziz and Aws, (2012)

Water quality conversions were made for field data in order to estimate the state variables modeled with CE-QUAL-W2 model. Due to limitations in water quality field data of the Tigris River, estimates were made for missing data of a given state variable as indicated below:

- TDS concentrations for the Upper Zap and the Lower Zab tributaries were assumed as the same TDS concentrations at Mosul and Samarra cities, respectively, while TDS concentrations for Audaim and Diyala tributaries were provided from the Ministry of Water Resources in Iraq.
- PO4 for input flows at Mosul Dam were assumed from PO4 field data provided by Al-Layla et al., 1990.
- NH3 concentrations for all input flows were assumed 0.1 mg/l with exception to NH3 concentration of the discharged wastewater at Tikirt city that were assumed 1 mg/l.
- NO3 for input flows at Mosul Dam were assumed 1.5 mg/l from January 1st to June 30th (due to high downstream NO3 concentration at Samarra Barrage and Baghdad city). NO3 data from July 1st to December 31st were assumed from field data provided by Al-Layla et al., 1990.
- LDOM, RDOM, LPOM, and RPOM were assumed zero for all input flows.
- BOD5 field data were converted to ultimate BOD (BOD_U), the following typical relationship was used (Cole and Wells, 2017) assuming a BOD decay rate of 0.1 day^{-1}:

$$BOD_u = 2.54 \times BOD_5$$

- BOD concentrations in the Lower Zab tributaries were assumed from BOD field data provided by Al-Jebouri and Edham (2012). Same BOD data were used for BOD of the Upper Zab. BOD concentrations in Audaim tributary were assumed as BOD field data in Baghdad city provided by Rabee et al., (2011), while BOD concentrations in Diyala River were assumed from BOD field data provided by Husain Amal (2009).
- BOD-P for all input flows were assumed 0.01 of BOD_u
- BOD-N for all input flows were assumed 0.08 of BOD_u
- Algae concentration was assumed 0.05 mg/l for all input flows.
- DO concentration for upstream boundary conditions was assumed as 90% of the saturation oxygen O_s which was determined from the following equation (APHA 1992):

$$lnO_s = -139.34411 + \frac{1.575701\times10^5}{T_a} - \frac{6.642308\times10^7}{T_a^2} + \frac{1.2438\times10^{10}}{T_a^3} - \frac{8.621949\times10^{11}}{T_a^4}$$

where:

O_s: Saturation concentration of dissolved oxygen in fresh water at 1 atm mg/l

T_a: absolute temperature (K), $T_a = T + 273.15$

T: water temperature (° C)

- DO Concentrations for Upper Zap, Lower Zab, and Diyala River were assumed as the same DO concentration at Mosul city, Baeji city, and Baghdad city, respectively.

Figure 54, Figure 55, and Figure 56 show field data used for boundary conditions of the Tigris River model at Mosul Dam for TDS, PO4, NH4, NO3, BODu, and DO. Except for TDS, other input constituent field data for both Upper Zab and Lower Zab Rivers were assumed the same, while other input constituent field data for both Audaim and Diyala Rivers were assumed the same as well.

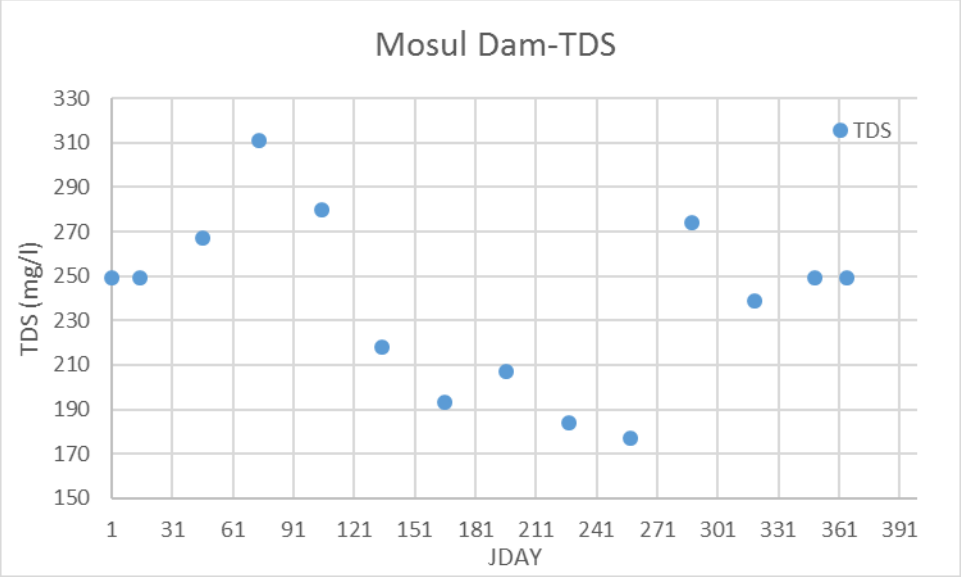

Figure 54: Input field data of TDS concentration for boundary conditions at Mosul Dam.

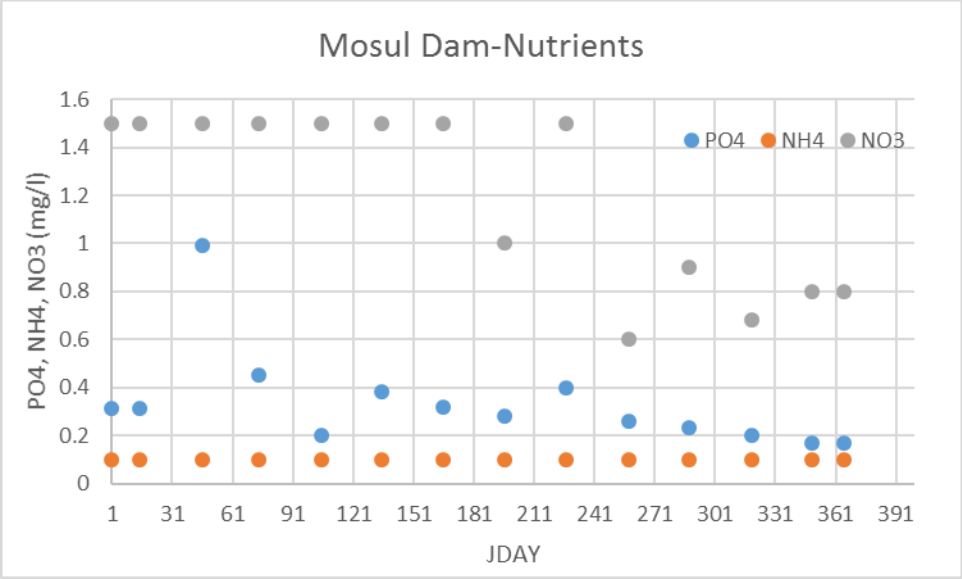

Figure 55: Estimated concentrations of PO4, NH4, and NO3 for boundary conditions at Mosul Dam.

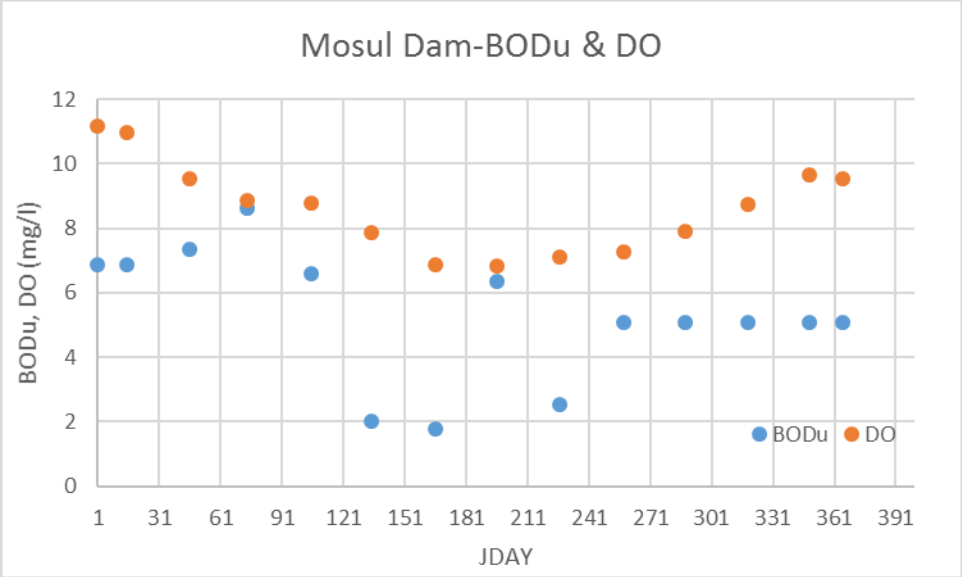

Figure 56: Estimated BODu and DO concentrations for boundary conditions at Mosul Dam

Chapter Six: The Tigris River Model Calibration

In this chapter, the calibration of the Tigris River model is described. Model predictions compared to field data included flow and water level at both Tharthar Lake and the mainstem of the Tigris River, water temperature, and water quality constituents such as total dissolved solids (TDS), phosphate (PO4), ammonia (NH4), nitrate (NO3), carbonaceous oxygen demand (CBOD), dissolve oxygen (DO), and chlorophyll-a (Chl-a).

Model Calibration: Flow-Tharthar Lake

According to the report of environmental statistics in Iraq (CSO, 2010), the water level of Tharthar Lake dropped from 45.75 m in October 2008 to 44 m in October 2009. Therefore, the initial condition of the lake's water level was assumed to be 45.5 m at the beginning of the model simulation in January 1st, 2009.

Figure 57 shows the model simulation of the water level at Tharthar Lake comparing it to the only 1 data point on October 2009. Figure 58 shows flowrates in both Tigris-Tharthar canal and Tharthar-Tigris canal for the model year 2009. The water level significantly increased in May due to a large volume of fresh water diverted through Tigris-Tharthar canal. The outflow from Tharthar Lake was diverted to both the Euphrates River through Tharthar-Euphrates canal and to the Tigris River through Tharthar-Tigris canal. Flowrates through the Tharthar-Tigris canal were assumed, while the excess lake's water was diverted to the Euphrates River.

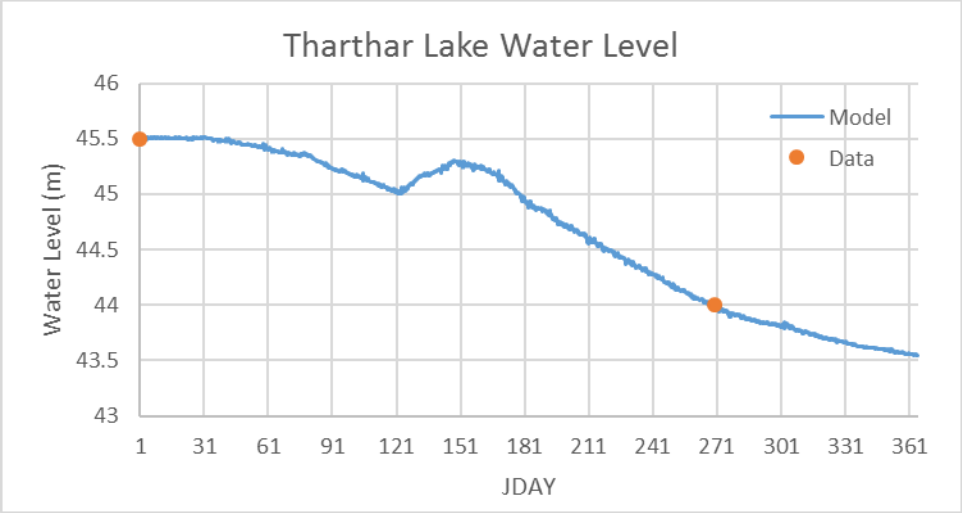

Figure 57: Model and data of the water level of Tharthar Lake in 2009.

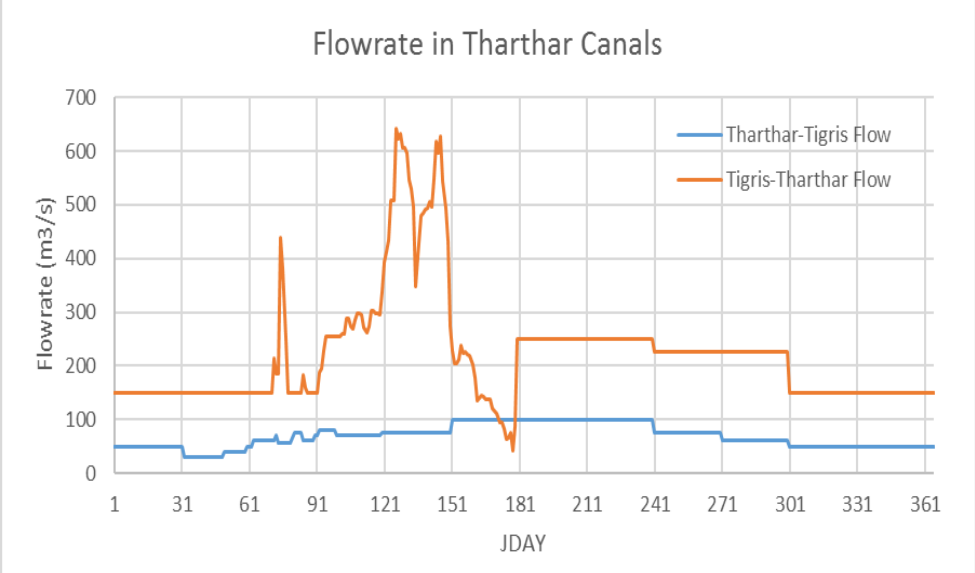

Figure 58: Model flowrate in Tharthar Lake canals in 2009.

Evaporation in Tharthar Lake

According to CSO (2010), the annual evaporation in Haditha Dam, 60 km northwest Tharthar Lake, was 2.27 m during the water year 2008-2009. Using default values for [AFW] and [BFW] evaporation coefficients in the wind speed formulation in the control file of the Tigris River model, model predictions of evaporation in Tharthar Lake was 2.2 m for the simulated year 2009. Figure 59 shows model flow balance in Tharthar Lake. As evaporation rates increase in the Tharthar Lake, the lake becomes more concentrated with high TDS concentrations causing more water quality issues as water diverts from the lake to both the Tigris and the Euphrates Rivers.

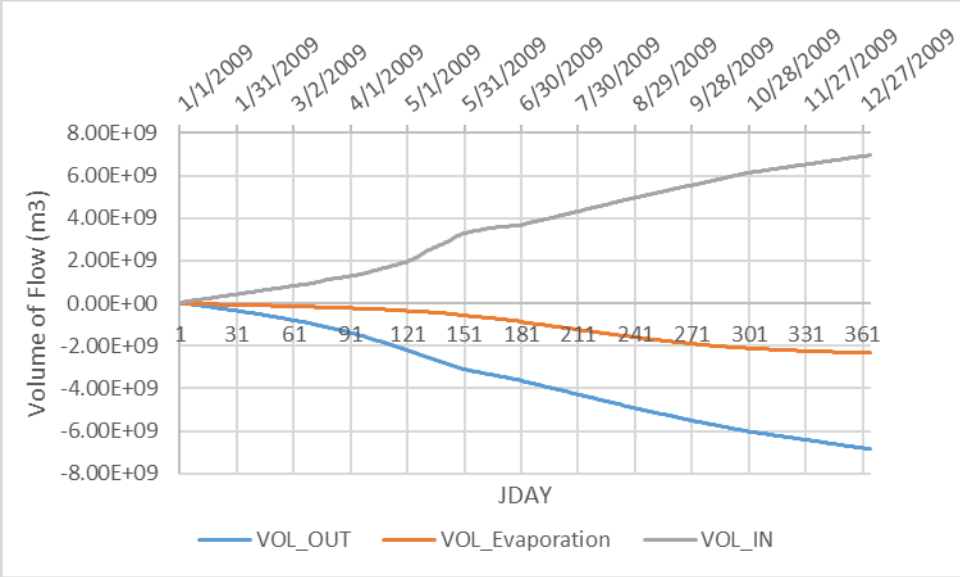

Figure 59: Flow balance in Tharthar Lake.

Model Calibration: Flow in the Tigris River

The model calibration of flowrate started at the upstream portions of the model and moved downstream comparing model predictions of flow and water level to field data of flow and water level along the mainstem of the Tigris River. Field data were provided by the Iraqi Ministry of Water Resources and were used for model-data comparisons during the model simulation year 2009. Calibration of flow and water level were done at Baeji city, Samarra Barrage, and Baghdad city. Flow calibration process is based on adding or subtracting flow through a distributed tributary. A distributed tributary accounts for ungaged inflows during storm events or outflow from the system such as numerous ungaged irrigation withdrawals along the river banks. This is done through multiple iterations until model predicted flows agree with field data. Figure 60 through Figure 65 show comparisons of model predictions and field data for flowrate and water level at Baeji city, Samarra Barrage, and Baghdad city, respectively.

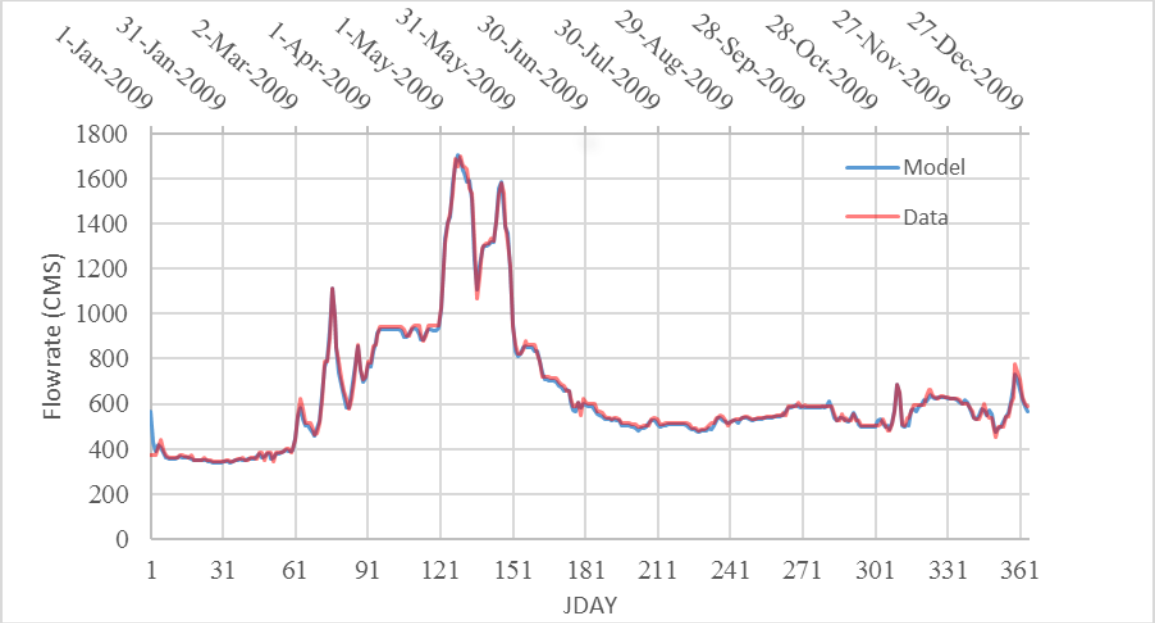

Figure 60: Model flowrate predictions compared to the Tigris River field data at Baeji city (segment 54).

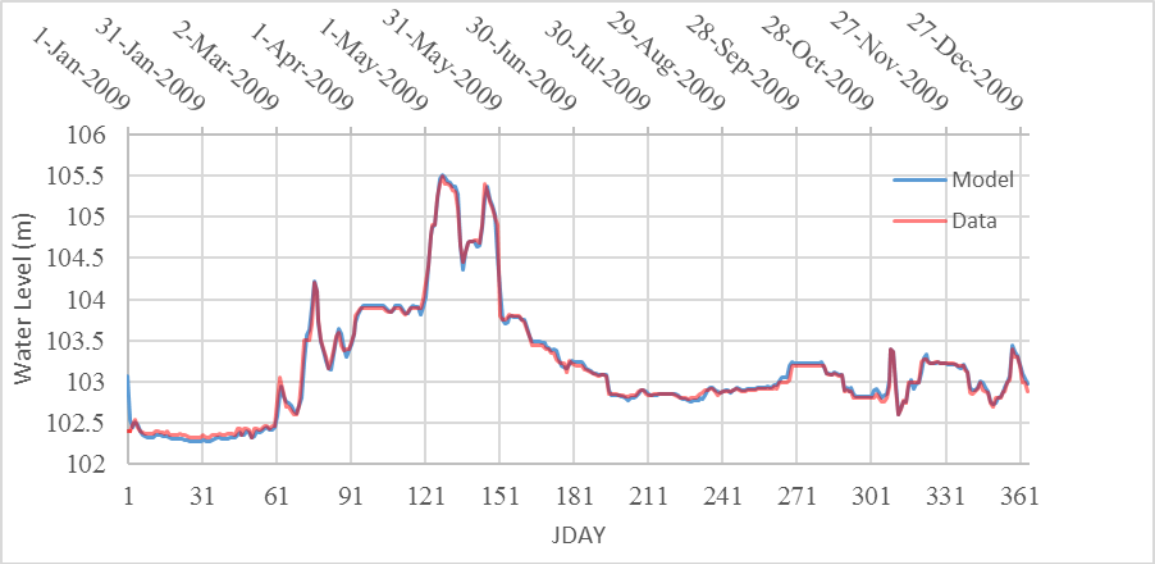

Figure 61: Model water level predictions compared to the Tigris River field data at Baeji city (segment 54).

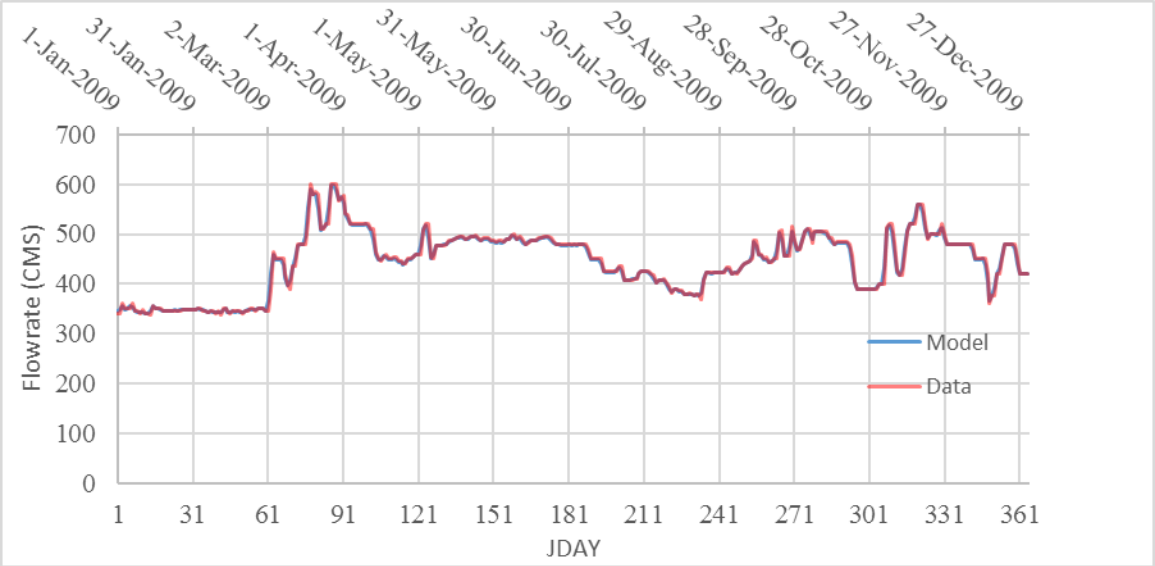

Figure 62: Model flowrate predictions compared to the Tigris River field data at Samarra Barrage (segment 83).

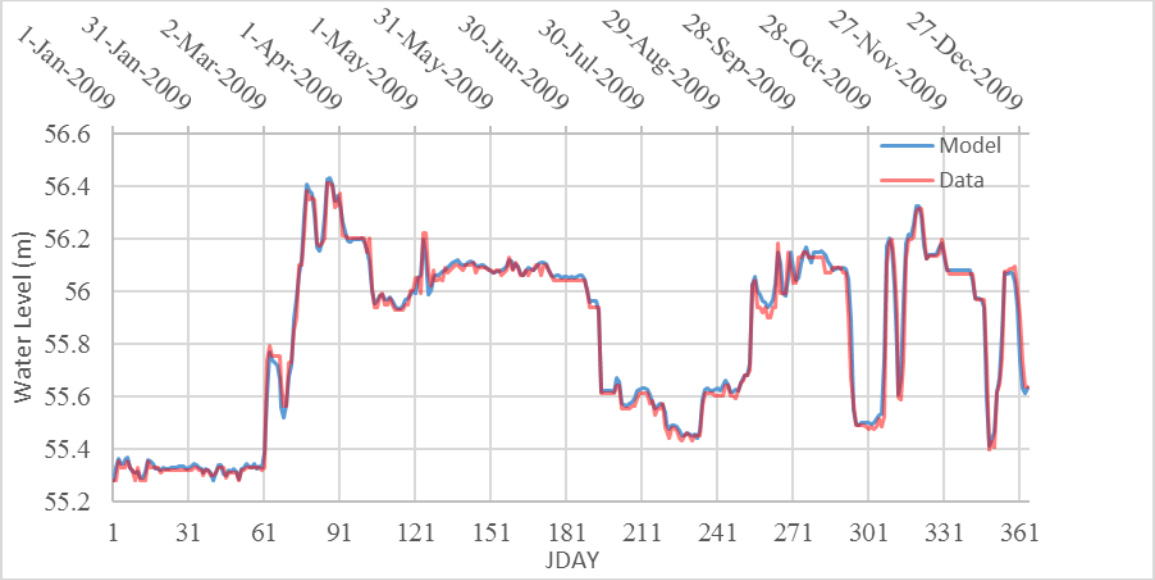

Figure 63: Model water level predictions compared to the Tigris River field data at Samarra Barrage (segment 83).

Figure 64: Model flowrate predictions compared to the Tigris River field data at Baghdad City (segment 123).

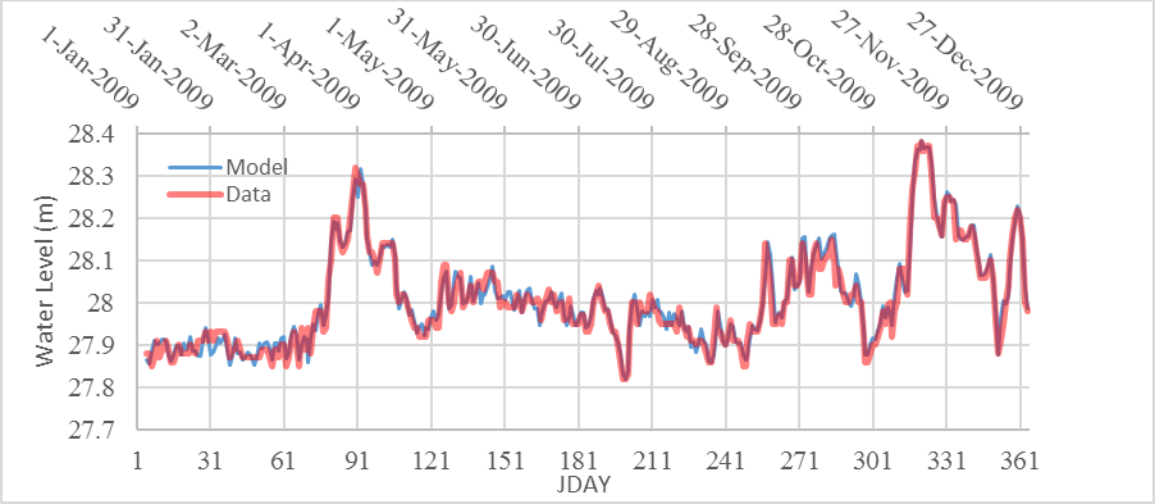

Figure 65: Model water level predictions compared to the Tigris River field data at Baghdad City (segment 123).

Flow Error Statistics

The model predicted flow and water level were compared to field data and error statistics using the mean error (ME) (Equation 15), absolute mean error (AME) (Equation 16), and root mean square error (RMSE) (Equation 17) were computed using the following equations:

Equation 15: Mean error.

$$ME = \frac{1}{N}\Sigma(Q_{model} - Q_{field\ data})$$

where

N is the number of model-field data comparisons

Q_{model} is the model flow output value

$Q_{field\ data}$ is the field flow data value

Equation 16: Absolute mean error.

$$AME = \frac{1}{N}\Sigma|(Q_{model} - Q_{field\ data})|$$

Equation 17: Root mean square error.

$$RMSE = \sqrt{\frac{1}{N}\Sigma(Q_{model} - Q_{field\ data})^2}$$

Error statistics for model comparisons with the field data are listed in Table 16. The goal was to have as minimum flow error as possible. Comparing the average error to the mean

flow at Baeji, Samarra, and Baghdad cities, the percentage error of flowrate at these cities are 1.93%, 0.83%, and 0.81%, respectively.

Table 16: Error statistics for model comparisons to field data for flow and water level (W.L.).

	Baeji City		**Samarra City**		**Baghdad City**	
	W.L.(m)	**Flow(cms)**	**W.L.(m)**	**Flow(cms)**	**W.L.(m)**	**Flow(cms)**
ME	0.001	-5.989	0.008	-0.731	0.003	0.031
AME	0.037	12.574	0.023	3.673	0.019	3.388
RMSE	0.057	17.036	0.038	6.921	0.025	4.475
N	360	360	360	360	360	360

Distributed Flows

Flow data were likely to contain uncertainty due to errors in gaged stream flow. Uncertainties of river flow data are mainly due to errors in measurements of a river rating curve (Di Baldassarre and Montanari, 2009). Other errors in flow measurements are due to errors in cross section areas, errors in mean stream velocity, or errors from the computed method (Sauer and Meyer 1992). To account for all inflows and outflow sources and sinks of water through precipitation, ground water, irrigation return flows, or seepage, additional flows were added or subtracted from the Tigris River system as distributed flows. Positive flows meant that water was added to the system, while negative flows meant that water was withdrawn from the system. Distributed tributaries were specified only for the mainstem of the Tigris River.

As soon as calibration was done at the first gage station (Baeji City), the same approach was followed with other downstream gage stations at Samarra and Baghdad Cities. Distributed tributaries at Baghdad city (branch 3) and Kut city (branch 4) mostly had negative flows indicating water was being withdrawn from the system because of irrigation. Figure 66 through Figure 68 show inflow and distributed flow with the ratio between flows in model branch 2, branch 3, and branch 4, respectively.

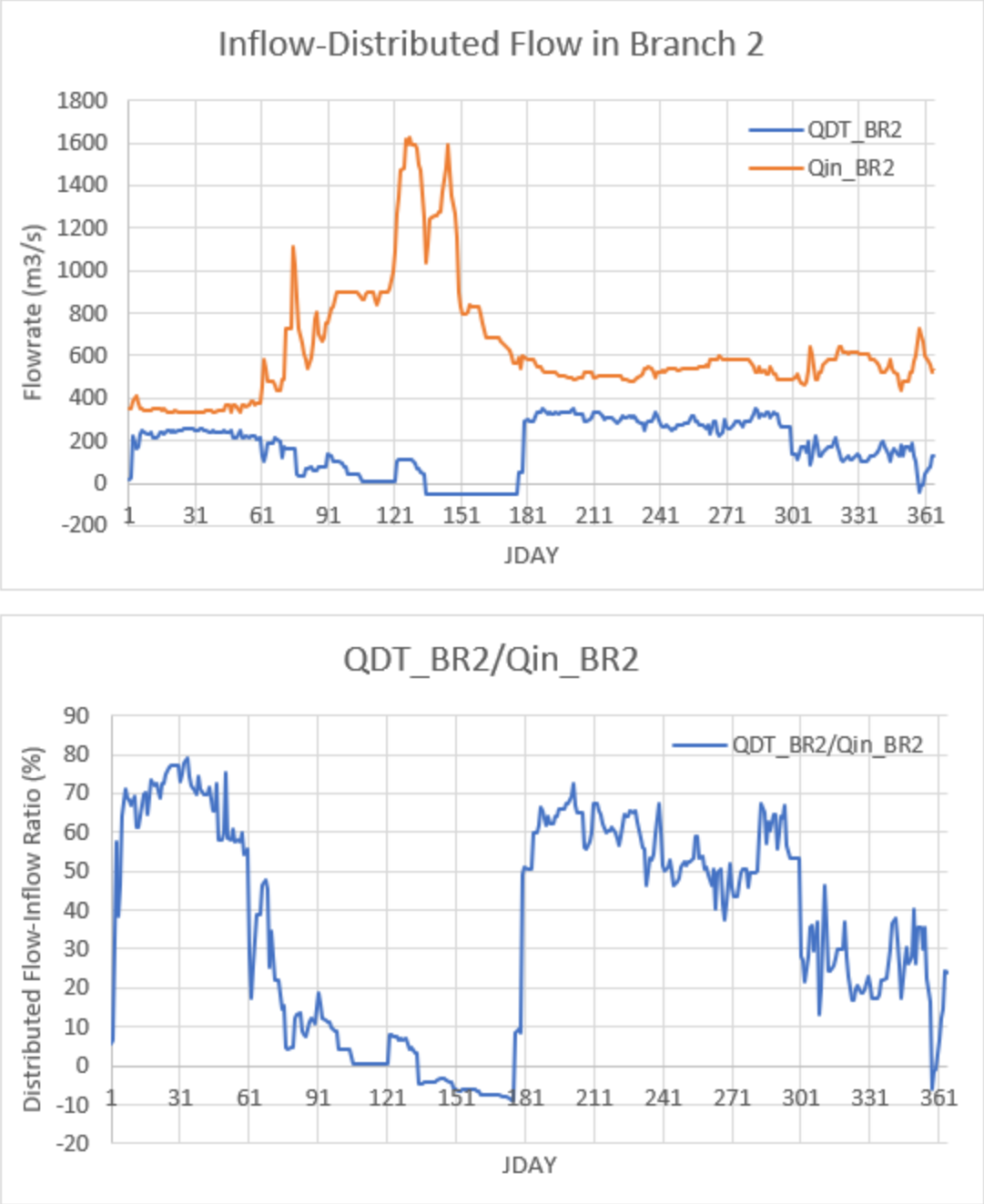

Figure 66: Inflow and distributed flow and the ratio of the flow in branch 2 of the Tigris River model.

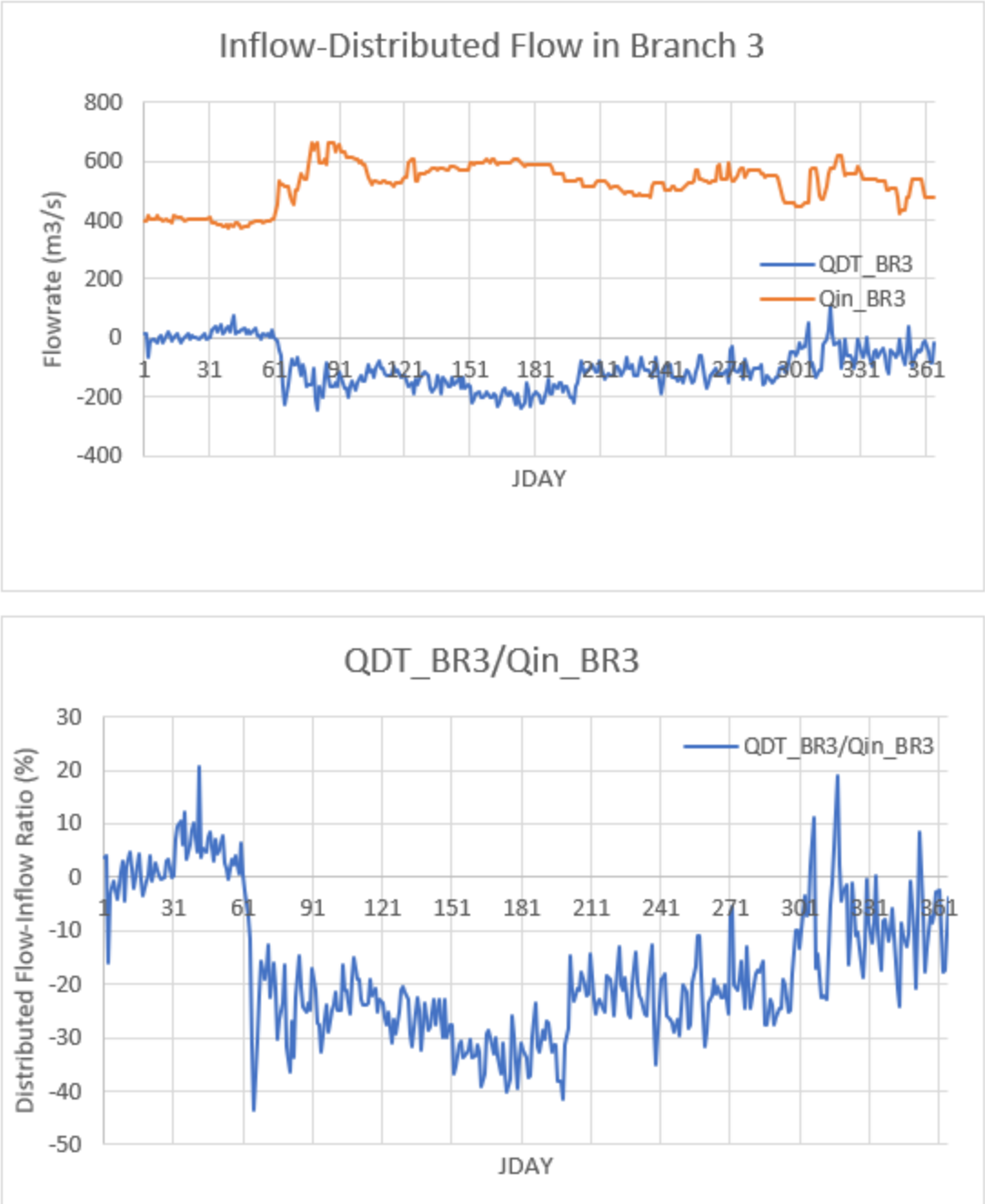

Figure 67: Inflow and distributed flow and the ratio of the flow in branch 2 of the Tigris River model.

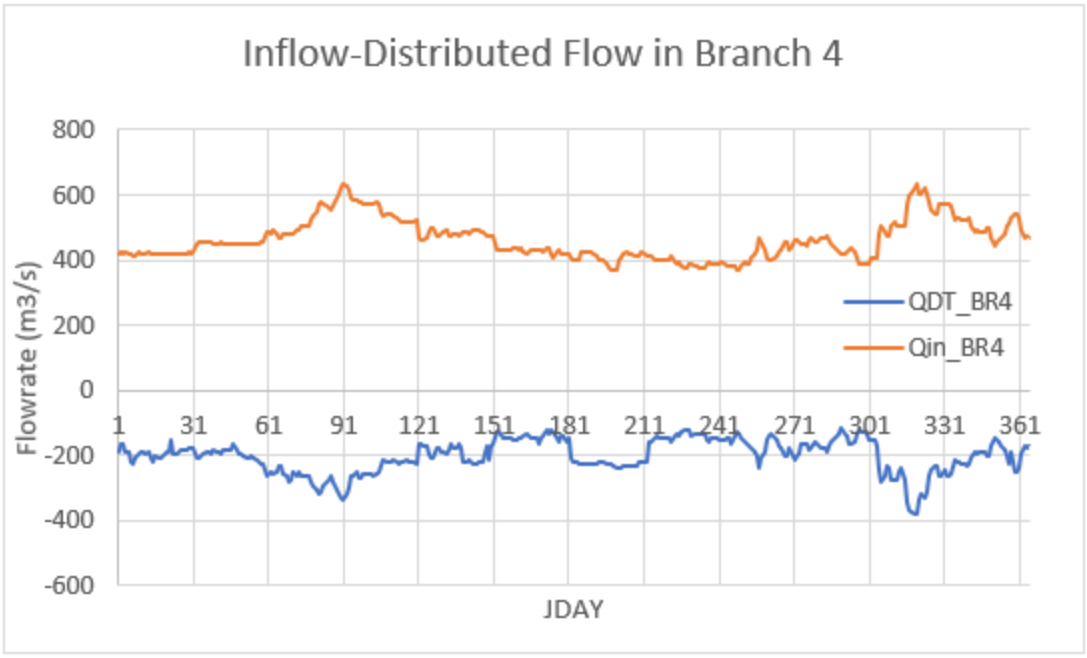

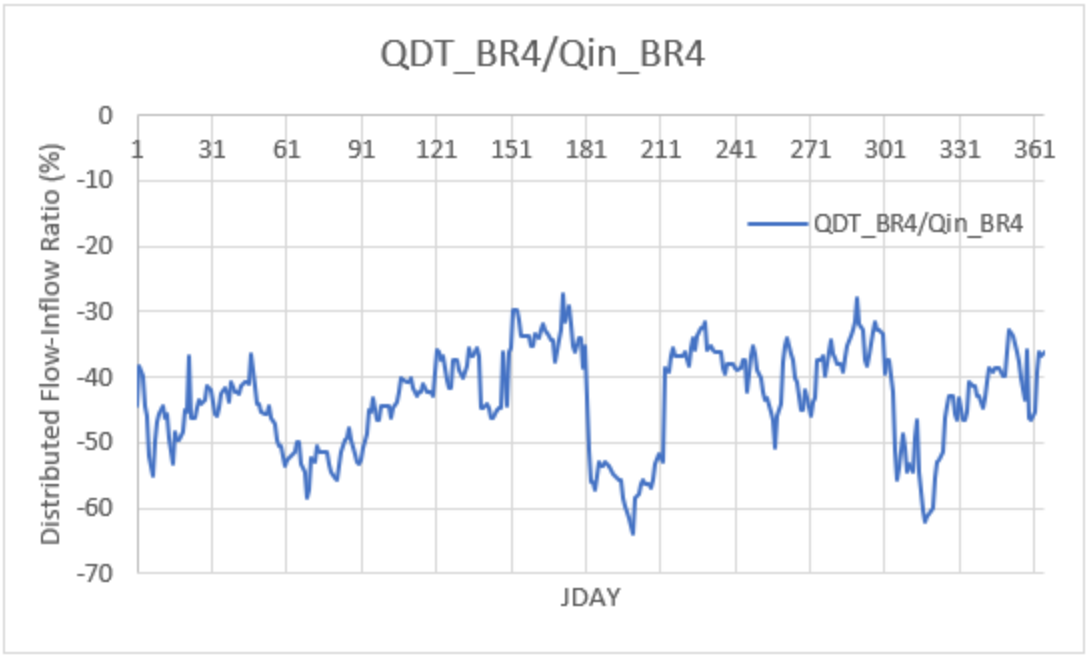

Figure 68: Inflow and distributed flow and the ratio of the flow in branch 2 of the Tigris River model.

In order to explore whether these distributed flows were reasonable, an estimate was made for typical irrigation demand along the Tigris River. The amount of irrigation water requirement is affected by many factors such as soil types, climate conditions, crop types, and loses through evaporation. Generally, an amount of 27154 gallons of water cover an area of one acre with one-inch depth (Hanson et al., 2004). Assuming 5 inches depth of water required for irrigated crops over a year, the estimated amounts of irrigation in Baghdad, Diyala, and Kut are listed in Table 17. Irrigation land measured in dunam, equivalent to 0.25 acre, in Baghdad, Diyala, and Kut cities is provided by CSO (2010). Theoretically, the average annual irrigation flow is 250 m^3/s in Kut city compared with 200 m^3/s average annual withdraw used in the model. The typical irrigation return flow is 20-25% of the original supplied volume (Aziz and Aws, 2012). Therefore, model estimations of irrigation flows as distributed tributaries were reasonable.

Table 17: Model and theoretical estimation of irrigation water in Baghdad, Diyala, and Kut.

City	Total Irrigated Area (Dunam)	Total Irrigated Area (Acre)	Model Estimation of Irrigation as Distributed Tributary (m3)	Theoretical Estimation of Irrigation (m3)
Baghdad and Diyala	18935718	4679118	3.00E+09	2.40E+09
Kut	62210000	15372426	6.35E+09	8.00E+09

Model Adjustments

Bathymetry was a crucial factor in flow calibration. Specifying the model grid properly includes describing the channel friction and slope, segment widths and depths.

Channel Friction and Slope

Water depths could be adjusted by altering Manning's coefficient. Decreasing Manning's coefficients cause the water to move more quickly in the system, while increasing Manning's coefficients slow the water in the system. Altering Manning's friction helped in matching water level to field data. According to Othman and Deguan (2004), 74% of the Tigris River bed within Mosul city was very coarse gravel. The bed of the Tigris River within Baghdad city is mainly covered by sand (Al-Ansari et al., 2015; Ali et al., 2012). Chow (1959) reported a minimum Manning's coefficient of 0.025 for natural streams that are clean with no deep pools and maximum Manning's coefficient of 0.05 for natural streams with sluggish reaches, while a maximum Manning's coefficient of 0.011 for constructed channels with concrete. Small concrete fragments remained in the Tigris River bed within Baghdad city after falling fom three major bridges, Al-Mu'alaq Bridge, Sarafia Bridge, and Jumhuriya Bridge, due to a considerable damage during the wars of 1991 and 2003. Bridge piers are obstacles to stream flows and cause backwater and consequently cause an effective increase in Manning's coefficient (Charbeneau and Holley 2001). Five bridges were constructed on the Tigris River within Mosul city, Figure 69, while 13 bridges were constructed on the Tigris River within Baghdad city, Figure 70. These can cause an increase in the channel friction. In this study, Manning's coefficient of the river within Mosul city to Samarra Barrage was 0.025, while Manning's coefficient of the river within Bagdad city was increased to 0.05. High Manning's friction in the Tigris River within

Baghdad city is due to the effect of channel irregularity (scoured banks), channel obstruction (debris deposits and bridge piers), the degree of meandering, and imperfections in the given cross-sectional geometry.

Figure 69: Bridges and meandering on the Tigris River within Mosul city.

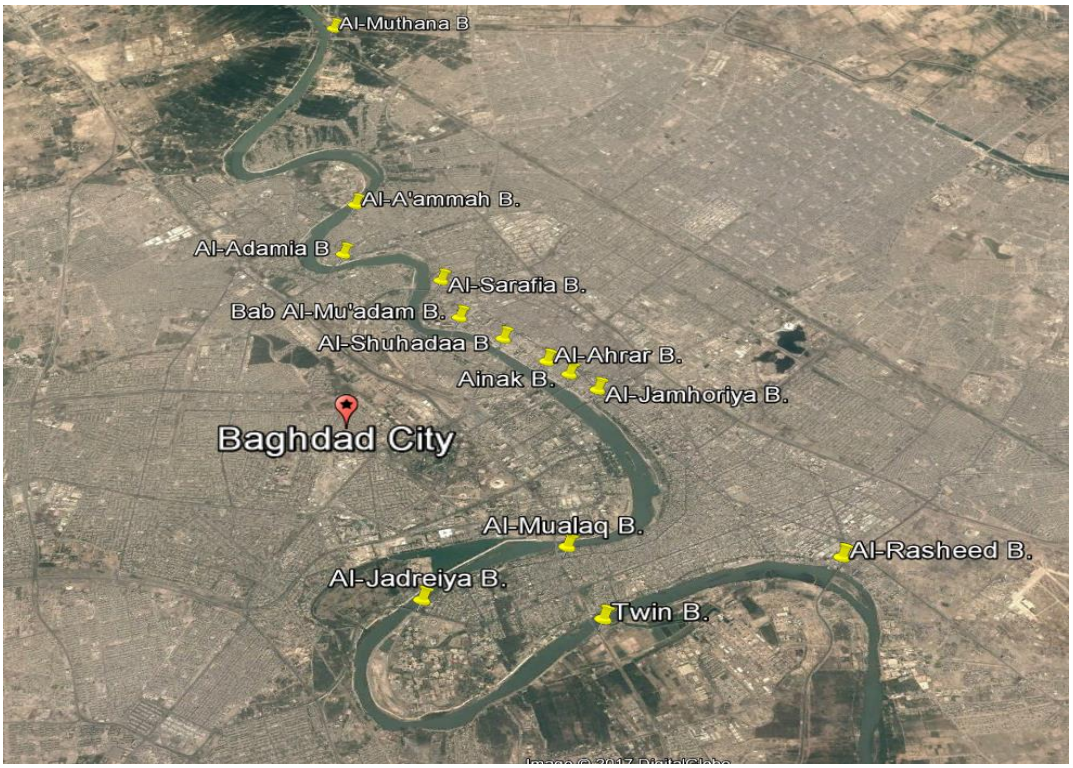

Figure 70: Bridges and meandering on the Tigris River within Baghdad city.

In the W2 model, each branch had a channel slope. This was the general slope of each branch and the included segments. However, the channel slope may not accurately capture the hydraulic gradient slope due to real channel characteristics, such as falls, riffles, or other features (Cole and Wells, 2017). Due to this reason, a separate variable, SLOPEC in the model control file, was specified for each branch and represented the hydraulic equivalent slope. This variable was used to calculate fluid acceleration in the momentum equations (Cole and Wells, 2017). In the Tigris River model, SLOPEC was assumed as the same as the actual channel slope. According to Al-Obaidy (1996), the slope of the Tigris River below Mosul city in the region between the Upper and the Lower Zabs is 0.000544. Table 18 lists Manning's coefficients and slopes used in the model.

Table 18: Manning's coefficients and slopes used in the Tigris River model

Model Branch	Manning's Coefficients	Slope	Details
1	0.025	0.00054	From Mosul Dam to 15 km DS Tikrit city
2	0.025	0	Samarra Barrage
3	0.05	0.000154	From Samarra B. to 70 km DS Baghdad city
4	0.05	0	Kut Barrage
5	0.011	0.00012	Tigris-Tharthar Canal
6	0.011	0	Tharthar Lake
7	0.011	0.00011	Tharthar Arm
8	0.011	0.0002	Tharthar-Tigris Canal
9	0.011	0.0001	Erwaeiya Canal

Water Age and Travel Time

Water age measures how long water has been in a waterbody. Water age of the Tigris River system was defined as a state variable and was set to zero in all flow inputs to the system, upstream boundary conditions and side tributaries. Figure 71 and Figure 72 show water age in the mainstem of the Tigris River and Tharthar Lake, respectively. Generally, water age increases as water moves downstream of the system. The water age started to significantly increase downstream of Samarra Barrage due to the fact that inflow from Tharthar-Tigris canal had relatively older water age and mixed with mainstem flow that was relatively newer.

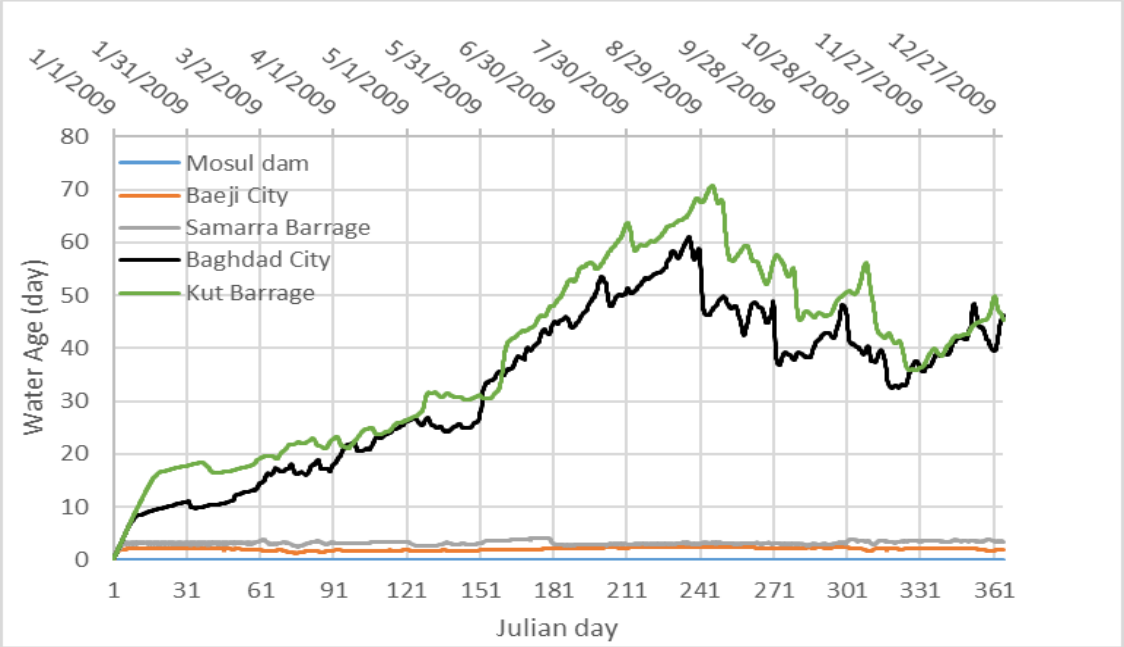

Figure 71: Model predictions of water age throughout the mainstem of the Tigris River system for the base model.

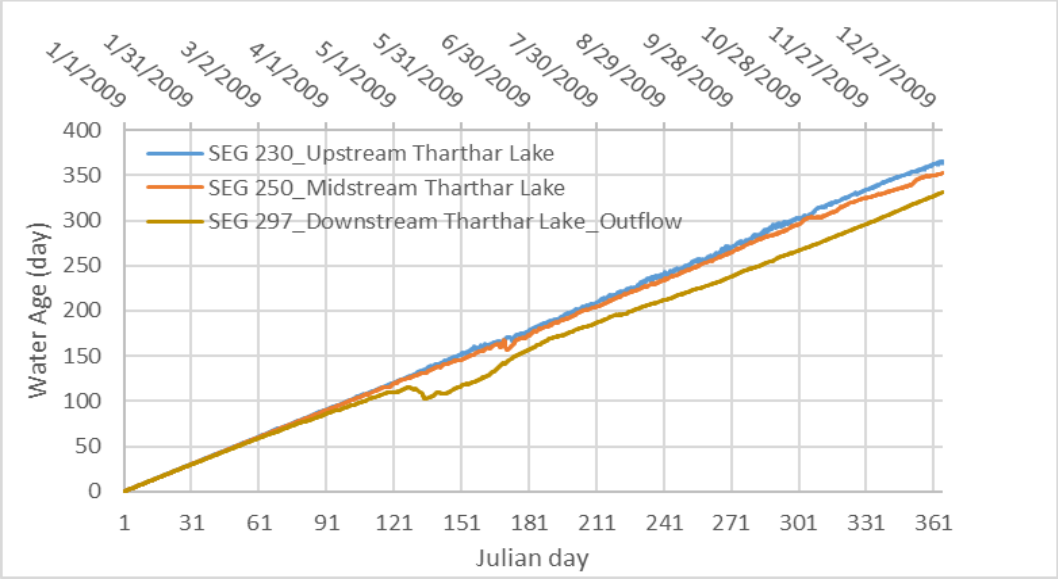

Figure 72: Model predictions of water age in Tharthar Lake.

The travel time of a parcel of water was estimated using a conservative tracer with an arbitrary concentration of 10,000 mg/l added at the upstream boundary (Mosul Dam) for 1 day and repeated every two months for the entire simulation period. As the pulse moved downstream, the time to peak at Baji city, Samarra Barrage, Baghdad city, and Kut Barrage was recorded. The difference between peak times downstream and the original pulse time injected upstream at the boundary reflected the travel time of the center of mass of the plume. Figure 73 shows the tracer concentration as the plume moved downstream. Tracer concentrations decreased, and associated travel times increased as the peak moved to different stations along the mainstem of the Tigris River. Figure 74 shows an example of a pulse injected at Julian day 1.0 at Mosul Dam and the travel time of the peak at Baeji city, Samarra Barrage, Baghdad city, and Kut Barrage. Figure 75 shows the travel time of the tracer at the output segment of Tharthar Lake. Table 19 lists downstream travel time in days of an upstream pulse injected every 60 days.

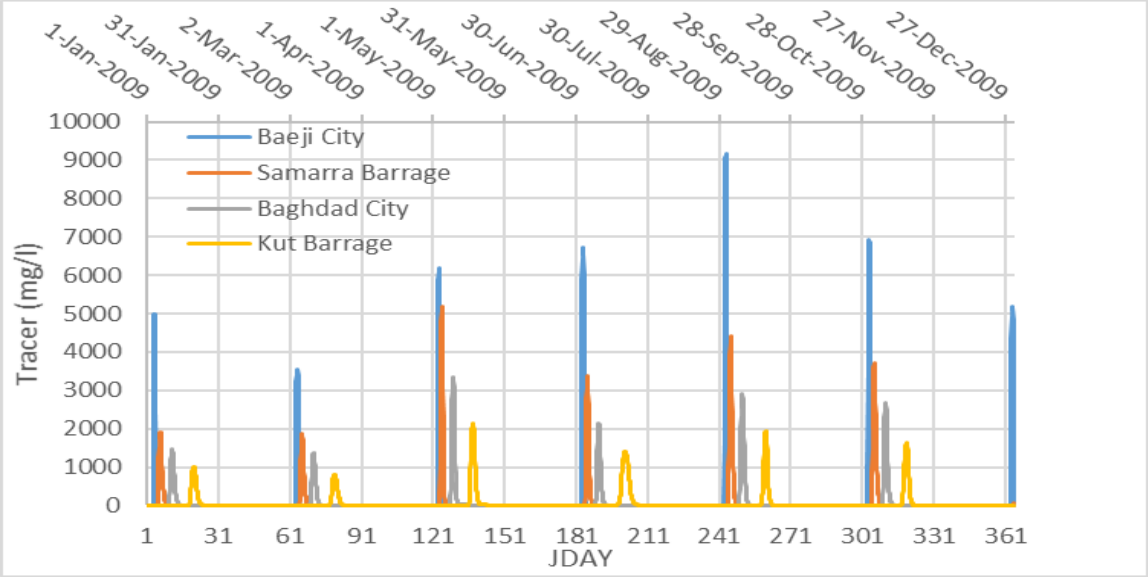

Figure 73: A tracer pulse input at upstream boundary condition and travel time of that pulse along the main stream of the Tigris River at Baeji city, Samarra Barrage, Baghdad city, and Kut Barrage.

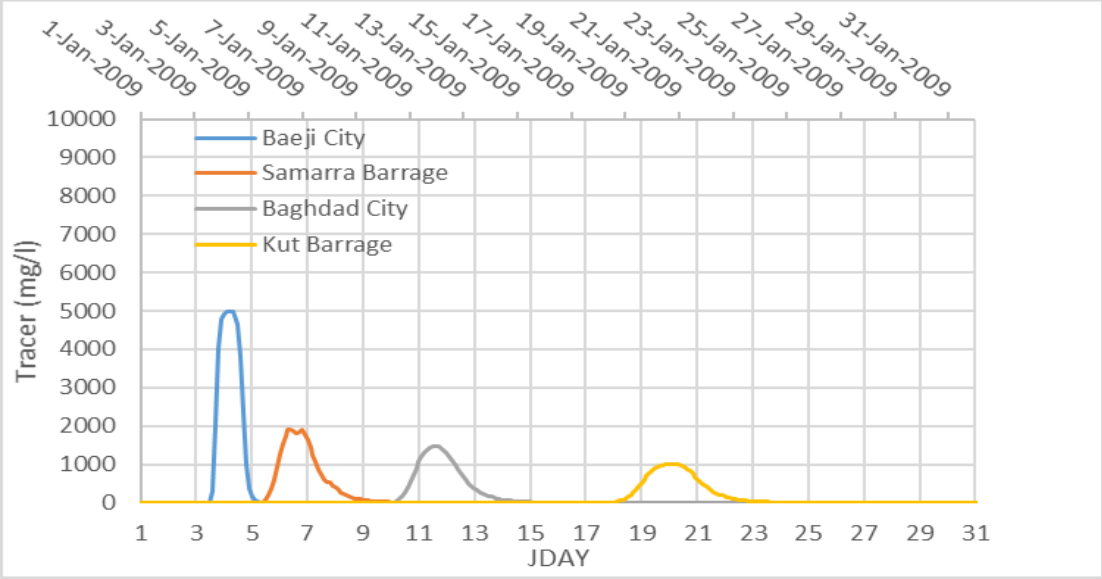

Figure 74: A tracer pulse input at JDAY 1.5 condition and travel time of that pulse along the main stream of the Tigris River at Baeji city, Samarra Barrage, Baghdad city, and Kut Barrage.

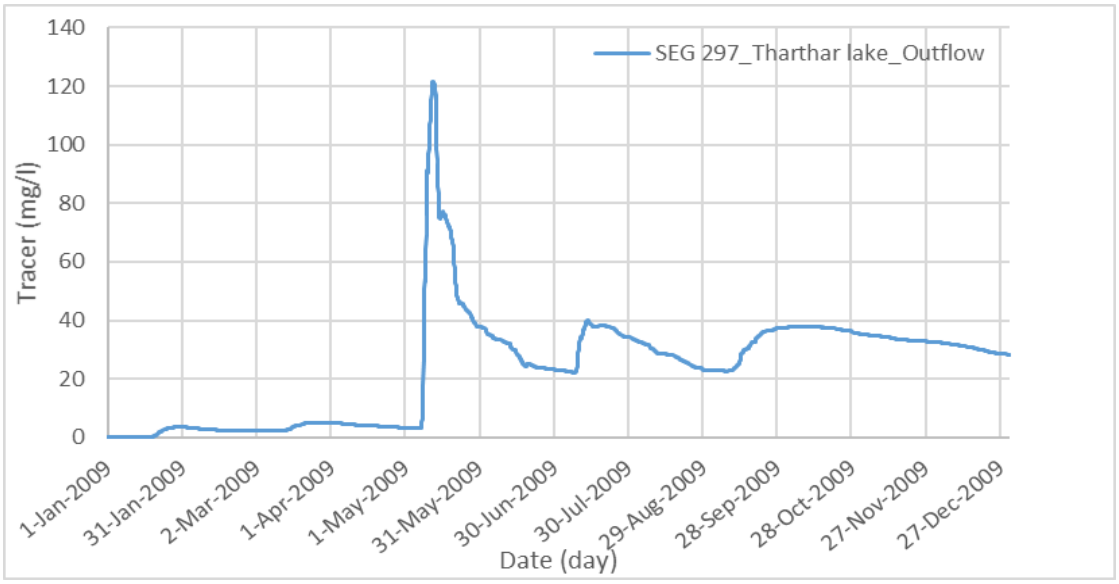

Figure 75: A tracer pulse input at JDAY 1.0 condition and travel time of that pulse in Tharthar Lake.

Table 19: Travel time of upstream pulse inputs every 2 months

		Travel Time (day)			
Initial Upstream Pulse JDAY	**Upstream Flow at Mosul Dam (m^3/s)**	**Baeji City**	**Samarra Barrage**	**Baghdad City**	**Kut Barrage**
1.5	200	3	5.5	10.5	18.5
61.5	200	2.8	4.8	9.5	18.5
121.5	810	2.3	3.5	8.2	16.5
181.5	400	2.7	4.5	9	20.5
241.5	480	2.5	4.5	9.5	19.3
301.5	400	2.7	4.8	9.5	18.1
361.5	300	2.9	-	-	-

Model Calibration: Temperature

Water Temperature of Tharthar Lake

Longitudinal water temperature of Tharthar Lake was estimated remotely using Landsat images and was compared to model predictions of water temperature at different segments along the North-South axis of the lake. Figure 76 and Figure 77 show model predictions of longitudinal surface water temperature in Tharthar Lake compared with satellite data estimated for Tharthar Lake at a distance from the North to the South: 15 km, 25 km, 35 km, 45 km, 55 km, 70.5 km (input of the lake), 80.5 km, and 90 km (outlet of the lake). Model predictions of surface water temperature of the lake agreed with satellite data in that there was a longitudinal variation in water temperature along the North-South axis of the lake and the southern part was warmer than the northern part. However, the model often estimated a larger surface temperature variation than the satellite-based estimates. Table 20 lists error statistics of model comparisons to satellite data in Tharthar Lake.

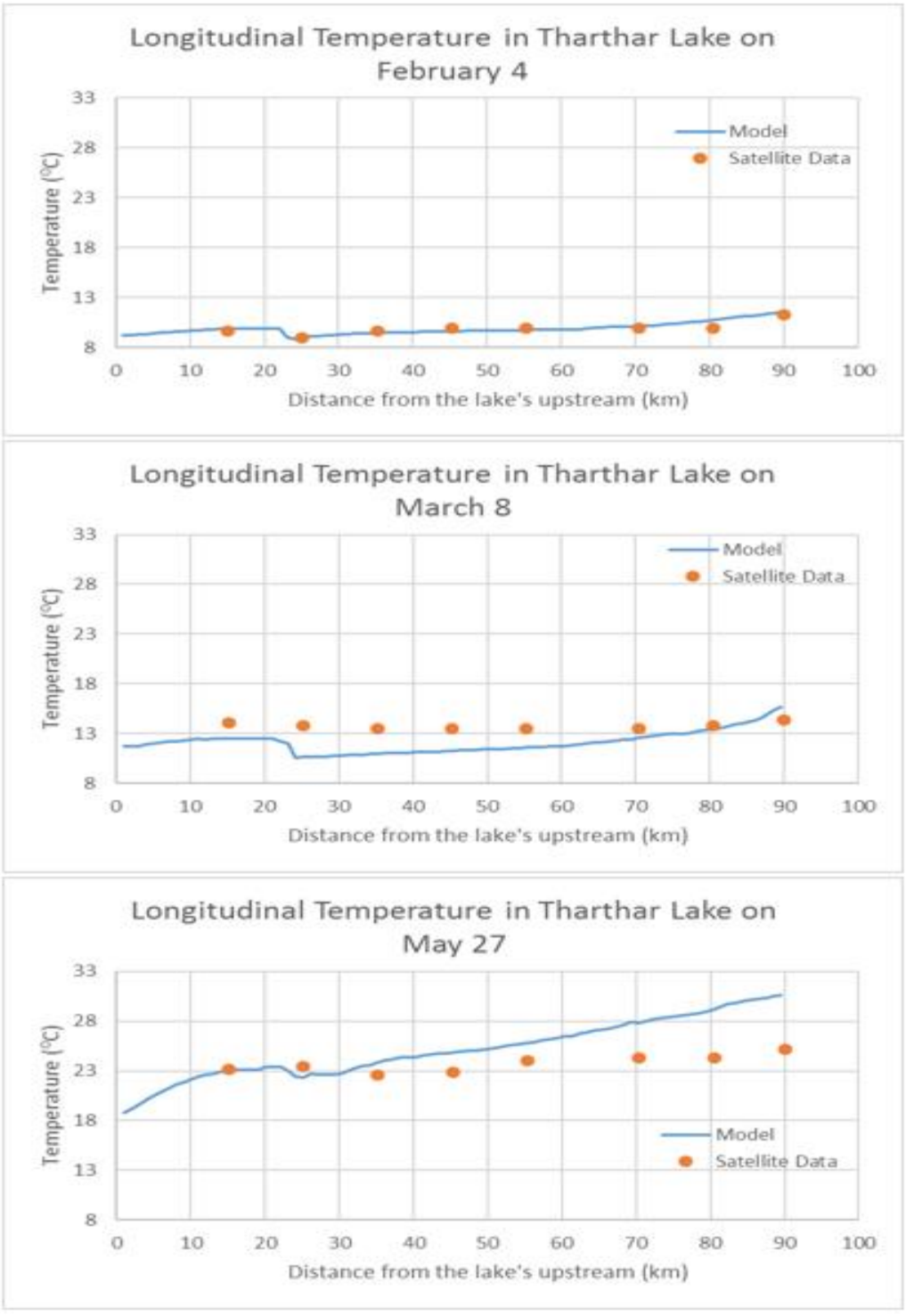

Figure 76: Model predictions of longitudinal surface water temperature in Tharthar Lake on February 4th, March8th, and May 27th.

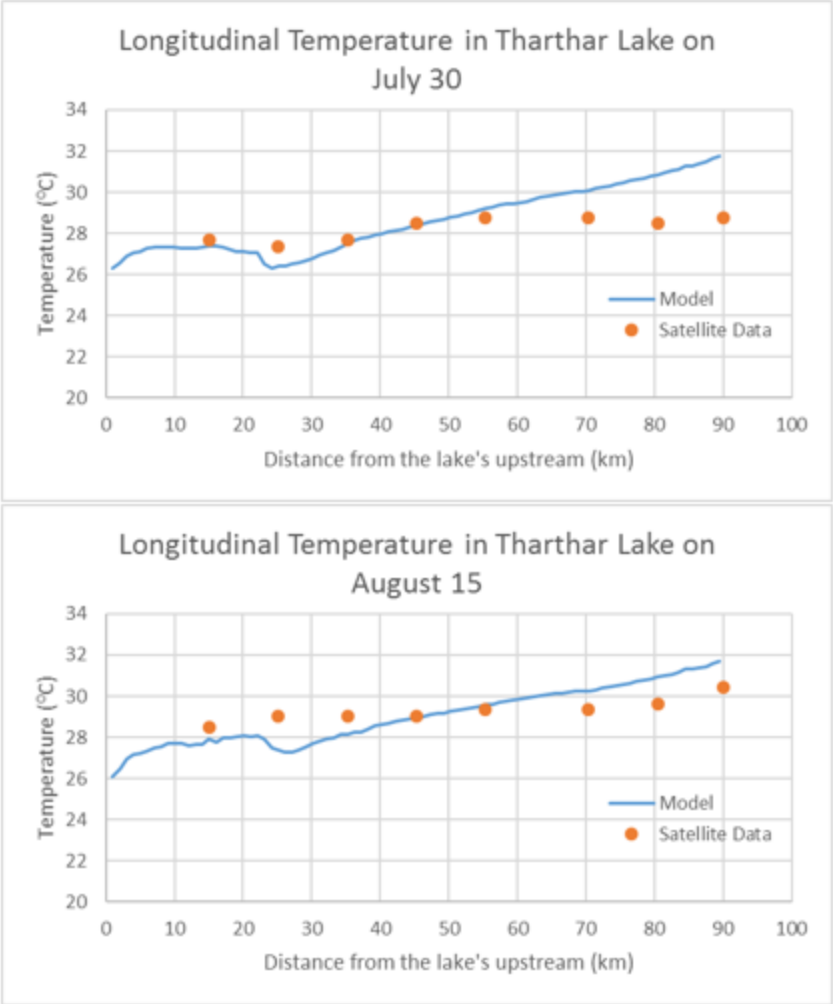

Figure 77: Model predictions of longitudinal surface water temperature in Tharthar Lake on July 30th and August 15th.

Table 20: Error statistics for model comparisons to satellite data for longitudinal water temperature in Tharthar Lake.

	February 4, 2009	**March 8, 2009**	**May 27, 2009**	**July 30, 2009**	**August 15, 2009**
ME	0.13	-1.39	2.24	0.69	0.06
AME	0.30	1.72	2.55	1.08	0.88
RMSE	0.37	1.90	3.11	1.48	1.01
N	8	8	8	8	8

Water Temperature of the Tigris River

Water temperature of the Tigris River was calibrated after the flowrate calibration since water temperature is highly dependent on water depth and travel time. Most of water quality constituent state variables were temperature dependent and therefore calibrating temperature was performed before water quality. The model predictions of surface water temperature were compared with remote sensed temperature data estimated from Landsat satellite at both Baeji City and Baghdad City. Figure 78 and Figure 79 show model predictions of water temperature compared with satellite data along the mainstem of the Tigris River at both Baeji and Baghdad cities, respectively. Unfortunately, field data of vertical temperature profiles were not available for model comparisons. Figure 80 and Figure 81 show temperature contour lines of Tharthar Lake, while Figure 82 and Figure 83 show temperature contour lines of Samarra Barrage and Kut Barrage for the simulated year 2009. The temperature profiles show that the lake's water was well mixed at the beginning of the simulation and started to stratify during the summer months, while weak stratification did occur from time to time at Samarra Barrage and Kut Barrage during low flow conditions.

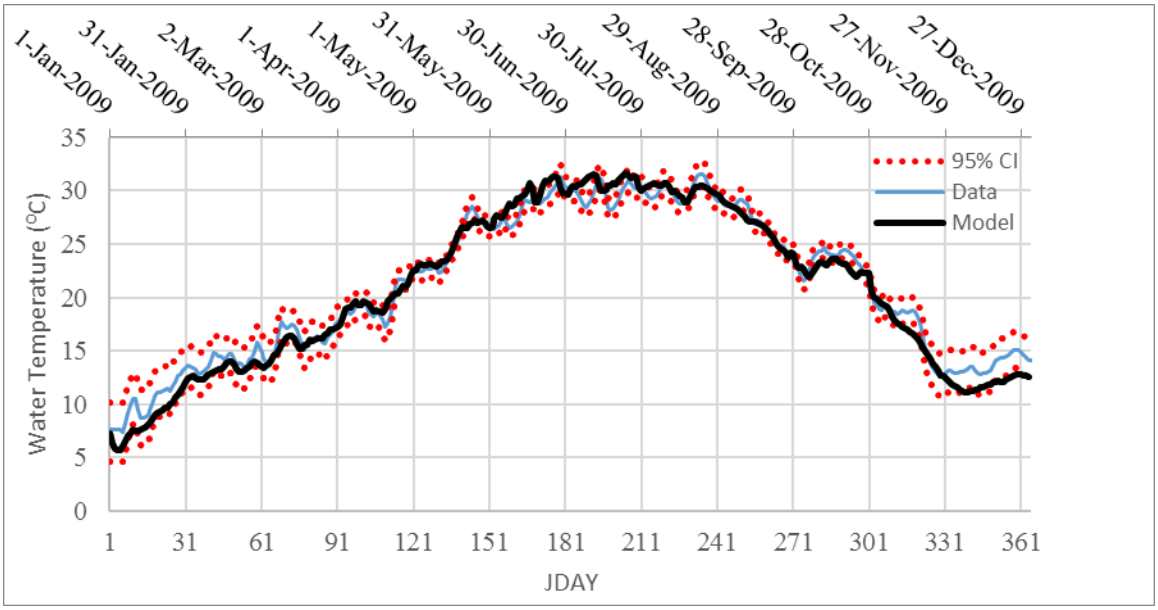

Figure 78: Model surface water temperature predictions compared to the Tigris River remote sensing data at Baeji City (segment 54).

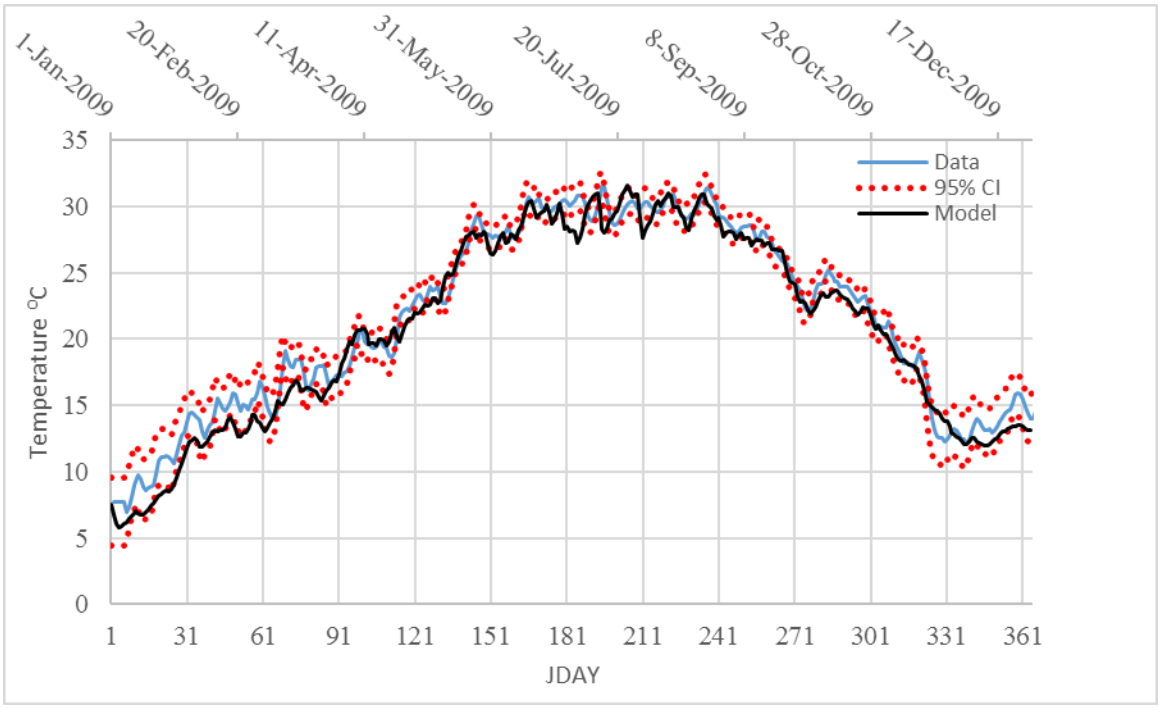

Figure 79: Model surface water temperature predictions compared to the Tigris River remote sensing data at Baghdad City (segment 123).

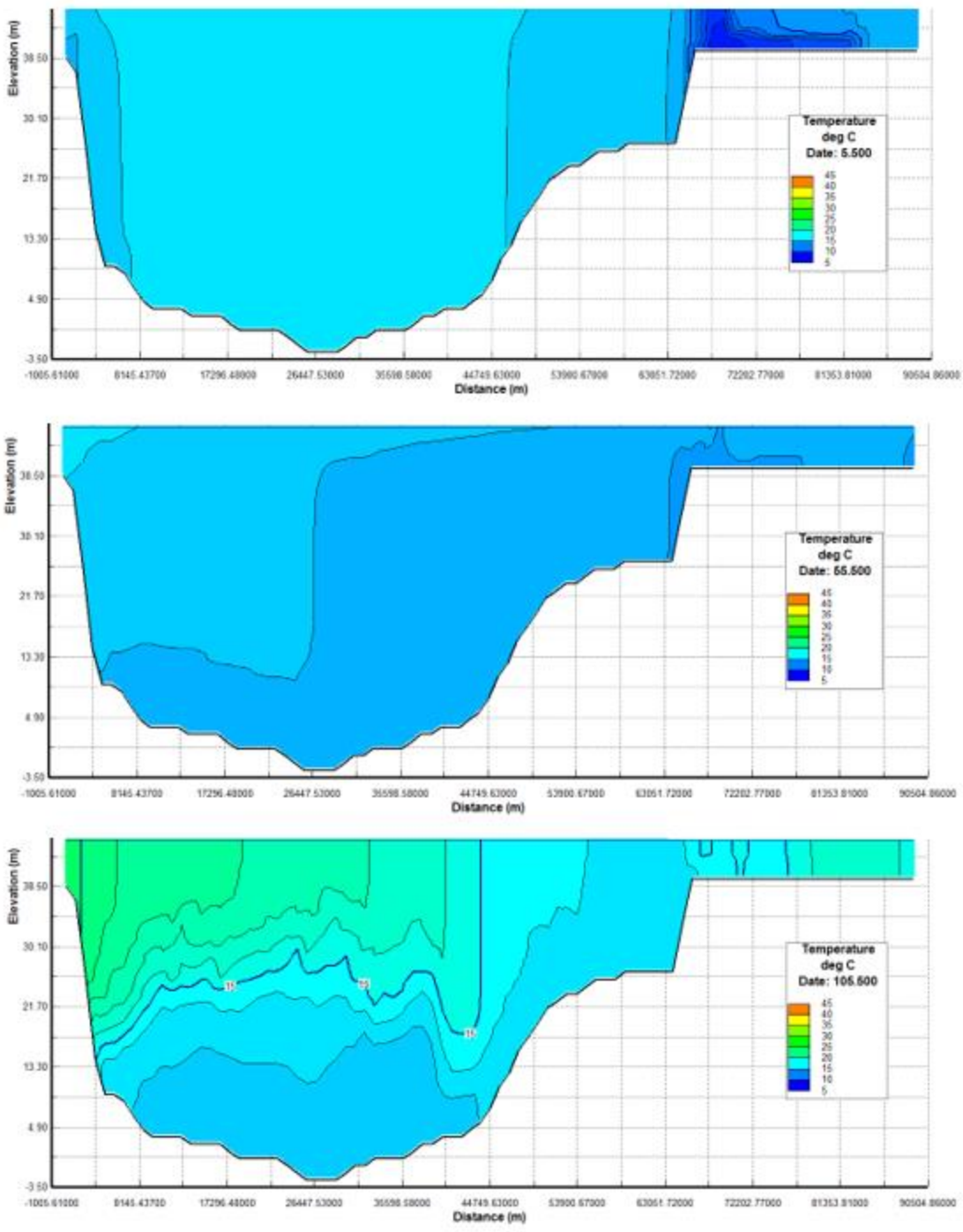

Figure 80: Model temperature contour lines of Tharthar Lake at JDAY 5.5, 55.5, and 105.5 of 2009 (Part 1).

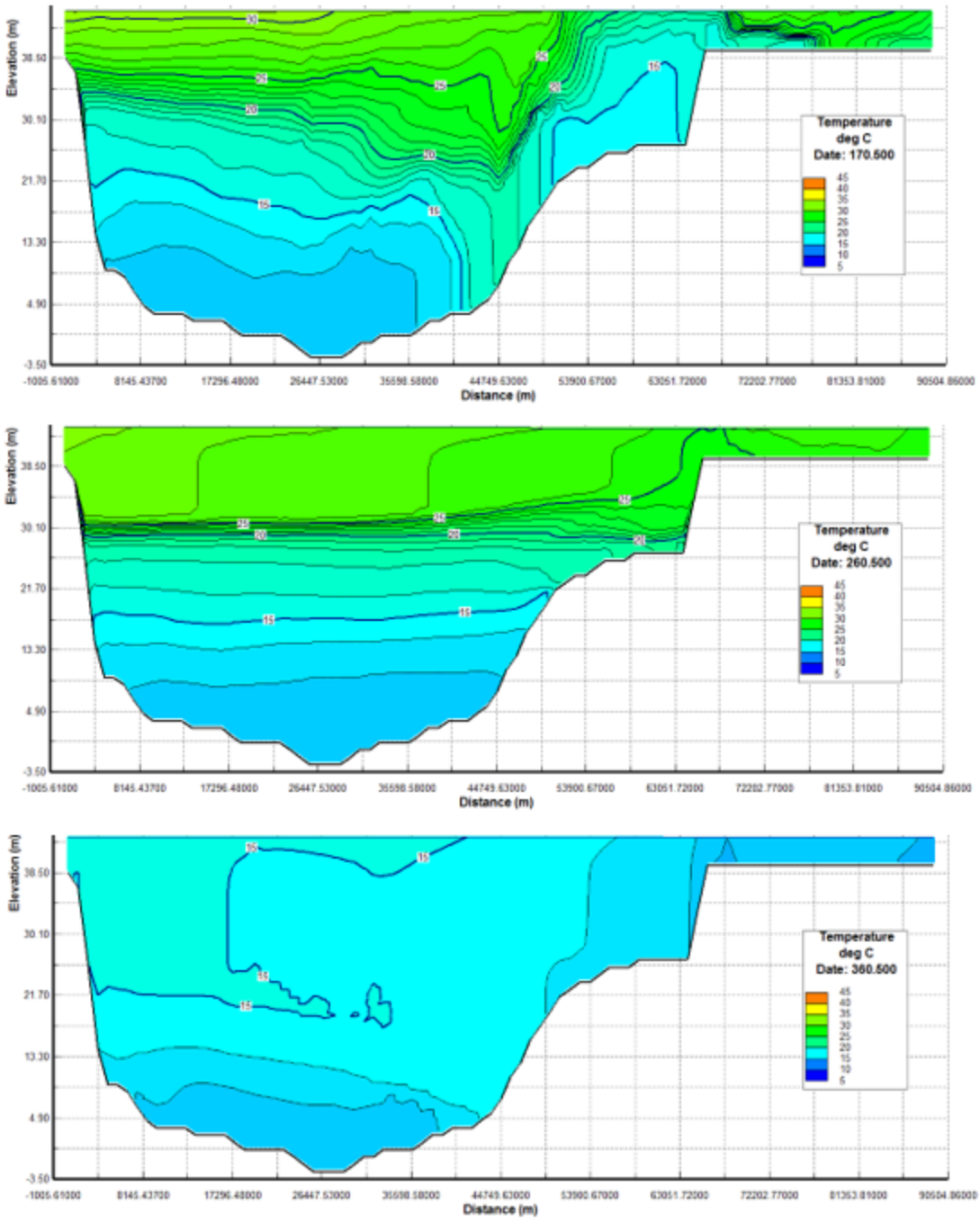

Figure 81: Model temperature contour lines of Tharthar Lake at JDAY 170.5, 260.5, and 350.5 of 2009 (Part 2).

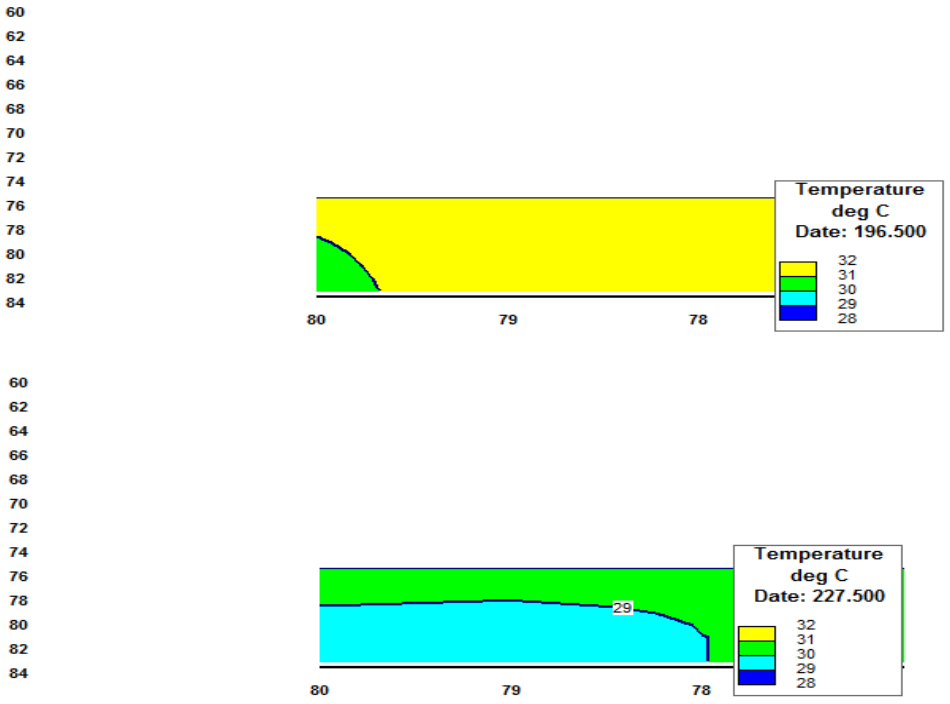

Figure 82: Model temperature contour lines of Samarra Barrage (model segment 80) at JDAY 196.5 and 227.5 of 2009.

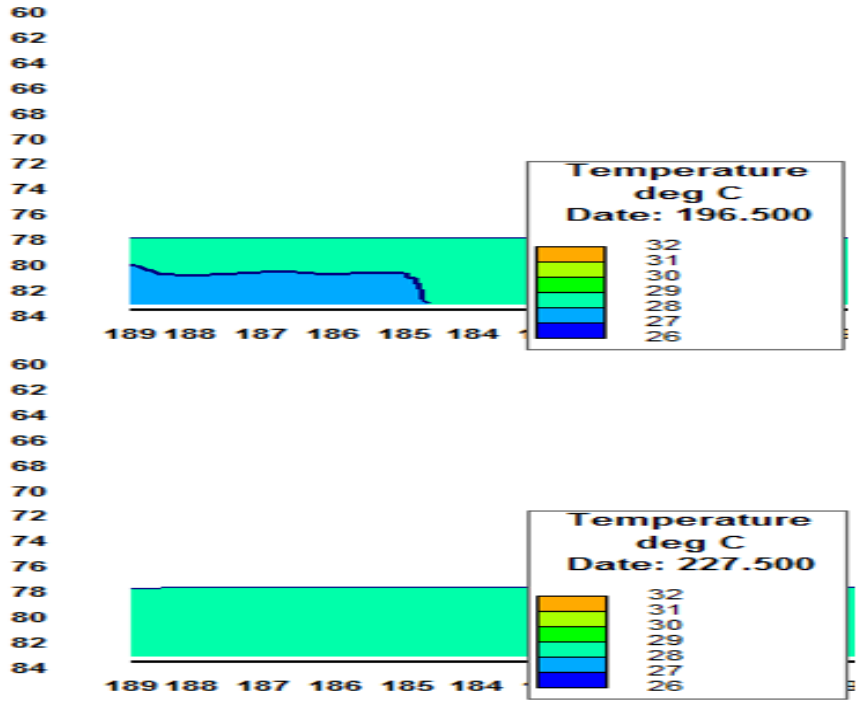

Figure 83: Model temperature contour lines of Kut Barrage (model segment 189) at JDAY196.5 and 227.5 of 2009.

Temperature Error Statistics

Following the same procedure as with flow, the model predicted temperature was compared to estimated temperatures using satellite data.

Table 21 lists error statistics for model predicted temperature values compared to satellite data at stations along the mainstem of the Tigris River at Baeji city and Baghdad city. Model predictions of temperatures were relatively colder than satellite data during winter months but were within the confidence interval. This could be attributed to a contamination of the satellite water pixels by land pixels. In addition, high image cloud cover and lack of Landsat images, as listed previously in Table 9 in chapter three, likely produced a bias between model predictions and the statistical models of water temperature at Baeji and Baghdad cities in winter months of the simulated year 2009; essentially, summertime conditions were optimized. According to Boer (2014), another possible error contribution could be introduced due to undetected thin clouds. Table 22 lists error statistics for model predicted temperature values from April to October compared to satellite data at stations along the mainstem of the Tigris River at Baeji city and Baghdad city.

Table 21: Error statistics for model comparisons to satellite data for water temperature from January to December 2009.

	Baeji City	**Baghdad City**
	Temp (º C)	**Temp (º C)**
ME	-0.324	-0.727
AME	0.911	1.047
RMSE	1.140	1.315
N	360	360

Table 22: Error statistics for model comparisons to satellite data for water temperature from April to October 2009.

	Baeji City [BFW 0.46]	**Baghdad City [BFW 0.46]**
	Temp (º C)	**Temp (º C)**
ME	0.337	-0.314
AME	0.710	0.775
RMSE	0.938	1.016
N	184	184

Model Calibration: Water Quality Constituents

Like flow and temperature calibration, model predictions of water quality constituents were compared to the measurements in the Tigris River when field data were available. Unfortunately, not all water quality field data were available for either the model boundary conditions or for comparisons to model predictions during model calibration. Monthly average field data of both total dissolved solids (TDS) and nitrates (NO3) were the only two water quality constituents provided by the Iraqi Ministry of Water Resources for the modeled year 2009. Other water quality constituents modeled in this study such as PO4, NO3, BOD_u, algae, and DO were estimated from literature values.

Total Dissolved Solids

In-situ monthly average data of total dissolved solids were provided by the Iraqi ministry of Water Resources (MOWR 2014). Data were provided at Mosul Dam, Samarra Barrage, Audaim tributary, Baghdad City (Al-Shahada Bridge), Diyala River tributary, and Kut Barrage. No TDS data are available for both Upper Zab and Lower Zab Rivers, and therefore TDS concentrations at these two tributaries were assumed based on the available data. Unfortunately, daily average data of TDS were unavailable and therefore the model calibration for TDS was based on the monthly average data.

Due to relatively low flowrates and high TDS concentrations introduced to the mainstem of the Tigris River upstream Baghdad city through the Tharthar-Tigris canal, TDS in the mainstem of the river at Baghdad city was relatively high during the first two months of the year (winter time). This peak in TDS concentration at Baghdad city and downstream areas (Kut Barrage) could mostly be due to ungaged irrigation return flows that were

directly discharged into the mainstem of the Tigris River through numerous man-made irrigation channels along both river banks. The effects of these return flows were added to the model as tributaries.

To account for high TDS concentration in Baghdad City during the first two months of the year, an extra tributary was introduced into the mainstem of the Tigris River system and was placed downstream of Samarra Barrage. This extra tributary had low flowrates (1 m^3/s) with high mass of TDS to adjust for the deficit in TDS concentrations during the winter months. This was like adding a mass source of TDS to the river. Another tributary was introduced downstream of Baghdad City to account for high TDS at Kut Barrage in winter months. Figure 84 through Figure 88show the model predictions of TDS compared with field data at Mosul Dam (boundary condition), Samarra Barrage, Baghdad City, Kut Barrage, and Tharthar Lake respectively. Unfortunately, field data of TDS in Tharthar Lake were not available for model comparison. TDS contour lines for the longitudinal and vertical at Tharthar Lake are shown in Figure 90. As water was continuously diverted to Tharthar Lake from Samarra Barrage through Tigris-Tharthar Canal, TDS concentrations in Tharthar Lake decreased during the simulated year due to continuous dilution. According to Ansari et al., (2012), TDS and other water quality constituents decrease with increasing dilution. The initial condition of TDS at Tharthar Lake was 1300 mg/l and dropped down to about 1150 mg/l at the end of the simulation. Table 23 lists error statistics of model predictions for TDS compared with the monthly averaged field data at Samarra Barrage, Baghdad city, and Kut Barrage.

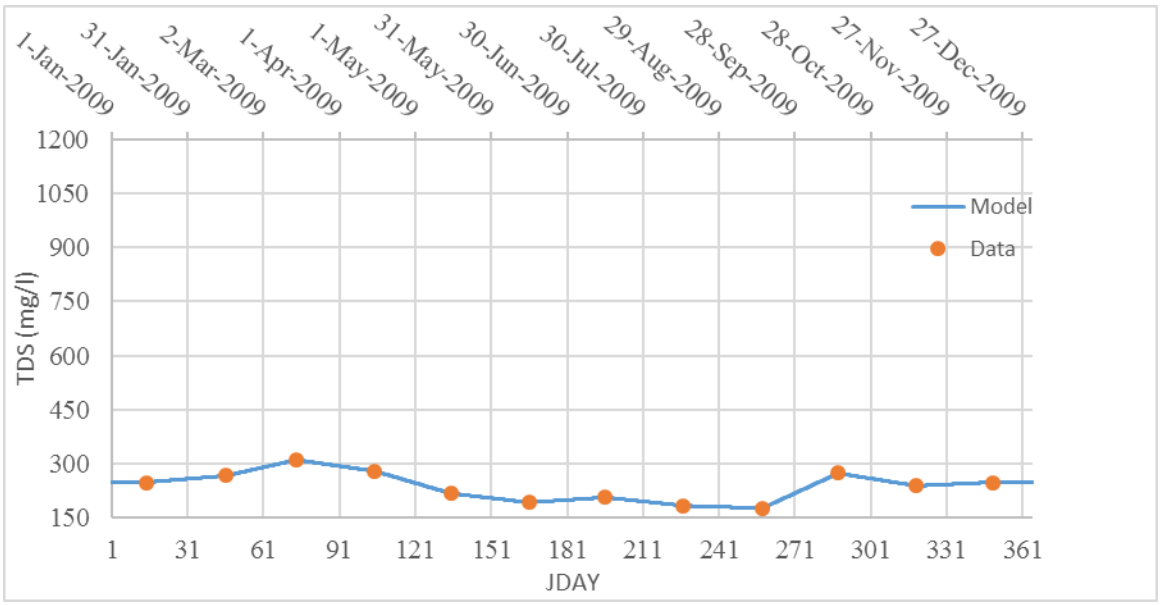

Figure 84: Model TDS predictions compared to the Tigris River field data at Mosul Dam (segment 2) the upstream boundary condition.

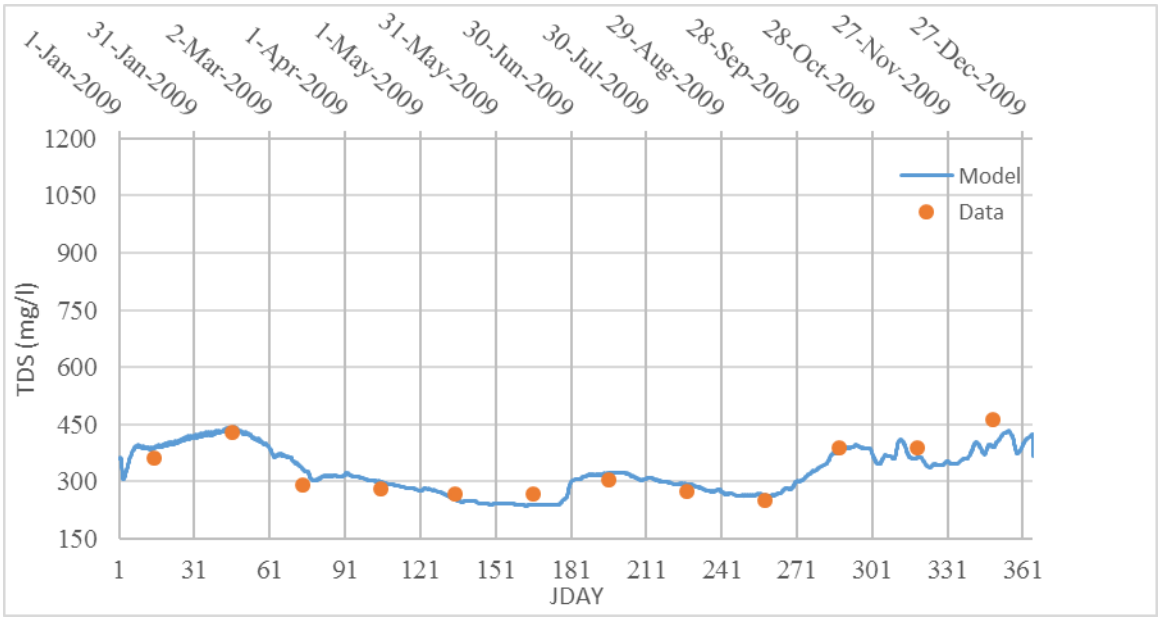

Figure 85: Model TDS predictions compared to the Tigris River field data at Samarra Barrage (segment 83).

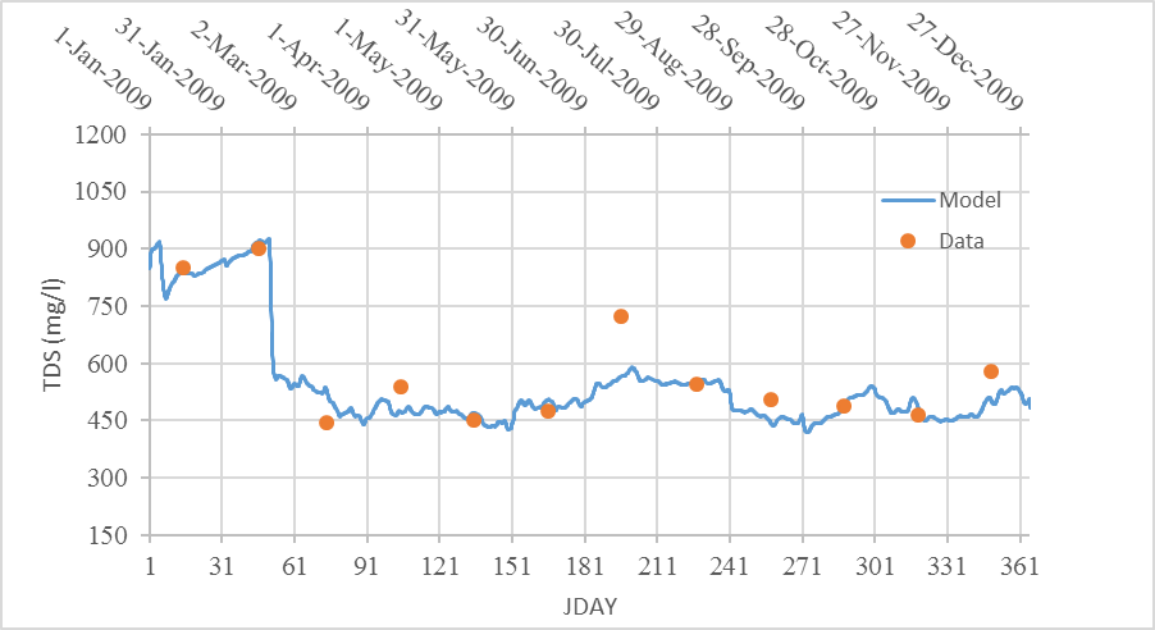

Figure 86: Model TDS predictions compared to the Tigris River field data at Baghdad City (segment 123).

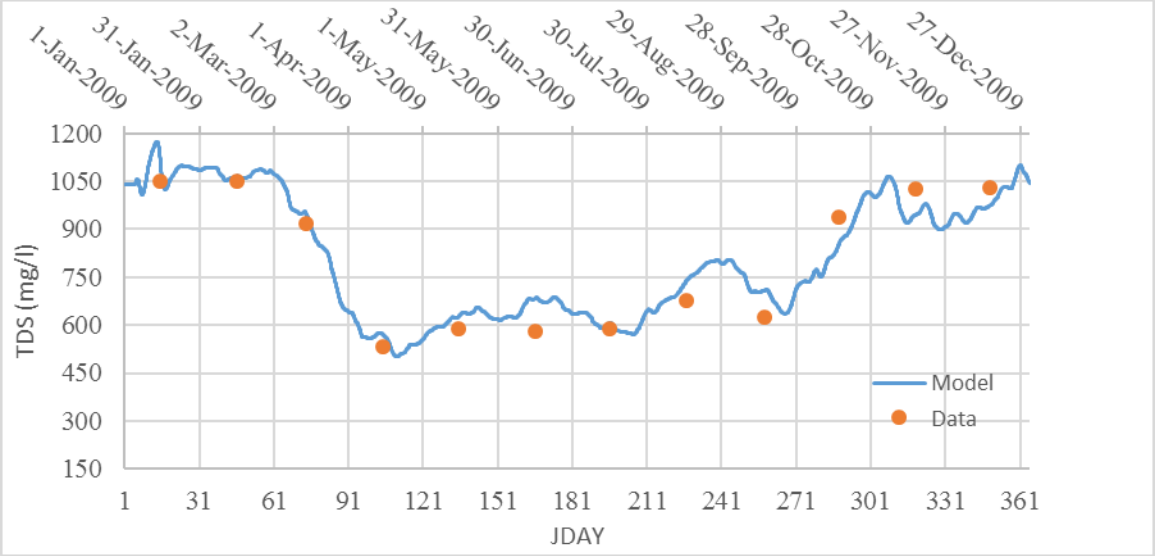

Figure 87: Model TDS predictions compared to the Tigris River field data at Kut Barrage (segment 189).

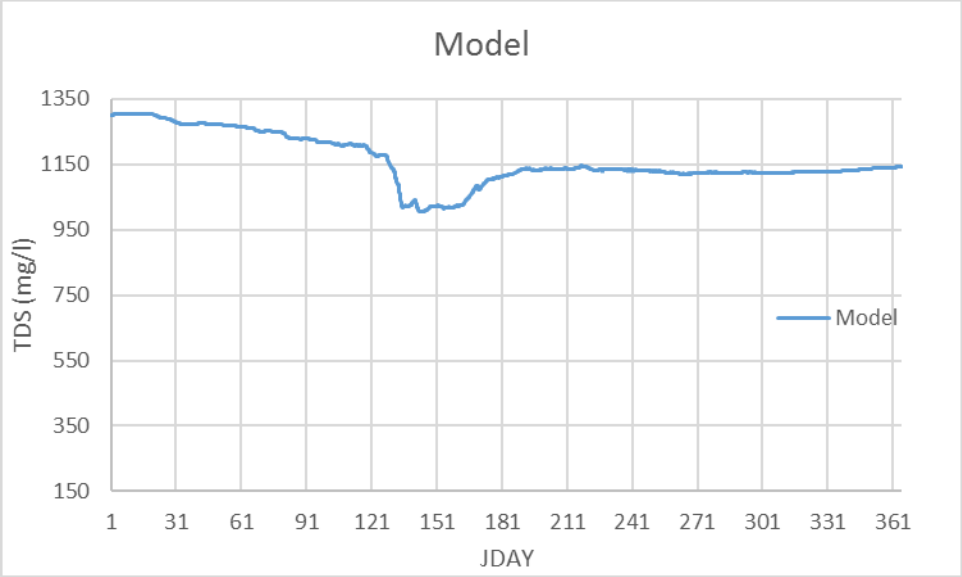

Figure 88: Model TDS predictions at the outlet of Tharthar Lake in 2009 (segment 297).

Table 23: Error statistics for model predictions of TDS in the middle of the month compared with field data.

	Samarra	**Baghdad**	**Kut**
ME (mg/l)	2.567	-12.896	17.692
AME (mg/l)	27.083	53.163	53.175
RMSE (mg/l)	31.692	64.778	60.361
N	12	12	12

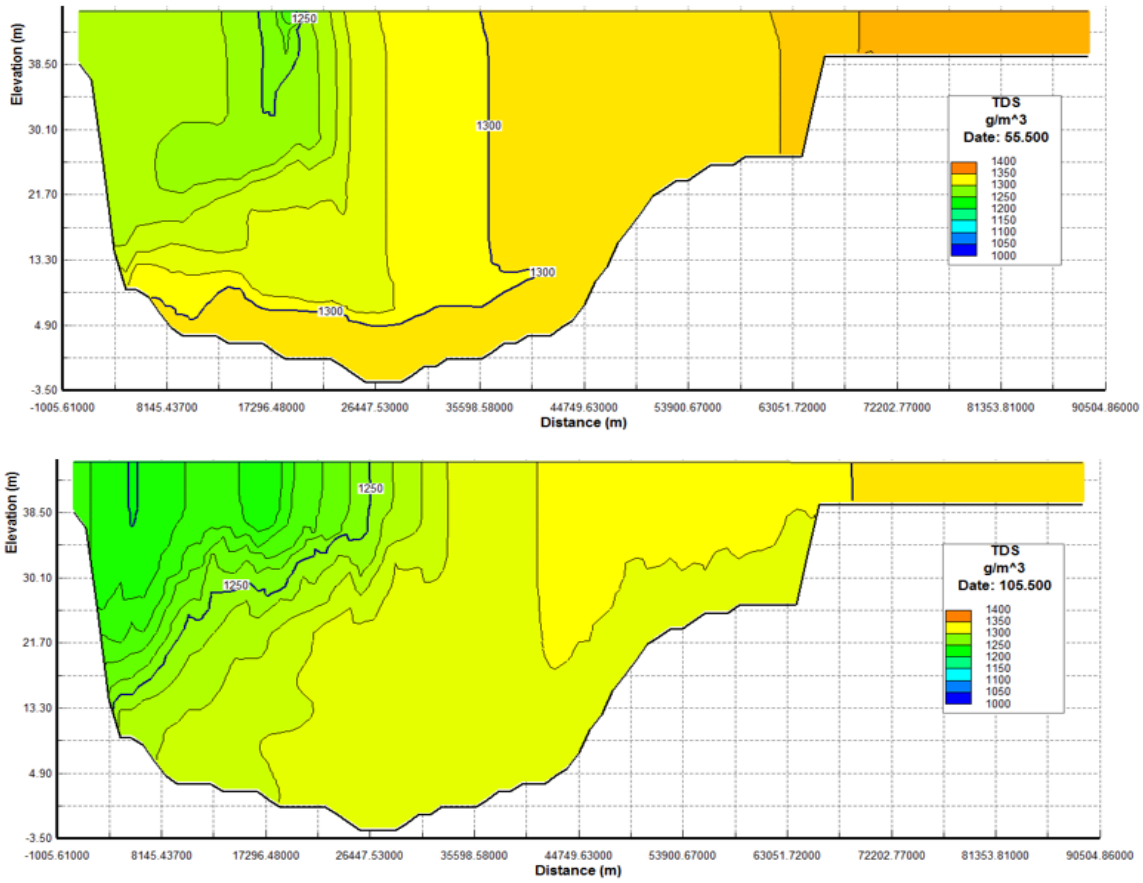

Figure 89: Model contours of TDS in Tharthar Lake at JDAY 55.5, and 105.5 of 2009 (Part 1).

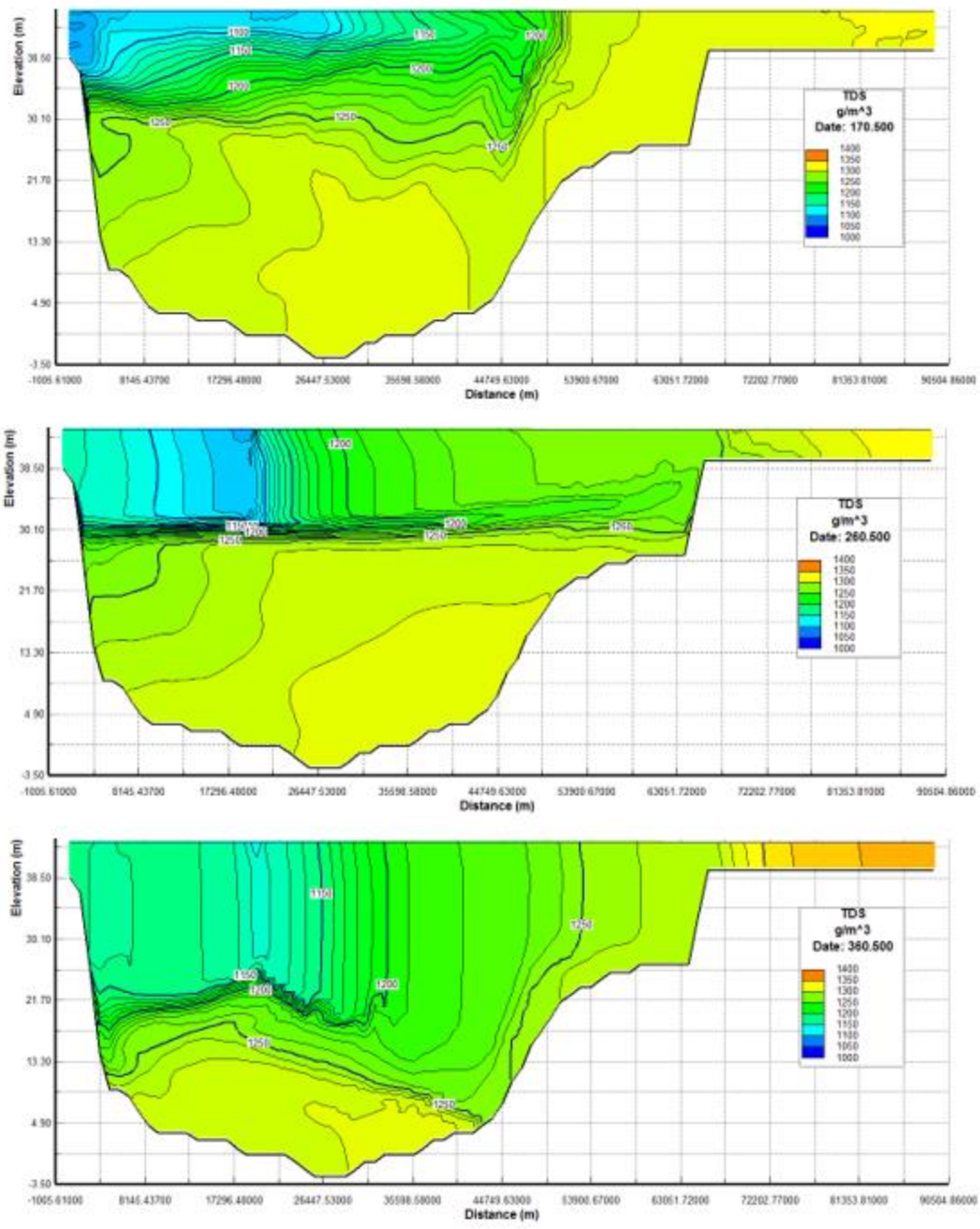

Figure 90: Model contours of TDS in Tharthar Lake at JDAY 170.5, 260.5, and 360.5 of 2009 (Part 2).

Other Water Quality State Variables

Other water quality state variables modeled in this study were phosphate (PO4), ammonium (NH4), nitrate (NO3), biochemical oxygen demand (BOD), algae, and dissolved oxygen (DO). Historical data of water quality state variables at Mosul Dam were determined from other field studies. Water quality constituents for tributaries of the Tigris River were assumed based on data availability from the literature as listed in Table 15 in chapter 5. For both Upper Zab and Lower Zab tributaries, PO4 concentrations were assumed the same. The same assumption was used for NO3 and BOD concentrations, while DO concentrations were estimated based on water temperature at Mosul Dam for the Upper Zab and water temperature at Beaji city for the Lower Zab. On the other hand, for both Audaim and Diyala tributaries, PO4 concentrations were assumed the same. The same assumption was used for NO3 and DO, while BOD concentrations were estimated from literature values. Figure 91 through Figure 96 show model results for PO4, NH4, NO3, DO, CBOD, and Chl-a at Mosul Dam, Samarra Barrage, Tharthar Lake, Baghdad city, and Kut Barrage, respectively. Unfortunately, field data of PO4, NH4, DO, and Chl-a were unavailable for model comparisons. Some monthly average of NO3 field data for the Tigris River at Samarra Barrage and Baghdad city were available, while seasonal BOD field data were available only at Baghdad city for the modeled year 2009 and were used for model comparisons. NO3 concentrations at Mosul Dam were assumed 1.5 mg/l from January 1st to June 30th for better model predictions at Samarra Barrage and Baghdad city as shown in Figure 93.

Model predictions of dissolved oxygen in the mainstem of the Tigris River and Tharthar Lake are shown in Figure 94. DO concentrations decreased during the summer with the exception at Kut Barrage where DO concentrations were relatively high in the period from May to August of the simulated year. This was mostly due to a significant high concentration in chlorophyll-a at Kut Barrage as shown in Figure 96.

Like the TDS calibration approach in Baghdad city, a high mass with a low flowrate of ultimate biochemical oxygen demand (BODu) was introduced into the mainstem of the Tigris River at Baghdad city through model branch 5 located downstream of Samarra Barrage to match seasonal field data as shown in Figure 95. This was essentially adding a mass load to the river. High BOD concentrations within Baghdad city were mainly related to the direct discharge of wastewater treatment plants and other industrial discharges. This was especially important during the summer months when flow in the Tigris River was low.

Model predictions of chlorophyll-a were high below Baghdad city and Tharthar Lake as shown in Figure 96. A sensitivity study, in the next section, was conducted to check if satellite images also show high Chl-a concentrations.

In summary, model predictions of phosphate, ammonium, nitrate, carbonaceous biological oxygen demand, dissolved oxygen, and chlorophyll-a for the base model of the Tigris River system will be compared with management scenarios in the next chapter.

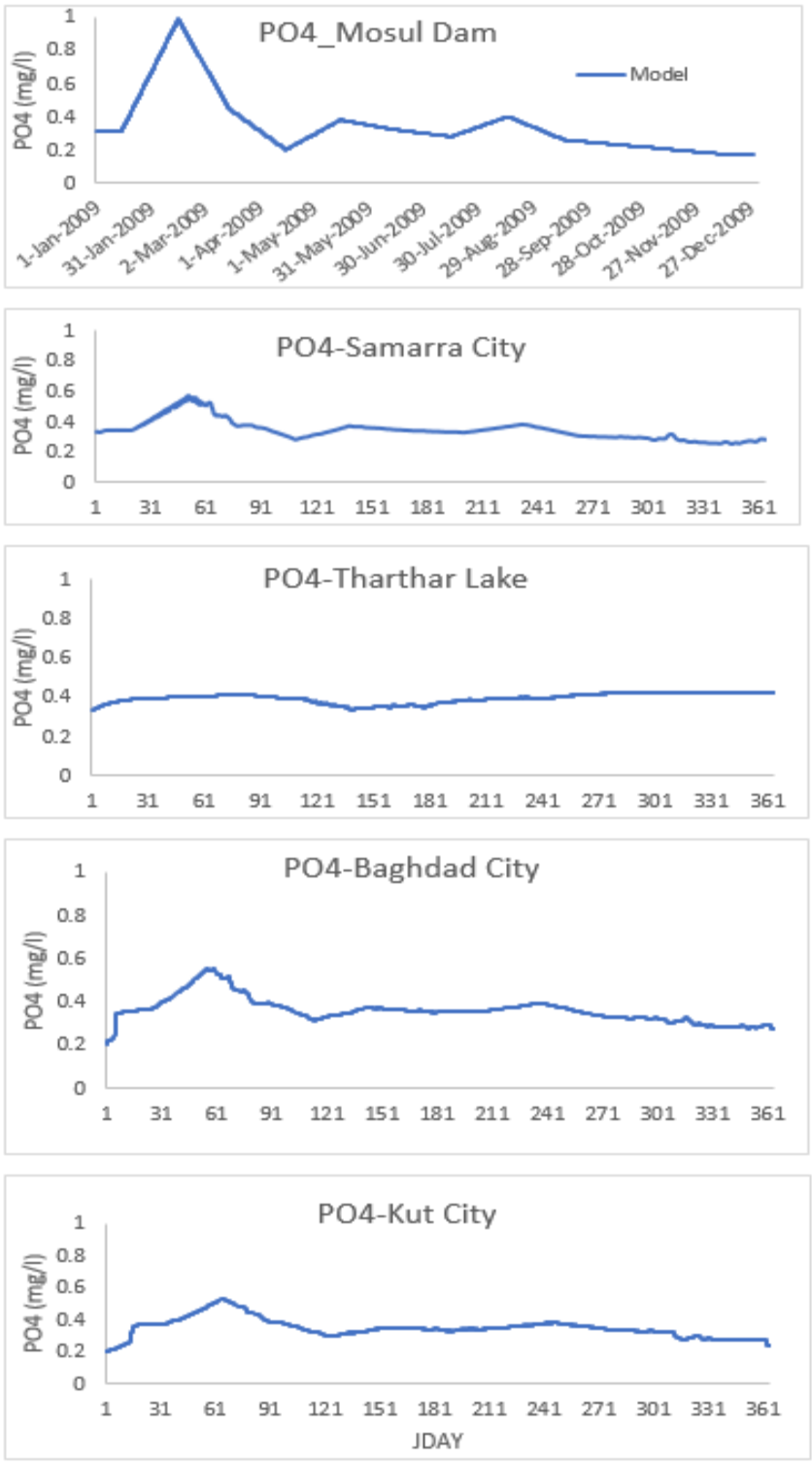

Figure 91: Model PO4 predictions at Mosul Dam, at Samarra Barrage, at Tharthar Lake, at Baghdad City, and at Kut City.

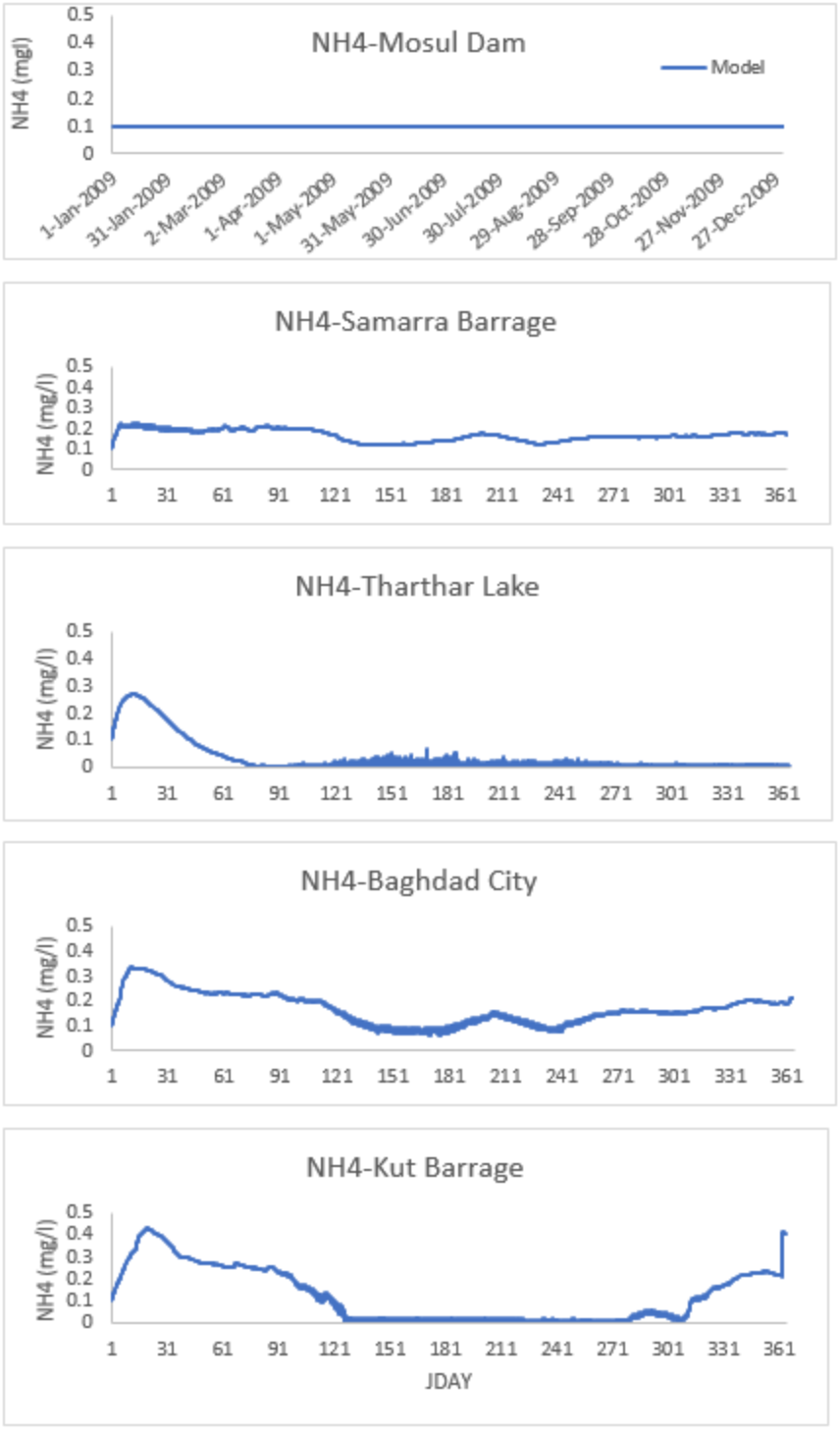

Figure 92: Model Ammonium predictions at Mosul Dam, at Samarra Barrage, at Tharthar Lake, at Baghdad City, and at Kut Barrage.

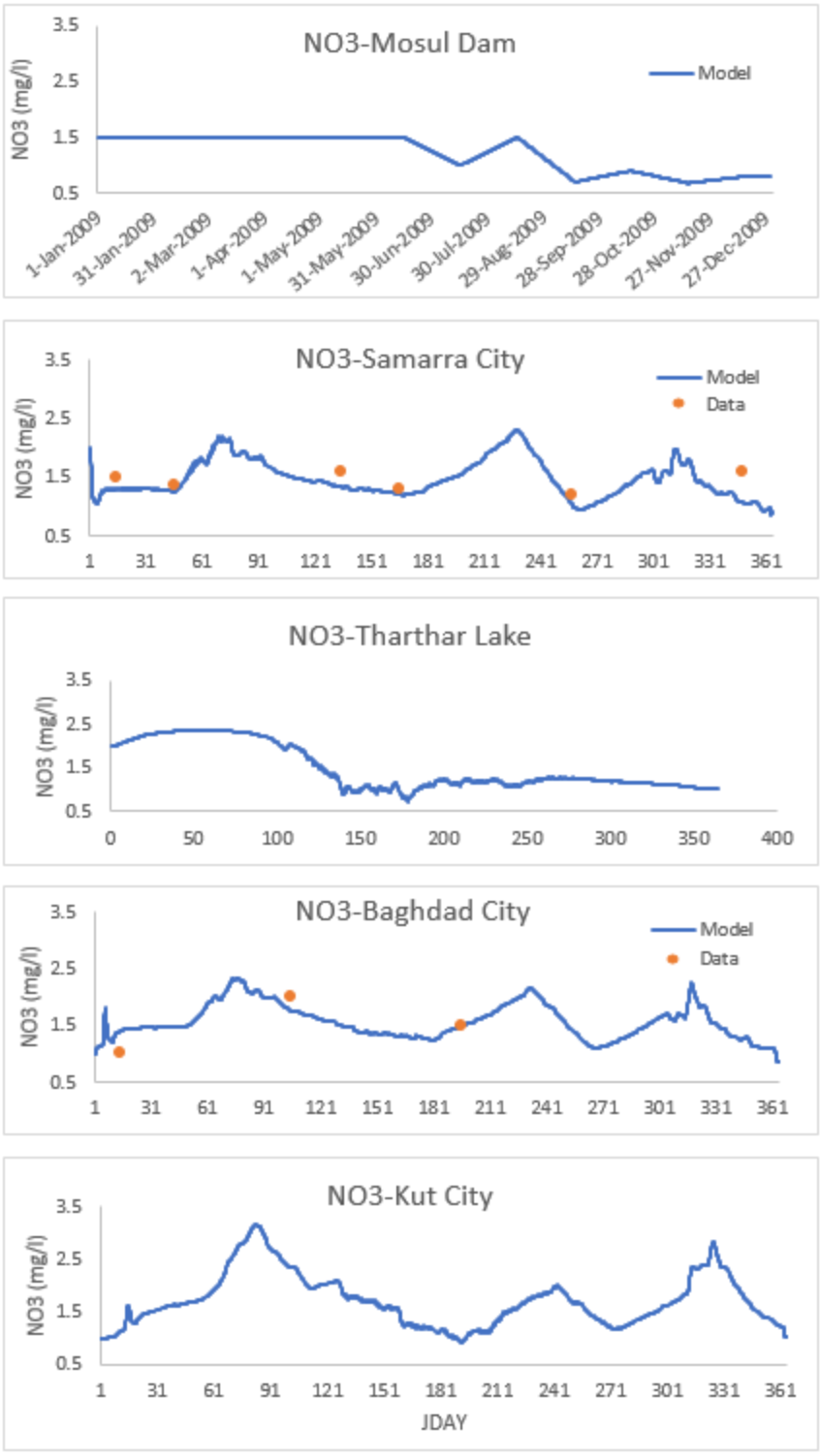

Figure 93: Model Nitrate predictions at Mosul Dam, at Samarra Barrage (model Vs. field data), at Tharthar Lake, at Baghdad City (model Vs. field data), and at Kut City.

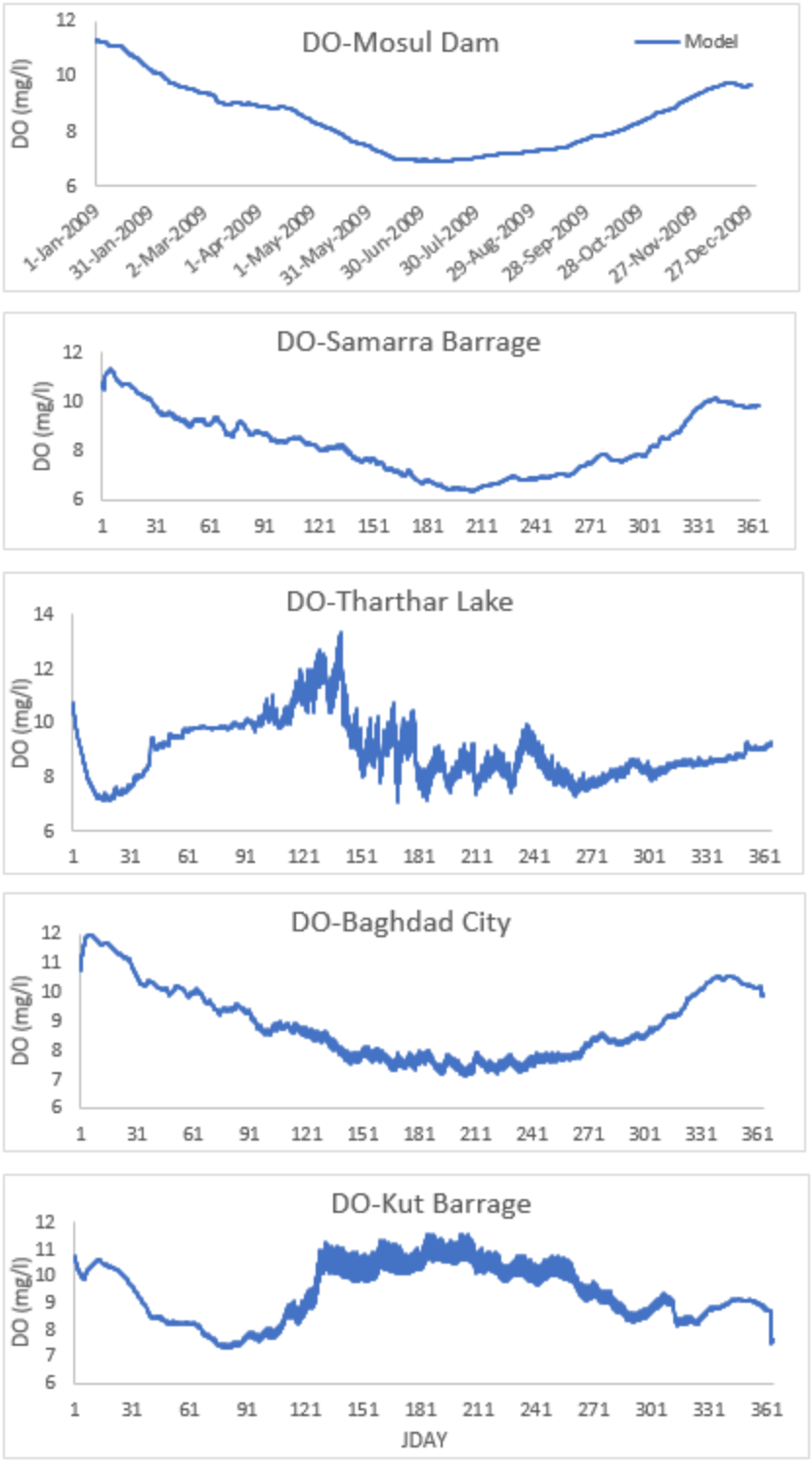

Figure 94: Model Dissolved Oxygen predictions at Mosul Dam, at Samarra Barrage, at Tharthar Lake, at Baghdad City, and at Kut Barrage.

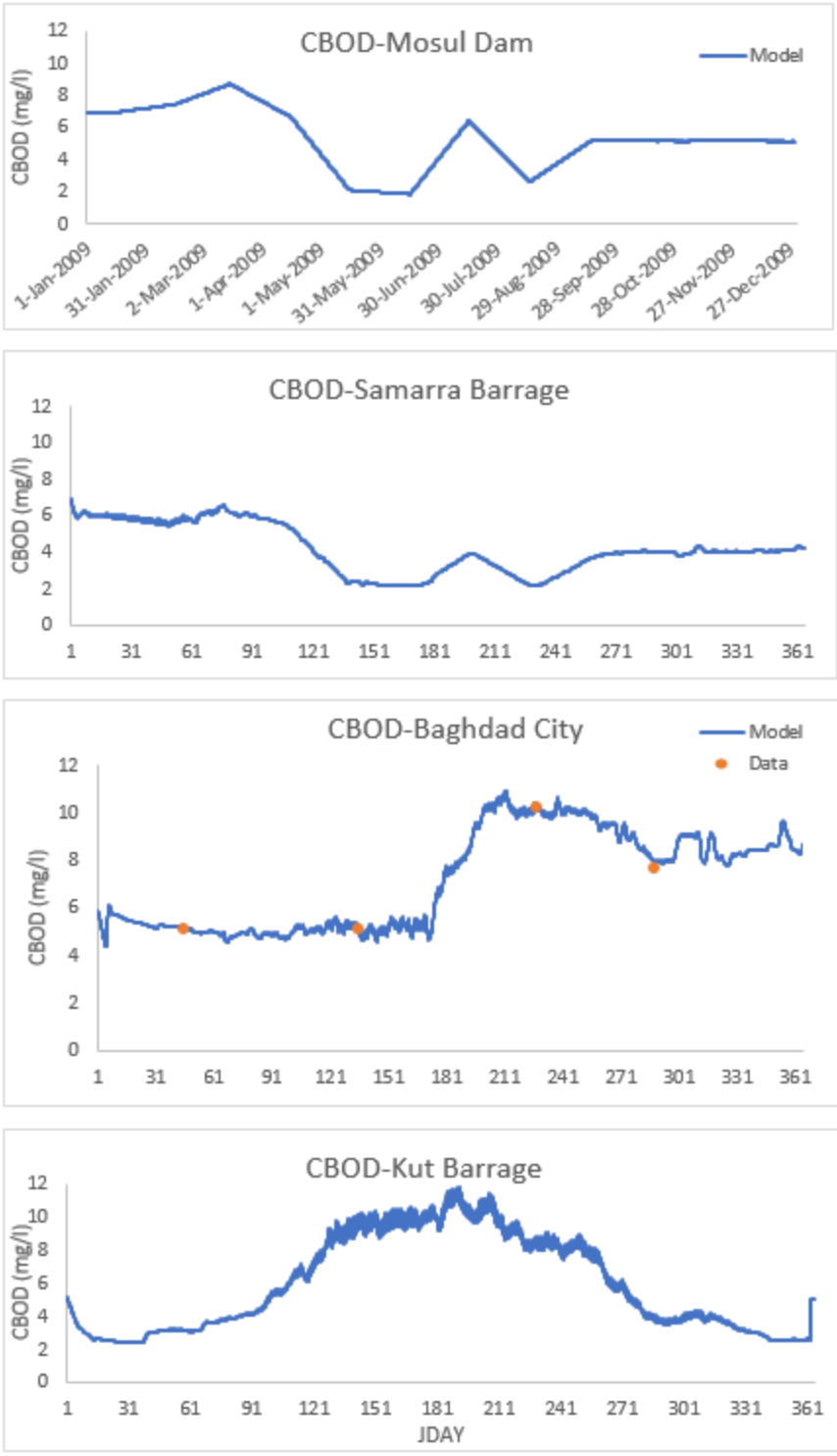

Figure 95: Model CBOD predictions at Mosul Dam, at Samarra Barrage, at Baghdad City (model Vs. field data), and at Kut Barrage.

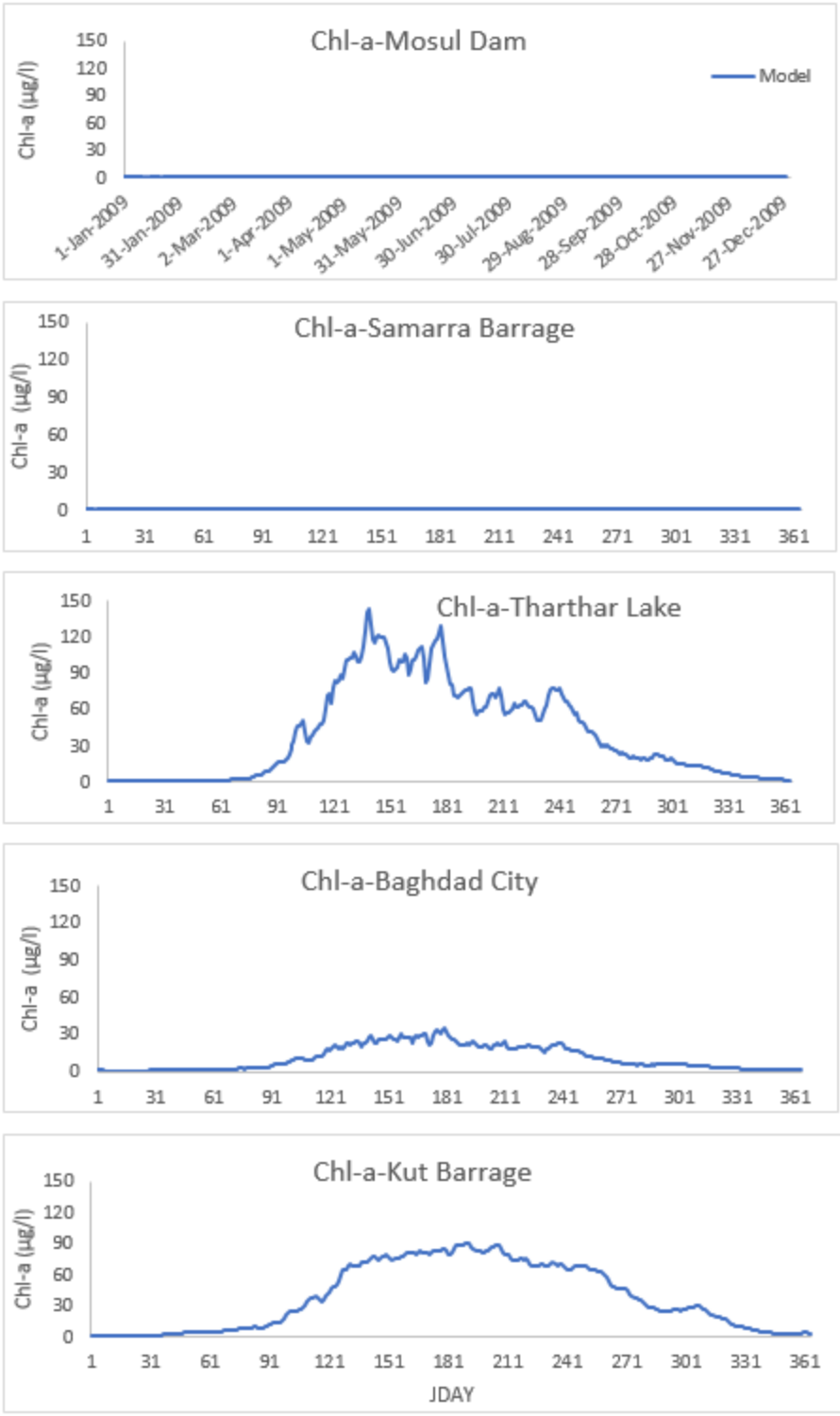

Figure 96: Model Chlorophyll-a predictions at Mosul Dam, at Samarra Barrage, at Tharthar Lake, at Baghdad City, and at Kut Barrage using algae growth rate of 1.5 d^{-1}.

Chlorophyll-a

The model predicts a large growth of algae below Baghdad city and Tharthar Lake. For the base model, a value of 1.5 day^{-1} was set as the maximum algal growth rate [AG] in the control file. A sensitivity study was conducted to check if satellite images also show high Chl-a concentrations using a Chl-a correlation provided from previous literature studies. 13 Landsat 5 TM images with path/row 169/36 were used to extract pixel's reflectance for both band 1 (B1) and band 2 (B2) at a point corresponding to model segment 230 in Tharthar Lake. B1 and B2 values were then used to estimate Chl-a concentration using a Chl-a correlation, Equation 18, estimated by Khattab et al. (2014) that was used to estimate Chl-a in Mosul Dam Lake. Figure 97 shows model predictions of Chl-a for model segment 230 in Tharthar Lake using [AG] of 1.5 d^{-1} compared with satellite data. Model predictions of Chl-a were too high compared with satellite data.

Equation 18: Chl-a correlation estimated by Khattab et al. (2014)

$$Chl - a = 111.236 - 27.416 * \frac{B1}{B2} - 70.17 * \frac{B2}{B1}$$

Multiple simulations were performed to evaluate model sensitivity to [AG]. The best fit was reached using [AG] 0.98 d^{-1}. Figure 98 shows model predictions of Chl-a for model segment 230 in Tharthar Lake using [AG] of 0.98 d^{-1} compared with satellite data. Therefore, the model is sensitive to the maximum algal growth rate.

B1 and B2 values were also estimated in the mainstem of the Tigris River at Baghdad city in an attempt to estimate Chl-a concentrations in the river using the same correlation used for Tharthar Lake. Unfortunately, the correlation did not work out to estimate Chl-a concentrations in the river.

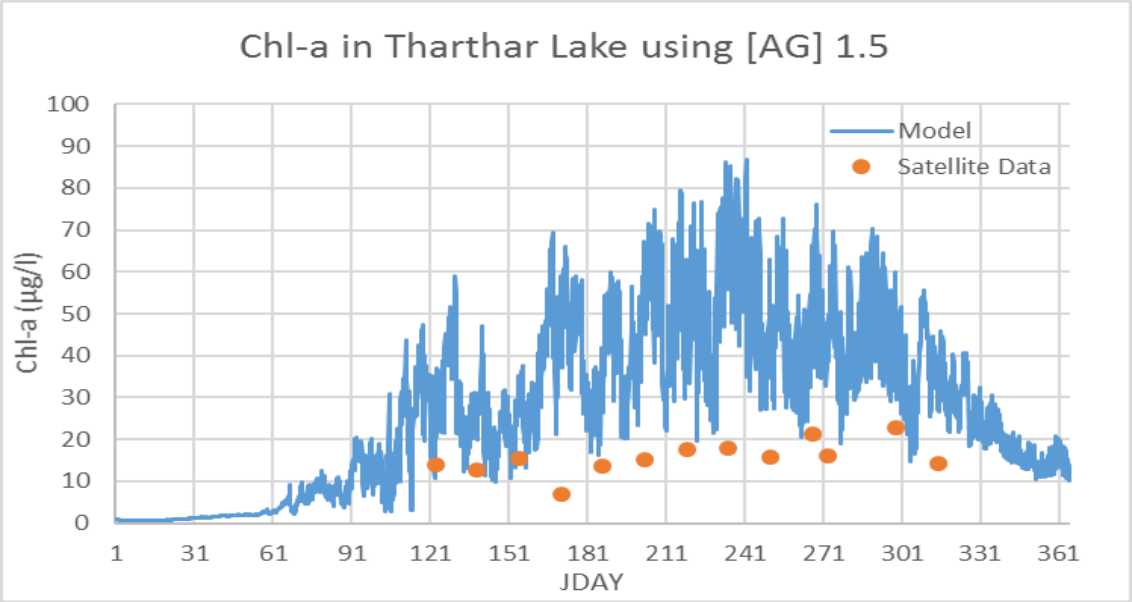

Figure 97: Model predictions of Chl-a in Tharthar Lake using [AG] 1.5 d^{-1} compared with Satellite data.

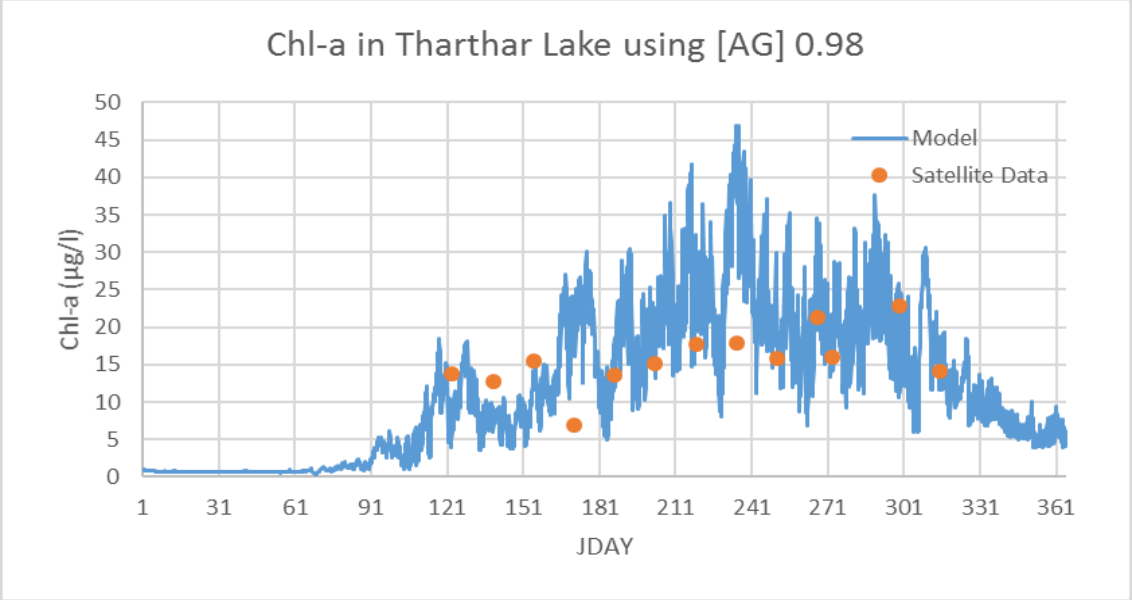

Figure 98: Model predictions of Chl-a in Tharthar Lake using [AG] 0.98 d^{-1} compared with Satellite data.

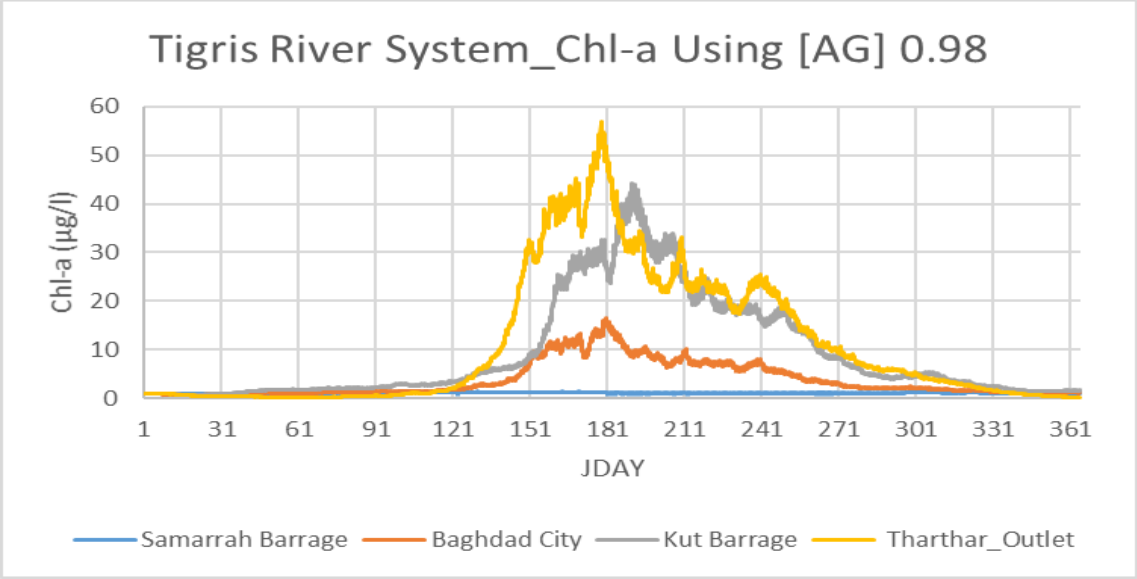

Figure 99: Model predictions of Chl-a in the Tigris River system using [AG] 0.98 d^{-1}

Nutrients

After a sensitivity study was conducted on Chl-a by decreasing algal growth to 0.98 d^{-1}, concentrations of NH4 (Figure 100) and NO3 (Figure 101) in the Tigris River system at Kut Barrage and Tharthar Lake were slightly affected, while no significant change was observed on PO4 concentration over all the Tigris River system.

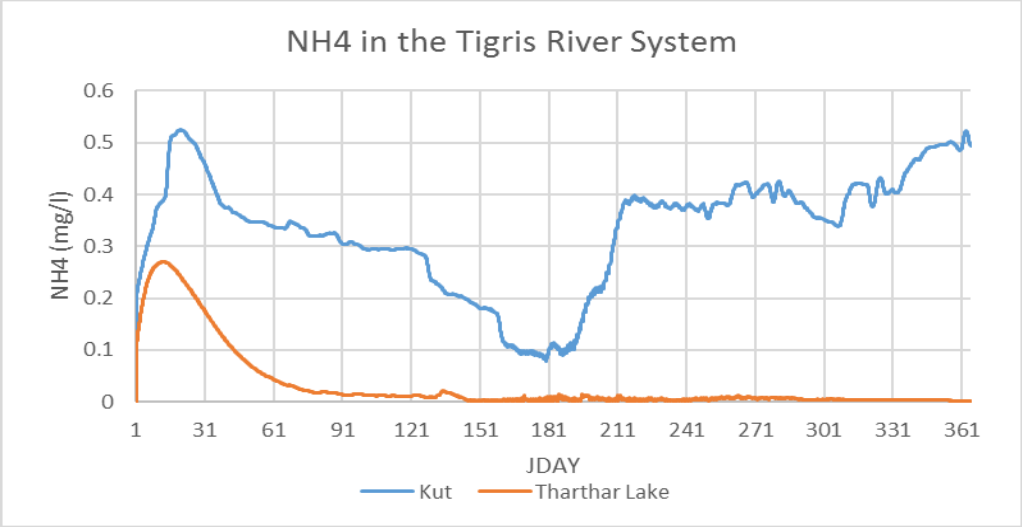

Figure 100: Model predictions of NH4 in Kut Barrage and Tharthar Lake.

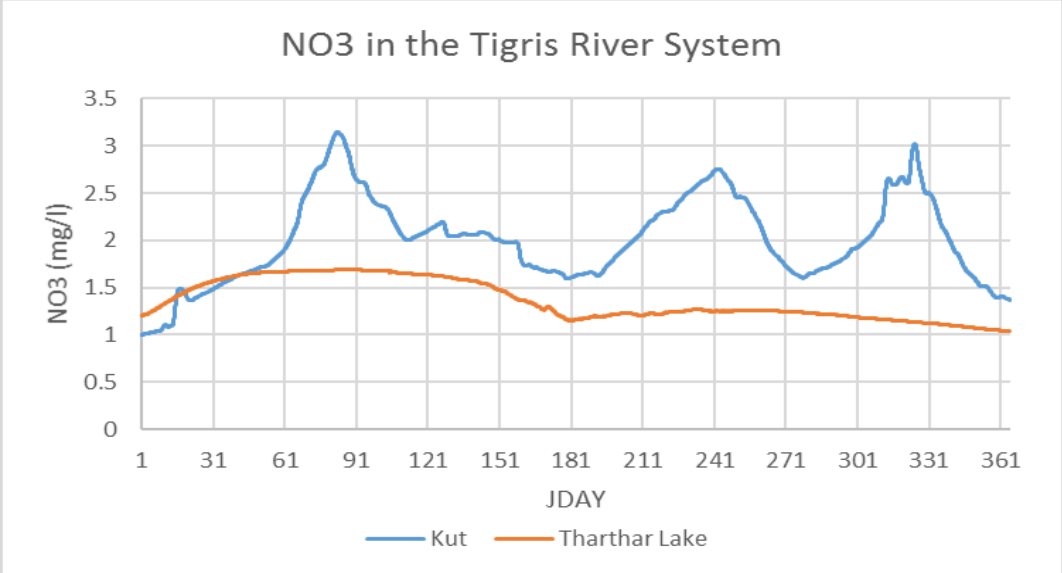

Figure 101: Model predictions of NO3 in Kut Barrage and Tharthar Lake.

Chapter Seven: The Tigris River Management Scenarios

Multiple management scenarios were applied to the model inputs to simulate the effect of changing flow regime (hydrology), upstream increase in nutrient concentrations from Turkey, the impact of climate change, disconnection of Tharthar Lake from the Tigris River system, and a 6-year simulation of the Tigris River model evaluating longer-term changes inn Tharthar Lake. Model scenarios were chosen based on potential change in upstream flow and nutrient concentrations from Turkey, future increase in air temperatures, and potential decrease in TDS concentrations in the mainstem of the Tigris River. Management scenarios were then compared with the base model of the simulated year 2009. For each management scenario, only pertinent results are showed and discussed, while the remaining results that caused little change are discussed and placed in appendix A. Table 24 lists all management scenarios applied to the Tigris River system.

Table 24: The Tigris River management scenarios

Run #	Description	Year 2009	6-Year Model	Existing Flow Conditions	Existing Meteorological data	Existing Nutrients	Increasing Upstream Flow	Decreasing Upstream Flow	Increasing Nutrients	Climate Change	Decreasing BOD by 50%
1	Base Model	X		X	X	X					
2	Increasing Upstream Flow	X			X	X	X				
3	Decreasing Upstream Flow	X			X	X		X			
4	Decreasing Upstream Flow with increasing nutrients	X			X			X	X		
5	Increasing Tharthar Lake's Flow from Samarra Barrage	X			X	X	X				
6	Climate change	X		X		X				X	
7	Climate change with decreasing upstream flow	X				X		X		X	
8	Disconnecting Tharthar Lake	X		X	X	X					
9	Decreasing BOD by 50%	X		X	X	X					X
10	Base Model		X	X	X	X					

Historical Hydrology of the Tigris River System

Hydrology of the Tigris River system has been significantly impacted by flows entering Iraq at the Turkey-Iraq border. Historical flow regime of the Tigris River at Mosul city before and after Mosul Dam operation in July 1986 is shown in Figure 102. Compared with the mean annual flow before Mosul Dam operation, the mean annual flow of the Tigris River system decreased by 12% after Mosul Dam operation in July 1986. Also, the mean annual discharge at Mosul city before 1984 was 701 m^3/s and dropped to 596 m^3/s afterwards. This is a 15% decrease of the river discharge (Al-Ansari and Knutsson, 2011). This is because of the construction projects that have been built in Turkey after 1984 causing increased upstream utilization.

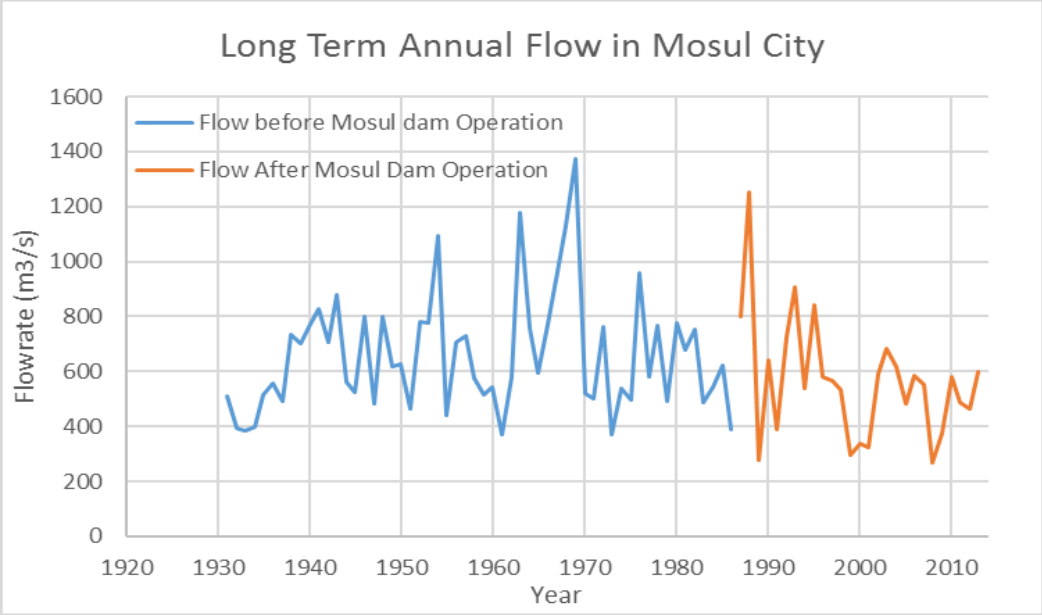

Figure 102: Historical flow regime in Mosul city before and after Mosul Dam Operation.

Management Scenario 1: Increasing Upstream Flow

Since the mean annual flow of the Tigris River system has decreased by 15% after the Mosul Dam was put into operation in July 1986, the first management scenario increased the mainstem flow by 15% and compared the results with the base. Figure 103 and Figure 104 show model predictions of management scenario 1 for total dissolved solids (TDS) and carbonaceous biological oxygen demand (CBOD) at Samarra Barrage, Baghdad city, Kut Barrage, and Tharthar Lake. Model predictions for water temperature (T_w), phosphate (PO4), ammonium (NH4), nitrate (NO3), dissolved oxygen (DO), and chlorophyll-a are shown in appendix A. Predictions of management scenario 1 were compared with the base model of the Tigris River system.

Due to an increase in upstream flowrate, most of water quality constituents were decreased compared with the base model with the exception of water temperature and DO. Since TDS is a conservative state variable and decreased by dilution, TDS concentrations decreased from 495 mg/l to 470 mg/l in the mainstem and from 1239 mg/l to 1226 mg/l in Tharthar Lake. CBOD concentrations decreased from 5.9 mg/l to 5.74 mg/l.

No major changes were observed in water temperature predictions in scenario 1 with an average temperature changed from 20.7 ° C to 20.8 ° C over all the mainstem of the river. No major changes were observed in model predictions for nutrients with a negligible decrease in PO4, NH4, and NO3 by 0.1%, 0.1%, and 1.3%, respectively in the mainstem of the Tigris River. Also, DO and Chl-a concentrations increased negligibly over all the mainstem of the river from 8.15 mg/l to 8.2 mg/l and from 1.97 µg/l to 2 µg/l, respectively.

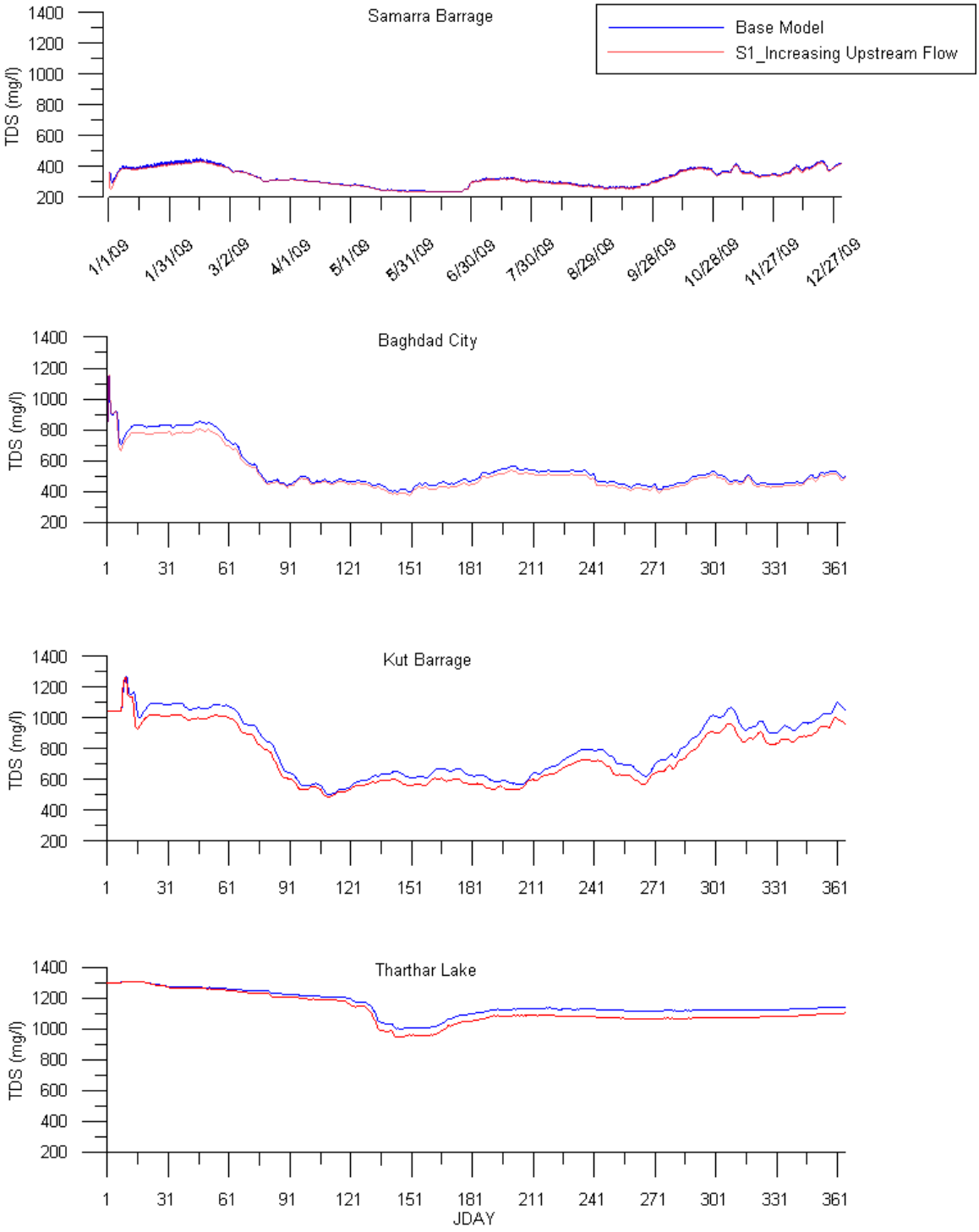

Figure 103: Model total dissolved solids (TDS) predictions for base model and management scenario 1 (increasing upstream flow) at Samarra Barrage, Baghdad City, Kut Barrage, and Tharthar Lake.

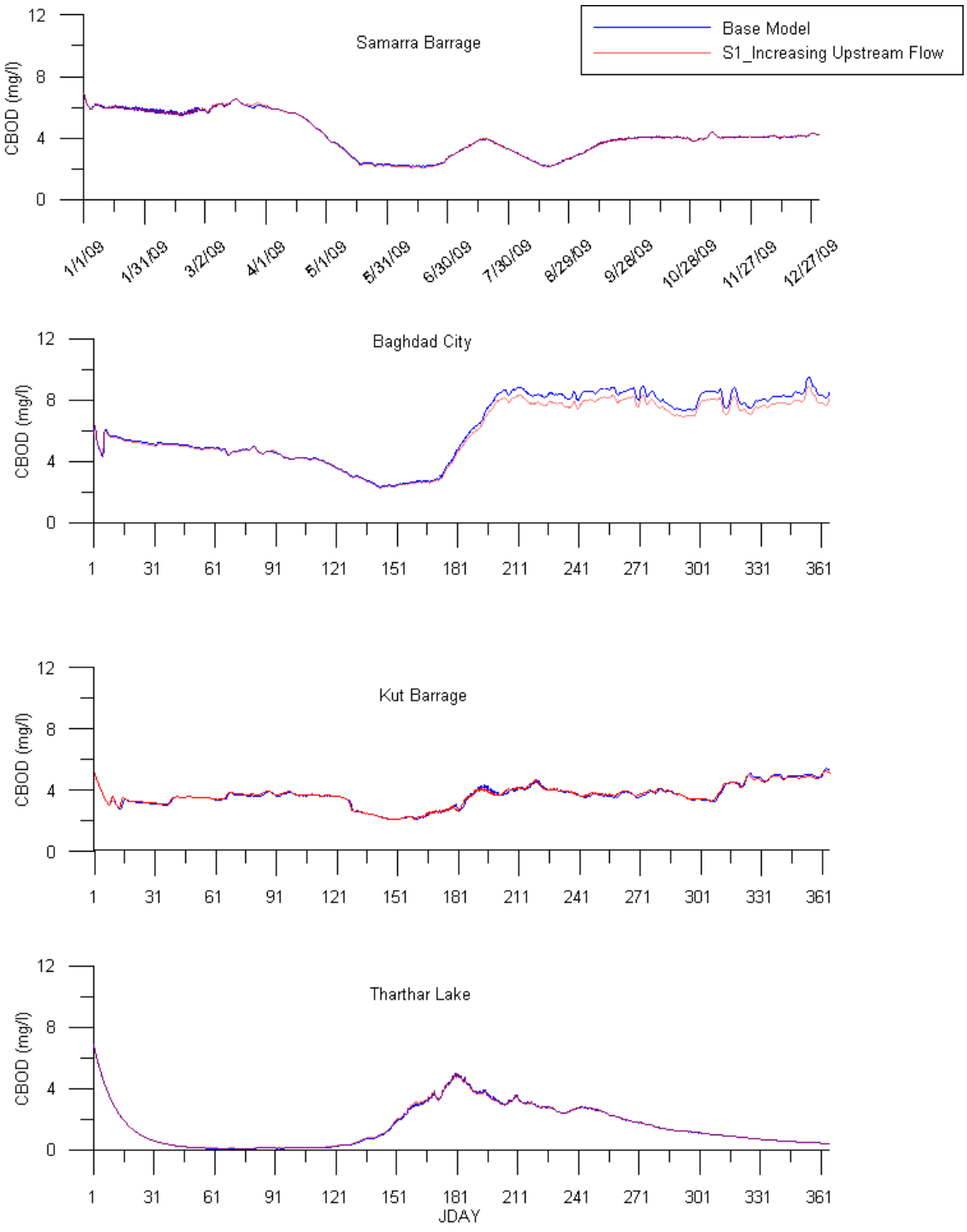

Figure 104: Model carbonaceous biological oxygen demand (CBOD) predictions for base model and management scenario 1 (increasing upstream flow) at Samarra Barrage, Baghdad City, Kut Barrage, and Tharthar Lake.

Management Scenario 2: Decreasing Upstream Flow

The upstream flow boundary condition of the Tigris River system at Mosul Dam was decreased by 15% to study the effect of altering flow on the mainstem of the river and thereby also decreasing the flow to Tharthar Lake. Figure 105 through Figure 109 show model predictions of management scenario 2 for total dissolved solids, phosphate, ammonium, nitrate, and carbonaceous biological oxygen demand, respectively at Samarra Barrage, Baghdad city, Kut Barrage, and Tharthar Lake. Model predictions for water temperature, dissolved oxygen, and chlorophyll-a are shown in appendix A. Predictions of management scenario 2 were compared with the base model of the Tigris River system.

As was expected, concentrations of the most of water quality constituents increased with decreasing upstream flow at Mosul Dam due to decrease in dilution. TDS concentrations were increased from 495 mg/l to 527 mg/l in the mainstem and from 1239 mg/l to 1253 mg/l in Tharthar Lake. Concentrations of PO4, NH4, and NO3 in the mainstem were increased from 0.35 mg/l, 0.23 mg/l, and 1.54 mg/l to 0.36 mg/l, 0.25 mg/l, and 1.57 mg/l, respectively. CBOD concentrations increased from 5.9 mg/l to 6.2 mg/l. There was no significant impact on water temperature, dissolved oxygen, and chlorophyll-a.

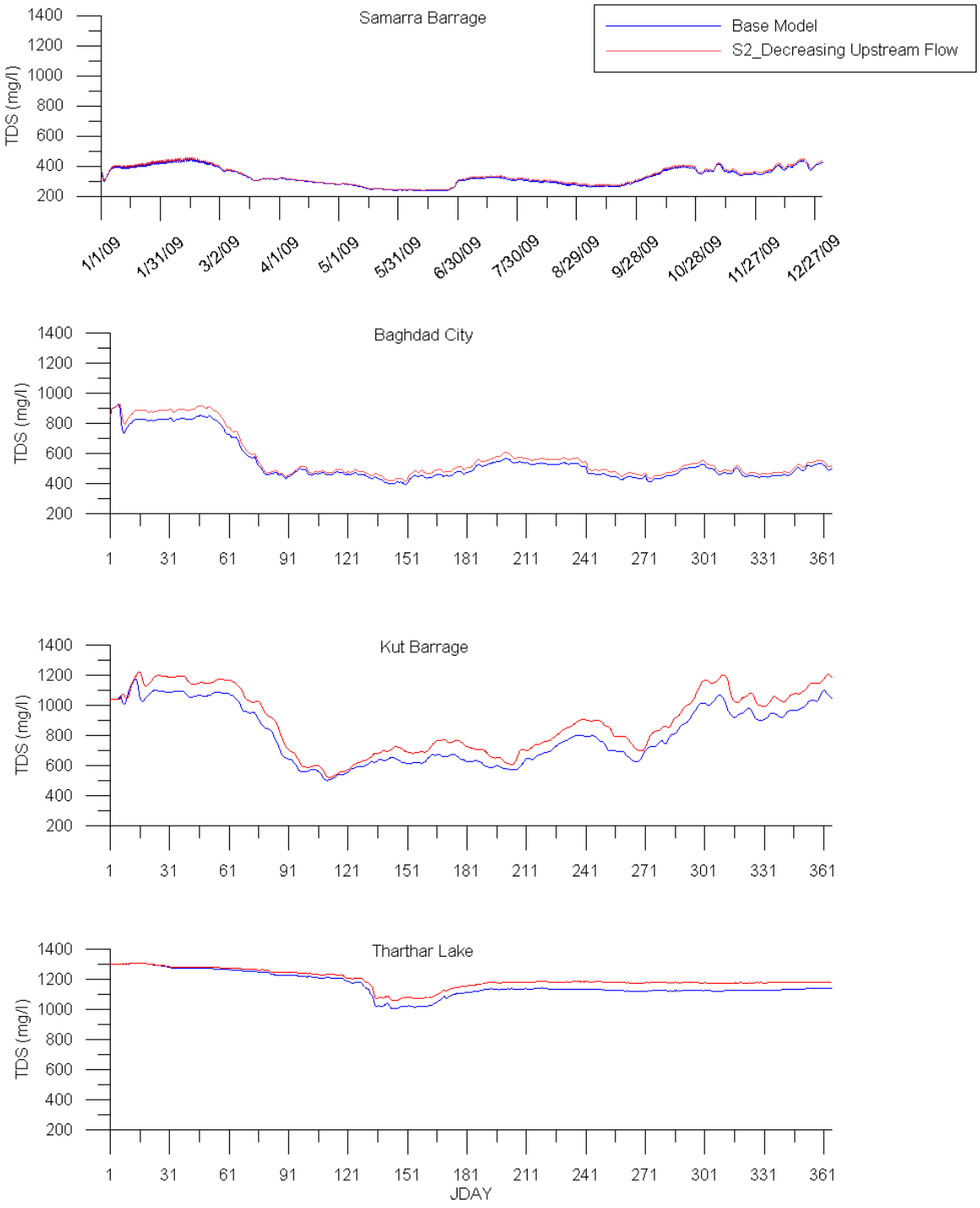

Figure 105: Model total dissolved solids (TDS) predictions for base model and management scenario 2 (decreasing upstream flow) at Samarra Barrage, Baghdad City, Kut Barrage, and Tharthar Lake.

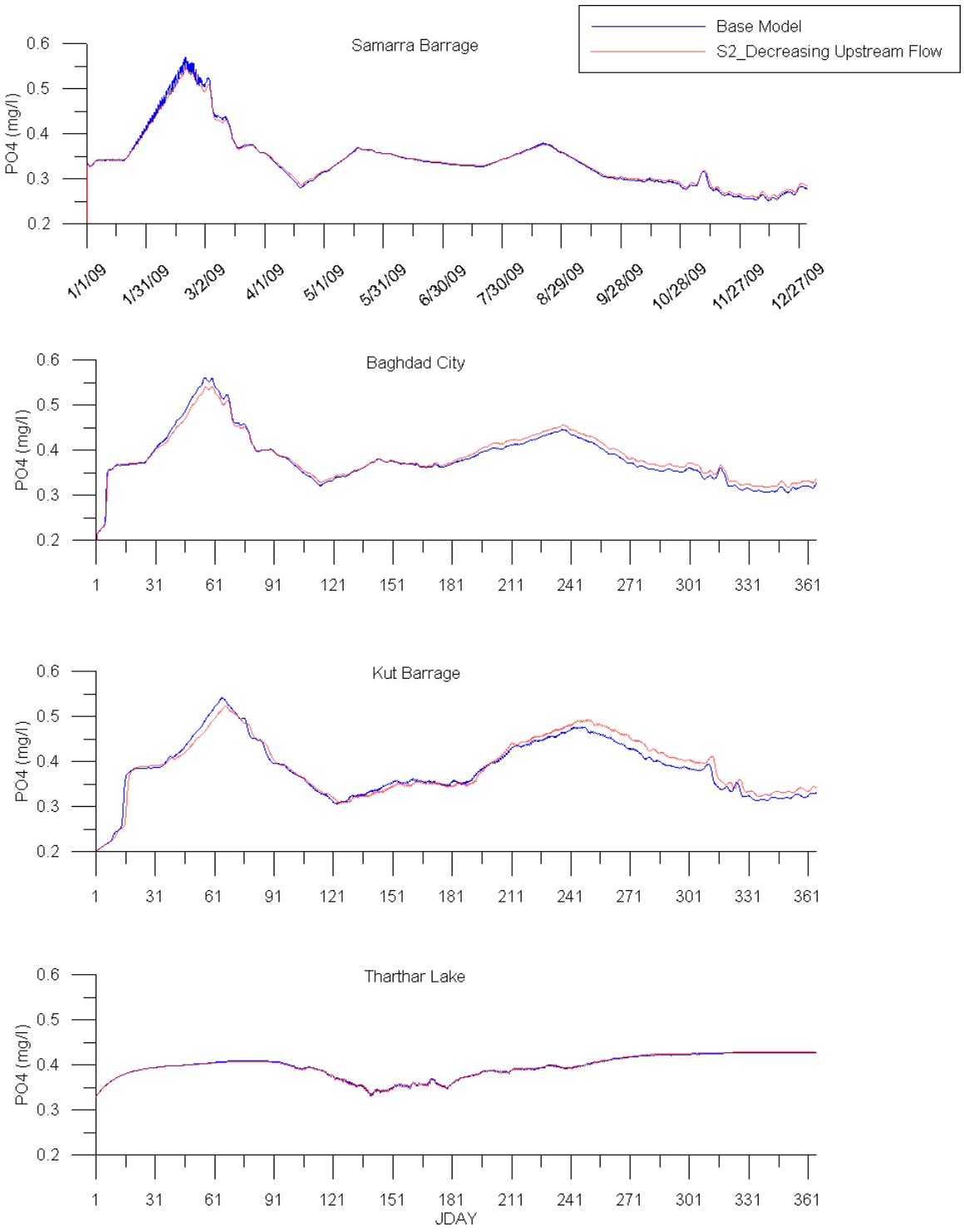

Figure 106: Model phosphate (PO4) predictions for base model and management scenario 2 (decreasing upstream flow) at Samarra Barrage, Baghdad City, Kut Barrage, and Tharthar Lake.

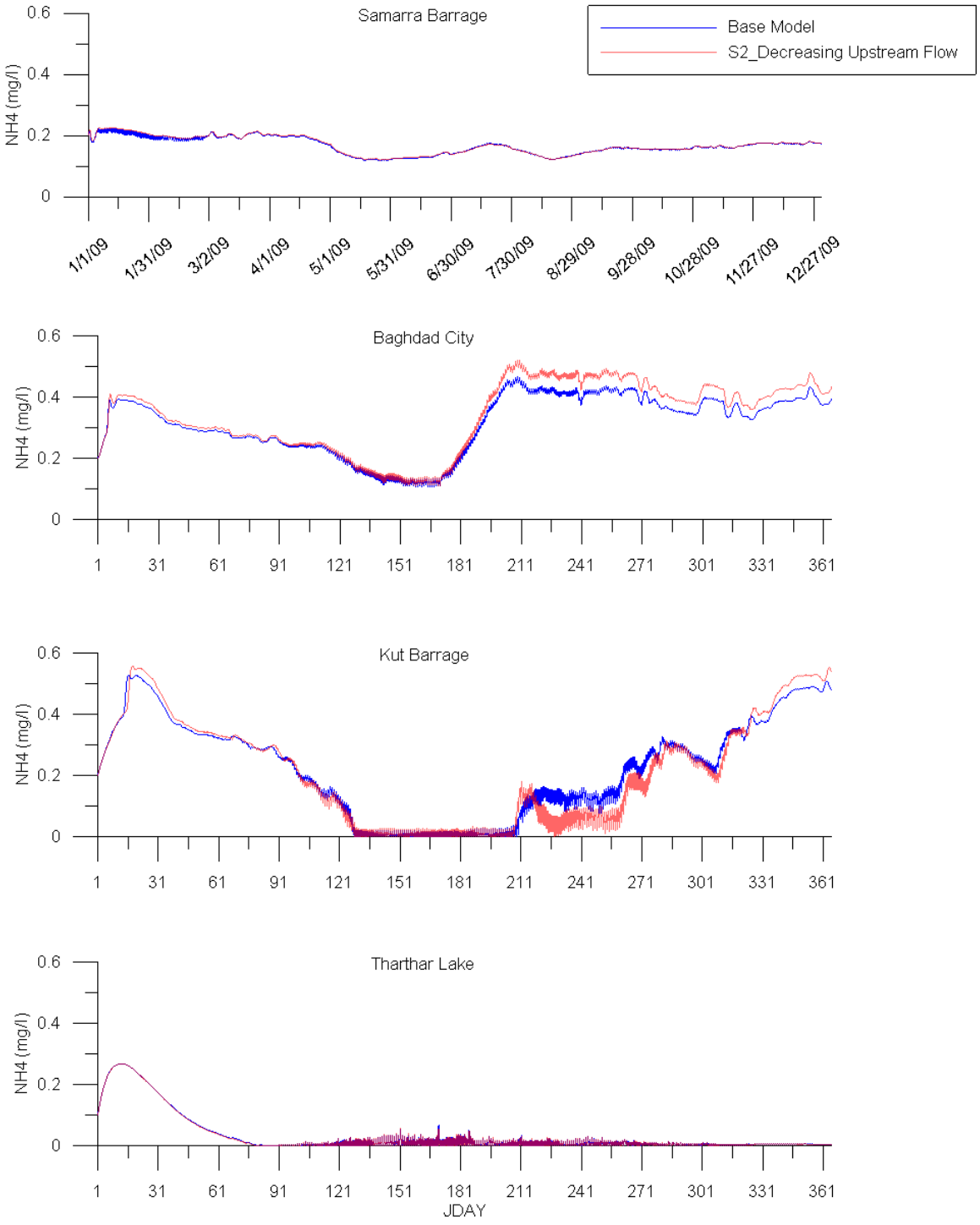

Figure 107: Model ammonia (NH4) predictions for base model and management scenario 2 (decreasing upstream flow) at Samarra Barrage, Baghdad City, Kut Barrage, and Tharthar Lake.

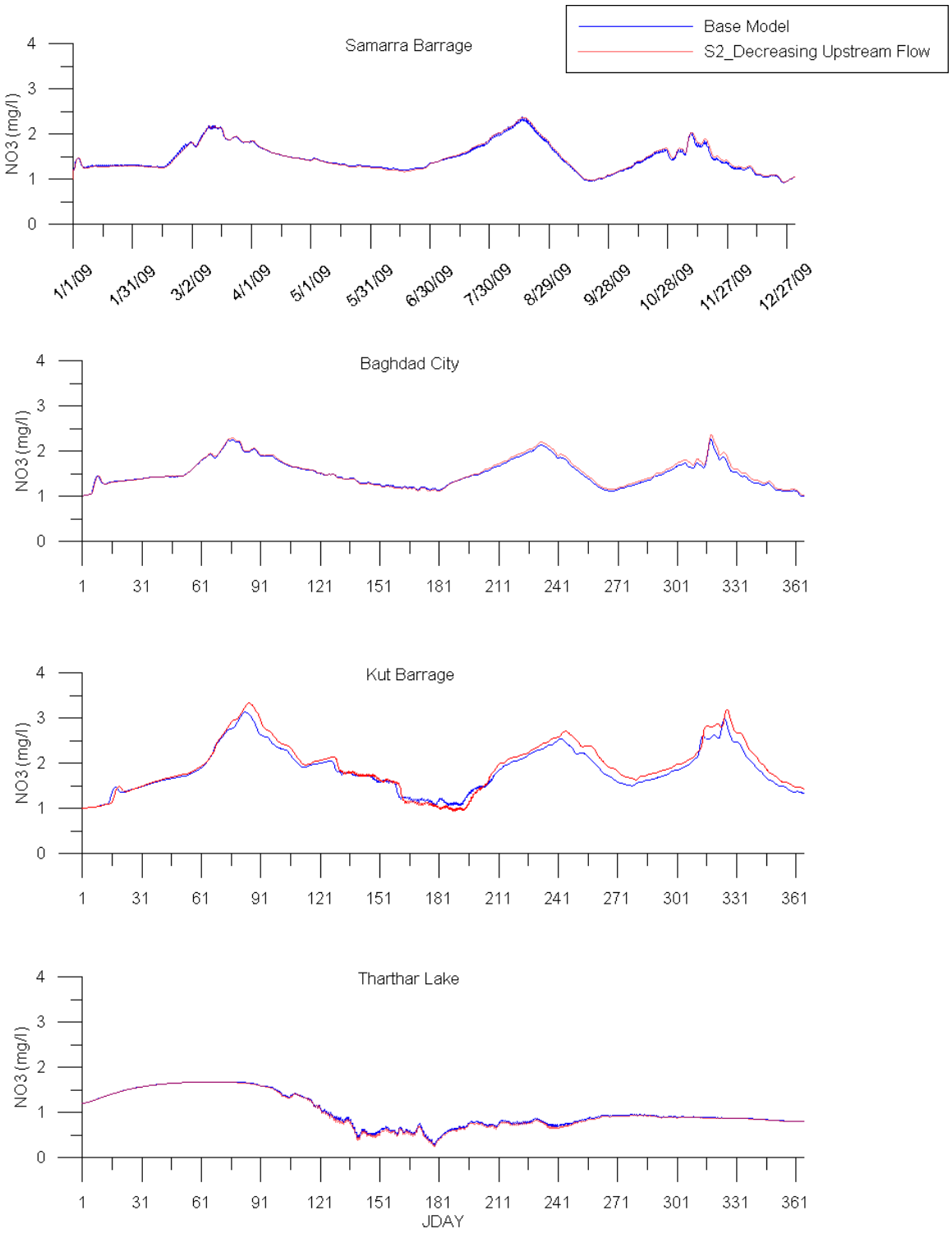

Figure 108: Model nitrate (NO3) predictions for base model and management scenario 2 (decreasing upstream flow) at Samarra Barrage, Baghdad City, Kut Barrage, and Tharthar Lake.

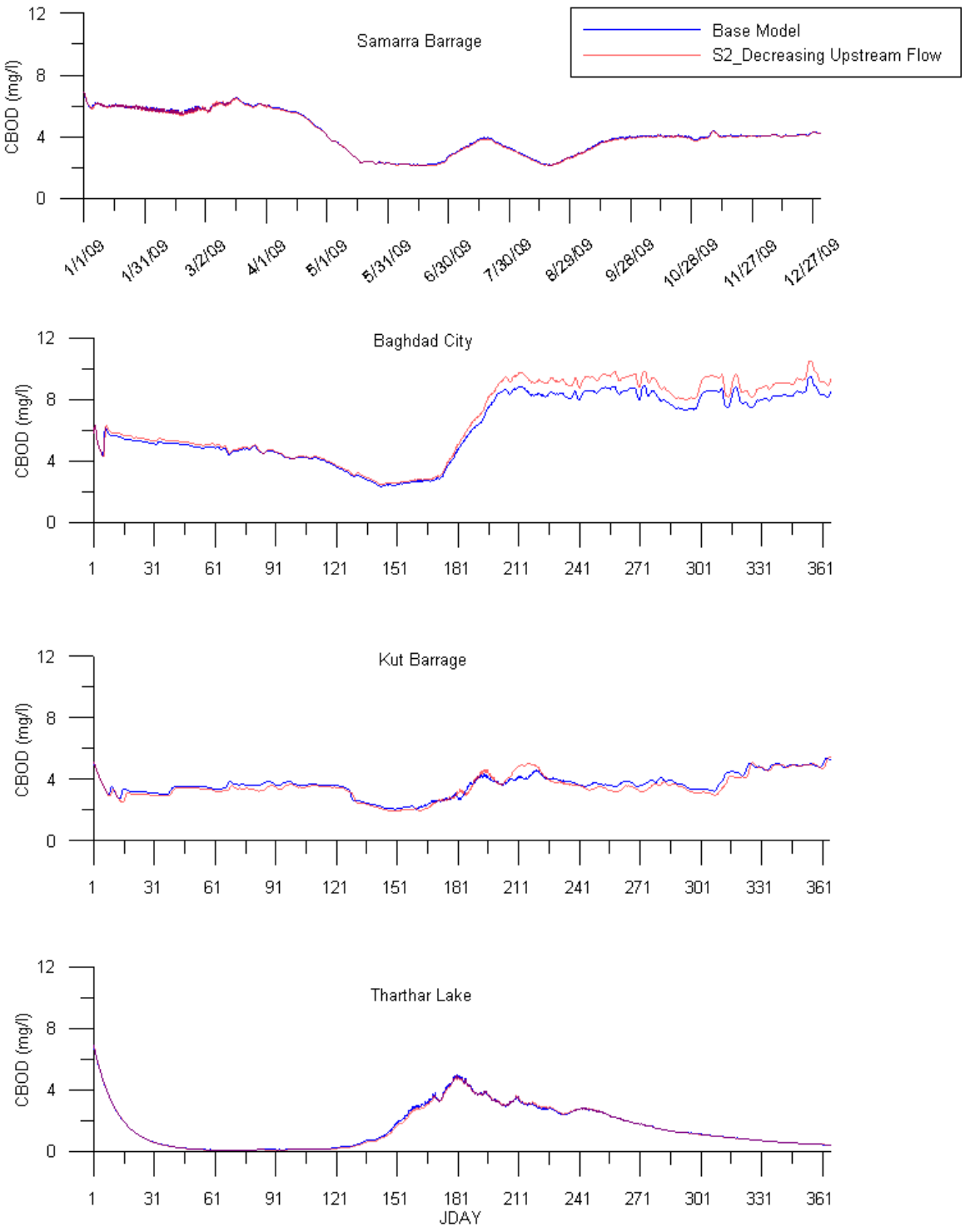

Figure 109: Model carbonaceous biological oxygen demand (CBOD) predictions for base model and management scenario 2 (decreasing upstream flow) at Samarra Barrage, Baghdad City, Kut Barrage, and Tharthar Lake.

Management Scenario 3: Decreasing Upstream Flow and Increasing Nutrients

Assuming a future increase in nutrient concentrations at Mosul Dam, a 10% increase in phosphate, ammonium, and nitrate concentrations was implemented along with a 15% decrease in upstream flow boundary conditions at Mosul Dam. Figure 110 through Figure 114 show model predictions of management scenario 3 for total dissolved solids, phosphate, ammonium, nitrate, and carbonaceous biological oxygen demand, respectively, at Samarra Barrage, Baghdad city, Kut Barrage, and Tharthar Lake. Model predictions for water temperature, dissolved oxygen, and chlorophyll-a are shown in appendix A. Predictions of management scenario 3 were compared with the base model of the Tigris River system.

In this scenario, a similar trend in water quality concentrations was noticed as in scenario 2 with a slight increase in nutrient concentrations. Compared with the base model, TDS concentrations increased by 9% in the mainstem and by 1.2% in Tharthar Lake. Concentrations of PO4, NH4, and NO3 increased in the mainstem from 0.35 mg/l, 0.23 mg/l, and 1.54 mg/l to 0.37 mg/l, 0.25 mg/l, and 1.63 mg/l respectively. CBOD concentrations increased from 5.9 mg/l to 6.2 mg/l. There were no significant impacts on water temperature and dissolved oxygen.

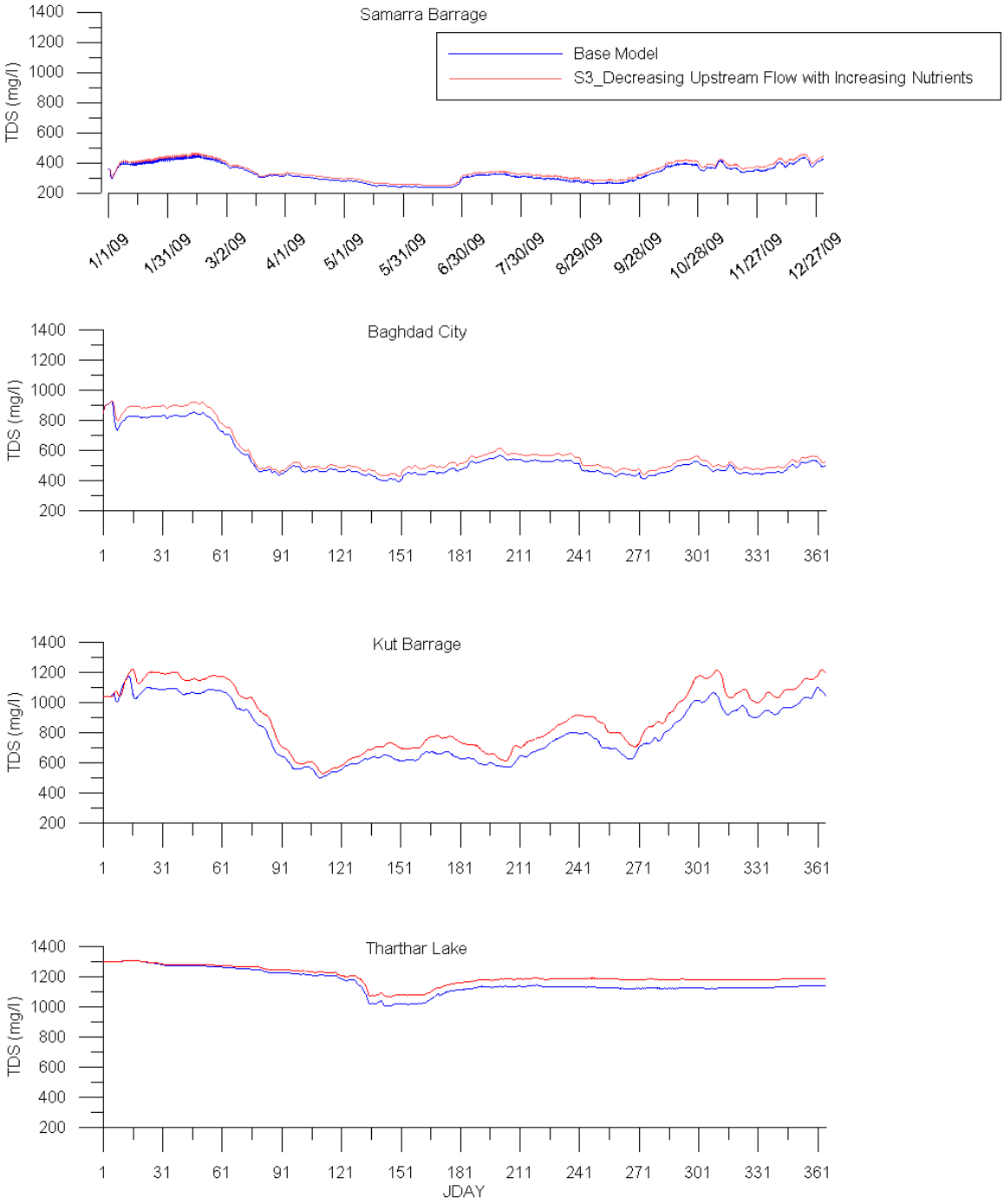

Figure 110: Model total dissolved solids (TDS) predictions for base model and management scenario 3 (decreasing upstream flow with increasing nutrients) at Samarra Barrage, Baghdad City, Kut Barrage, and Tharthar Lake.

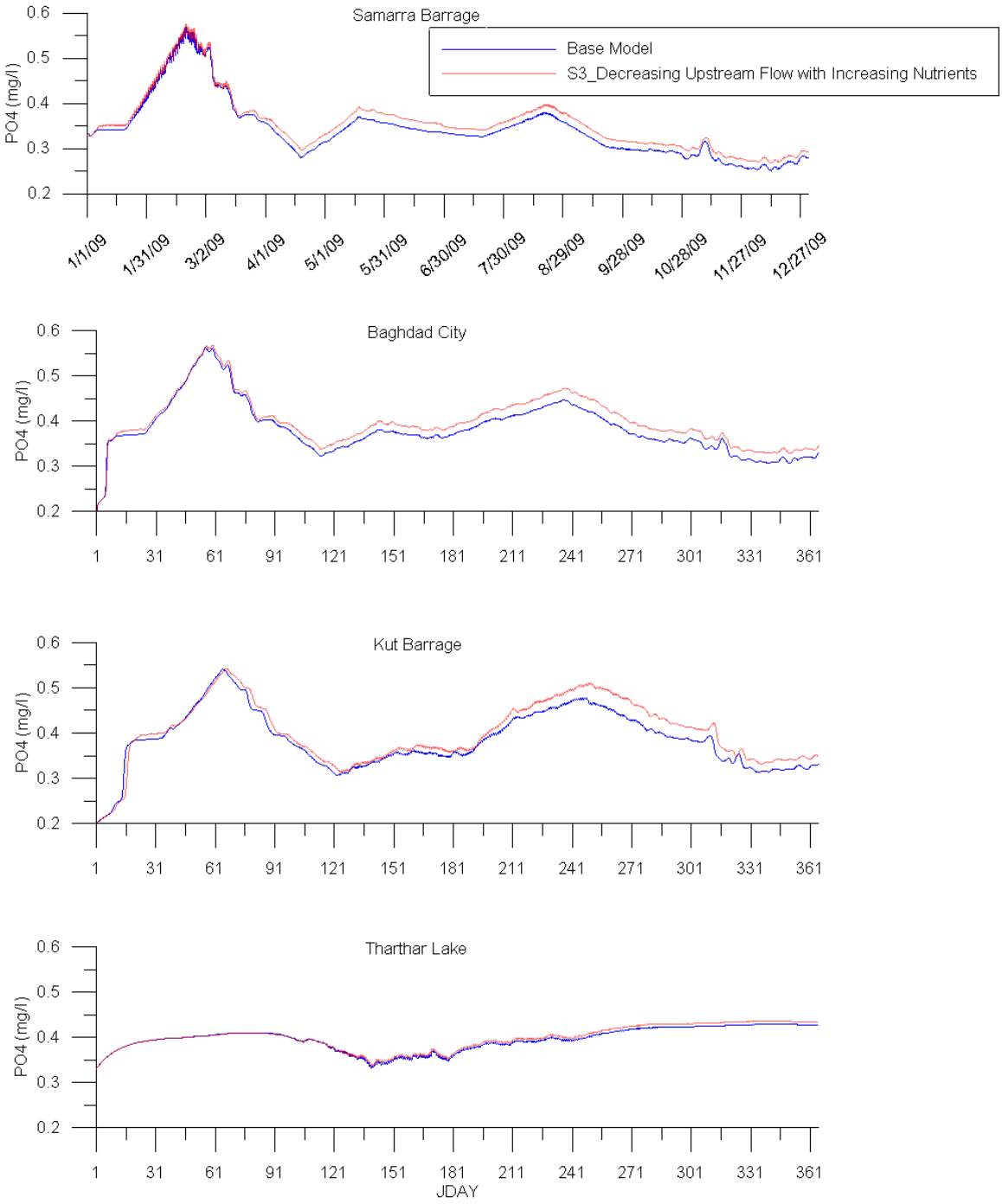

Figure 111: Model phosphate (PO4) predictions for base model and management scenario 3 (decreasing upstream flow with increasing nutrients) at Samarra Barrage, Baghdad City, Kut Barrage, and Tharthar Lake.

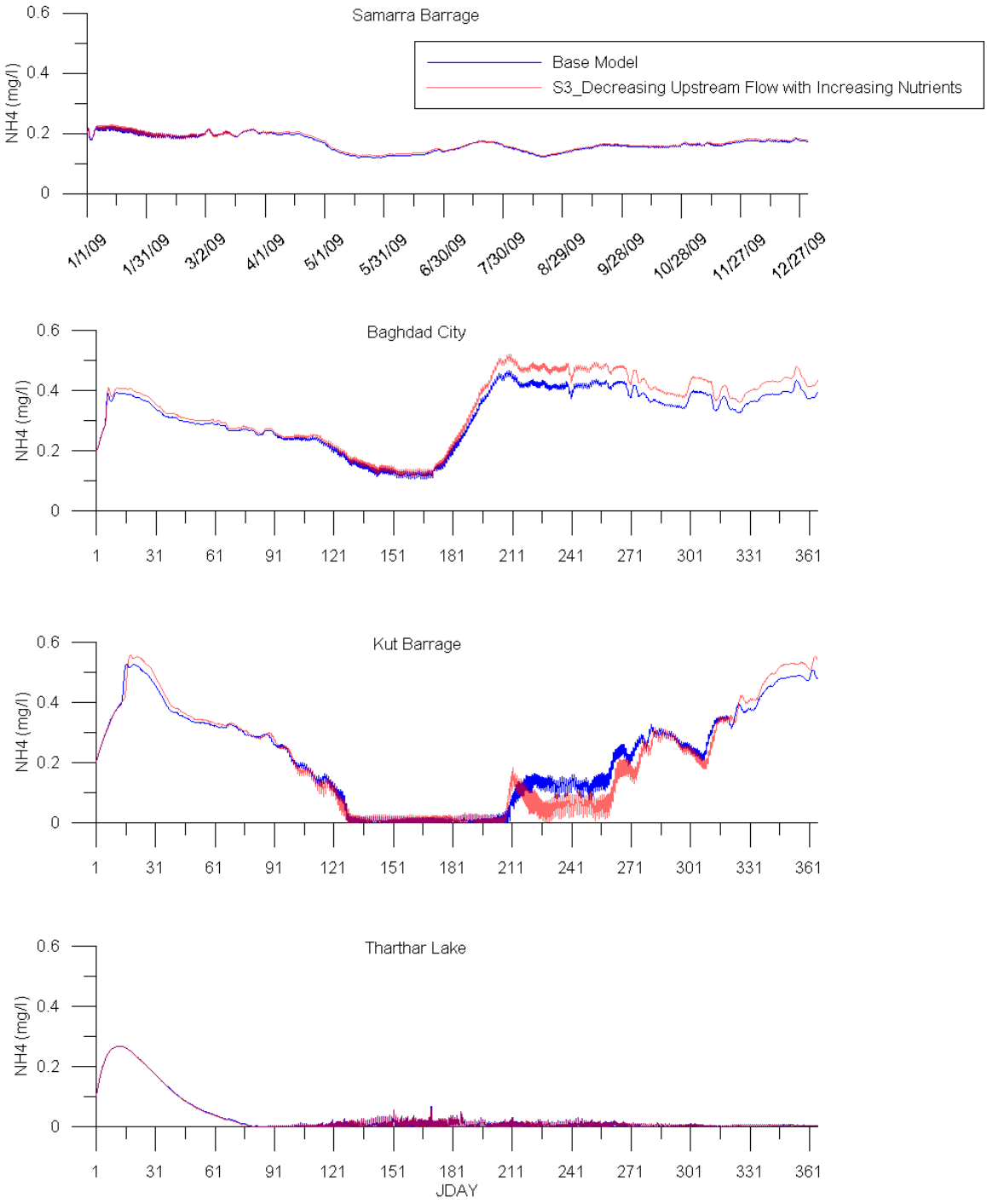

Figure 112: Model ammonia (NH4) predictions for base model and management scenario 3 (decreasing upstream flow with increasing nutrients) at Samarra Barrage, Baghdad City, Kut Barrage, and Tharthar Lake.

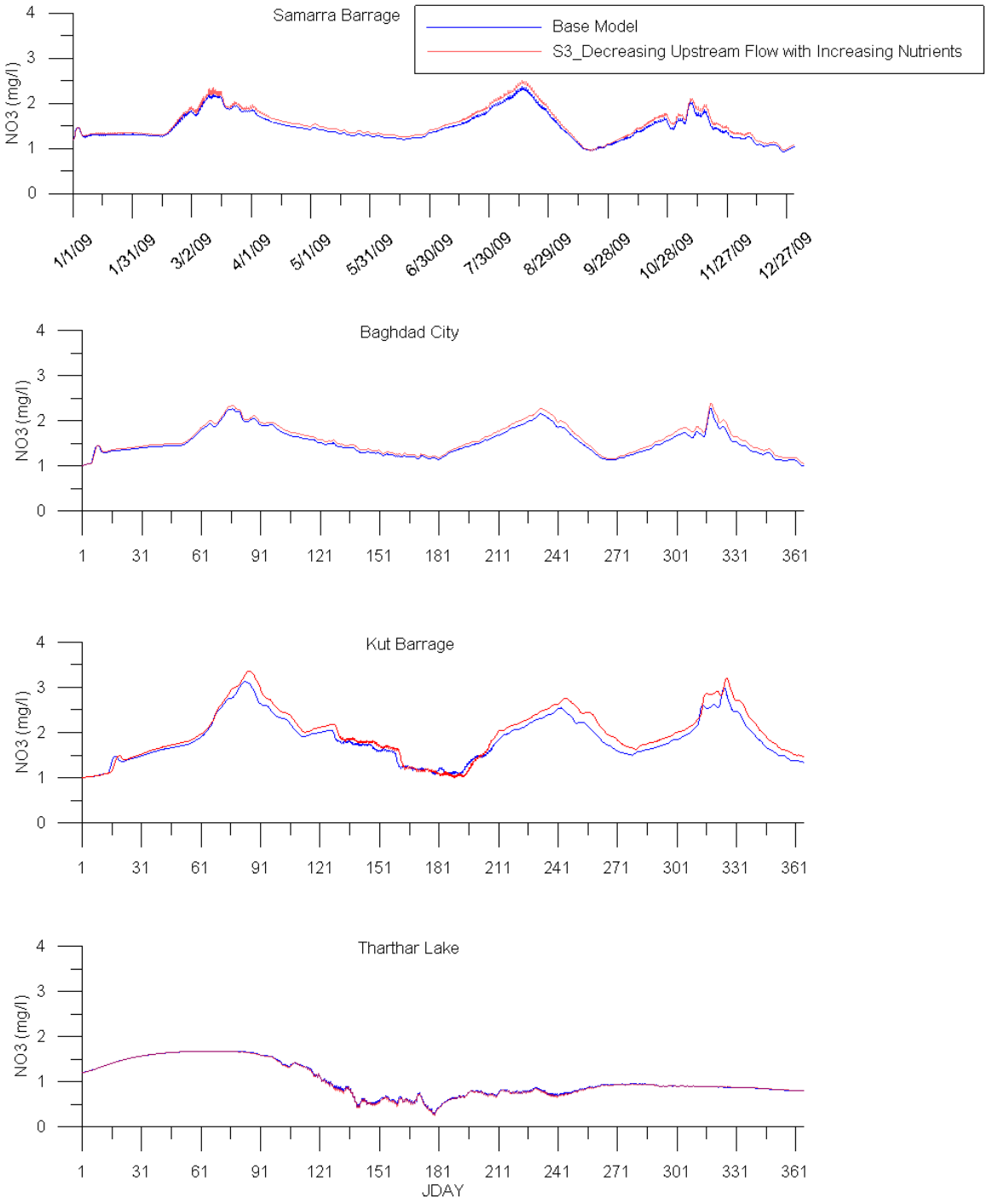

Figure 113: Model nitrate (NO3) predictions for base model and management 3 (decreasing upstream flow with increasing nutrients) at Samarra Barrage, Baghdad City, Kut Barrage, and Tharthar Lake.

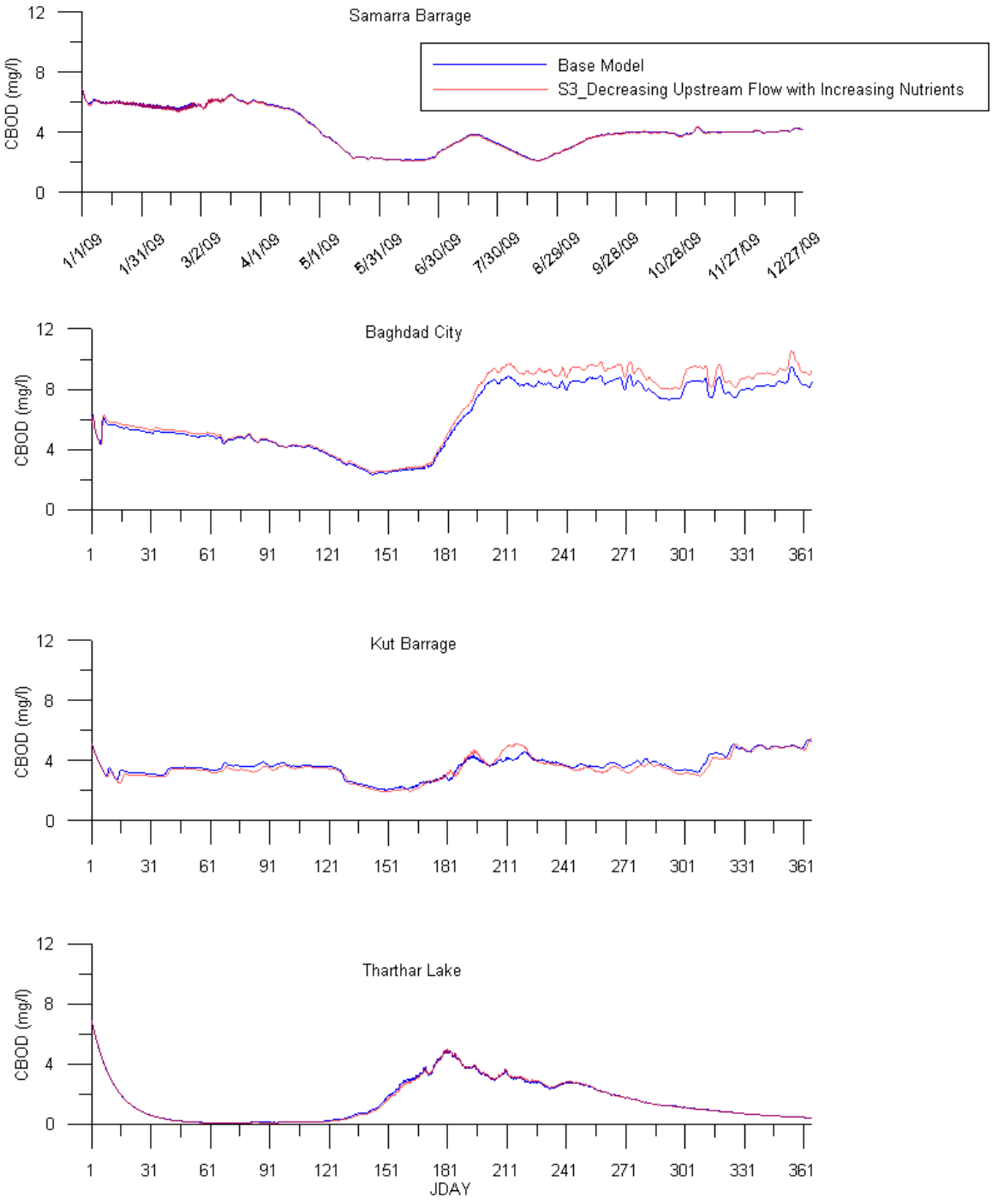

Figure 114: Model carbonaceous biological oxygen demand (CBOD) predictions for base model and management scenario 3 (decreasing upstream flow with increasing nutrients) at Samarra Barrage, Baghdad City, Kut Barrage, and Tharthar Lake.

Management Scenario 4: Increasing Tharthar Lake's Flow

In this management scenario, a 10% increase in flow was diverted from Samarra barrage to Tharthar Lake through Tigris-Tharthar canal to study the effect of increasing the lake's flow on Tharthar Lake and the mainstem of the Tigris River downstream Samarra Barrage. Figure 115 shows model predictions of management scenario 4 for total dissolved solids at Samarra Barrage, Baghdad city, Kut Barrage, and Tharthar Lake. Model predictions of phosphate, ammonium, nitrate, carbonaceous biological oxygen demand, and chlorophyll-a are shown in appendix A. Predictions of management scenario 4 were compared with the base model of the Tigris River system.

There was no substantial impact on TDS concentrations in the mainstem with an average concentration decreased from 495 mg/l to 493 mg/l, while a decrease from 1239 mg/l to 1231 mg/l was recorded in Tharthar Lake. There were no major changes in water temperature, nutrients, CBOD, DO, and Chl-a.

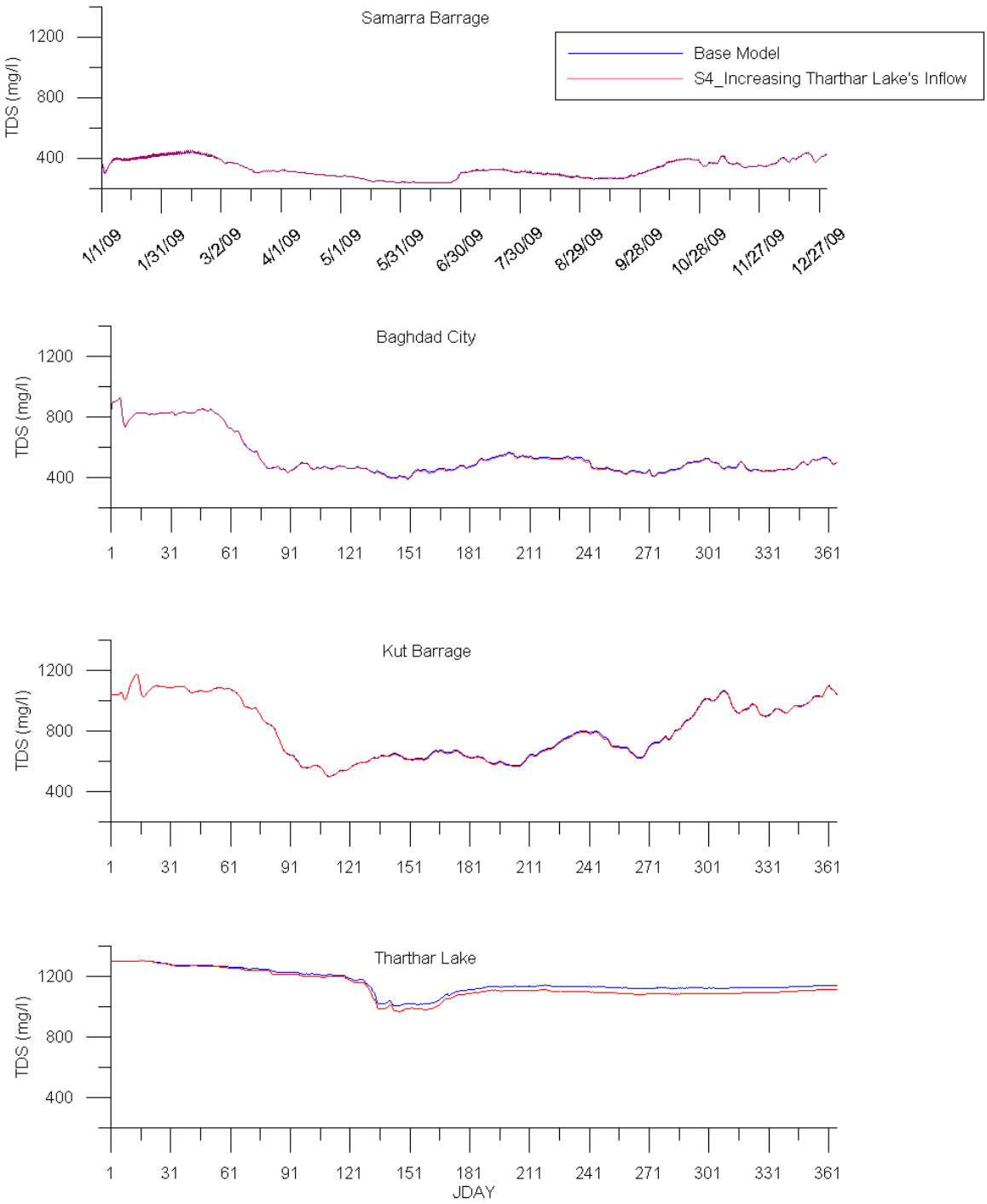

Figure 115: Model total dissolved solids (TDS) predictions for base model and management scenario 4 (increasing Tharthar Lake's inflow) at Samarra Barrage, Baghdad City, Kut Barrage, and Tharthar Lake.

Management Scenario 5: The Effect of Climate Change

Climate change was evaluated on the Tigris River system assuming that air temperature was increased by 2 ° C. This affected all the meteorological input files for the Tigris River model. Assuming constant relative humidity, dew point temperatures were then estimated based on Equation 19:

Equation 19: Dew point Temperature estimation (Wanielista, 1997)

$$T_{dewpoint} = (\frac{RH}{100})^{\frac{1}{8}} * (112 + 0.9 * T) + 0.1 * T - 112$$

Figure 116 shows the new dewpoint temperatures compared with that of the base model at Mosul, Baeji, and Baghdad cities. The average change in dew point temperature over the simulated year 2009 at Mosul, Baeji, and Baghdad cities are 24%, 22%, and 24%, respectively. The climate change management scenario was implemented and compared to the base model.

Figure 117 through Figure 119 show model predictions of management scenario 5 for water temperature, dissolved oxygen, and chlorophyll-a respectively at Samarra Barrage, Baghdad city, Kut Barrage, and Tharthar Lake. Model predictions of total dissolved solids, phosphate, ammonium, nitrate, and carbonaceous biological oxygen demand are shown in appendix A. Predictions of management scenario 5 were compared with the base model of the Tigris River system.

Water temperature increased by 5% with an average temperature increased from 20.7 ° C to 21.7 ° C in the mainstem and from 17.44 ° C to 18.35 ° C in Tharthar Lake. On the other hand, DO concentrations decreased from 8.15 mg/l to 7.98 mg/l and from 6.98 mg/l to 6.66 mg/l in the mainstem and Tharthar Lake, respectively. Chl-a concentrations slightly

increased in the mainstem due to climate change effect with an average concentration changed from 1.97 µg/ to 2 µg/l. There was no significant change in the average TDS, nutrients, and CBOD concentrations in the mainstem and in the lake.

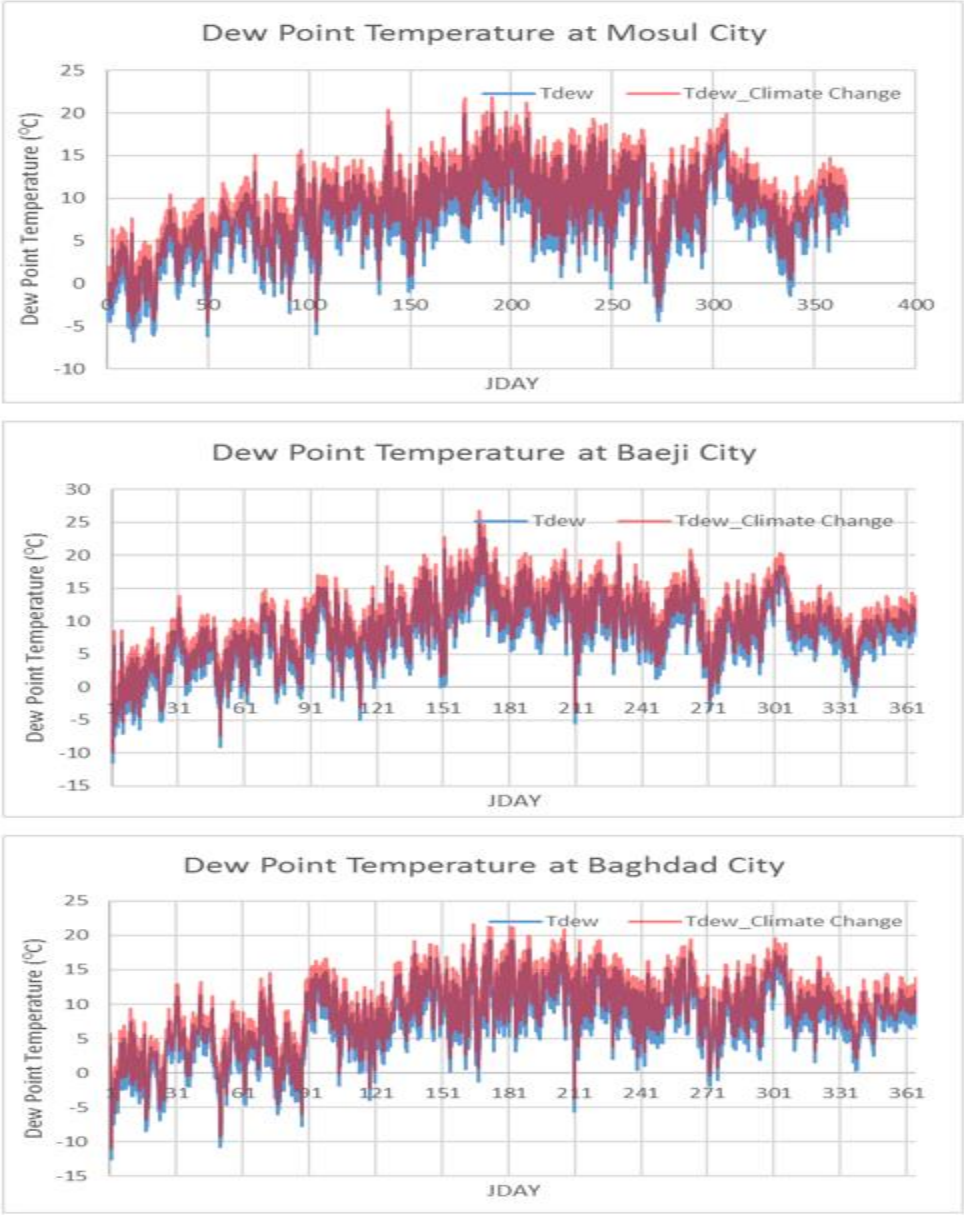

Figure 116: Dew point temperature of the base model and management scenario 5 (Climate Change) at Mosul, Baeji, and Baghdad cities in 2009.

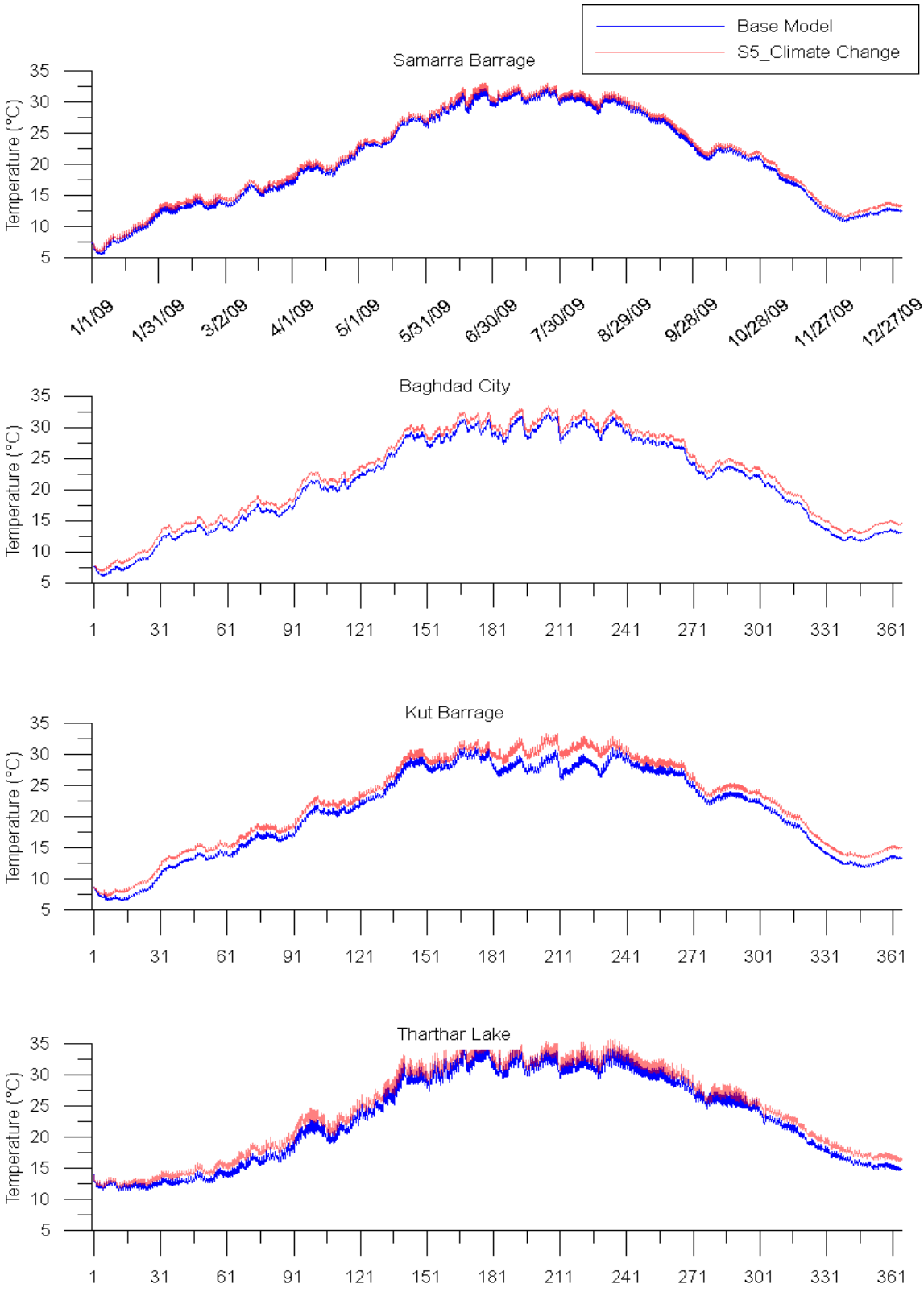

Figure 117: Model water temperature (T) predictions for base model and management scenario 5 (climate change) at Samarra Barrage, Baghdad City, Kut Barrage, and Tharthar Lake.

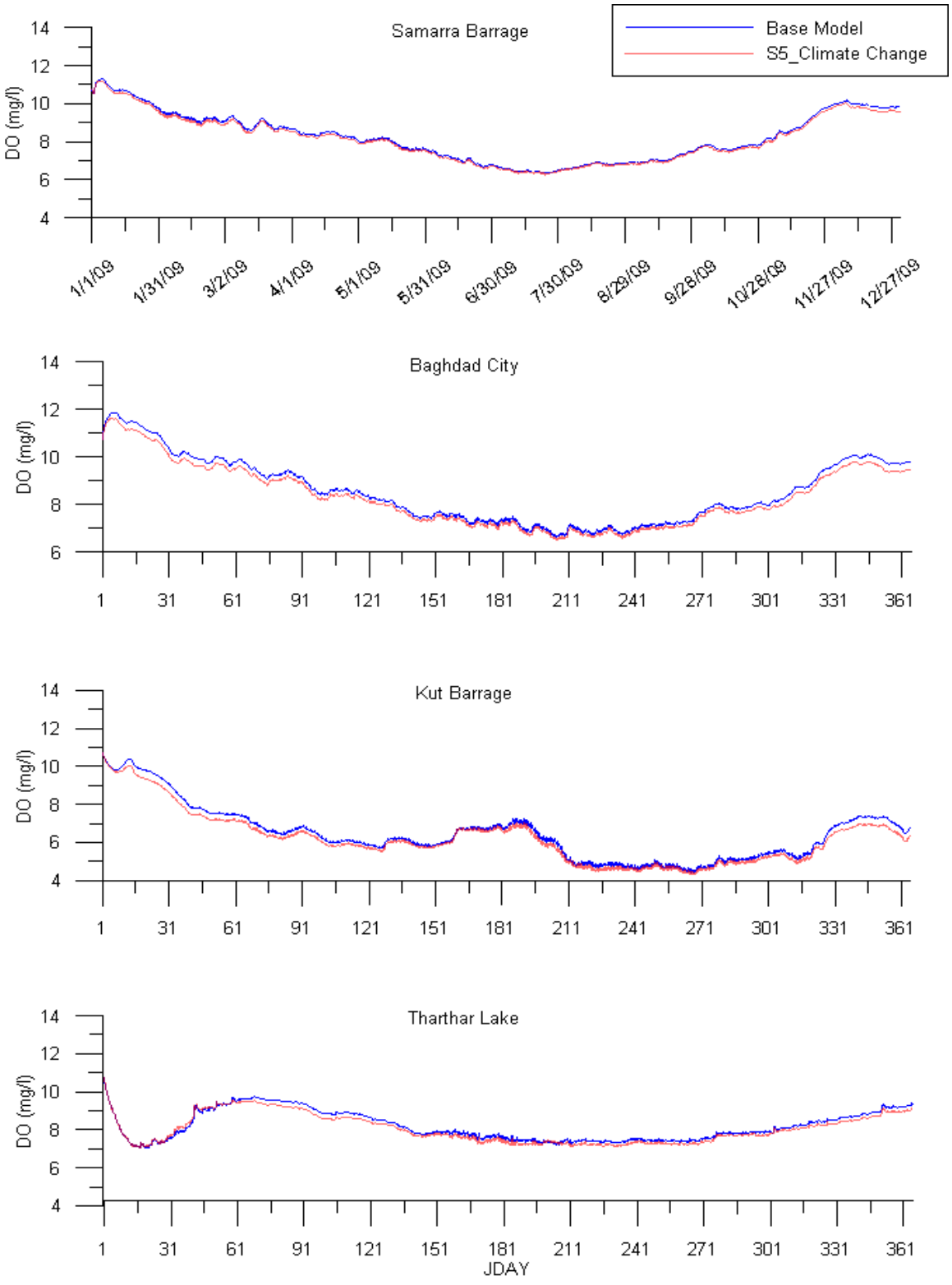

Figure 118: Model dissolved oxygen (DO) predictions for base model and management scenario 5 (climate change) at Samarra Barrage, Baghdad City, Kut Barrage, and Tharthar Lake.

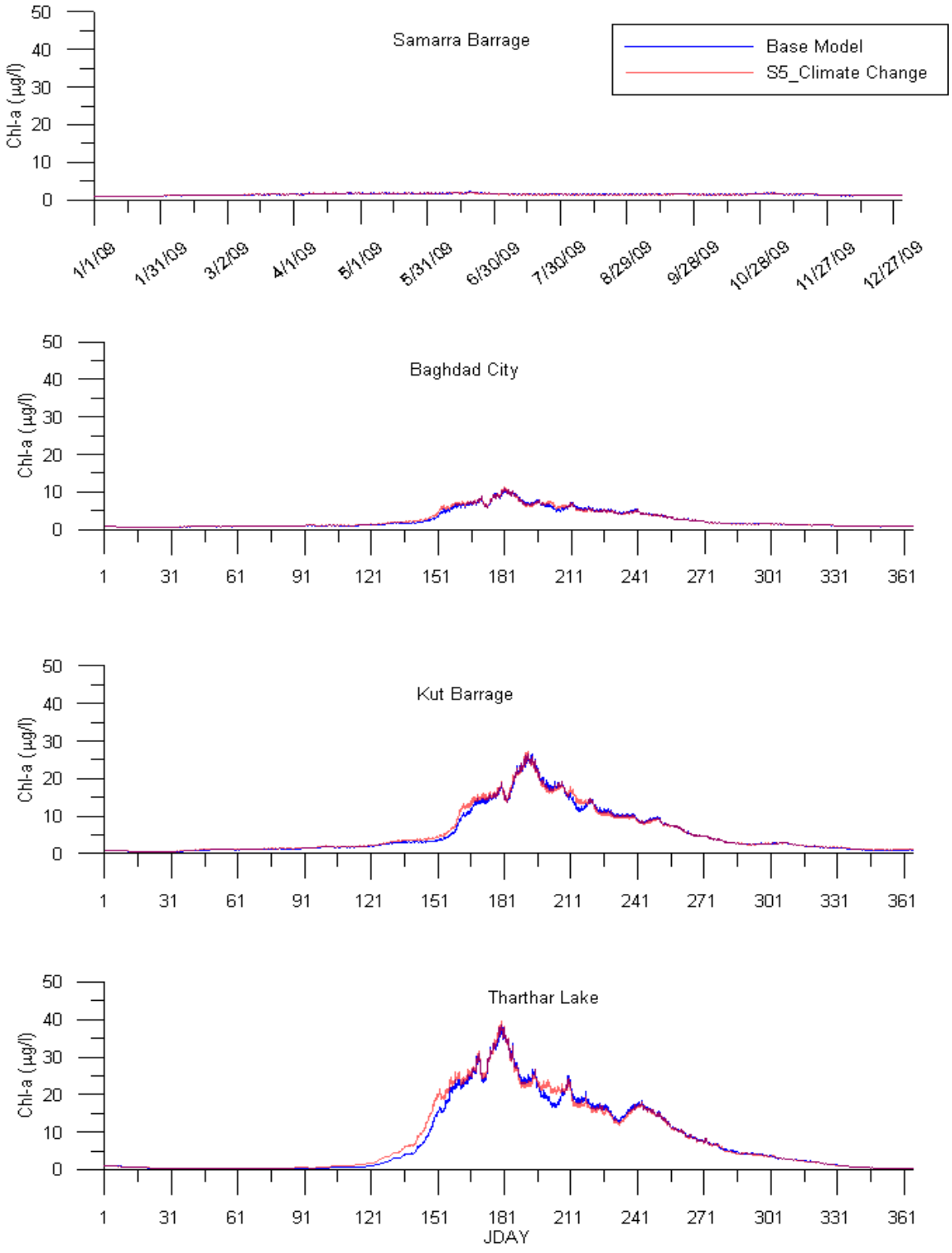

Figure 119: Model chlorophyll-a (Chl-a) predictions for base model and management scenario 5 (climate change) at Samarra Barrage, Baghdad City, Kut Barrage, and Tharthar Lake.

Management Scenario 6: The Effect of Climate Change with Decreasing Upstream Flow

In this management scenario, the effect of climate change was implemented along with an expected decrease in the system's hydrology. Upstream flow boundary conditions at Mosul Dam were decreased by 15%. Like scenario 5, a 2 ° C increase in air temperature and subsequent increase in dew point temperatures was implemented in this management scenario also. Figure 120 through Figure 124 show model predictions of management scenario 6 for water temperature, total dissolved solids, carbonaceous biological oxygen demand, dissolved oxygen, and chlorophyll-a, respectively, at Samarra Barrage, Baghdad city, Kut Barrage, and Tharthar Lake. Model predictions of phosphate, ammonium, and nitrate are shown in appendix A. Predictions of management scenario 6 were compared with the base model of the Tigris River system.

Like scenario 5, temperature predictions were warmer than the temperature predictions of the base model. There was also a corresponding decrease in DO concentrations in the Tigris River system was at all four stations. The average temperatures in the mainstem and Tharthar Lake were increased from 20.7 ° C and 17.44 ° C to 21.56 ° C and 18.37 ° C respectively. A 6.7% and 1.3% increase in TDS concentration were recorded in the mainstem and Tharthar Lake respectively. There was no major impact on PO4, NH4, and NO3 concentrations in the mainstem. On the other hand, CBOD concentrations increased from 6 mg/l to 6.15 mg/l, while DO concentrations decreased from 8.15 mg/l to 7.93 mg/l in the mainstem. Chl-a concentrations decreased in the mainstem with an average concentration decreasing from 1.97 µg/l to 1.91 µg/l.

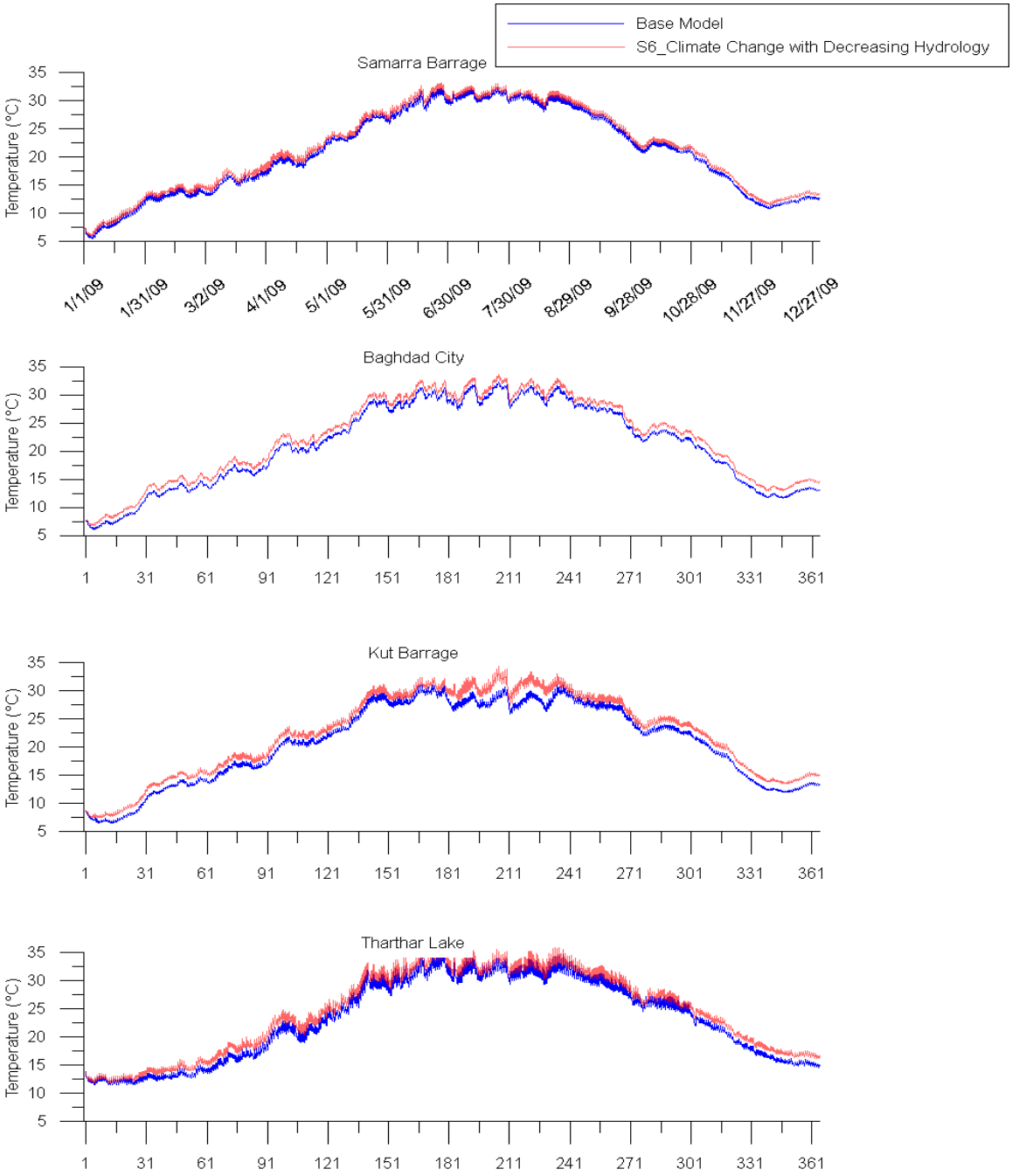

Figure 120: Model water temperature (T_w) predictions for base model and management scenario 6 (climate change with decreasing hydrology) at Samarra Barrage, Baghdad City, Kut Barrage and Tharthar Lake.

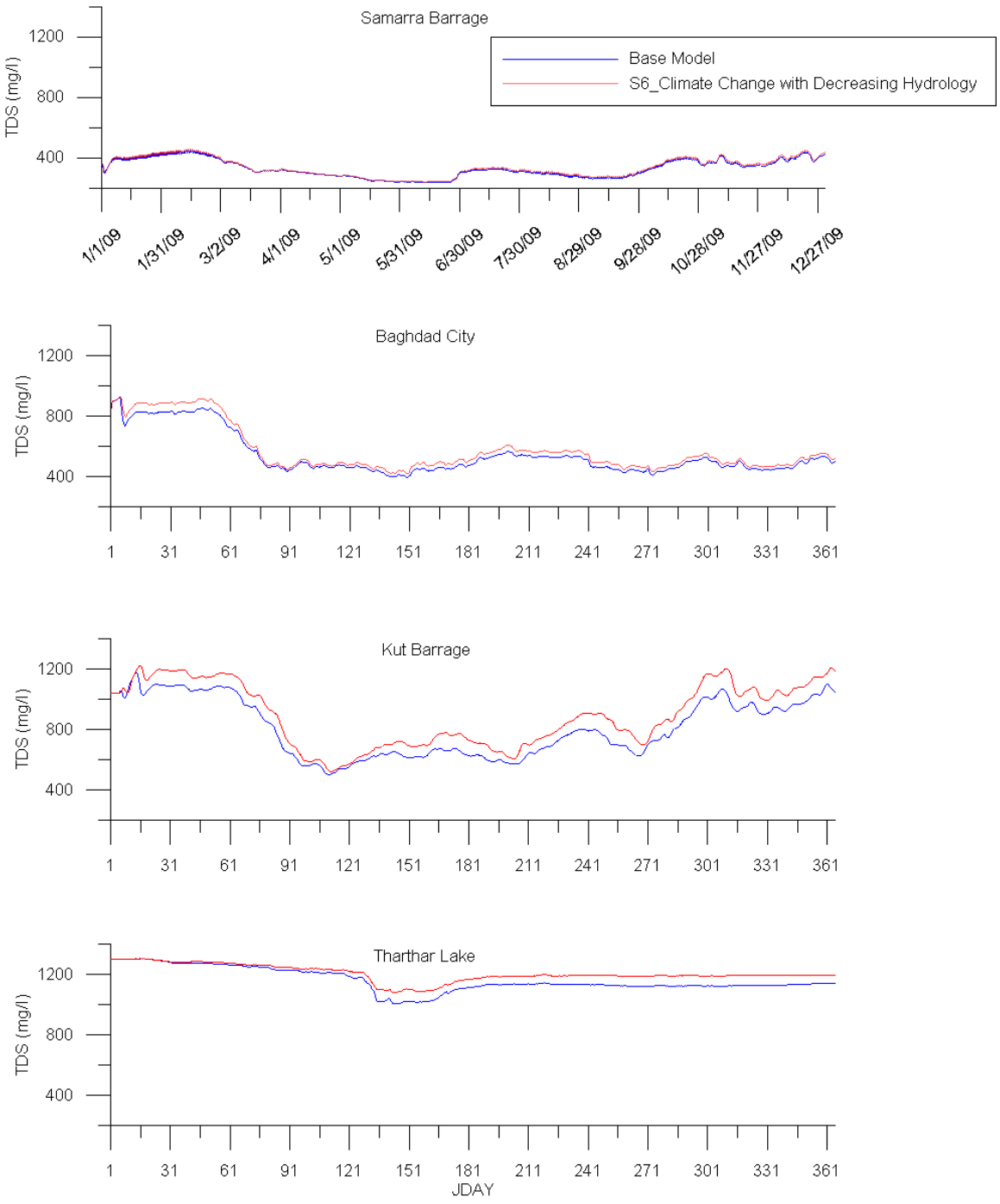

Figure 121 Model total dissolved solids (TDS) predictions for base model and management scenario 6 (climate change with decreasing hydrology) at Samarra Barrage, Baghdad City, Kut Barrage and Tharthar Lake.

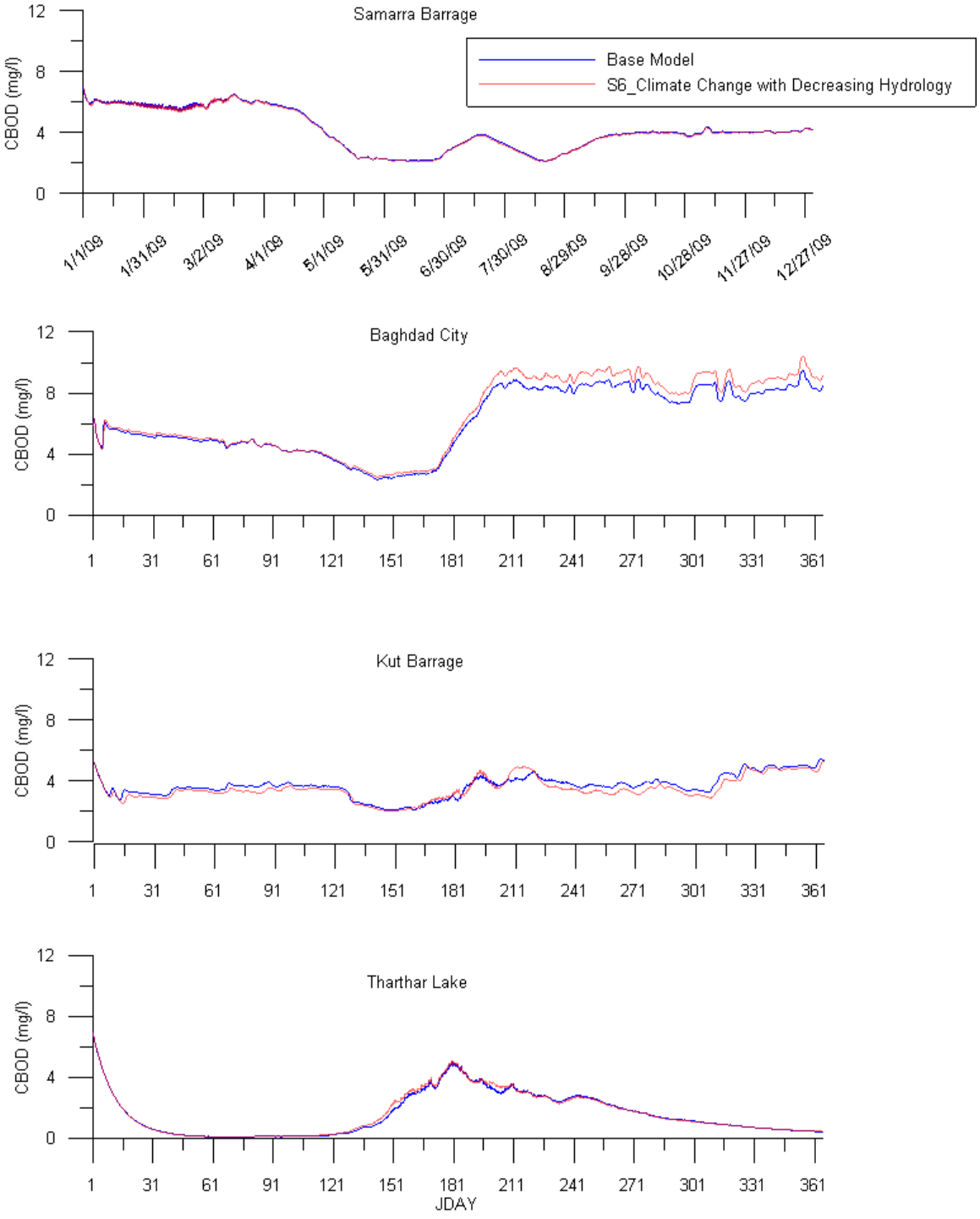

Figure 122: Model carbonaceous biological oxygen demand (CBOD) predictions for base model and management scenario 6 (climate change with decreasing hydrology) at Samarra Barrage, Baghdad City, Kut Barrage and Tharthar Lake.

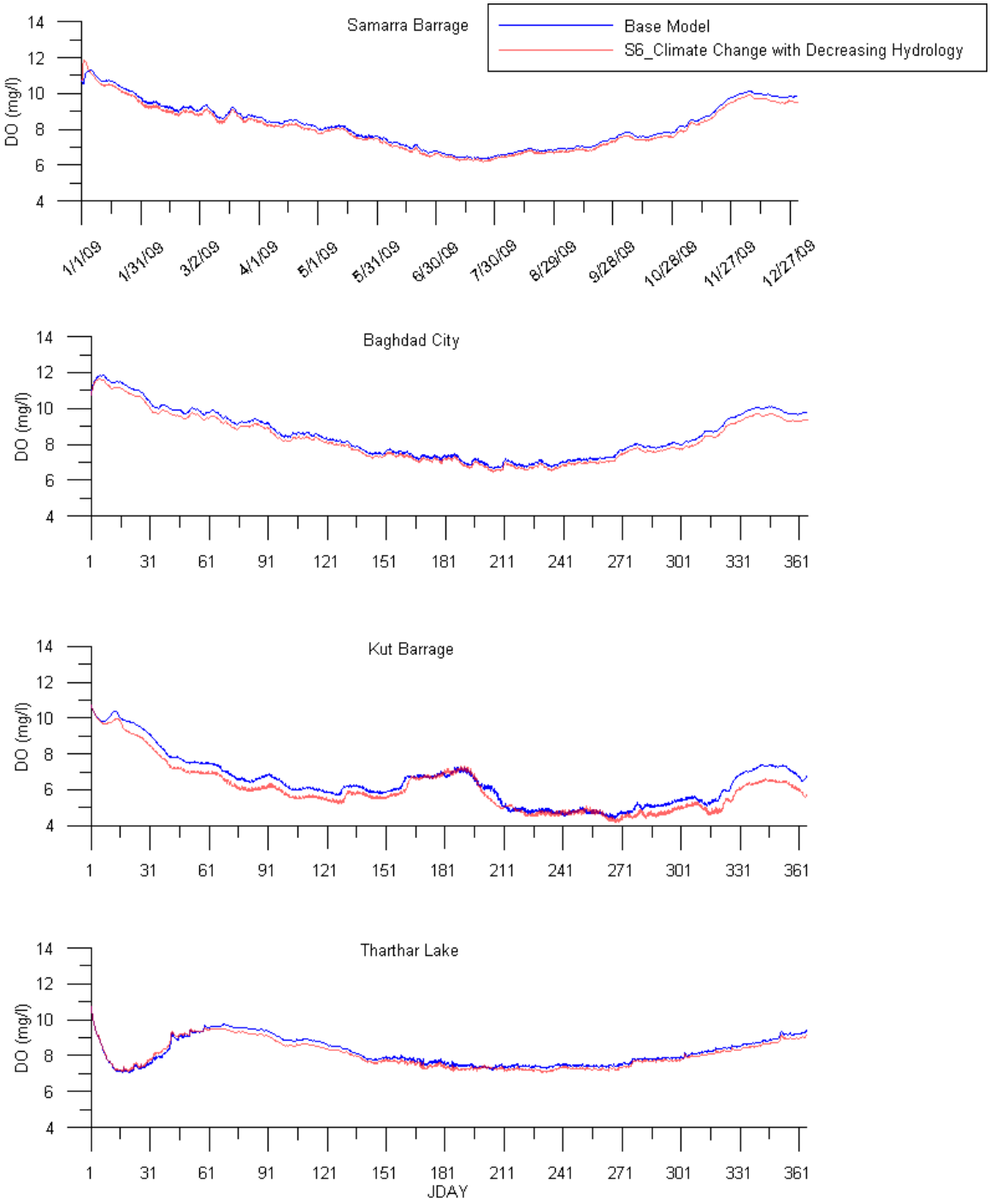

Figure 123: Model dissolved oxygen (DO) predictions for base model and management scenario 6 (climate change with decreasing hydrology) at Samarra Barrage, Baghdad City, Kut Barrage and Tharthar Lake.

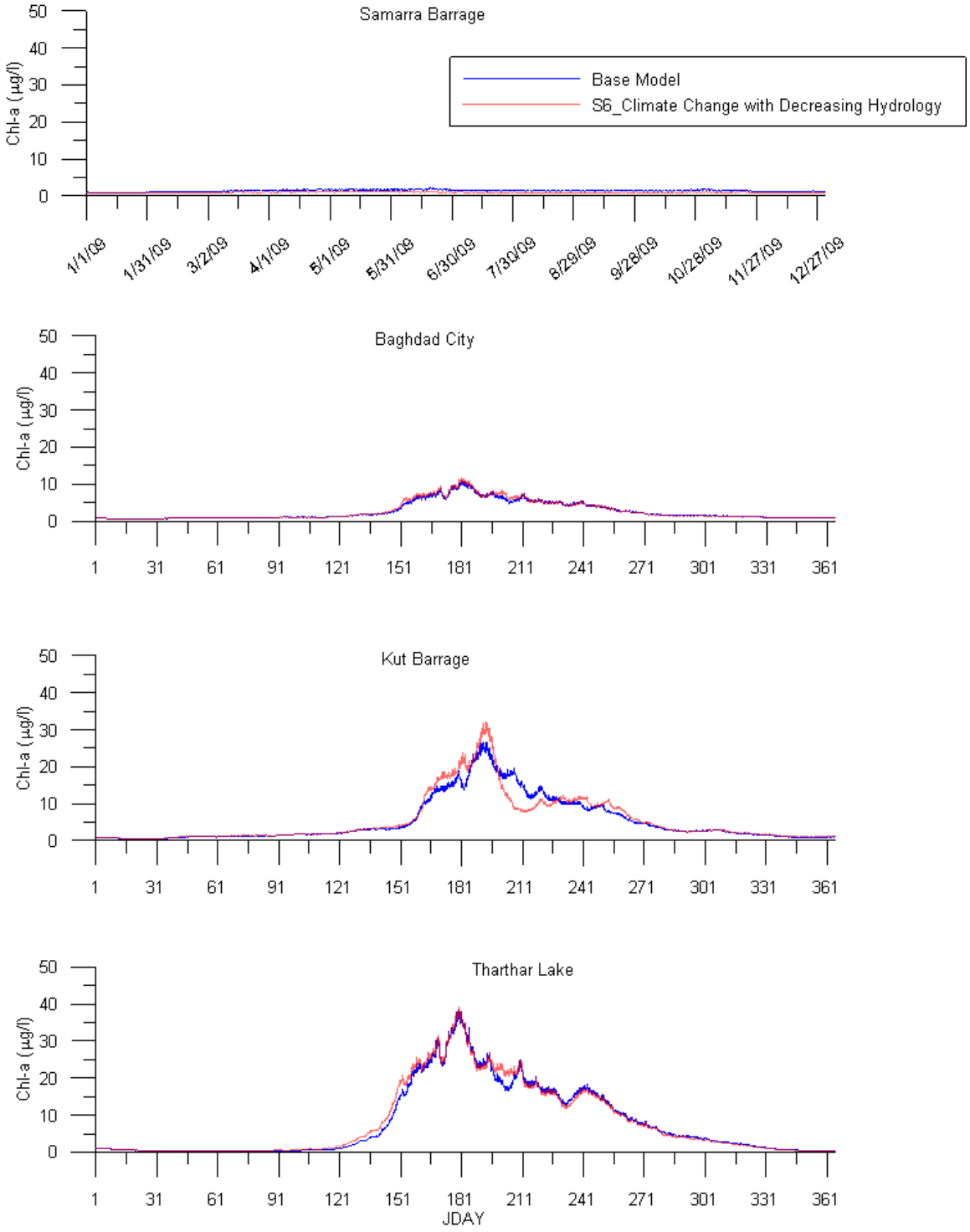

Figure 124 Model chlorophyll-a (Chl-a) predictions for base model and management scenario 6 (climate change with decreasing hydrology) at Samarra Barrage, Baghdad City, Kut Barrage and Tharthar Lake.

Management Scenario 7: Disconnecting Tharthar Lake

To study the importance of Tharthar Lake on the Tigris River system and its water quality, Tharthar Lake and its canals (Tigris-Tharthar canal, Tharthar arm, and Tharthar-Tigris canal) were disconnected from the entire system. Figure 125 through Figure 128 show model predictions of management scenario 7 for total dissolved solids, carbonaceous biological oxygen demand, dissolved oxygen, and chlorophyll-a, respectively, at Samarra Barrage, Baghdad city, Kut Barrage. Model predictions of water temperature, phosphate, ammonium, nitrate are shown in appendix A. Predictions of management scenario 7 were compared with the base model of the Tigris River system.

There was a significant 25% decrease in TDS concentrations in the mainstem due to a 36% increase in flow from Samarra Barrage to Baghdad city. CBOD concentrations decreased from 6 mg/l to 5.2 mg/l in the mainstem. Chl-a concentrations significantly decreased by 40% with an average concentration decreasing from 2 µg/l to 1.2 µg/l. Figure 129 shows flow of the mainstem of the Tigris River at Samarra Barrage and Baghdad city. High volumes of water passed to Baghdad city through Samarra Barrage. There were no major changes noticed in the system's temperature and nutrients.

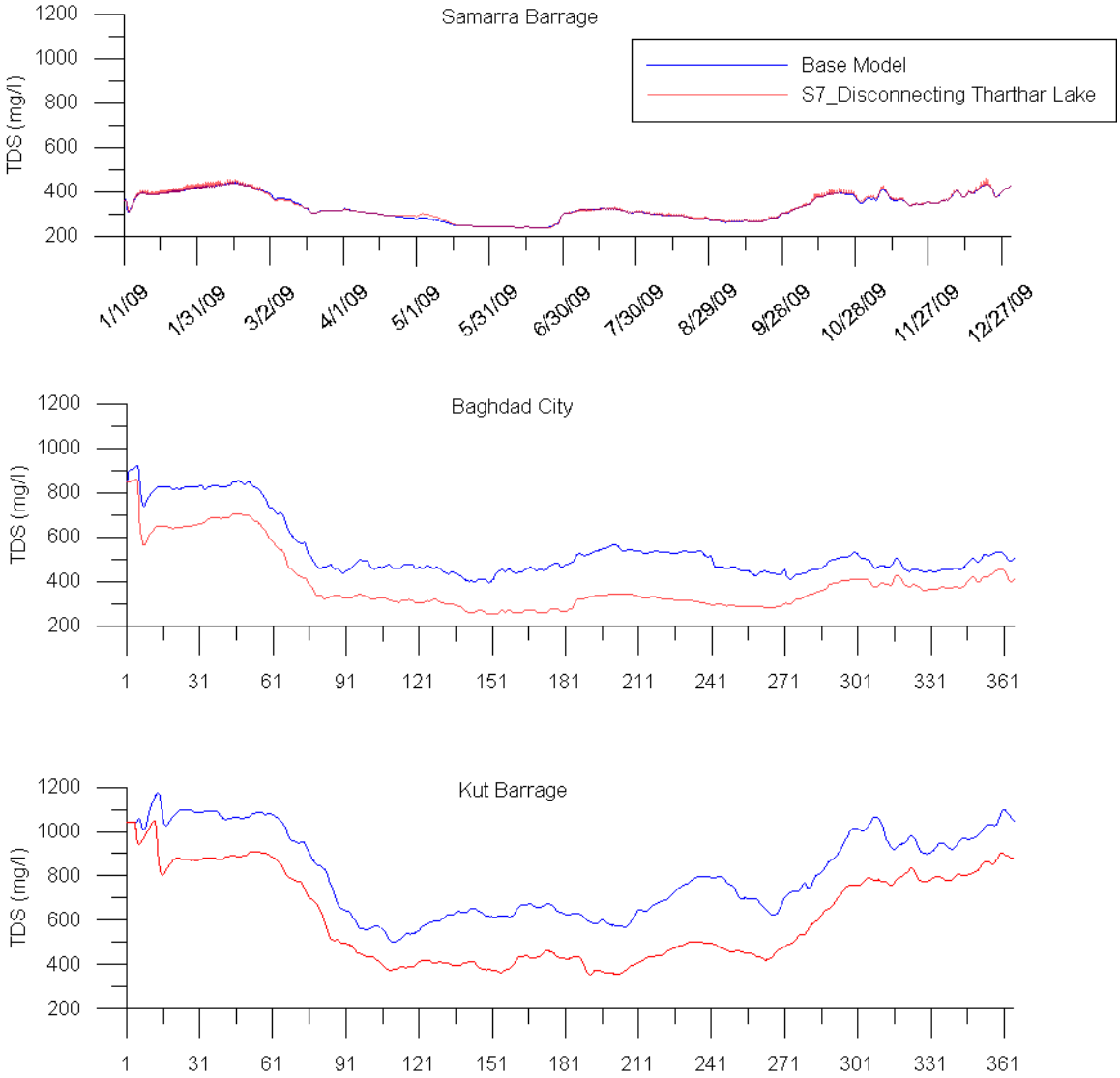

Figure 125 Model total dissolved solids (TDS) predictions for base model and management scenario 7 (disconnecting Tharthar Lake) at Samarra Barrage, Baghdad City, Kut Barrage.

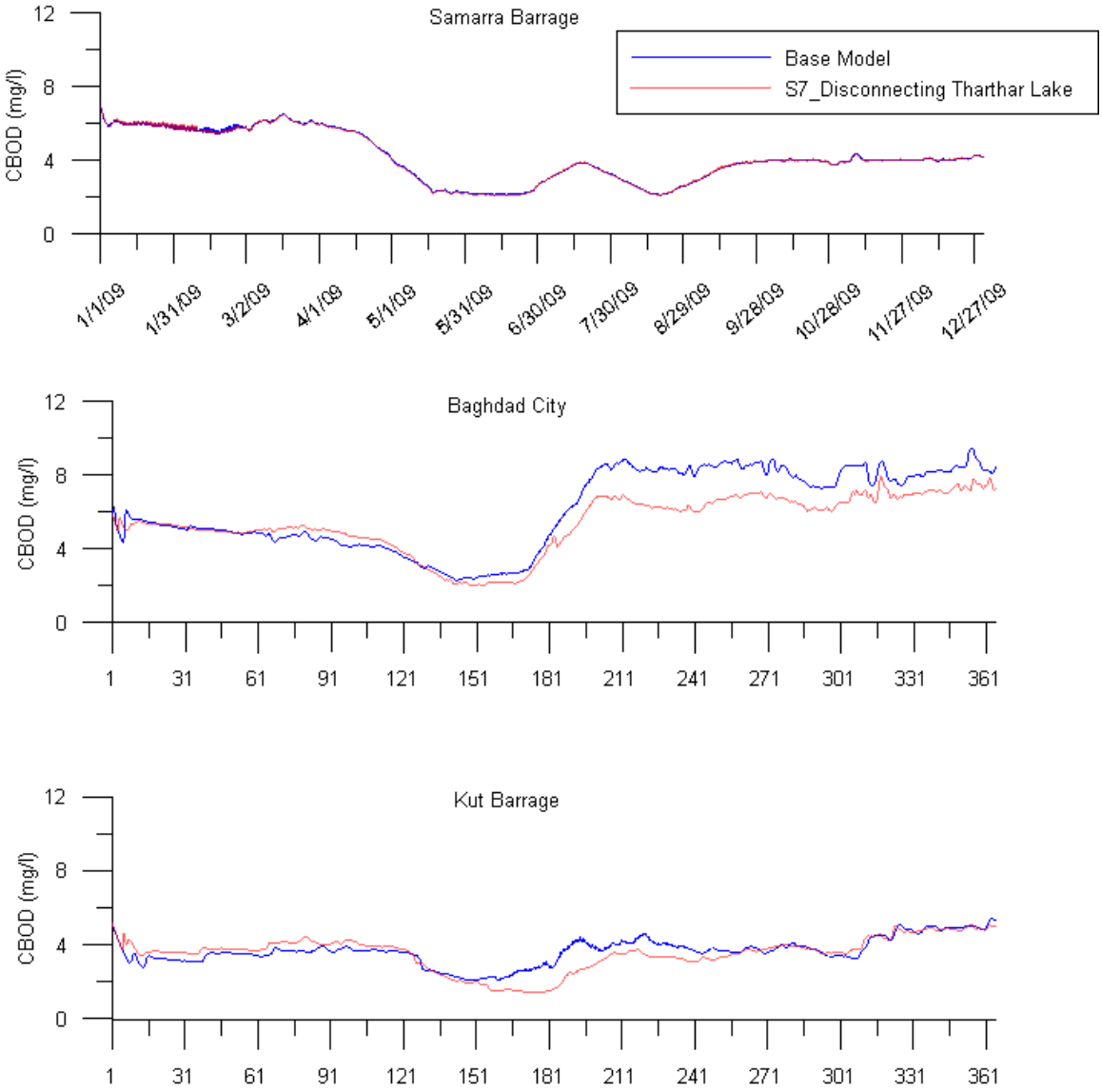

Figure 126: Model carbonaceous biological oxygen demand (CBOD) predictions for base model and management scenario 7 (disconnecting Tharthar Lake) at Samarra Barrage, Baghdad City, Kut Barrage.

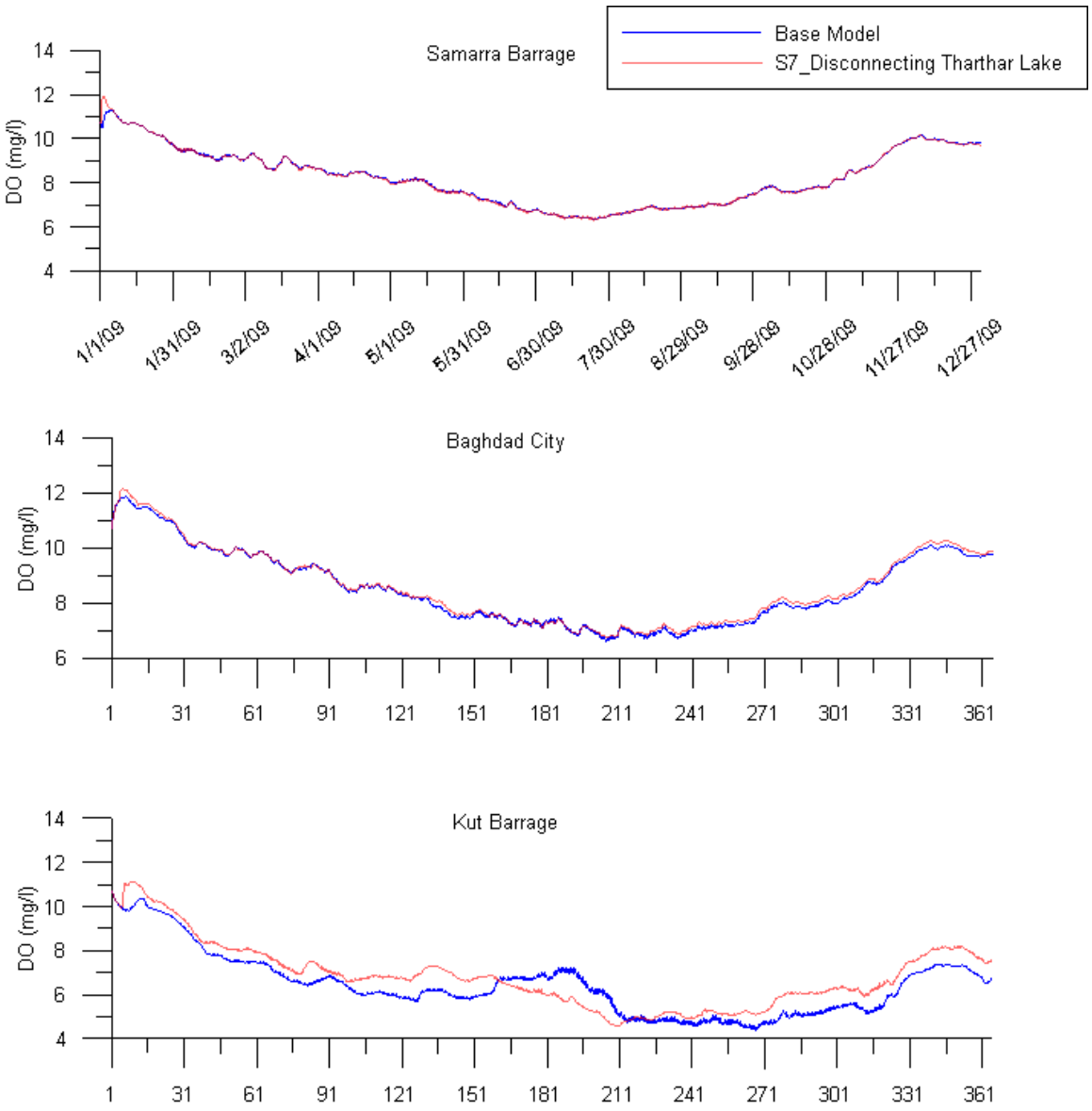

Figure 127: Model dissolved oxygen (DO) predictions for base model and management scenario 7 (disconnecting Tharthar Lake) at Samarra Barrage, Baghdad City, Kut Barrage.

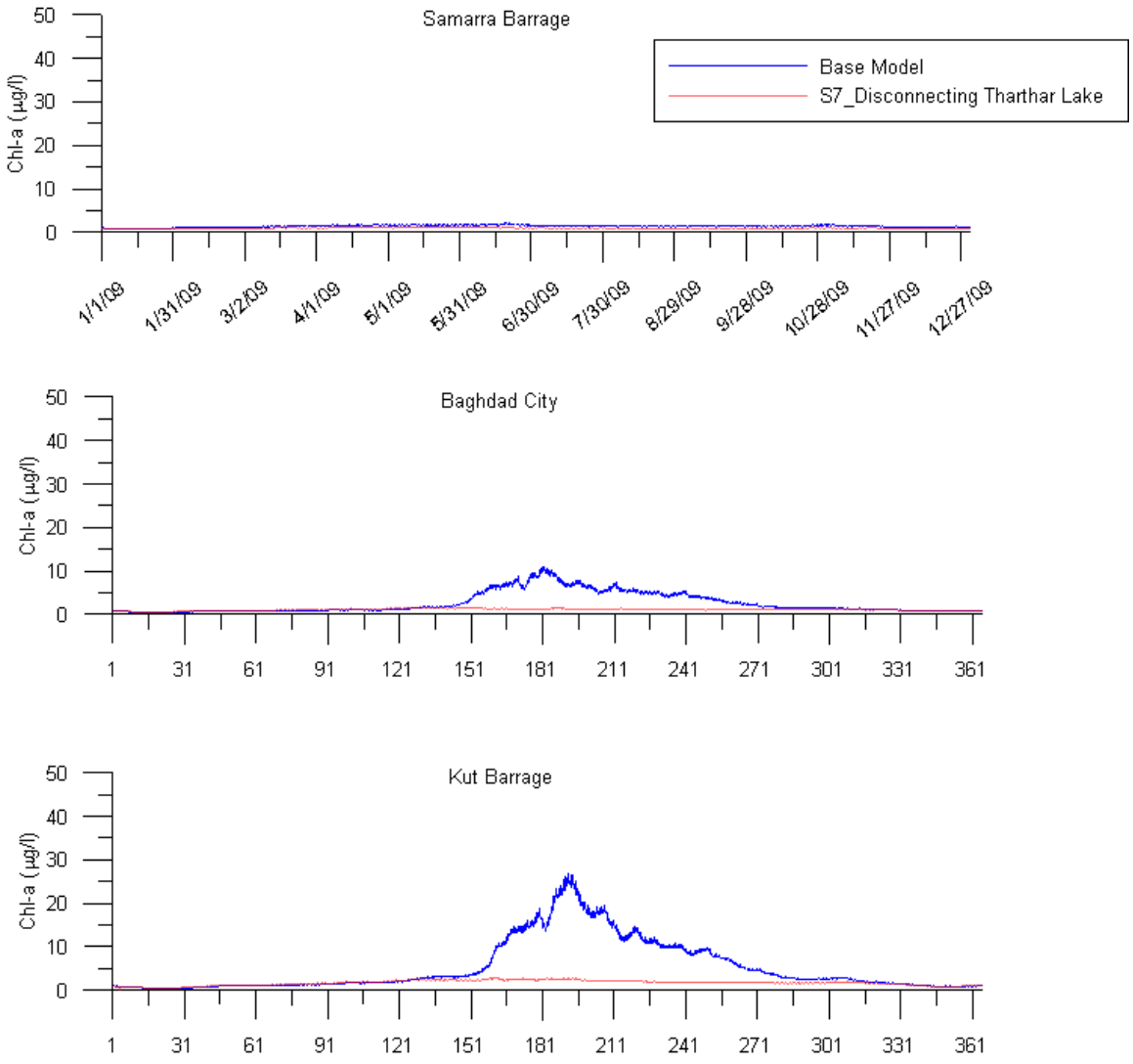

Figure 128: Model chlorophyll-a (Chl-a) predictions for base model and management scenario 7 (disconnecting Tharthar Lake) at Samarra Barrage, Baghdad City, Kut Barrage.

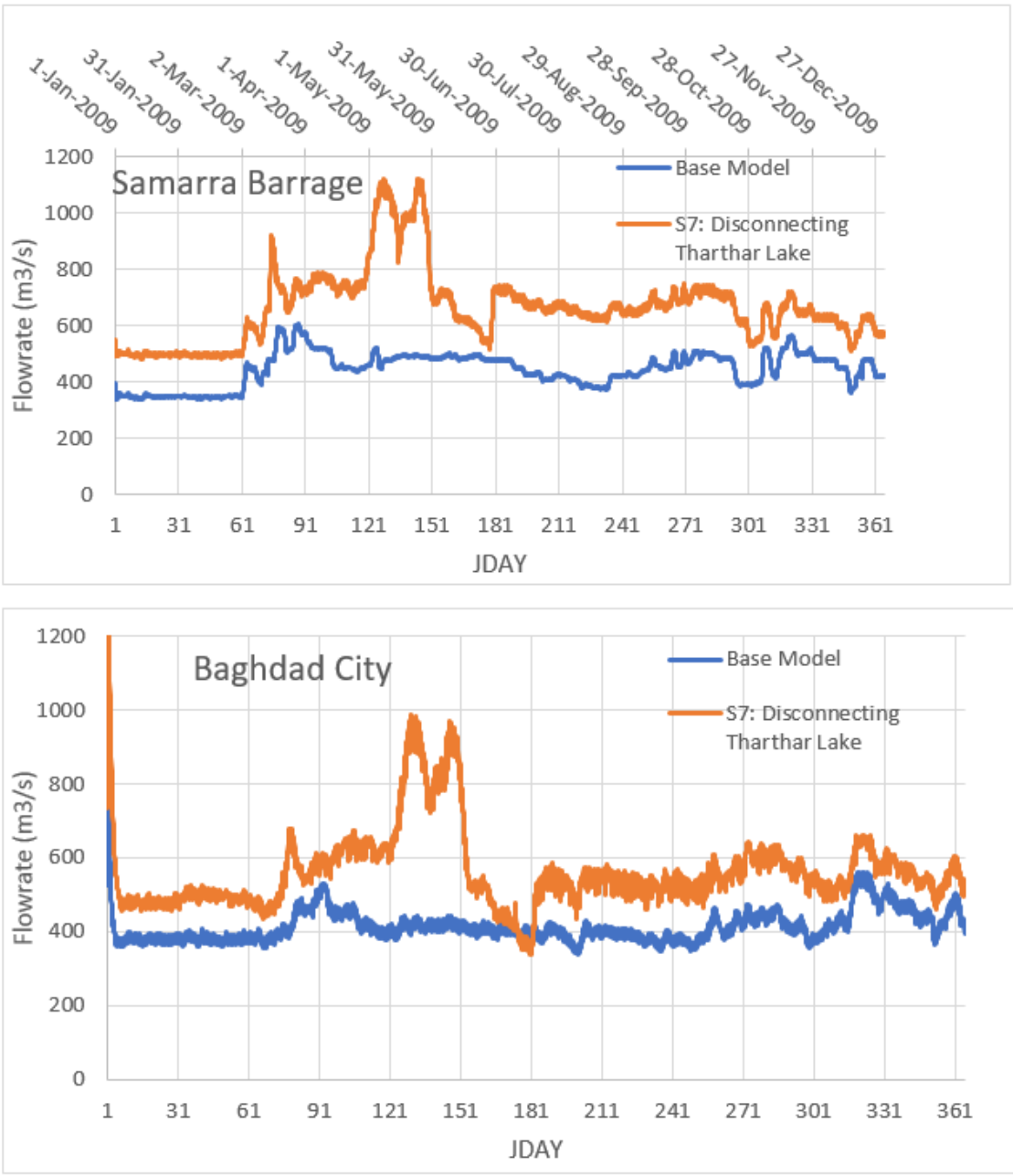

Figure 129: Model flowrate (Q) predictions for base model and management scenario 7 (disconnecting Tharthar Lake) at Samarra Barrage and Baghdad City.

Management Scenario 8: Long Term Model

In this management scenario, a 6-year model simulation of the Tigris River system was performed to have an insight of how water quality constituents vary in Tharthar Lake. Detention time in the lake was approximately 6 years with a volume of 28245 E6 m^3 and average inflow and outflow of 150 m^3/s and 200 m^3/s, respectively. Boundary conditions for the long-term model (2009-2014) were developed using the same boundary conditions of the Tigris River model for year 2009. Figure 130 through Figure 137 show model predictions of management scenario 8 for water age, temperature, total dissolved solids, phosphate, ammonium, nitrate, carbonaceous biological oxygen demand, dissolved oxygen, and chlorophyll-a, respectively, at the outlet of Tharthar Lake. The average temperature in the lake increased from 17.44 ° C to 17.56 ° C, while no change in water temperatures was noticed in the mainstem. The average TDS concentration decreased by 16% from 1239 mg/l to 1041 mg/l in Tharthar Lake due to a continuous dilution by fresh waters diverted from Samarra Barrage. Fresh water enters the lake at a point located close to the lake's outlet and causes a high dilution in the water near the lake's outlet. PO4, NH4, and NO3 concentrations decreased by 2%, 66%, and 26%, respectively. Average concentrations of CBOD and Chl-a were decreased from 0.71 mg/l and 2 µg/l to 0.63 mg/l and 1.61 µg/l, respectively.

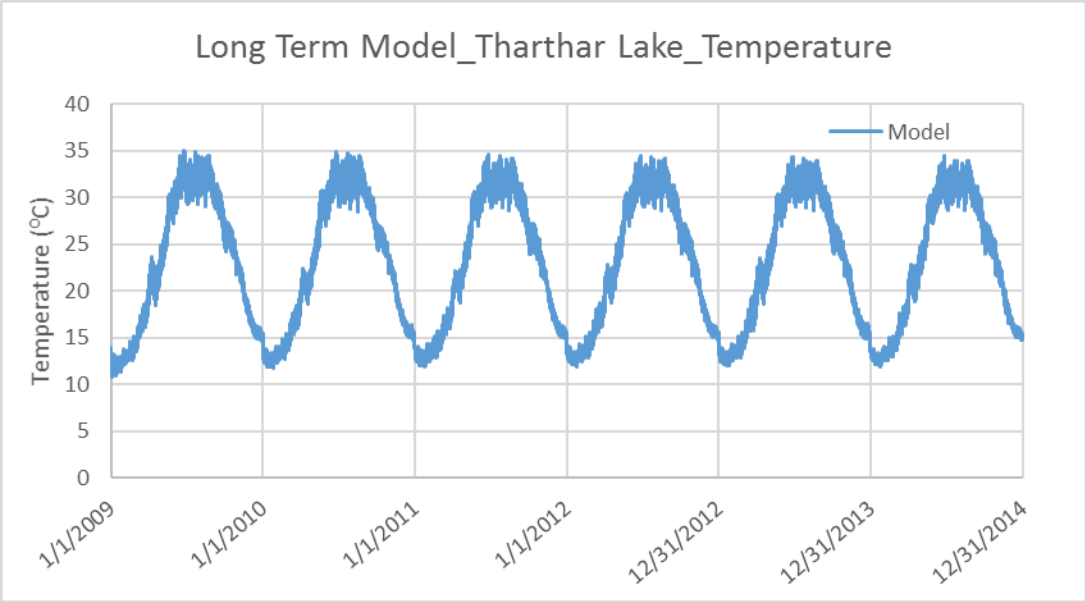

Figure 130: Model water temperature (T_w) predictions for management scenario 8 (Long Term simulation) in Tharthar Lake.

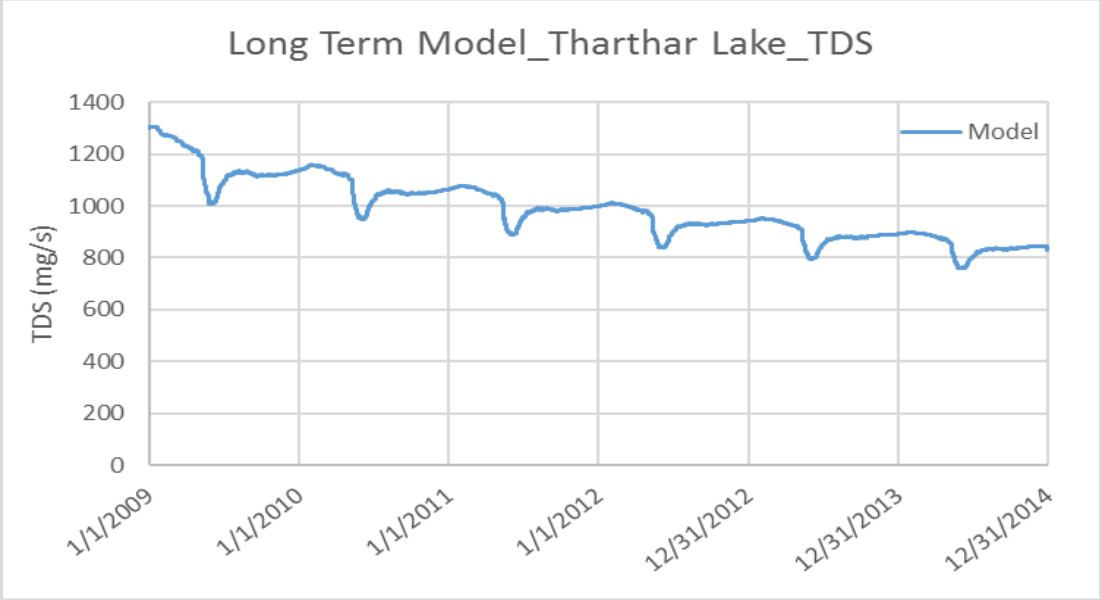

Figure 131: Model total dissolved solids (TDS) predictions for management scenario 8 (Long Term simulation) in Tharthar Lake.

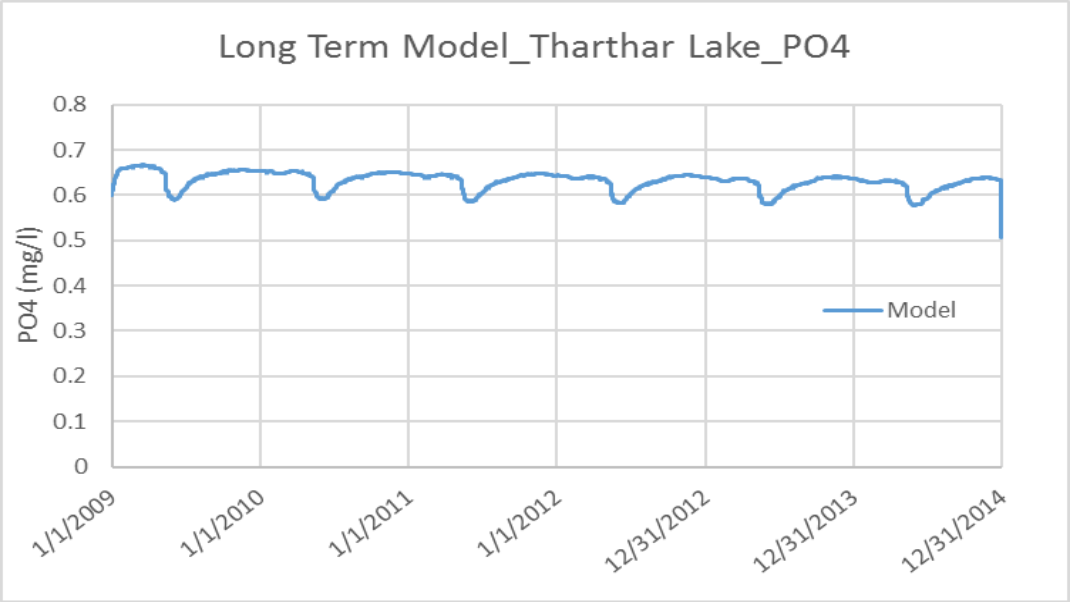

Figure 132: Model phosphate (PO4) predictions for management scenario 8 (Long Term simulation) in Tharthar Lake.

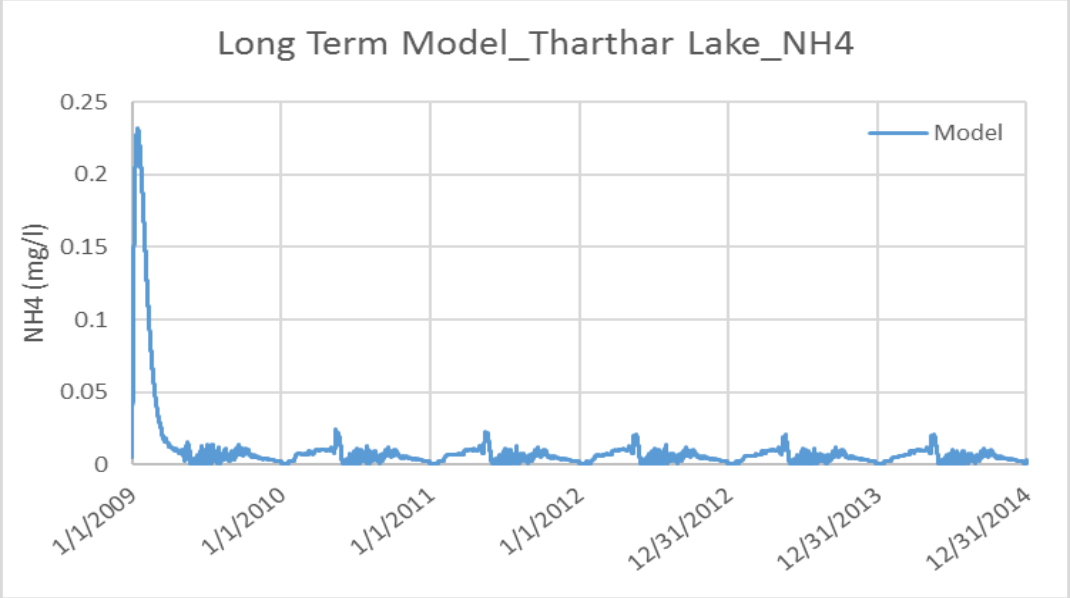

Figure 133: Model ammonia (NH4) predictions for management scenario 8 (Long Term simulation) in Tharthar Lake.

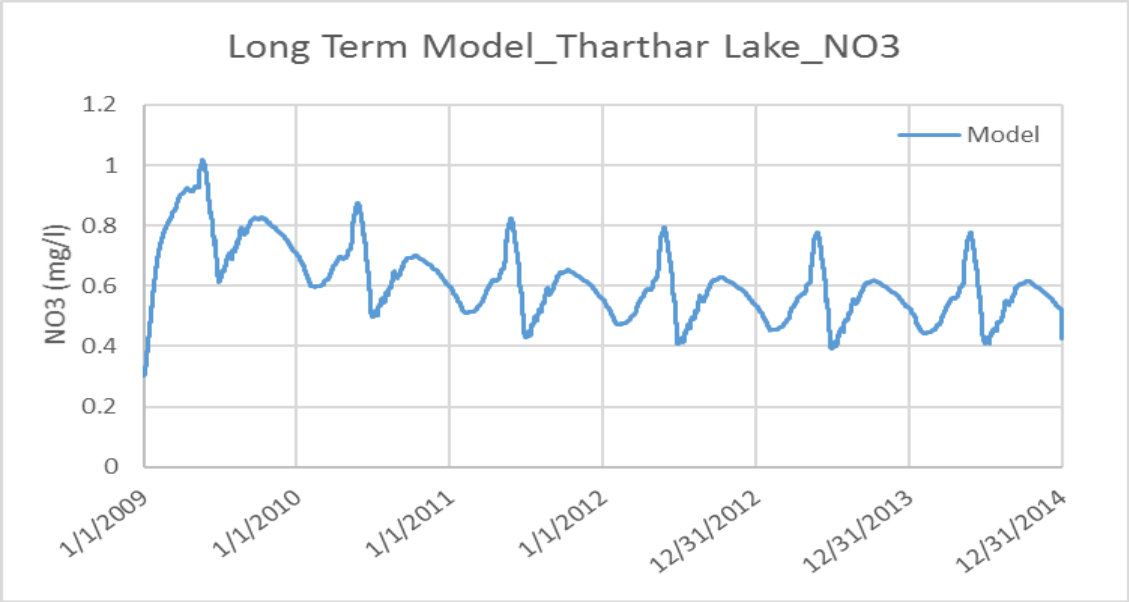

Figure 134: Model nitrate (NO3) predictions for management scenario 8 (Long Term simulation) in Tharthar Lake.

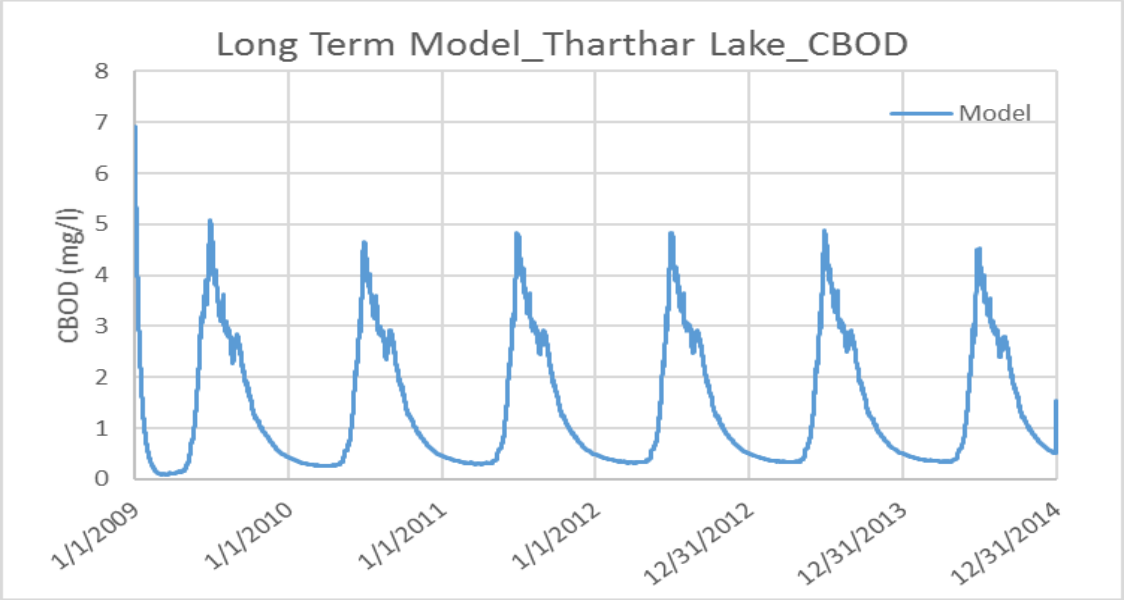

Figure 135: Model carbonaceous biological oxygen demand (CBOD) predictions for management scenario 8 (Long Term simulation) in Tharthar Lake.

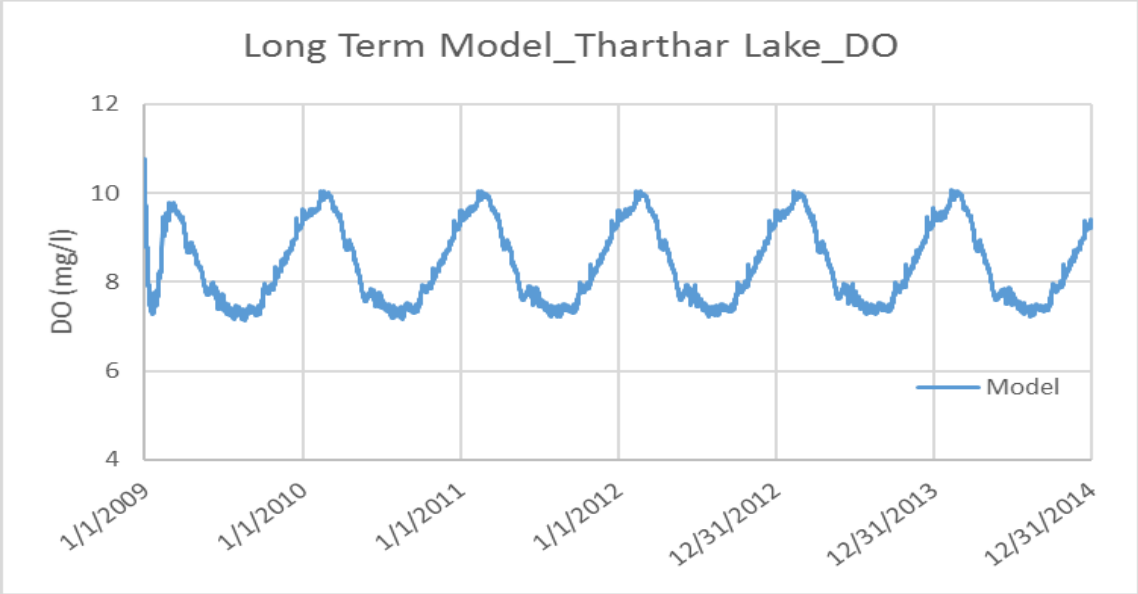

Figure 136: Model dissolved oxygen (DO) predictions for management scenario 8 (Long Term simulation) in Tharthar Lake.

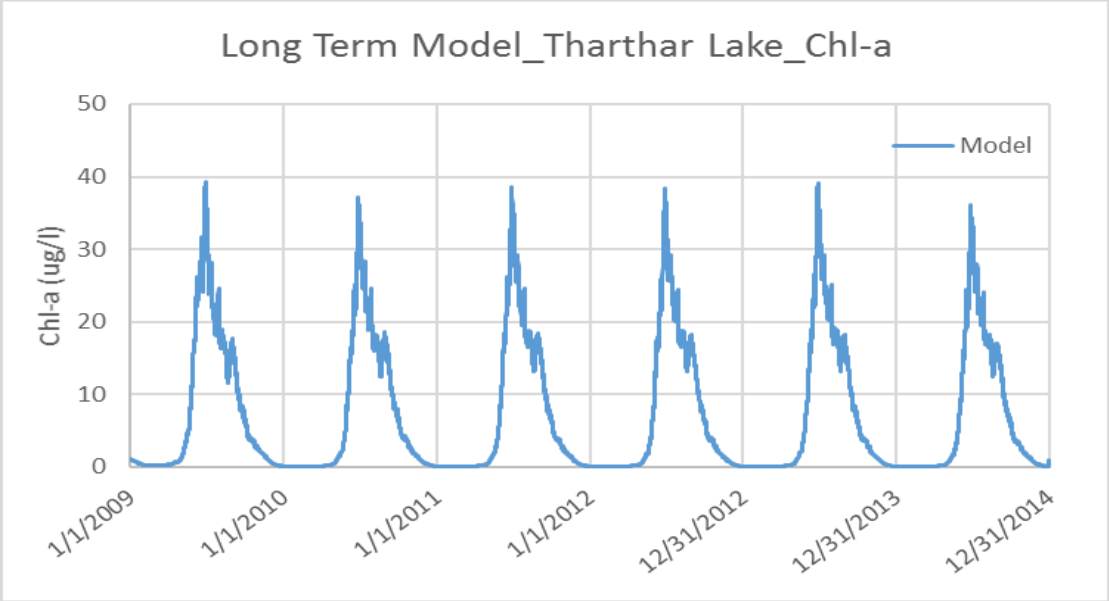

Figure 137: Model chlorophyll-a (Chl-a) predictions for management scenario 8 (Long Term simulation) in Tharthar Lake.

Management Scenario 9: Decreasing BOD in the Tigris River within Baghdad City

In this management scenario, BOD concentrations in the Tigris River within Baghdad city were decreased by 50% to study its impact on DO and Chl-a concentrations in Baghdad city and downstream cites. Effluents with high BOD concentrations were directly discharged into the mainstem of the river causing significant increase in BOD concentrations in Baghdad city and downstream cities. Figure 138 through Figure 140 show model predictions of management scenario 9 for carbonaceous biological oxygen demand, dissolved oxygen, and chlorophyll-a, respectively, at Baghdad city and Kut Barrage. Predictions of management scenario 9 were compared with the base model of the Tigris River system. BOD concentrations in the mainstem decreased by 24%, while DO concentrations increased by 2.8%. There were no significant impacts on Chl-a concentrations in the mainstem of the river.

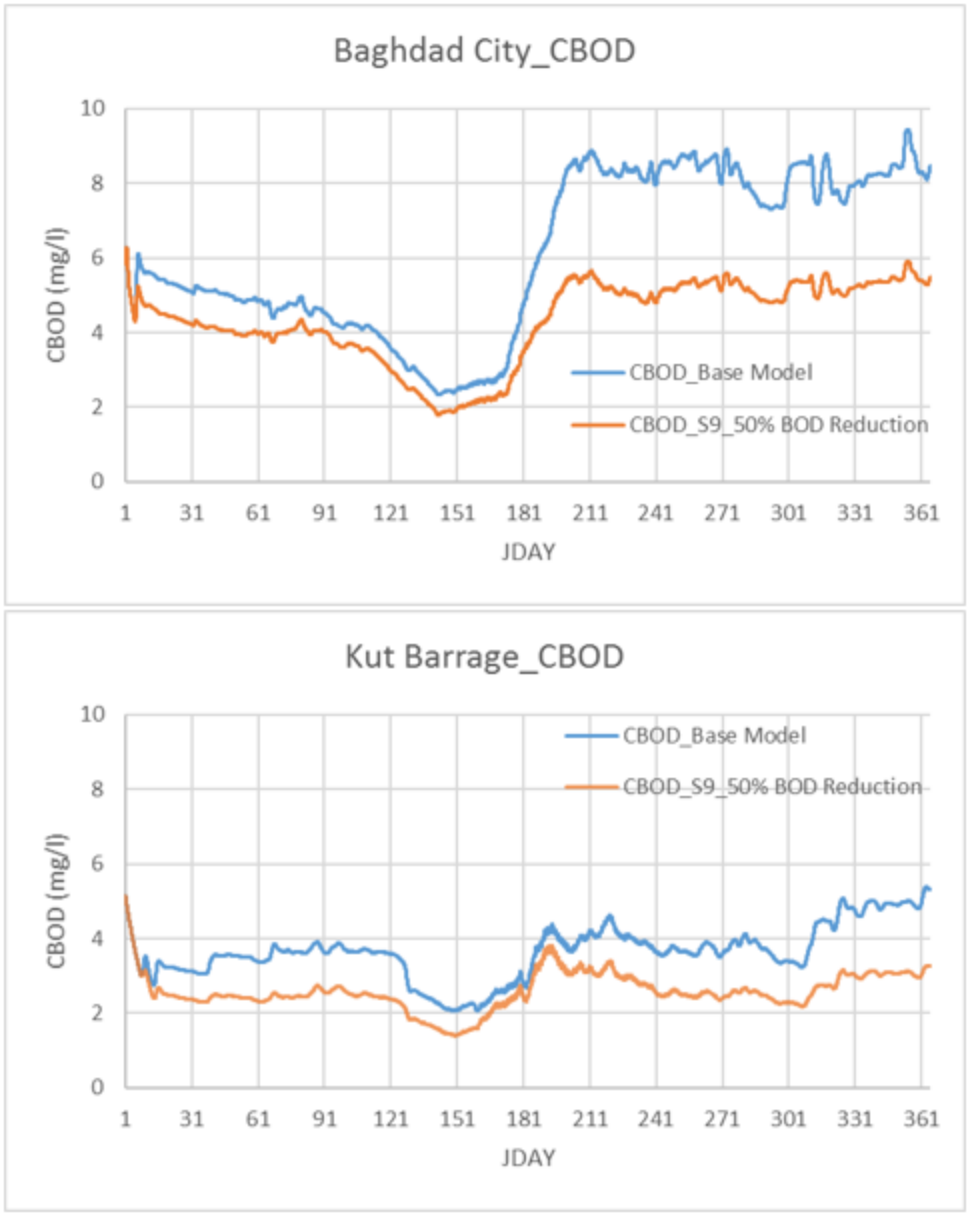

Figure 138: Model carbonaceous biological oxygen demand (CBOD) predictions for base model and management scenario 9 (50% BOD Reduction) at Baghdad City and Kut Barragel.

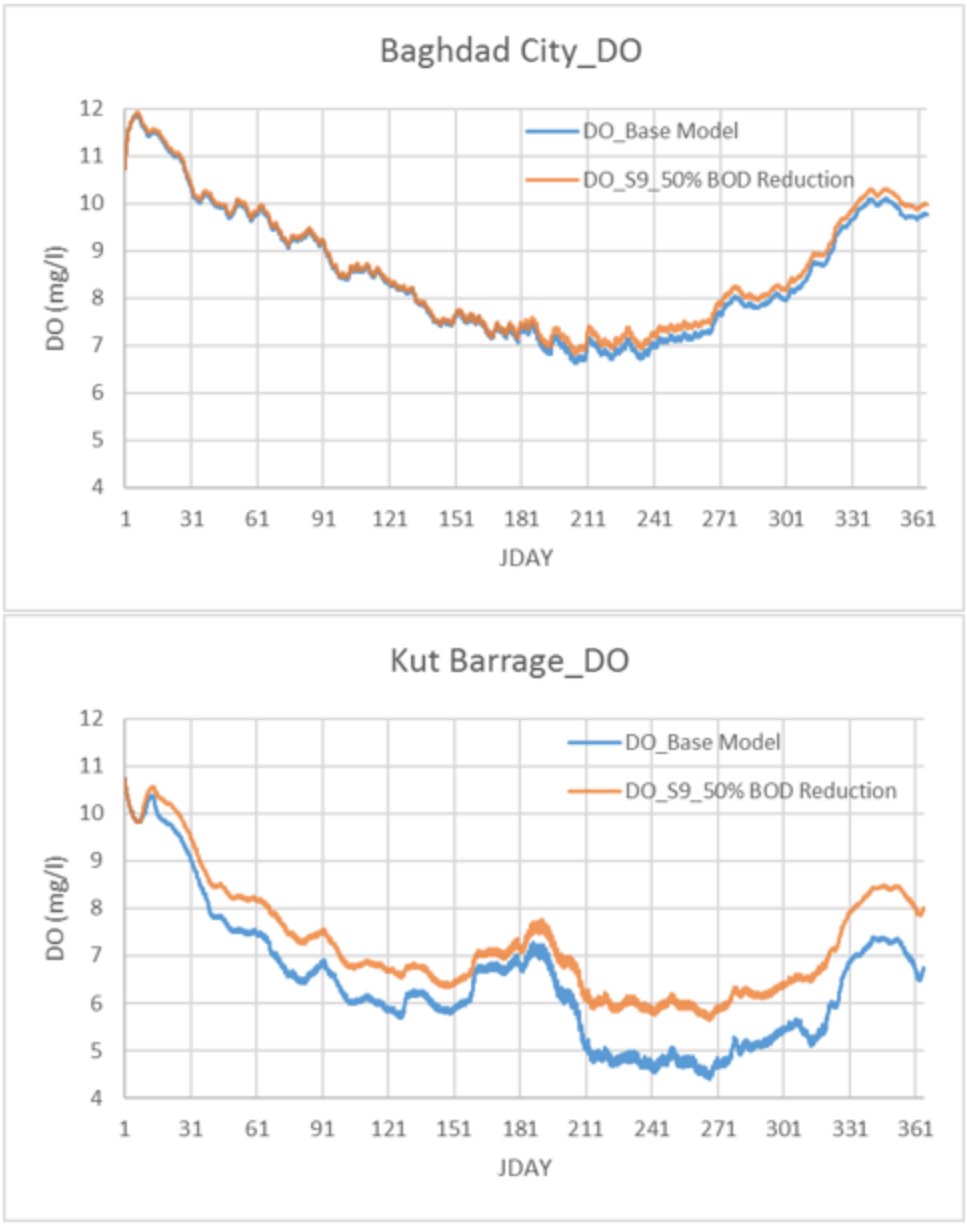

Figure 139: Model dissolved oxygen (DO) predictions for base model and management scenario 9 (50% BOD Reduction) at Baghdad City and Kut Barrage.

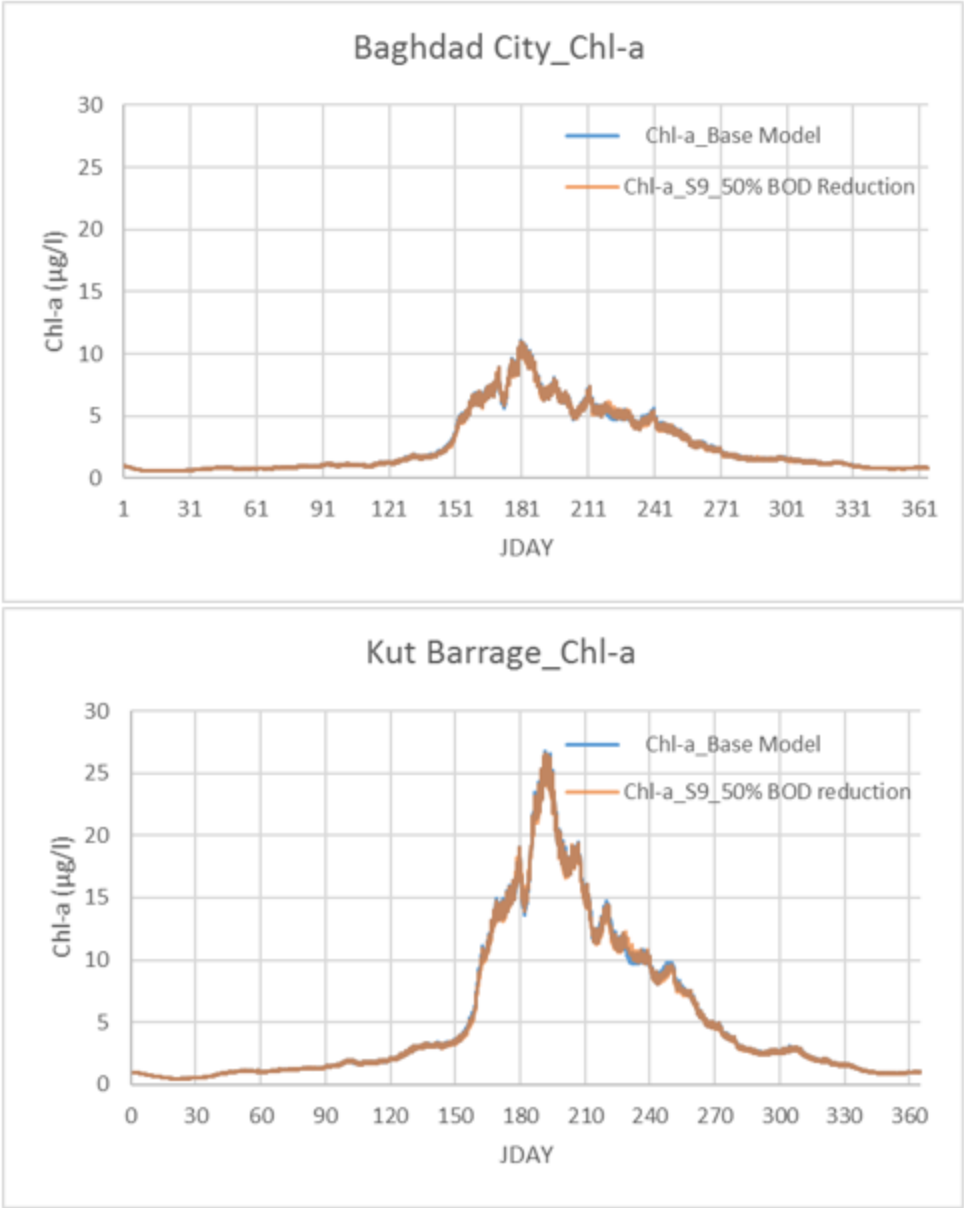

Figure 140: Model chlorophyll-a (Chl-a) predictions for base model and management scenario 9 (50% BOD Reduction) at Baghdad City and Kut Barrage.

Management Scenario 10: Dissolved Oxygen Release from Mosul Dam

Dissolve oxygen (DO) concentrations released upstream from Mosul Dam were set to 1.5 mg/l from June 15th to August 15th to evaluate how long it takes for DO water from Mousul dam to reach saturation in the summer. Figure 141 shows model predictions of DO at model segments 2, 4, 6, 7, 8, 9, and 11. DO reached an equilibrium concentration at model segment 11, 50 km downstream Mosul Dam after about a day of the release. Therefore, upstream boundary conditions affect model predictions of DO for approximately 50 km downstream the point of the release.

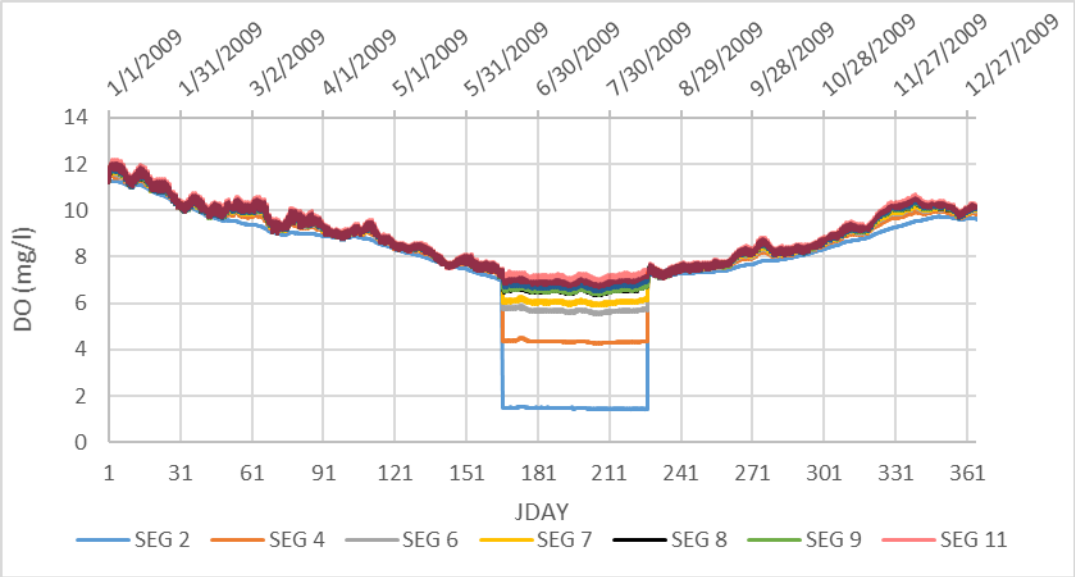

Figure 141: Model predictions of DO in the Mainstem of the Tigris River at model segments 2, 4, 6, 7, 8, 9, and 11.

Summary of Management Scenarios

Different management scenarios were implemented on the Tigris River system and compared with the base model to study the effect of each individual scenario on the mainstem of the Tigris River and Tharthar Lake. Increasing the upstream flow rates at Mosul Dam decreased TDS and nutrient concentrations, while increasing nutrient concentrations at Mosul Dam directly affected the entire system's water quality by increasing in the system's nutrient concentrations. Temperatures in the Middle East region are expected to increase due to the impact of climate change (AFED, 2009; IPCC, 2007; and WRI, 2002). A study conducted by Zakaria et al. (2013) showed an increase in temperatures due to the impact of climate change. In this study, climate change directly impacted the system's temperatures and decreased DO concentrations at Samarra Barrage, Baghdad city, Kut Barrage, and Tharthar Lake.

Most water quality constituents such as TDS, NH4, CBOD, and Chl-a concentrations tended to increase downstream of Samarra Barrage at both Baghdad city and Kut Barrage. The DO concentrations at Kut Barrage and Tharthar Lake were highly affected by algae production at these stations. On the other hand, disconnecting Tharthar Lake changed the entire hydrologic regime in the mainstem of the Tigris River downstream of Samarra Barrage by passing high volumes of water to Baghdad city and downstream areas. In addition, Chl-a concentrations in the mainstem were reduced after disconnecting Tharthar Lake from the Tigris River system, and DO concentrations decreased at Kut Barrage as a result. Appendix B shows histograms for different scenario runs comparing water temperatures, total dissolved solids, phosphate, ammonium, nitrate, carbonaceous biological oxygen demand, dissolved oxygen, and chlorophyll-a in the mainstem of the

Tigris River and Tharthar Lake. Table 25 and Table 26 list the average of water quality constituents in the mainstem of the Tigris River and Tharthar Lake for the base model and model simulations for the year 2009.

Table 25: Average of water quality constituents in the mainstem of the Tigris River for the base model and management scenarios.

Water Quality Parameter	Base Model Run # 1	Increasing Hydrology Run # 2	Decreasing Hydrology Run#3	Decreasing Hydrology with Increasing Nutrients Run# 4	Increasing Tharthar Lake's Flow Run# 5	Climate Change Run# 6	Climate Change with Decreasing Hydrology Run# 7	Disconnecting Tharthar Lake Run# 8	Long Term_6 Years 2009-2014 Run# 9	50%BOD Reduction Run# 10
Temp (^{0}C)	20.71	20.80	20.59	20.60	20.73	21.68	21.56	20.91	20.83	20.73
TDS (mg/l)	495	470	527	539	493	495	528	397	500	493
PO4 (mg/l)	0.357	0.357	0.358	0.374	0.357	0.358	0.359	0.354	0.367	0.349
NH4 (mg/l)	0.235	0.230	0.246	0.249	0.236	0.234	0.244	0.236	0.222	0.188
NO3 (mg/l)	1.540	1.520	1.575	1.627	1.542	1.542	1.576	1.549	1.457	1.518
CBOD (mg/l)	5.912	5.744	6.181	6.183	5.913	5.875	6.140	5.229	5.727	4.511
DO (mg/l)	8.147	8.191	8.086	8.086	8.149	7.989	7.926	8.283	8.199	8.371
Chl-a (µg/l)	1.968	1.998	1.857	1.869	2.000	2.018	1.912	1.177	2.238	1.961

Table 26: Average of water quality constituents in Tharthar Lake for the base model and management scenarios.

Water Quality Parameter	Base Model Run#1	Increasing Hydrology Run# 2	Decreasing Hydrology Run#3	Decreasing Hydrology with Increasing Nutrients Run#4	Increasing Tharthar Lake's Flow Run#5	Climate Change Run#6	Climate Change with Decreasing Hydrology Run#7	Long Term_6 Years 2009-2014 Run# 8	50%BOD Reduction Run#9
Temp (^{0}C)	17.44	17.42	17.46	17.46	17.44	18.35	18.37	17.56	17.49
TDS (mg/l)	1239	1226	1253	1254	1231	1241	1255	1041	1239
PO4 (mg/l)	0.405	0.405	0.405	0.406	0.405	0.405	0.405	0.397	0.405
NH4 (mg/l)	0.042	0.042	0.042	0.042	0.042	0.041	0.040	0.014	0.042
NO3 (mg/l)	1.245	1.248	1.242	1.245	1.244	1.196	1.190	0.920	1.246
CBOD (mg/l)	0.712	0.716	0.705	0.705	0.711	0.729	0.721	0.634	0.709
DO (mg/l)	6.981	6.963	7.004	7.006	6.970	6.663	6.684	7.691	6.984
Chl-a (µg/l)	2.017	2.036	1.990	1.991	2.014	2.082	2.045	1.609	2.005

Chapter Eight: Conclusions and Recommendations

The Tigris River system (the mainstem of the Tigris River and Tharthar Lake with its canals) in Iraq was modeled using the 2-D hydrodynamics and water quality model CE-QUAL-W2 Version 4.0 from Mosul Dam (river km 0) upstream Mosul City to Kut Barrage (river km 880) in Kut City. The model was run from January 1st, 2009 to December 31st, 2009. The model state variables included longitudinal and vertical velocity, water level, water temperature, total dissolved solids, phosphate, ammonia, nitrate, carbonaceous oxygen demand, dissolve oxygen, and algae. Chlorophyll-a was also included in the Tigris River model as a derived water quality constituent. Scenarios were performed with the base model of the Tigris River to give more insight into how the river responds to changes in hydrology, an upstream increase in nutrients at Mosul Dam, and possible climate change of increasing air temperatures. The Tigris River system was classified into 9 waterbodies with 9 branches, 343 longitudinal segments, and 84 vertical layers for each segment with 1 m height for each layer.

Field data such as flow, water level, bathymetry and some water quality constituents (total dissolved solids and nitrate) were provided from the Water Resources Ministry in Iraq (MOWR, 2014) and were used to develop the model's input files and to calibrate the model by comparing model predictions to field data. Meteorological data for the Tigris River model were obtained from the Iraqi Ministry of Transportation, the General Organization for Meteorology and Seismic Monitoring (MOT-IMOAS 2014).

Field data for water temperature were extremely scarce in Iraq and therefore water temperatures for upstream boundary conditions at Mosul Dam and model calibration at Baeji and Baghdad cities were estimated from Landsat using remote sensing and image processing technique.

Model predictions of flow and water level were compared to field data at three stations along the mainstem of the Tigris River located at Baeji city, downstream Samarra Barrage and Baghdad city with flow absolute mean error varying from 12.57 to 3.38 m^3/s and water level absolute mean error varying from 0.036 to 0.018 m. The average percentage errors of flowrate at Baeji city, downstream Samarra Barrage and Baghdad city were 1.93%, 0.83%, and 0.81% respectively. Adding a distributed tributary to the Tigris River model allowed for flow calibration by accounting for ungaged flow such as ground water, runoff, and irrigation return flow. Model predictions of flow could be improved by having more field data at different gaging stations along the mainstem of the Tigris River and Tharthar Lake.

Model predictions of temperatures were compared to remotely sensed temperature data at both Baeji and Baghdad cities. Model predictions of temperatures significantly agreed with the estimated data since model predictions were within 95% confidence interval with a noticeable bias in winter months due to uncertainty in Landsat estimations at both Baeji and Baghdad cities. The absolute mean error of temperature predictions varied from 0.91 to 1.04 ° C. Model predictions of temperatures could significantly be improved by providing temperature field data at multiple gaging stations both longitudinally and vertically to compare with the model vertical profile.

Model predictions of total dissolved solids and nitrate were compared to monthly averaged field data. Model predictions of TDS were compared to field data at Samarra Barrage, Baghdad city, and Kut Barrage. TDS concentrations in the Tigris River started to significantly increase from Mosul dam to Kut Barrage with a peak in winter months due to storm water runoff. Unregulated effluents from three waste water treatment plants (WWTPs) within Baghdad city cause a significant increase in TDS concentrations in addition to irrigation back flow in Baghdad city and downstream areas since this region contains agricultural lands. Model predictions of NO3 were compared to field data at both Samarra Barrage and Baghdad city. There was no significant increase in NO3 concentrations between Samarra Barrage and Baghdad city.

Model predictions of other water quality state variables such as phosphate, ammonium, biochemical oxygen demand, algae and chlorophyll-a and dissolved oxygen were estimated based on field data collected from the literature. BOD concentrations within Baghdad city were extremely high due to direct discharge of industrial wastewater into the mainstem of the Tigris River from numerous factories located along the river banks. There were no considerable changes in both PO4 and NH4 concentrations in Baghdad and downstream cites. A sensitivity study was conducted to check if satellite images show high Chl-a concentrations using a Chl-a correlation provided from previous literature studies. The study showed that the best algal growth rate was 0.98 d^{-1} that subsequently used for all management scenarios of the Tigris River system. Evaporation rate in Tharthar Lake was 2.2 m for the simulated year 2009 which compared well with measured evaporation of 2.27 m for a nearby lake (CSO, 2010).

Multiple scenarios were implemented using the base 2009 model of the Tigris River by altering hydrology, increasing upstream nutrients, increasing air temperature, disconnecting Tharthar Lake from the Tigris River system, and simulating a long-term model of the Tigris River system. Increasing upstream flowrates at Mosul Dam by 15% decreased TDS concentrations from 495 mg/l to 470 mg/l in the mainstem. CBOD concentrations in the mainstem were also decreased by 3%.

On the other hand, decreasing upstream flow showed a significant impact on water quality in the Tigris River causing a significant increase in concentrations of TDS by 6.55%, PO4 by 3%, NH4 by 4.5%, NO3 by 2.3%, and CBOD by 5%, while DO concentration decreased by 0.33%. Increasing nutrient concentrations by 10% at Mosul Dam increased PO4, NH4, and NO3concentrations in the mainstem by 4.6%, 5.65%, and 5.65%, respectively.

Assuming an increase in air temperatures of 2 ºC and a corresponding increase in dew point temperatures increased water temperatures in the mainstem of the Tigris River from 20.7 º C to 21.7 º C causing a subsequent decrease in DO levels from 8.15 mg/l to 7.98 mg/l. Average TDS concentrations in the mainstem and Tharthar Lake increased from 494.5 mg/l and 1239 mg/l to 495 mg/l and 1241 mg/l, respectively. NO3 concentration in the lake decreased from 1.24 mg/l to 1.196 mg/l, while there were no changes in PO4 and NH4 concentrations compared with the base model. There were no significant impacts on CBOD concentration in the mainstem. Chl-a concentrations were slightly increased in the mainstem due to climate change effect with an average concentration changed from 1.97 µg/ to 2 µg/l.

Disconnecting Tharthar Lake from the Tigris River system significantly affected the hydrologic regime downstream of Samarra Barrage by passing 36% more water from Samarra Barrage to Baghdad city causing a substantial decrease in TDS concentration by 25%. In addition, Chl-a concentrations were decreased dramatically from 1.97 µg/l to 1.18 µg/l in the mainstem of the Tigris River.

A long-term 6-year simulation was performed on the Tigris River system. The average temperature in Tharthar Lake increased from 17.44 º C to 17.5 º C, while no change in water temperatures was noticed in the mainstem. The average TDS concentration decreased from 1239 mg/l to 1041 mg/l in Tharthar Lake, while the average TDS concentration was increased from 495 mg/l to 500 mg/l in the mainstem. There were no major changes in the average concentrations of PO4, NH4, and NO3 in the mainstem. PO4, NH4, and NO3 concentrations decreased by 2%, 62%, and 95.4%, respectively. Average concentrations of CBOD and Chl-a decreased from 0.71 mg/l and 2 µg/l to 0.63 mg/l and 1.6 µg/l, respectively.

After decreasing BOD concentrations of the Tigris River by 50%, BOD concentrations in the mainstem decreased by 24%, while DO concentrations increased by 2.8%. There were no significant impacts on Chl-a concentrations in the mainstem of the river.

Finally, it was found that approximately 50 km below Mosul Dam was affected by extremely low dissolved oxygen release from Mosul Dam before DO concentrations reached an equilibrium concentration.

The following conclusions can be made:

- Due to extremely low flow rates, there was no significant effect of highly saline water discharged through Audiam tributary to the mainstem of the Tigris River.
- Ungaged flow in the Tigris River system was significantly important in the model flow calibration and can be accounted for using distributed tributaries.
- Water Treatment plants in Baghdad city withdrew about 6% of the average flow in the Tigris River.
- Saline water diverted from Tharthar Lake, irrigation return flow, wastewater effluents, and urban runoff caused high TDS concentration in the Tigris River from Baghdad city to Kut Barrage.
- The mainstem of the Tigris River within Mosul city was not affected by treated wastewater as it discharged to natural Wadies. Also, the Tigris River from Tikrit city to Samarra Barrage was not affected by discharging 25% of the treated wastewater due to extremely low flow rates.
- Landsat images proved a good resource to estimate water temperatures in the Tigris River for upstream boundary conditions at Mosul Dam and for in-river calibration.
- Chlorophyll-a concentrations in Tharthar Lake could be retrieved from Landsat images.
- Air temperature is a significant predictor of surface water temperature of the Tigris River.
- Temperature calibration in the Tigris River system was highly sensitive to meteorological input data.

- There was no noticeable stratification found in both Samarra Barrage and Kut Barrage.
- Surface water temperature in Tharthar Lake varied longitudinally along the North-South axis with warmer temperatures in the lower part compared with the upper part of the lake.
- High Manning's friction in the Tigris River within Baghdad city was observed due to the effect of channel irregularity and obstruction (such as debris deposits and bridge piers), the degree of meandering, and imperfections in the given cross-sectional geometry.
- Diverted water from Tharthar Lake to the Tigris River caused a significant increase in the water age of the river within Baghdad and downstream cites.
- A parcel of water released from Mosul Dam reaches to Baeji, Samarra Barrage, Baghdad, and Kut Barrage after approximately 3 days, 5 days, 10 days, and 19 days, respectively.
- Increasing upstream flow by 15% at Mosul Dam significantly improved TDS concentrations in the mainstem and in Tharthar Lake, while decreasing upstream flow negatively impacted TDS concentrations in the Tigris River system.
- A 10% increase in the annual average flow diverted from Samarra Barrage to Tharthar Lake should be allocated to constantly reduce salinity in the lake.
- 50 km long in the mainstem of the Tigris River below Mosul Dam was affected by extremely low DO release from Mosul Dam before DO concentrations reached steady state.

The following recommendations can be made:

- The head water quantity and quality of the Tigris River as it inters Iraq through the Turkey-Iraqi border should be monitored based on previously signed agreements between the two countries because this is an important boundary condition for predicting downstream water quality
- Since the model started at the base on Mosul dam, the reservoir itself should be monitored and modeled to assess water quality transformations within the reservoir
- The average annual flow of the Tigris River in Baghdad city should not be less than the existing annual average flow of 420 m^3/s to keep the average TDS concentration in the mainstem less than 500 mg/l. A decrease in the river flow will negatively impact its quality by increasing TDS, nutrients, BOD, and Chl-a concentrations.
- Since the Upper Zab tributary is the biggest contributor, after the upper Tigris basin, to the Tigris River with 33% of its annual volume, its flow should be managed through constructing a new dam that controls its discharge to the mainstem of the river.
- Wastewater in Baghdad city should efficiently be treated.
- Man-made canals used for irrigation should strictly be monitored to understand the impact of irrigation return flow on the mainstem of the Tigris River.
- Unregulated water withdrawn from the main stream of the Tigris River for irrigation should be controlled and new polices should be strictly implemented.

- More strategies on restoring the Tigris River should be planned a head as the future climate change will significantly impact the river's thermal regime.

The Tigris River Model Improvements and Recommendations

The mainstem of the Tigris River and Tharthar Lake was modeled for the year of 2009. The current model can be improved by the following suggestions organized by data type.

Flow Data

Having flow rate data, the Tigris River system model uncertainty can be reduced. Flowrate data in Tharthar Lake and its canals are extremely important for model comparisons and currently no such data were available for this study. Flowrate data are also needed for the mainstem of the Tigris River in the area between Baghdad city and Kut Barrage where numerous unmonitored withdrawals, runoff, and irrigation return flow occurred. These data give more understanding and more insight of how water is entering and leaving the system. It is also very important to have flow data for both the Upper Zab and Lower Zab tributaries since they are significant contributors to the Tigris water. Currently, the Upper Zab tributary was completely unmonitored for flow. Finally, flow data from Samarra Barrage to Erwaeiya canal are needed as well.

Temperature Data

In-situ water temperature data of the Tigris River system would be important for improving model calibration. The current model was evaluated utilizing surface water temperatures estimated from Landsat which add a level of uncertainty in model predictions and ultimately affect the temperature calibration. The mainstem of the Tigris River and Tharthar Lake lack temperature monitoring stations. Moreover, vertical temperature

profiles in Tharthar Lake would be very important to verify the model's predicted thermal dynamics in the water column. In addition, all tributaries of the Tigris River had no available temperature data, and therefore it is crucial to monitor flow temperature of at least both the Upper Zab and Lower Zab which are the main tributaries of the Tigris River. Availability of field temperature data gives the opportunity to validate satellite temperate and to reduce the level of uncertainty in the satellite estimates.

Water Quality Data

The mainstem of the Tigris River and Tharthar Lake lack most of water quality constituents used in the model study. Most of the available data of the Tigris River were monthly average TDS and nitrates during the simulated year 2009, while there were no data available for phosphate, dissolved oxygen, ammonia, organic matter, alkalinity, inorganic carbon, and algae. Although some monthly average data were available, it was difficult to distinguish specific seasonal and diurnal trends. Upstream of the Tigris River model at Mosul Dam, there were no water quality data available except for monthly average data of TDS. Knowing that the Mosul Dam can affect water quality significantly, knowing the discharge water quality coming from Mosul Dam is an important aspect of understanding how this inflow affects the Tigris River. Tharthar Lake also had no water quality data available during the simulated year. In addition, more water quality monitoring stations should be available along the main tributaries of the Tigris River such as Upper Zab and Lower Zab. Also, no water quality data were available from the WWTPs that discharge effluents into Diyala River, a tributary of the Tigris River, and eventually discharge into the mainstem of the Tigris River. Therefore, water quality data from WWTPs would be important for assessing water quality impacts on the Tigris River.

Model Grid and Bathymetry Data

Having 500 m or 1 km cross sections of the Tigris River would allow for more accurate calibration of flow and depths, temperature, and water quality constituents. The current cross section data of the mainstem of the Tigris River were provided with 5 km increments with some areas with missing data filled by interpolation. Moreover, more accurate bathymetric data of Tharthar Lake could significantly improve model calibration of the lake. A new cross section survey of the mainstem of the Tigris River would be important to provide bathymetric data of the system as a result of sediments were introduced into the water system after numerous wars in Iraq.

Meteorological Data

Improved meteorological data would be useful for temperature and water quality calibration. Solar radiation data would be a valuable and would significantly affect the water temperature calibration. Moreover, metrological data were only available from a meteorological station near Baghdad airport in Baghdad city and therefore more metrological data in the western parts of Iraq where Tharthar Lake is located would be important to understand thermal dynamics and summer stratification in Tharthar Lake.

References

Abdul Jabar, R. A., Al-Lami, A. A-Z., Abdul Khader, R. S., Radhi, A. G., (2008). "Effects of some physical and chemical factors of Lower Zab water on Tigris River." Tikrit J. of Pure Sci. 13, 132-142.

Abdul Razzak, I. A., Sulaymon, A. H., and Al-Zoubaidy, A. R. (2009). "Modeling the distribution of BOD and TDS in part of Tigris River within Baghdad." J. Engineering, 15, 3673-3691.

Abdul Razzak, I., (2006) "Studying and modeling the effects of pollution sources in Tigris river between Al-A'imma Bridge and al-Jumhuriya Bridge in Baghdad." Master's thesis, University of Baghdad, Iraq.

Adams, E. E. and Wells, S. A. (1984) "Field Measurements on Side Arms of Lake Anna, Virginia," Journal of Hydraulic Engineering, ASCE, Vol. 110, No. 6, 773-793.

Aenab, A. M., and Singh, S. K., (2012). "Evaluation of drinking water pollution and health effects in Baghdad, Iraq." J. Environ. Protection, 3, 533-537.

AFED (Arab Forum for Environment and Development) (2009). "Impact of Climate Change on Arab Countries."
http://www.afedonline.org/en/ (October/19/2017)

Alena, A. M., and Singh, S. K., (2012). "Evaluation of drinking water pollution and health effects in Baghdad, Iraq." J. Environ. Protection, 3, 533-537.

Ali, A. A., Al-Ansari, N. A., and Knutsson, S., (2012). "Morphology of Tigris River within Baghdad city." J. Hydrol. Earth Syst. Sci., 16, 3783-3790.

Alobaidy, A. H., Maulood, B. K., and Kadhem, A. J. (2010). "Evaluating raw and treated water quality of Tigris River within Baghdad by index analysis." J. Water Res. and prot., 2, 629-635.

Ansari, F., Awasthi, A. K., and Srivastava, B. P. (2012). "Physico-chemical Characterization of Distillery Effluent and its Dilution Effect at Different Levels." Scholars Research Library Archives of Applied Science Research, 4(4), 1705–1715.

Al-Anbari, R. A., Mahmood, T. A., and Yousif, W. F., (2006). "Hydraulic geometry of the Tigris River from Mosul to Bejee related to water temperature modeling." J. Env. Hydrol., 14, 1-11.

Al-Ansari, N., Ali, A. A., Al-Suhail, Q., & Knutsson, S. (2015). Flow of River Tigris and its Effect on the Bed Sediment within Baghdad, Iraq. Open Engineering, 5(1), 465–477. https://doi.org/10.1515/eng-2015-0054

Al-Ansari, N. and Knutsson, S., (2011). "Toward prudent management of water resources in Iraq." J. Advanced Science and Eng. Res., 1, 53-67.

Al-Badry, M., and Artin, Y., (1972). "Study of salinity of Tigris and Euphrates Rivers and Tharthar Lake with reference to sweetening period of Tharthar lake "unpublished report", Ministry of Irrigation, D.G of Dams and Reservoirs.

Al-Dabbas, M., and Hassan, H. A., (1987). "On condition Tharthar salinity problem model." J. Agriculture and Water Resources Research, AWRRC, Council for Scientific research, Iraq.

Al-Dabbas, M. and Al-Juburi, H., (1985). "Hydrochemical analysis and sediment distribution of Tharthar reservoir." Unpublished report, Water Resources Dept., AWRRC., Council for Scientific Research, Iraq.

Al-Jebouri, M. M., and Edham, M. H., (2012). "An Assessment of biological pollution in certain sector of lower Al-Zab and river Tigris waters using bacterial indicators and related factors in Iraq." J. Water Resources and Pollution, 4, 32-38

Al-Jubori, M.A.M. (1998). "Watercourse flow pattern of the River Tigris between the two Zabs." Ph.D. thesis, Mosul Univ., Iraq.

Al-Layla, M. A, and Al-Rizzo, H. M., (1989). "A water quality model for the Tigris River downstream of Sadam Dam, Iraq." J. Hydro. Sci., 34:6, 687-704.

Al-Layla, M. A, Kharrufa, S. N., Akrawi, S. M., (1990). "Effect of Saddam Dam on Tigris River water quality." J. Environ. Sci. Health, A25(1), 47-66.

Al-Marsoumi, A. H., Al-Bayati, K. M., and Al-Mallah, E. A., (2006). "Hydrogeochemical aspects of Tigris and Euphrates Rivers within Iraq: A comparative study." J. RAF. Sci., 17, 2, 34-49.

Al-Murib, M. (2014) "Application of CE-QUAL-W2 on Tigris River in Iraq." Civil and environmental Engineering Master's Project Report.
http://pdxscholar.library.pdx.edu/cengin_gradprojects/9

Al-Obaidy, F. M. Sh. (1996). "Hydrological study of the stage and other characteristics of Tigris River." M.S. thesis, Mosul Univ., Iraq.

Al-Rawi, S. M., (2005). "Contribution of Man – Made Activities to the Pollution of the Tigris within Mosul Area/IRAQ." International J. Environ. Research & Public Health, 2, 245-250.

Al-Samak, M.A.S., Al-Saati, B.A, Al-Janabi, F.H., Al-Timimi, A.A. and Ghalib, S.A. (1985). "Iraq-Regional Study." Vol.1, Dar Al-Kutib, Mosul Univ., P304 (in Arabic).

Al-Shahrabaly, Q. M. (2008). "River discharges for Tigris and Euphrates gauging stations." Ministry of water Resources, Baghdad.

APHA (American Public Health Association) (1992). Standard methods for the examination of water and wastewater, 18ed., Washington, DC.

Aziz, A. M., Aws, A. (2012). "Wastewater production treatment and use in Iraq country report." Ministry of water Resources, Iraq.

Baban, I. J., (1977). "General survey of hardness in natural waters of Iraq and effects of drainage schemes on it." M.S. thesis, Baghdad Univ., Iraq.

Boer, T. (2014). "Assessing the Accuracy of Water Temperature Determination and Monitoring of Inland Surface Waters Using Landsat 7 ETM + Thermal Infrared Images A Case Study on the Rhine River, North Sea Canal, and Hollands Diep." M.S. thesis, Delft University of Technology, Delft, The Netherlands.

Burnham, G., Lafta, R., Doocy, S., and Roberts, L., (2006). "Mortality after the 2003 Invasion of Iraq: A cross-sectional cluster sample survey." Lancet, 368, 9545, 1421-1428.

Camberato, J., (2001). "Irrigation water quality." Clemson University, http://www.scnla.com/Irrigation_Water_Quality.pdf (Apr.19, 2017)

Charbeneau, R. J., and Holley, E. R., (2001). "Backwater effects of bridge piers in subcritical flow." Research report conducted for the Texas Dept. of Transportation. http://ctr.utexas.edu/wp-content/uploads/pubs/1805_1.pdf

CSO (2010). "Central Statistical Organization in Iraq_Environmental Statistics Report in Iraq for the year 2009." In Arabic. Accessed on April-21-2017. http://www.cosit.gov.iq/ar/env-stat/envi-stat

Chander, G., & Markham, B. (2003). Revised Landsat-5 TM radiometric calibration procedures and post calibration dynamic ranges. IEEE Transactions on Geoscience and Remote Sensing, 41, 2674–2677.

Chow, V.T., (1959). "Open-channel hydraulics": New York, McGraw-Hill, 680 p.

Chipman, J. W., Lillesand, T. M., Schmaltz, J. E., Leale, J. E., & Nordheim, M. J. (2004). Mapping lake water clarity with Landsat images in Wisconsin, USA. Canada Journal of Remote Sensing, 30, 1–7.

Cole, T. M., Wells, S. A. (2017). "CE-QUAl-W2: a two-dimensional, laterally averaged, hydrodynamic and water quality model." version 3.71. Instruction Report EL-2000. US Army Engineering and Research Development Center, Vicksburg.

Coll, C., Galve, J. M., Sánchez, J.M., and Caselles, V. (2010), "Validation of Landsat-7/ETM+ Thermal-Band Calibration and Atmospheric Correction with Ground-Based Measurements", IEEE Trans. Geosci. Remote Sens., vol. 48, no. 1, pp. 547–555.

Di Baldassarre, G., & Montanari, A. (2009). Uncertainty in river discharge observations: a quantitative analysis. Hydrology and Earth System Sciences, 13(6), 913–921. https://doi.org/10.5194/hess-13-913-2009

Edinger, J.E., and Buchak, E.M. 1975. "A Hydrodynamic, Two-Dimensional Reservoir Model: The Computational Basis", prepared for US Army Engineer Division, Ohio River, Cincinnati, Ohio.

Fan, D., Huang, Y., Song, L., Liu, D., & Zhang, G. (2014). "Prediction of chlorophyll a concentration using HJ-1 satellite imagery for Xiangxi Bay in Three Gorges Reservoir." Water Science and Engineering, 7(1), 70–80.

FAO (2008) "Irrigation in the Middle East region in figures – AQUASTAT Survey" http://www.fao.org/nr/water/aquastat/basins/euphrates-tigris/Euphrates.tigris-CP_eng.pdf. (Sep. 12, 2017).

Fuller, R. M., Groom, G. B., & Jones, A. R. (1994). "The land cover map of Great Britain: An automated classification of Landsat Thematic Mapper data", Photogrammetric Engineering and Remote Sensing, 60, 553−562.

Giardino, C., Pepe, M., Brivio, P. A., Ghezzi, P., and Zilioli, E., (2001). "Detecting chlorophyll. Secchi disk depth and surface temperature in a sub-alpine lake using Landsat Imagery." J. Sci. Total Environ. 268, 19-29.

Hanson, B., Schwankl, L., and Fulton, A., (2004). "Introduction to irrigation scheduling." Scheduling irrigations: When and how much water to apply, Water Management Handbook Series, UC ANR publication 3396.

Hikmat, M. (2005). "Two-dimensional numerical model for the distribution of pollutants in Tigris River downstream of Tharthar-Tigris channe1." M.S. thesis, University of Baghdad, Baghdad, Iraq.

Husain, A. (2009). "Monthly changes of some physiochemical parameters for Tigris River-Baghdad between 2002-2003. J. Engineering and Technology, 27, 64-70.

IPCC (Intergovernmental Panel on Climate Change) (2007) Climate Change 2007: Climate Change Impacts, Adaptation and Vulnerability. Cambridge University Press, Geneva.

Ismail, A. H., and Abed, G. A., (2013). "BOD and DO modeling for Tigris River at Baghdad city portion using QUAL2K model." J. Kerbala University. 11, 257-273.

Issa, I. E., Al-Ansari, N. A., Sherwany, G, and Knutsson, S., (2014). "Expected future of water resources within Tigris-Euphrates Rivers, Iraq." J. water Resources and Protection, 6, 421-432.

Jasim, H. A. J. (1988). "Some effects of Tharthar-Tigris canal on water quality of the Tigris River." M.S. thesis, Baghdad Univ., Iraq.

Jehad, A. A., (1983). "Effect of Tharthar canal salty water on the quality of Euphrates water." M.S. thesis, Technology Univ., Iraq.

Jimeneze-Munoz, J. C., Sobrino, J. A. (2003) "A generalized single-channel method for retrieving land surface temperature from remote sensing data." J. Geophysical Research, 108, (D22).

Kabbara, N., Benkhelil, J. Awad, M., and Barale, V., (2008) "Monitoring water quality in the coastal area of Tripoli (Lebanon) using high-resolution satellite data." J. Photogrammetry &Remote sensing, 63, 488-495.

Kadhem, A. J., (2013). "Assessment of water quality in Tigris River-Iraq by using GIS mapping." J. Natural Resources, 4, 441-448.

Khattab, M. F. O., and Merkel, B. J., (2014) "Application of Landsat 5 and Landsat 7 images data for water quality mapping in Mosul Dam Lake, northern Iraq." Arab J. Geosci. 7, 3557-3573.

Lamaro, A. A., Marinelarena, A., Torrusio, S. E., and Sala, S. E., (2013) "Water surface temperature estimation from Landsat 7 ETM+ thermal infrared data using the generalized single-channel method: Case study of Embalse del Rio tercero (Corodoba, Argentina)." J. Advances in Space Research, 51, 492-500.

Leopold, L. B., and Maddock, T.J., (1953) "hydraulic geometry of stream channels and some physiographic implication." USGS professional paper 252, 55p.

Liu X, Wang L, Sherman DJ, Wu Q, Su H (2011) Algorithmic foundation and software tools for extracting shoreline features from remote sensing imagery and LiDAR data. J Geogr Inf Syst 3(2):99–119.

Lu, D., Mausel, P., Brondizio, E. and Moran, E., (2002), Assessment of atmospheric correction methods for Landsat TM data applicable to Amazon basin LBA research. International Journal of Remote Sensing, 23, pp. 1671–2651.

Ministry of Environment, "System Maintenance of River and Public Water Pollution in Iraq," 1998. http://www.moen.gov.iq

Ministry of Water Resources-Iraq (MWR) (2005), Schematic diagram of main control structures in Iraq, General directorate of water resources management, hydrological studies center.

Mix Max (2009). "Iraq the Lasting Love"
http://iraqthelastinglove.blogspot.com/2009/09/more-from-iraqs-old-days.html.
(September 21, 2017)

MOT-IMOAS (2014) "Ministry of Transportation-Iraqi Meterological Organization and Seismology" http://www.meteoseism.gov.iq/index.php (Oct. 18, 2017).

MOWR (2014) "Ministry of Water Resources in Iraq" https://www.mowr.gov.iq/en (Oct. 16, 2017).

Mutlak, S. M., Salih, B. M., and Tawfiq, S. J., (1980). "Quality of Tigris River passing through Baghdad for irrigation." J. Water, Air, and Soil Pollut. 13, 9-16.

Nas, B., Ekercin, S., and Karabork, H., (2010). "An application of Landsat-5TM image data for water quality mapping in Lake Beysehir, Turkey." J. Water Air Soil Pollut. 212, 183-197.

NASA (2014). "Land Remote-Sensing Satellite System 7" https://www.nasa.gov/directorates/heo/scan/services/missions/earth/Landsat7.html (Nov. 25, 2017).

Odemis, B., Sangun, M. K., and Evrendilek, F. (2010). "Quantifying long-term changes in water quality and quantity of Euphrates and Tigris rivers, Turkey." J. Environ. Monit. Assess, 170, 475-490.

Olmanson, L. G., Bauer, M. E.,&Brezonik, P. L. (2008). "A 20-year Landsat water clarity census of Minnesota's 10, 000 Lakes". Remote Sensing of Environment, 122(11), 4086–4097.

Othman, K. I., and Deguan, W. (2004). "Characteristics of Tigris River bed at Mosul City, Iraq." Journal of Lake Sciences, 16, 61–71.

Rabee A-M., Abdul-Kareem., B. M., Al-Dhamin, A. S., (2011). "Seasonal variations of some ecological parameters in Tigris River water at Baghdad region, Iraq." J. Water Resources and Protection, 3, 262-267.

Rahi, K. A., and Halihan, T. (2010). "Changes in the salinity of the Euphrates River system in Iraq." Regional Environmental Change, 10(1), 27–35.

Reddy, M. A. (1997). A detailed statistical study on selection of optimum IRS LISS pixel configuration for development of water quality models. International Journal of Remote Sensing, 18, 2559–2570.

Ritchie, R., Cooper CM., Schiebe, FB., (1990) "The relationship of MMS and TM digital data with suspended sediments, chlorophyll and temperature in Moon Lake, Mississippi." J. Remote Sensing of Environment, 33, 137-148.

Ryu, JH, Won JS, Min, KD (2002). "Waterline exreaction from Landsat TM data in a tidal flat: a case study in Gomso Bay, Korea." J. Remote Sens Environ, 83(3), 442-456

Sauer, V. B., & Meyer, R. W. (1992). "Determination of error in individual discharge measurements." United States Geological Survey Open - File Report.

Simon, R. N., Tormos, T., and Danis, P. A., (2014) "Retrieving water surface temperature from archive Landsat thermal infrared data: Application of the mono-channel atmospheric

correction algorithm over two freshwater reservoirs." International J. Applied Earth Observation and Geoinformation, 30, 247-250.

Sissakian, V. K., (2011). "Genesis and age estimation of the Tharthar depression, central west Iraq." J. Iraqi Bulletin of Geology and Mining, 7, 47-62.

Swiss Consultants. (1979). "Tigris River water resources study." "unpublished report", Ministry of Irrigation.

The World Bank. (2006). "Iraq - Country water resource assistance strategy: addressing major threats to people's livelihoods." 1–97. https://doi.org/36297-IQ

UN-ESCWA and BGR, (2013), Inventory of Shared Water Resources in Western Asia, United Nations Economic and Social Commission for Western Asia and Bundesanstalt für Geowissenschaften und Rohstoffe, Beirut.

United Nation (UN) factsheet (2013) "Water in Iraq Factsheet" http://www.iraqicivilsociety.org/wp-content/uploads/2014/02/Water-Factsheet.pdf (Aug. 28, 2017).

U.S. Army Corps of Engineers, (2010). "HEC-RAS" manual. http://www.hec.usace.army.mil/ (Aug. 31, 2017).

United States Geological Survey (USGS) http://glovis.usgs.gov/ (Aug. 31, 2017).

United States Geological Survey (USGS) http://www.earthexplorer.usgs.gov/ (Aug. 31, 2017).

USAID (2003) "Providing Sanitation to Iraq" http://pdf.usaid.gov/pdf_docs/Pdack151.pdf (Aug. 31, 2017).

USAID (2007) "Iraq Private Sector Growth and Employment Generation." http://www.iajd.org/files/3_1.pdf. (Aug. 31, 2017).

Wanielista M, Kersten R, Eaglin R. (1997) "Hydrology: Water Quantity and Quality Control," 2nd edition. John Wiley & Sons, Inc. pp. 68–72.

Wang, F., Han, L., Kung, H., and Ardale, R. (2006) "Application of Landsat5 TM imagery in assessing and mapping water quality in Reelfoot Lake, Tennessee" International J. Remote sensing, 27, 5269-5283.

Water Research Foundation (2015). "EPA Secondary Maximum Contaminant Levels: A Strategy for Drinking Water Quality and Consumer Acceptability." Web report#4537. http://www.waterrf.org/Pages/Projects.aspx?PID=4537 (April/19/2017).

Worldometers. "World Population." http://www.worldometers.info/world-population/iraq-population/ (December/23/2017).

Wulder, M. A.,White, J. C., Goward, S. N., Masek, J. G., Irons, J. R., Herold, M., Cohen,W. B., Loveland, T. R., &Woodcock, C. E. (2008). "Landsat continuity: Issues and opportunities for land cover monitoring", Remote Sensing of Environment, 112, 955−969.

WRI (World Resources Institute) (2002) Drylands, People, and Ecosystem Goods and Services: A Web-Based Geo-Spatial Analysis. http://www.wri.org

Zakaria, S., Al-ansari, N., & Knutsson, S. (2013). "Historical and Future Climatic Change Scenarios for Temperature and Rainfall for Iraq," *7*(12), 1574–1594.

Appendix A: Management Scenarios of the Tigris River Model

Management Scenario 1: Increasing Upstream Flow

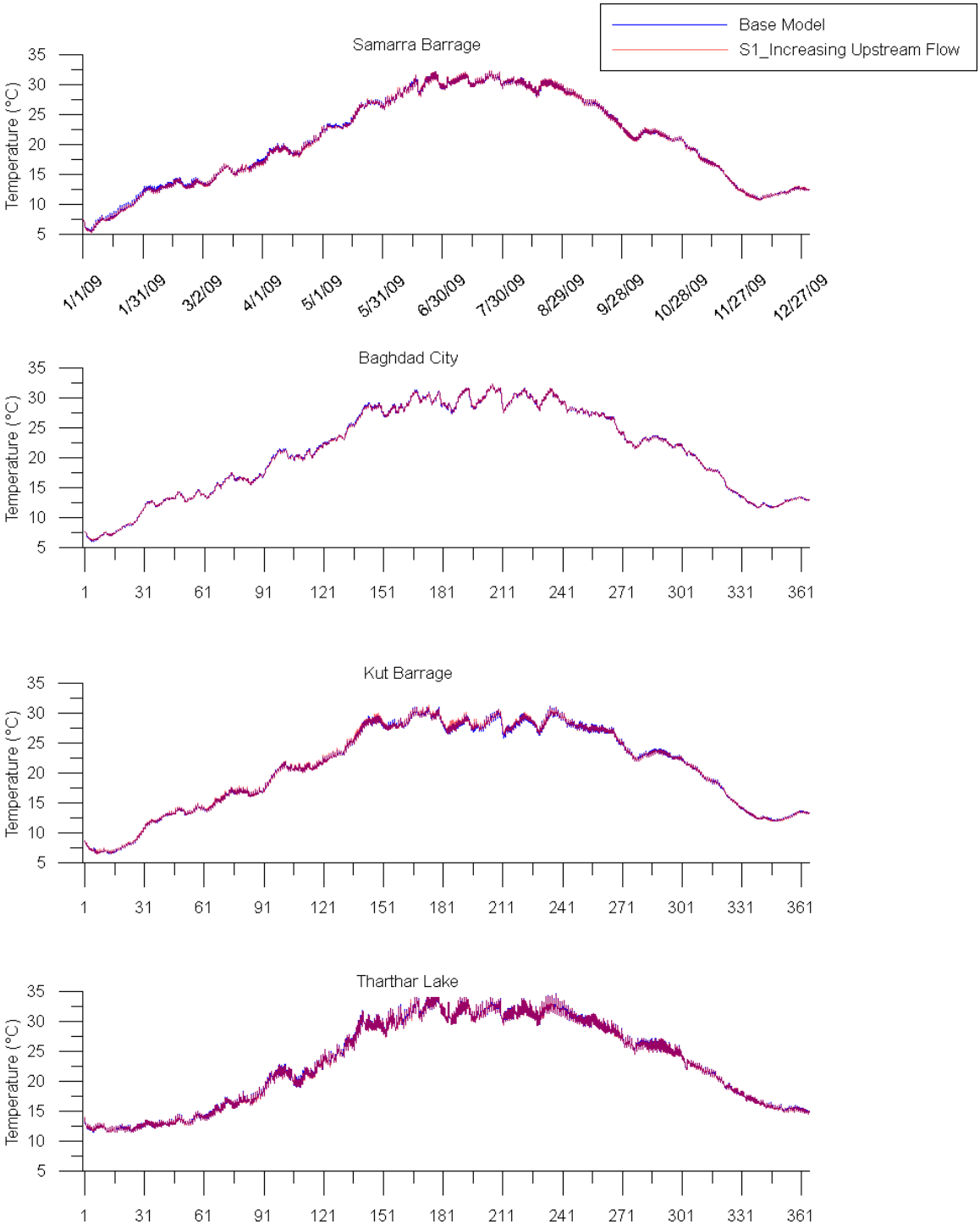

Figure 142: Model temperature (T_w) predictions for base model and management scenario 1 (increasing upstream flow) at Samarra Barrage, Baghdad City, Kut Barrage, and Tharthar Lake.

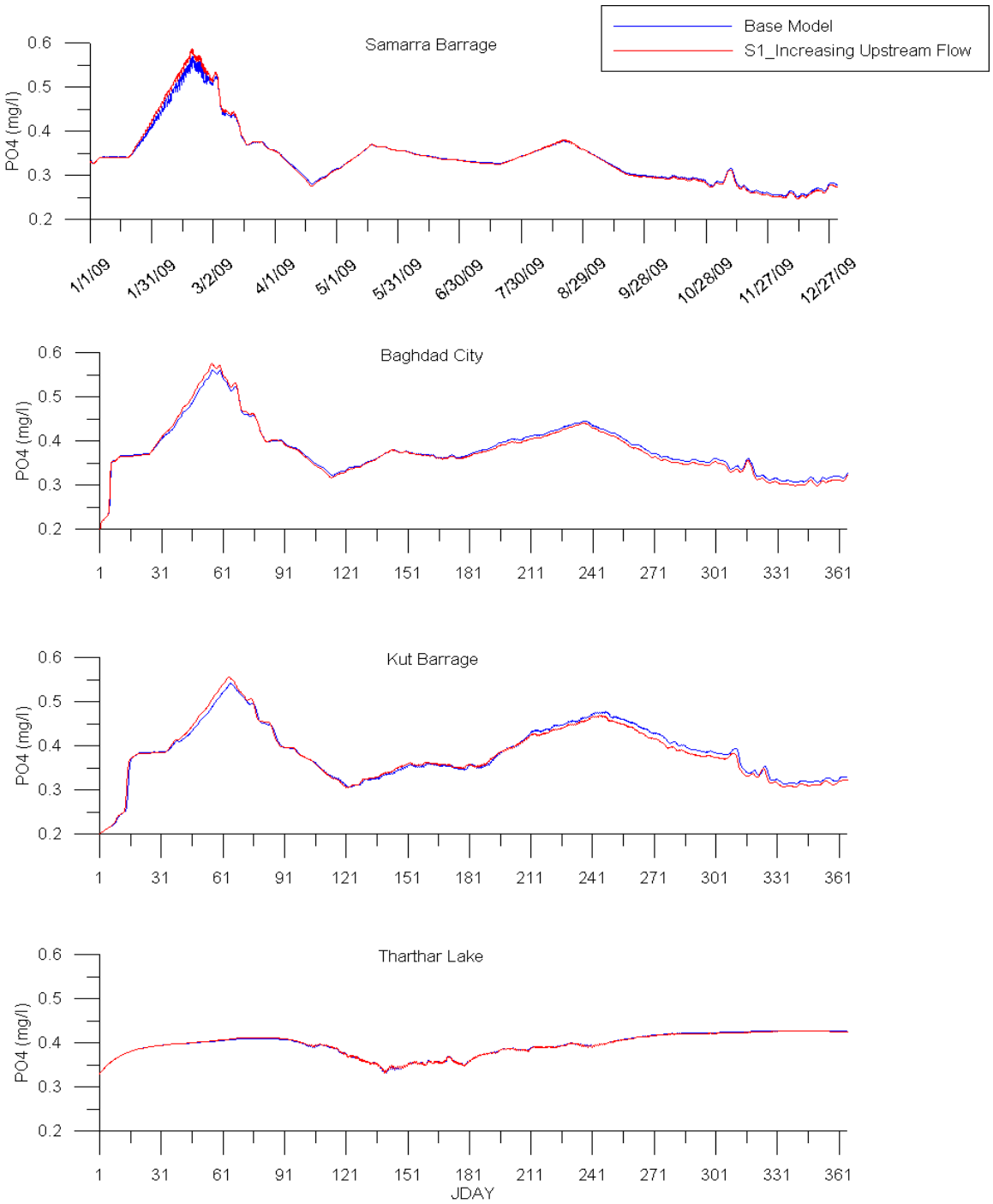

Figure 143: Model phosphate (PO4) predictions for base model and management scenario 1 (increasing upstream flow) at Samarra Barrage, Baghdad City, Kut Barrage, and Tharthar Lake.

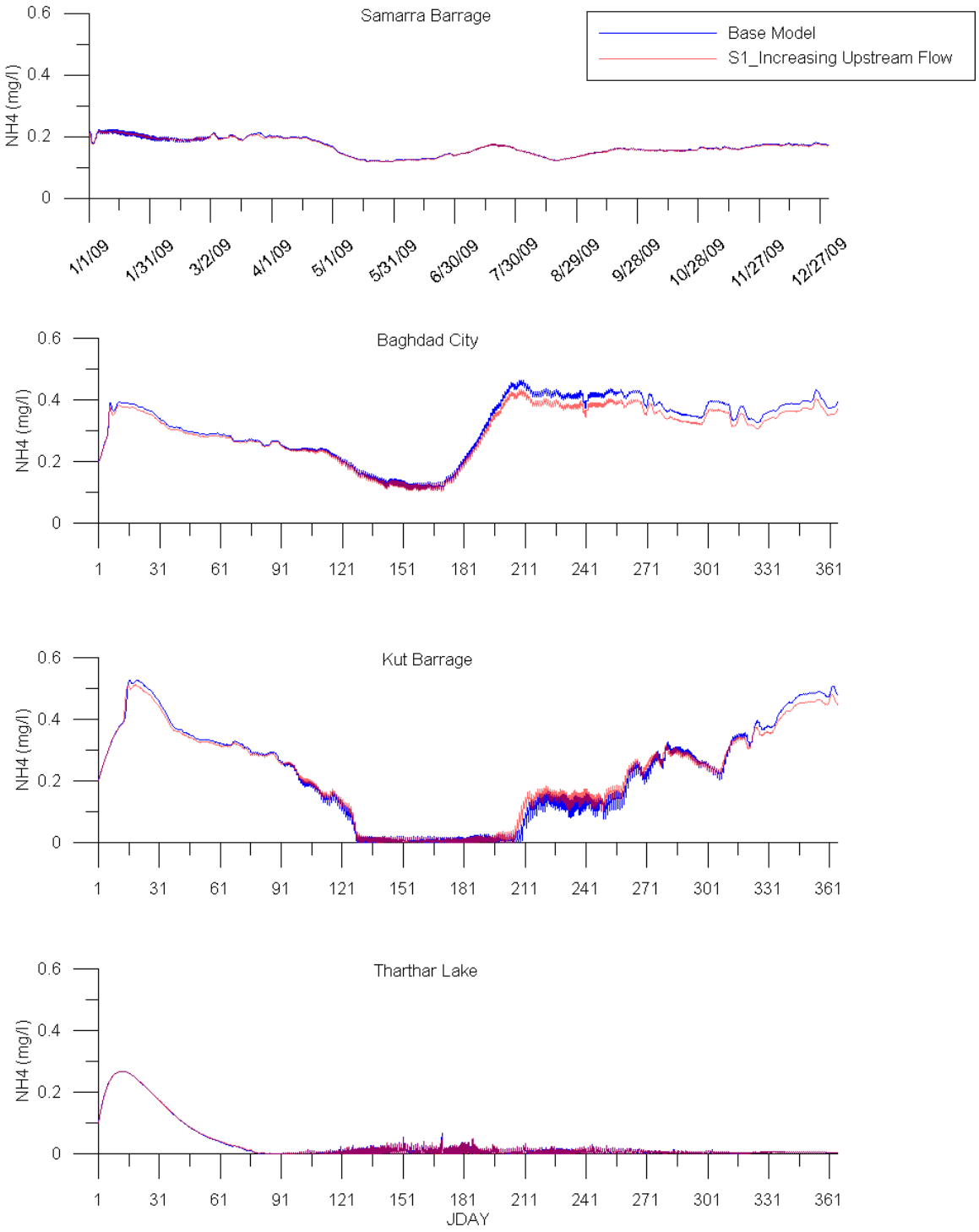

Figure 144: Model ammonia (NH4) predictions for base model and management scenario 1 (increasing upstream flow) at Samarra Barrage, Baghdad City, Kut Barrage, and Tharthar Lake.

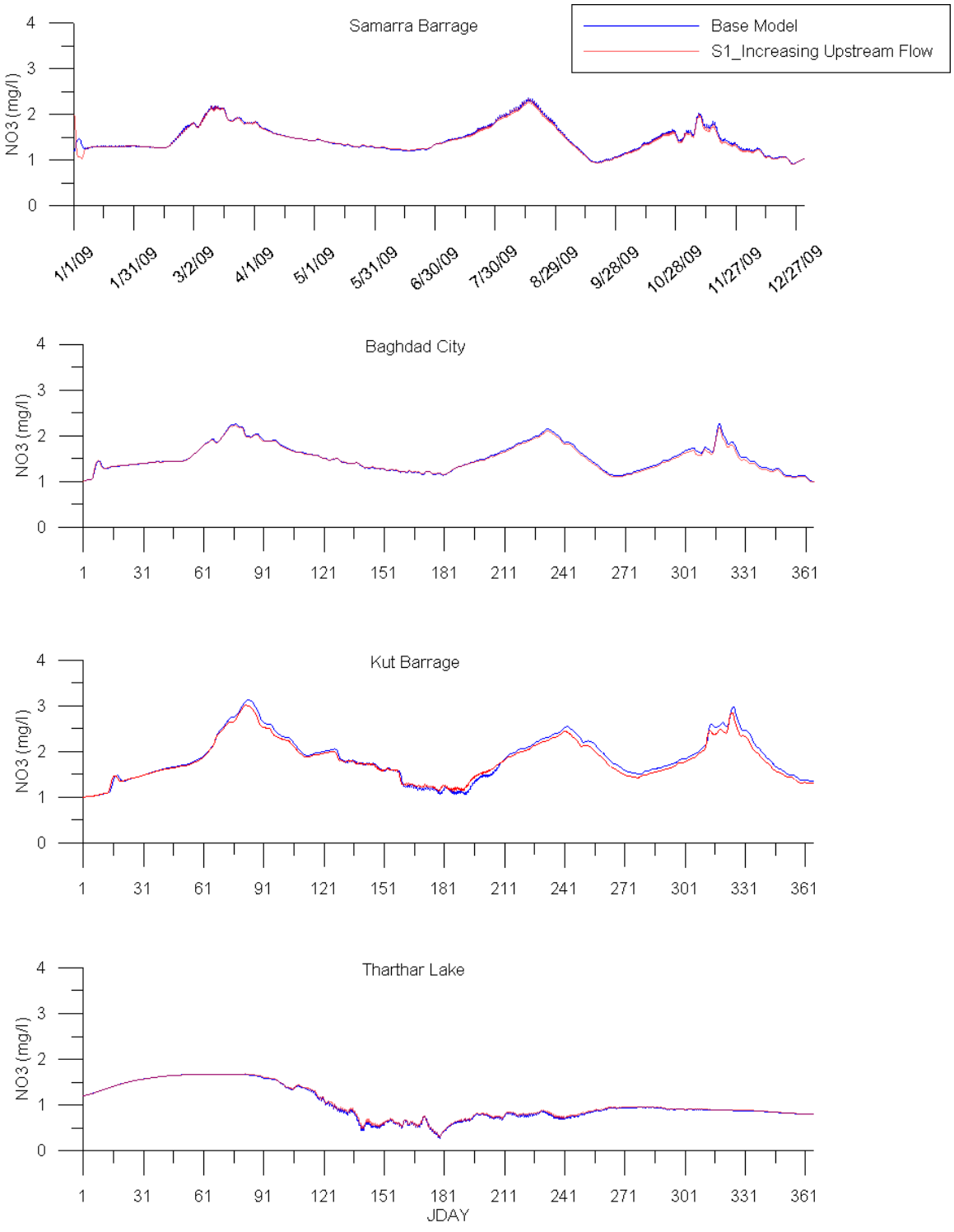

Figure 145: Model nitrate (NO3) predictions for base model and management scenario 1 (increasing upstream flow) at Samarra Barrage, Baghdad City, Kut Barrage and Tharthar Lake.

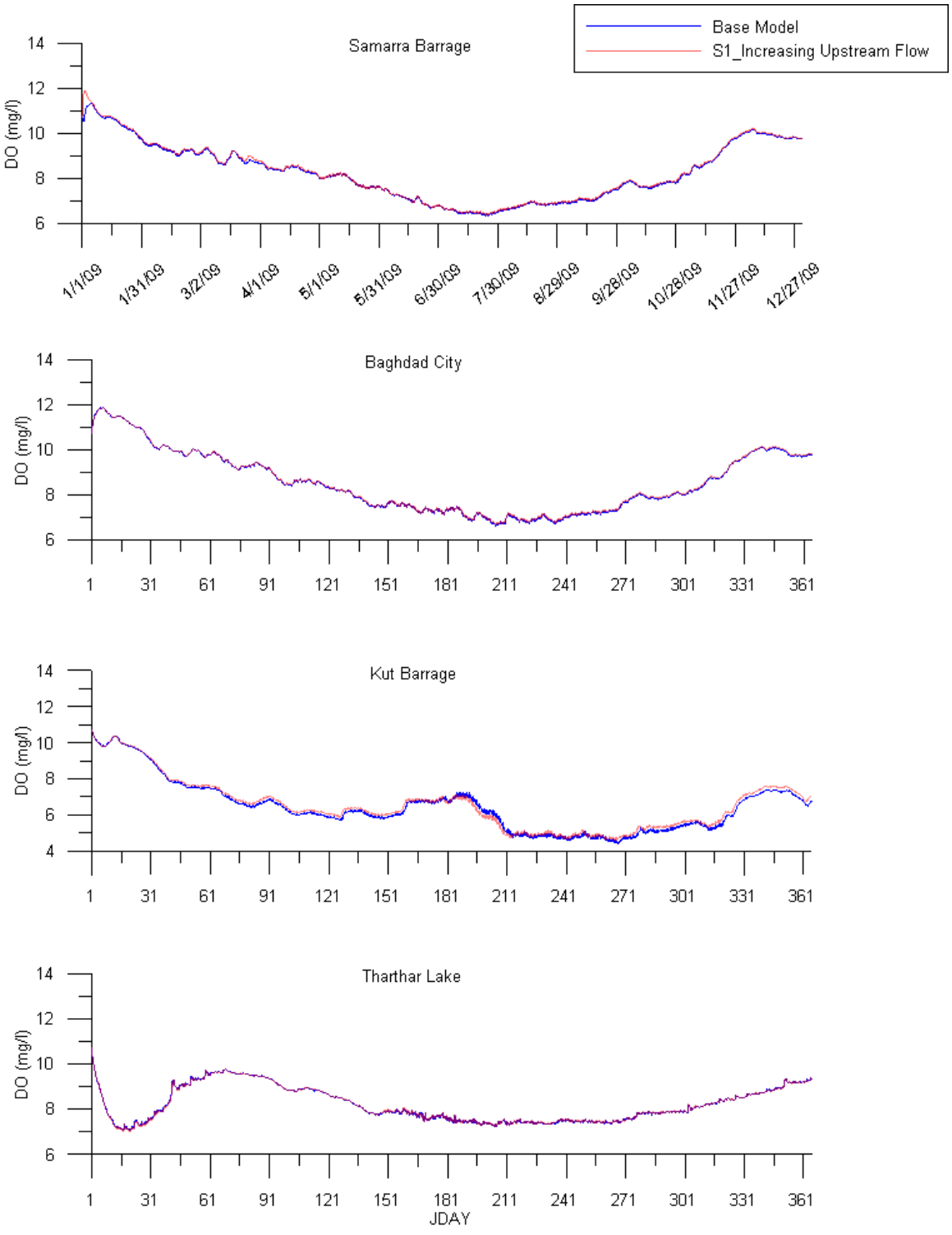

Figure 146: Model dissolved oxygen (DO) predictions for base model and management scenario 1 (increasing upstream flow) at Samarra Barrage, Baghdad City, Kut Barrage, and Tharthar Lake.

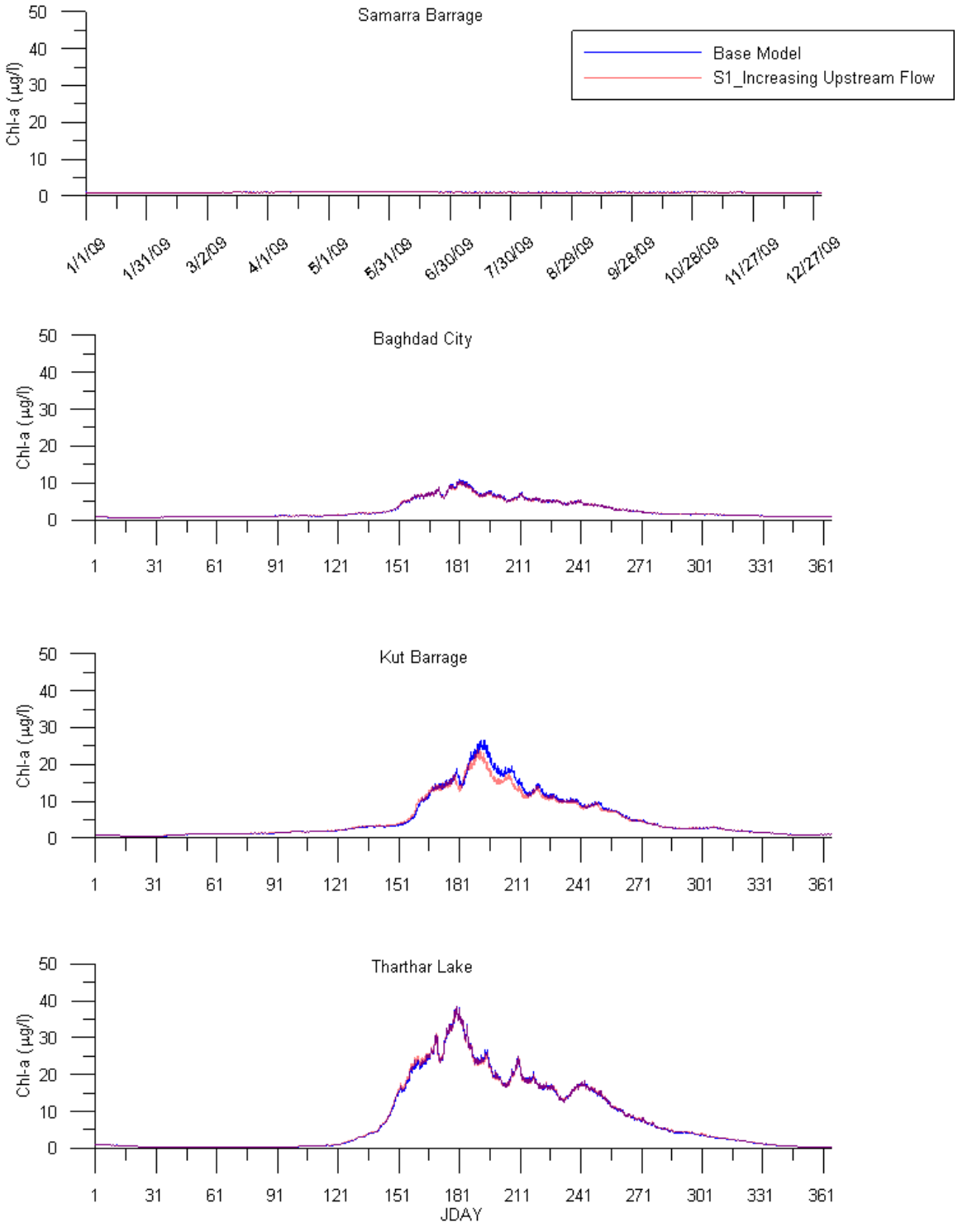

Figure 147: Model chlorophyll-a (Chl-a) predictions for base model and management scenario 1 (increasing upstream flow) at Samarra Barrage, Baghdad City, Kut Barrage, and Tharthar Lake.

Management Scenario 2: Decreasing Upstream Flow

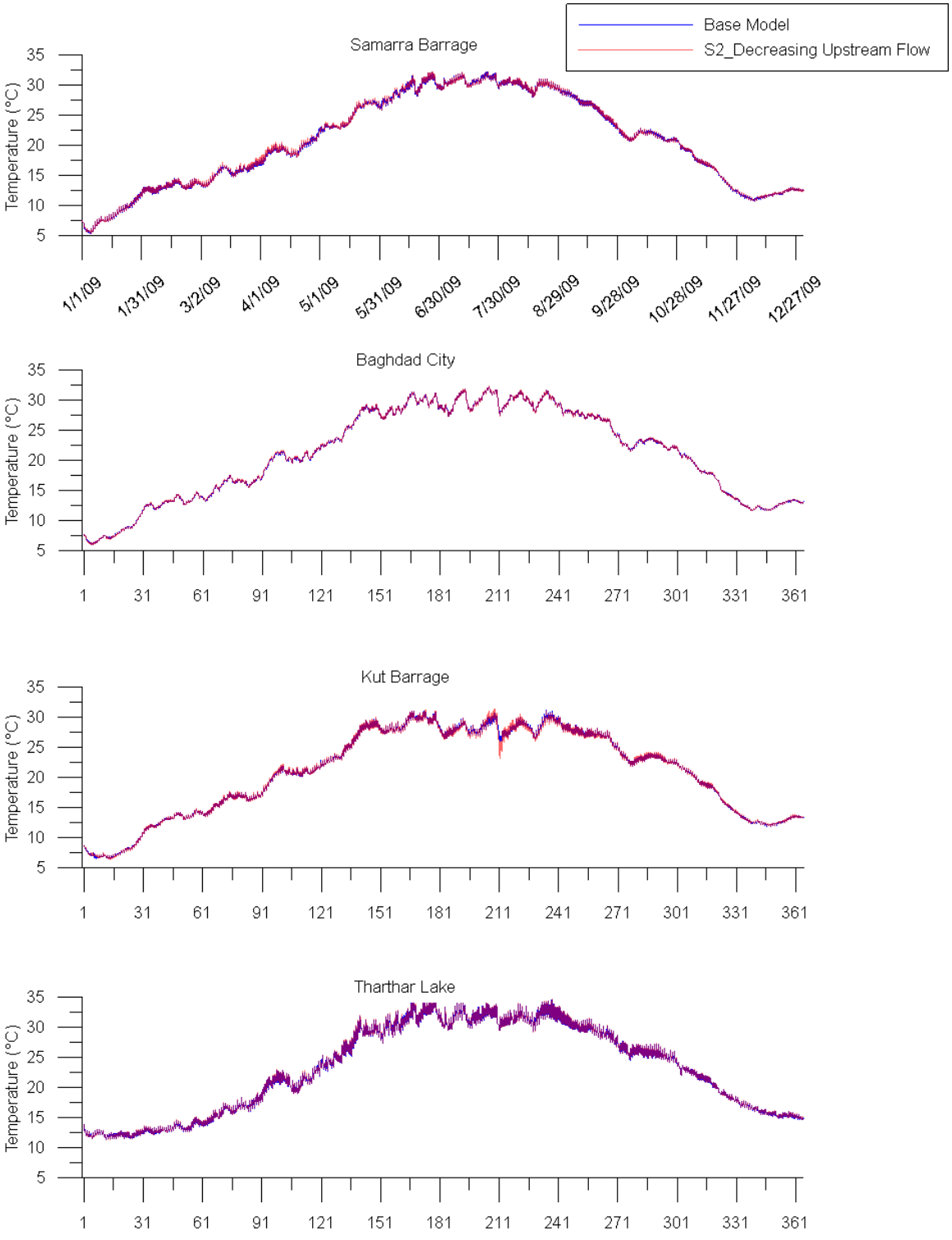

Figure 148: Model temperature (T_w) predictions for base model and management scenario 2 (decreasing upstream flow) at Samarra Barrage, Baghdad City, Kut Barrage, and Tharthar Lake.

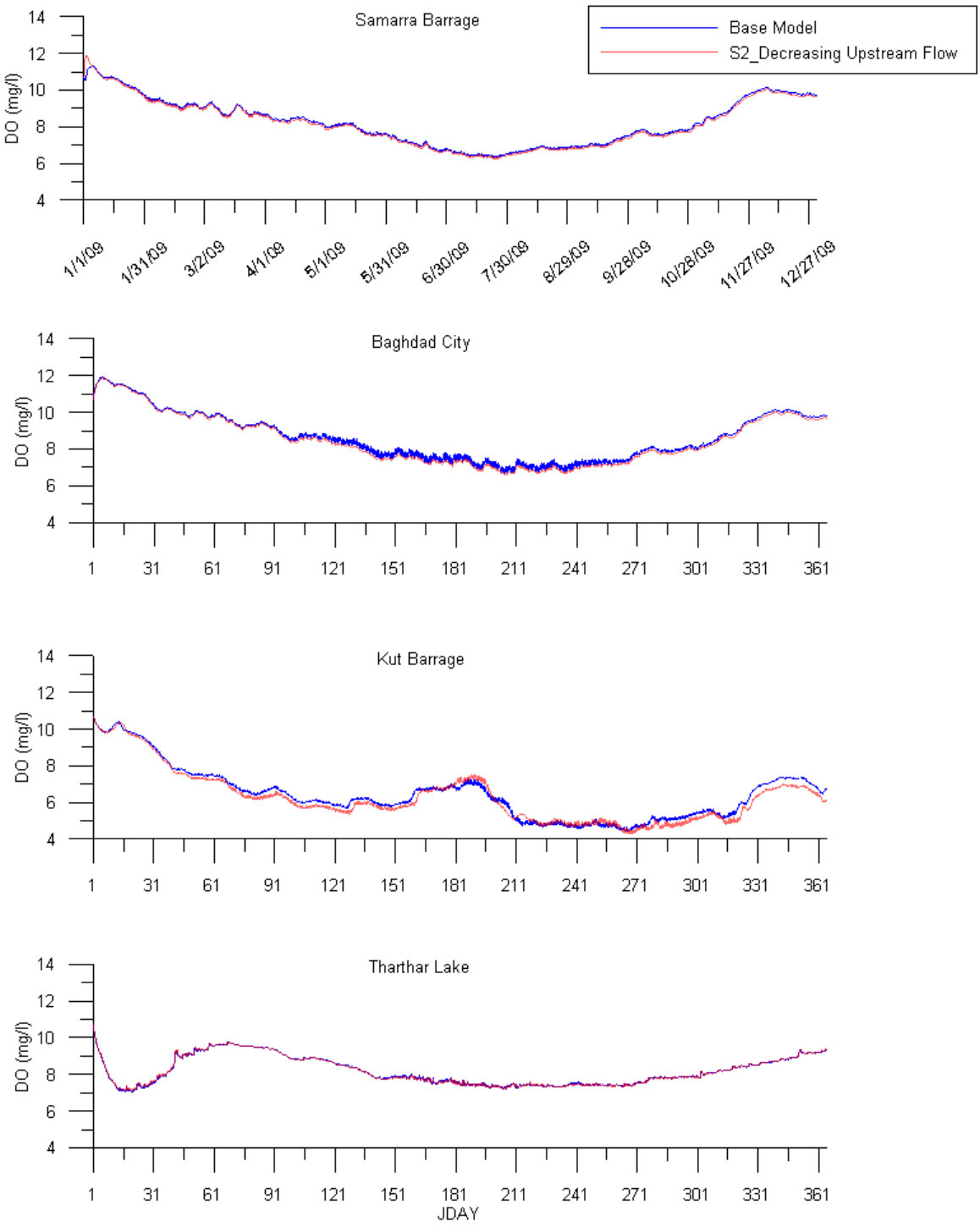

Figure 149: Model dissolved oxygen (DO) predictions for base model and management scenario 2 (decreasing upstream flow) at Samarra Barrage, Baghdad City, Kut Barrage and Tharthar Lake.

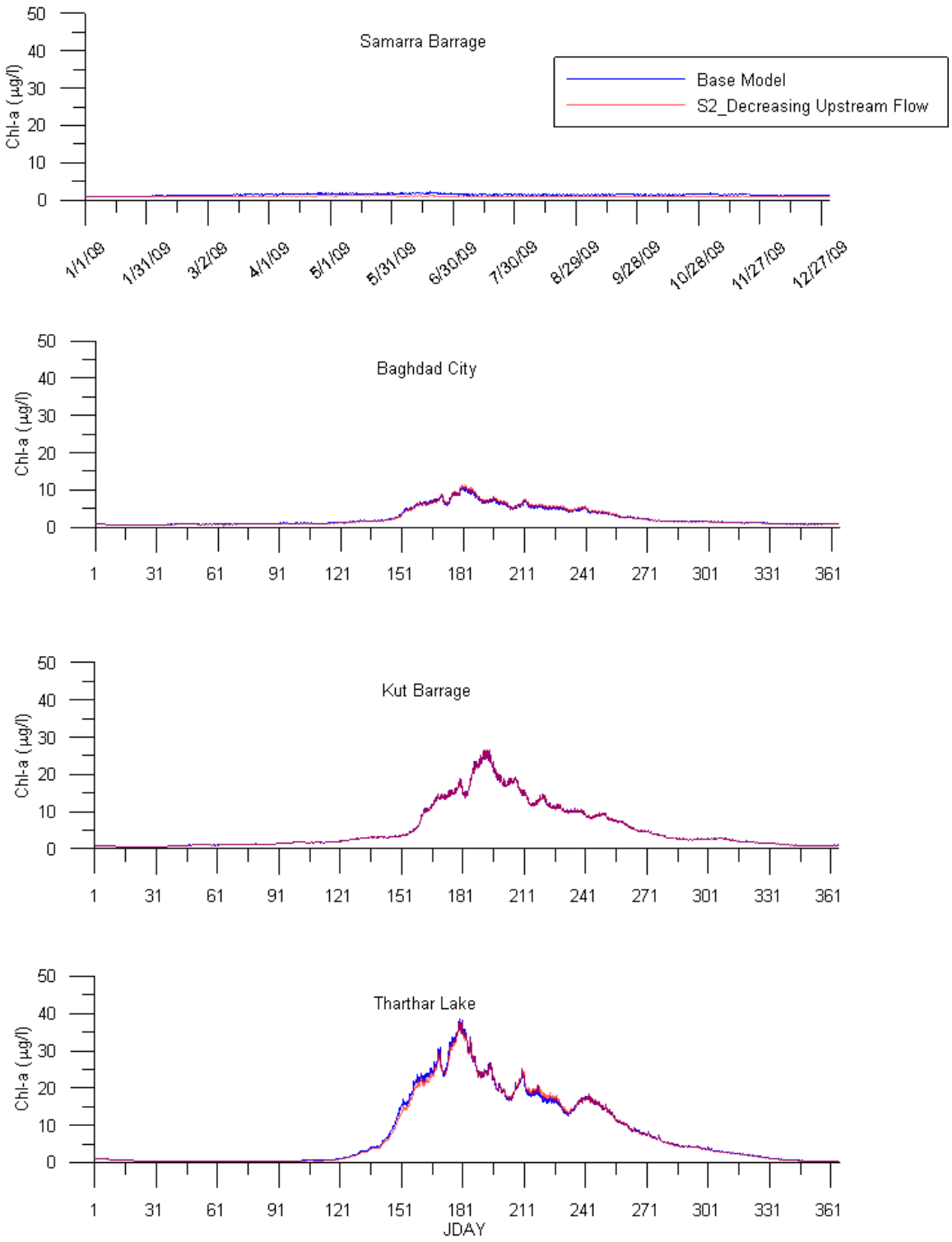

Figure 150: Model chlorophyll-a (Chl-a) predictions for base model and management scenario 2 (decreasing upstream flow) at Samarra Barrage, Baghdad City, Kut Barrage, and Tharthar Lake.

Management Scenario 3: Decreasing Upstream Flow and Increasing Nutrients

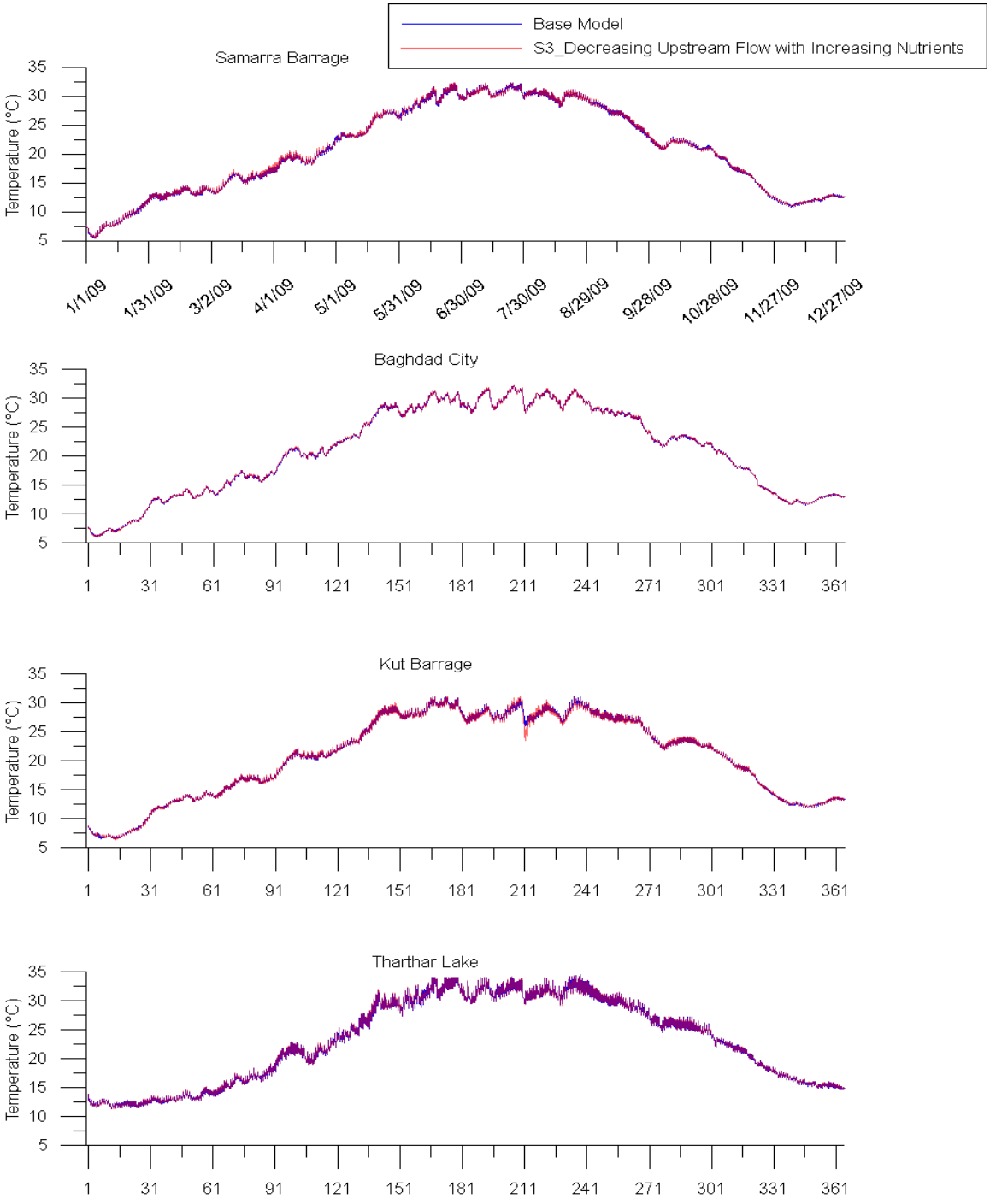

Figure 151: Model temperature (T_w) predictions for base model and management scenario 3 (decreasing upstream flow with increasing nutrients) at Samarra Barrage, Baghdad City, Kut Barrage, and Tharthar Lake.

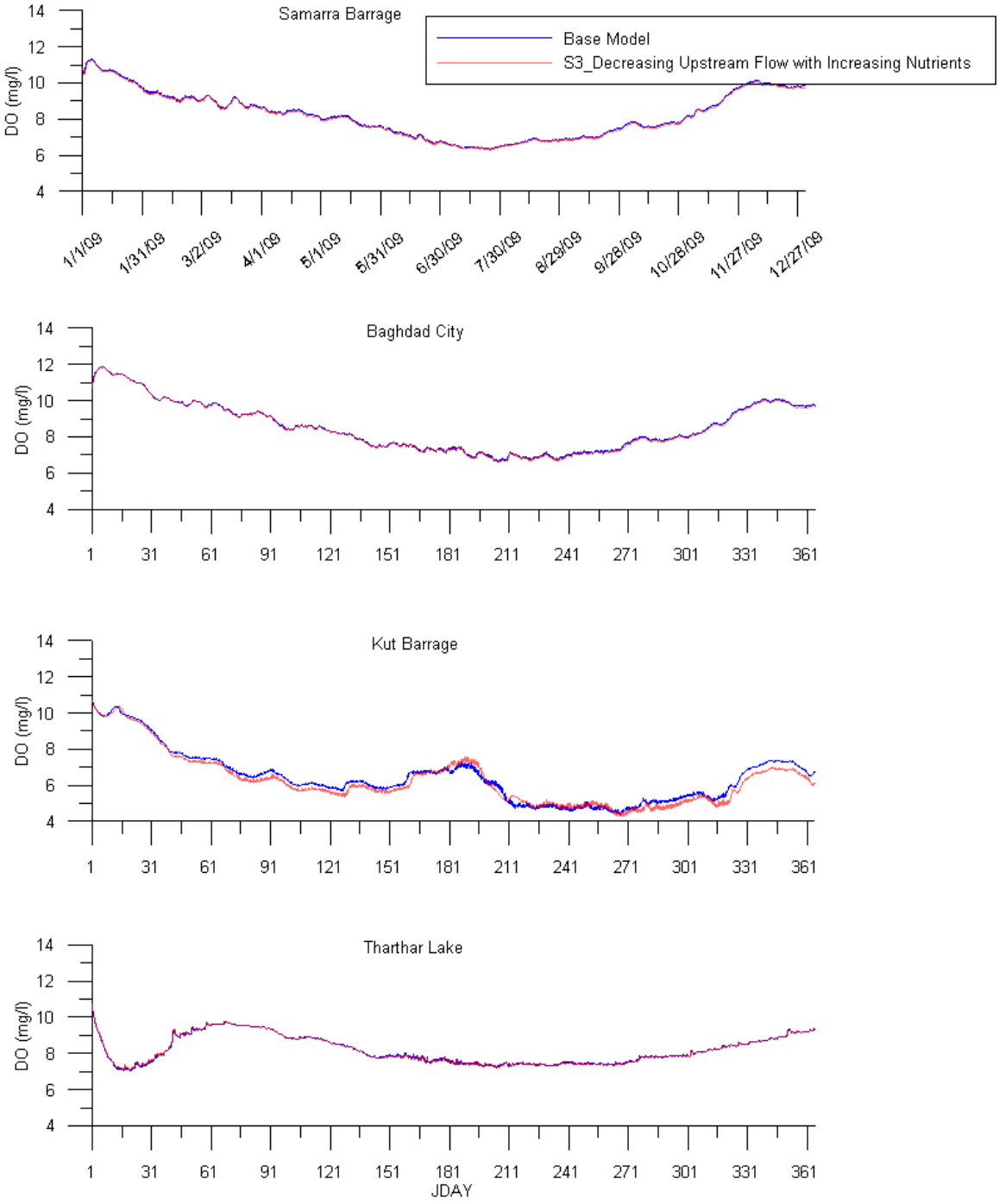

Figure 152: Model dissolved oxygen (DO) predictions for base model and management scenario 3 (decreasing upstream flow with increasing nutrients) at Samarra Barrage, Baghdad City, Kut Barrage, and Tharthar Lake.

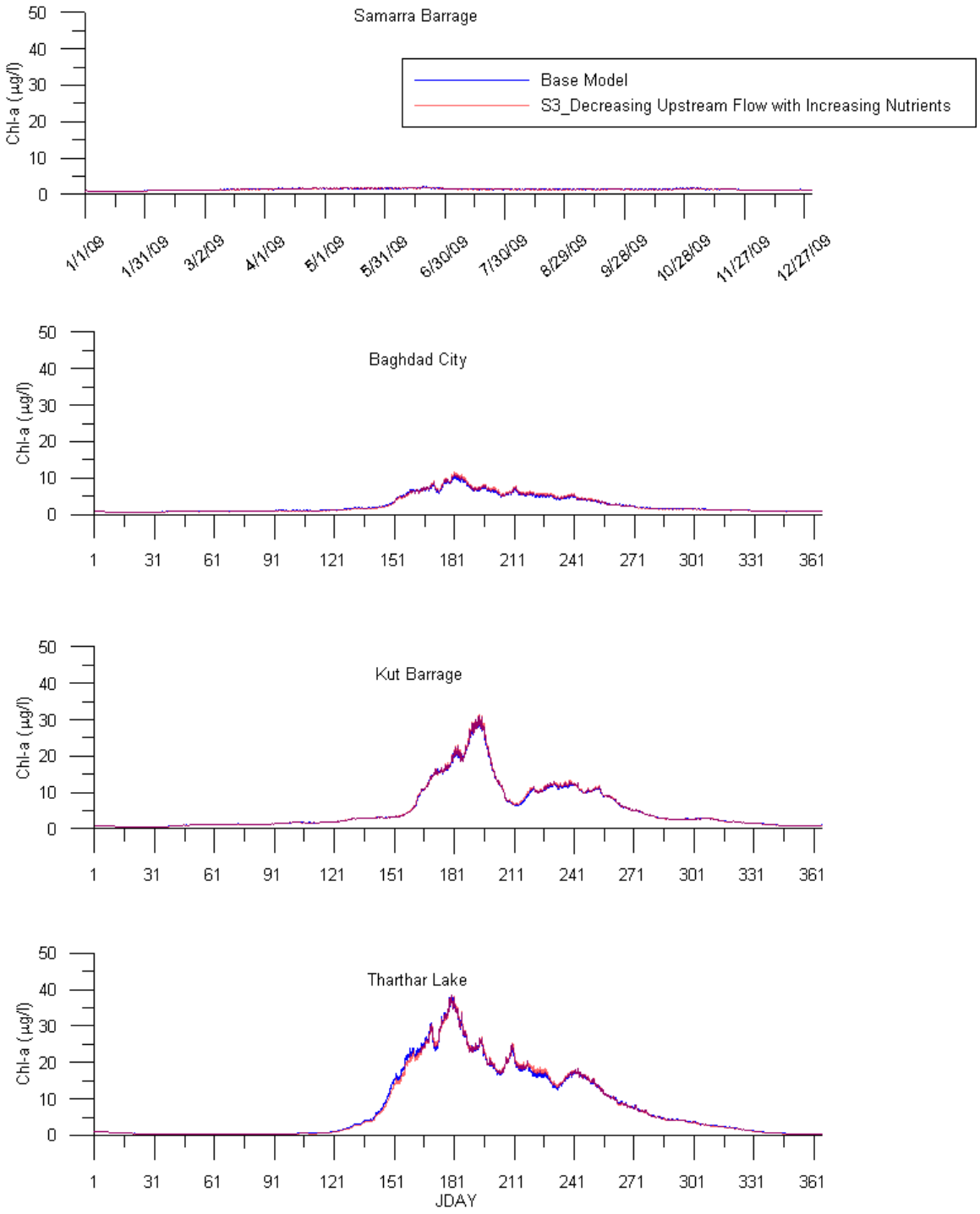

Figure 153: Model chlorophyll-a (Chl-a) predictions for base model and management scenario 3 (decreasing upstream flow with increasing nutrients) at Samarra Barrage, Baghdad City, Kut Barrage, and Tharthar Lake.

Management Scenario 4: Increasing Tharthar Lake's Flow

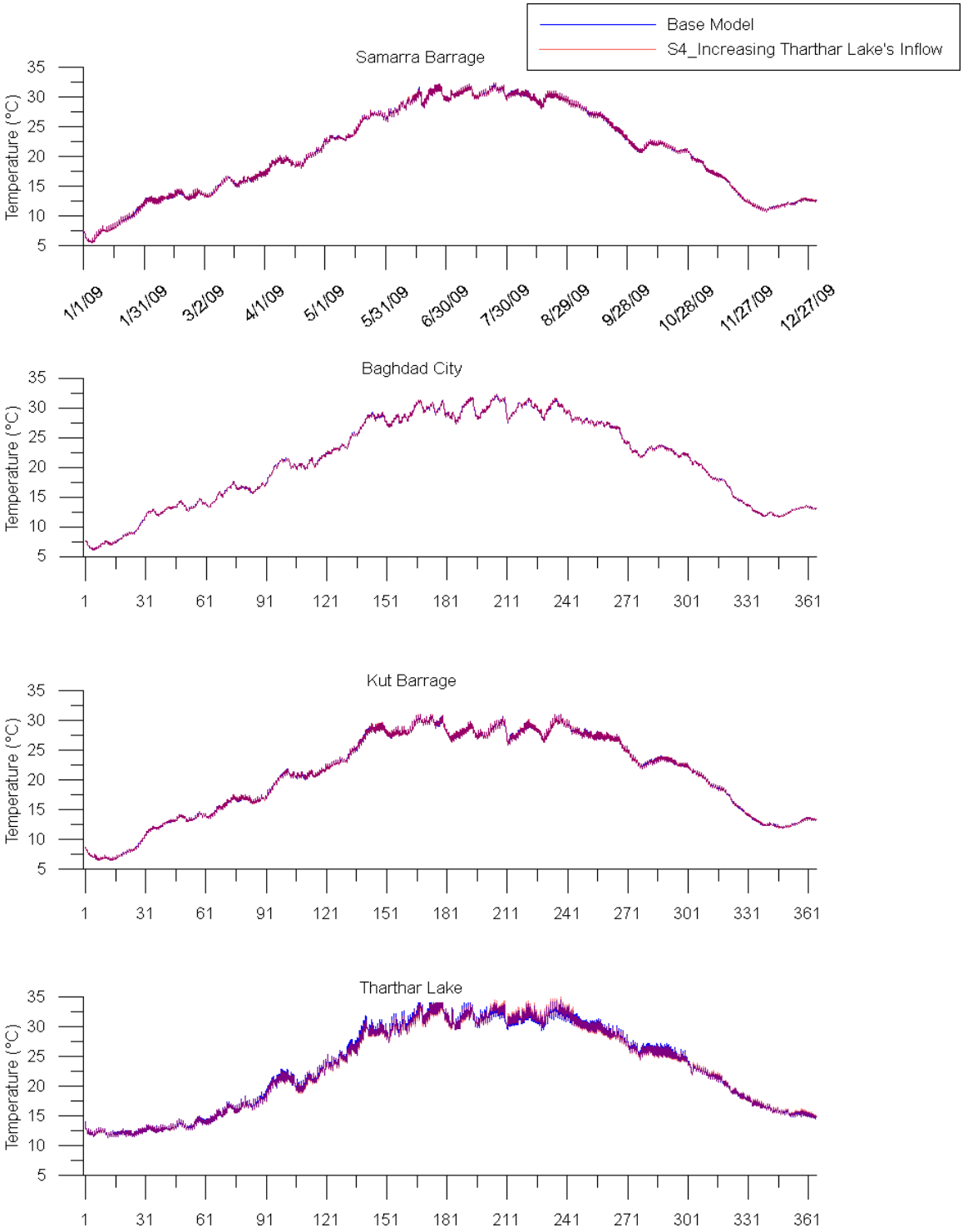

Figure 154: Model temperature (T_w) predictions for base model and management scenario 4 (increasing Tharthar Lake's inflow) at Samarra Barrage, Baghdad City, Kut Barrage, and Tharthar Lake.

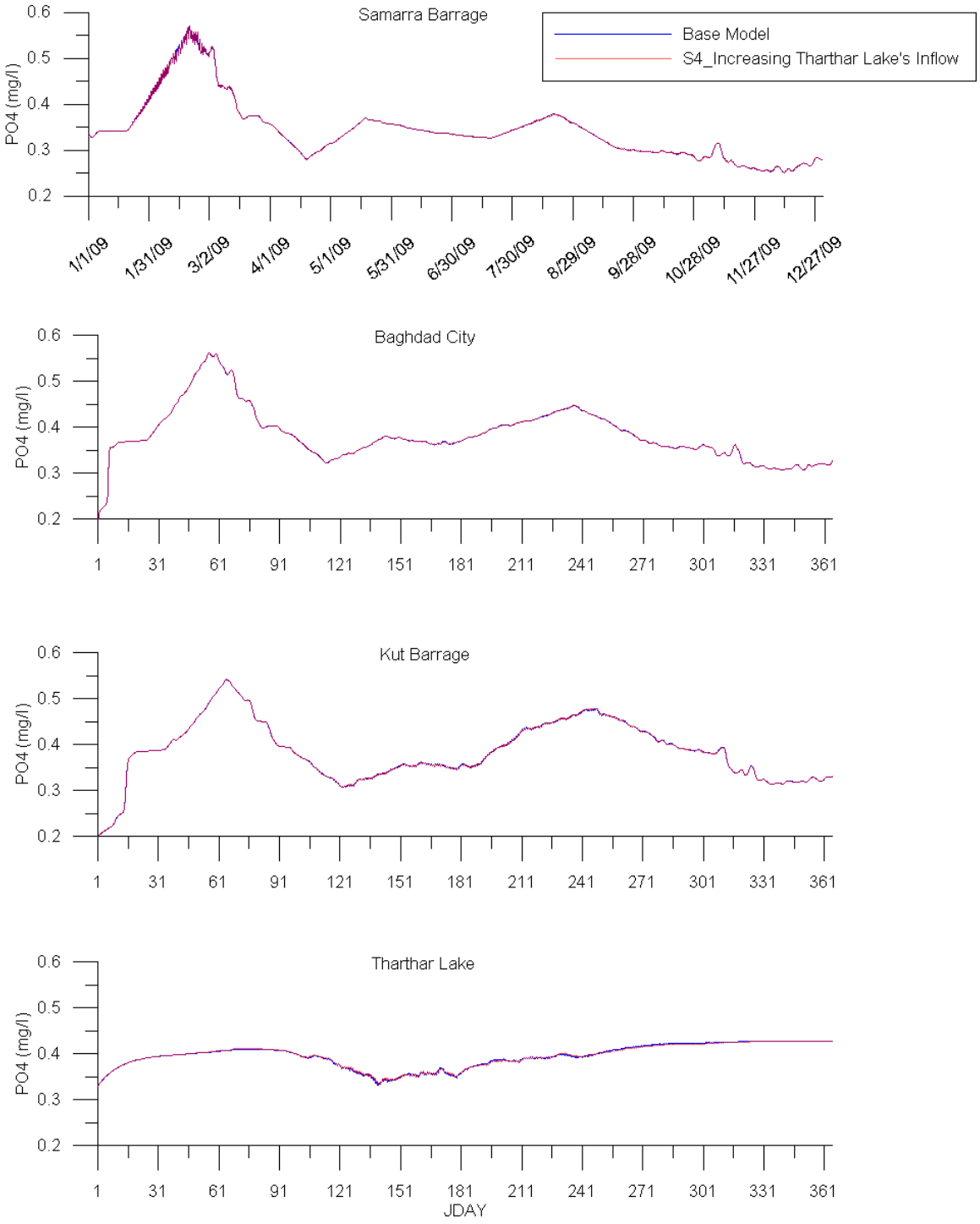

Figure 155: Model phosphate (PO4) predictions for base model and management scenario 4 (increasing Tharthar Lake's inflow) at Samarra Barrage, Baghdad City, Kut Barrage, and Tharthar Lake.

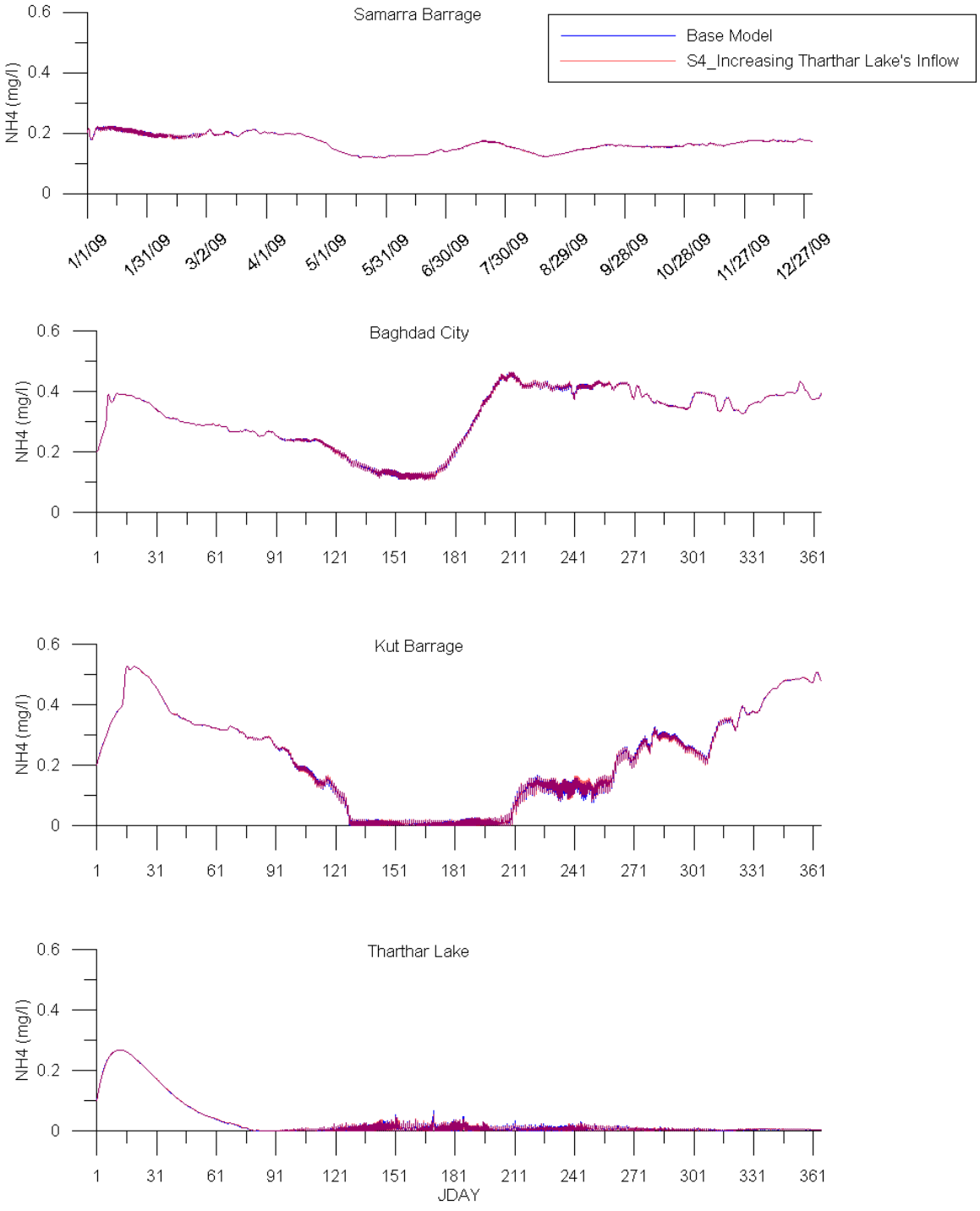

Figure 156: Model ammonia (NH4) predictions for base model and management scenario 4 (increasing Tharthar Lake's inflow) at Samarra Barrage, Baghdad City, Kut Barrage, and Tharthar Lake.

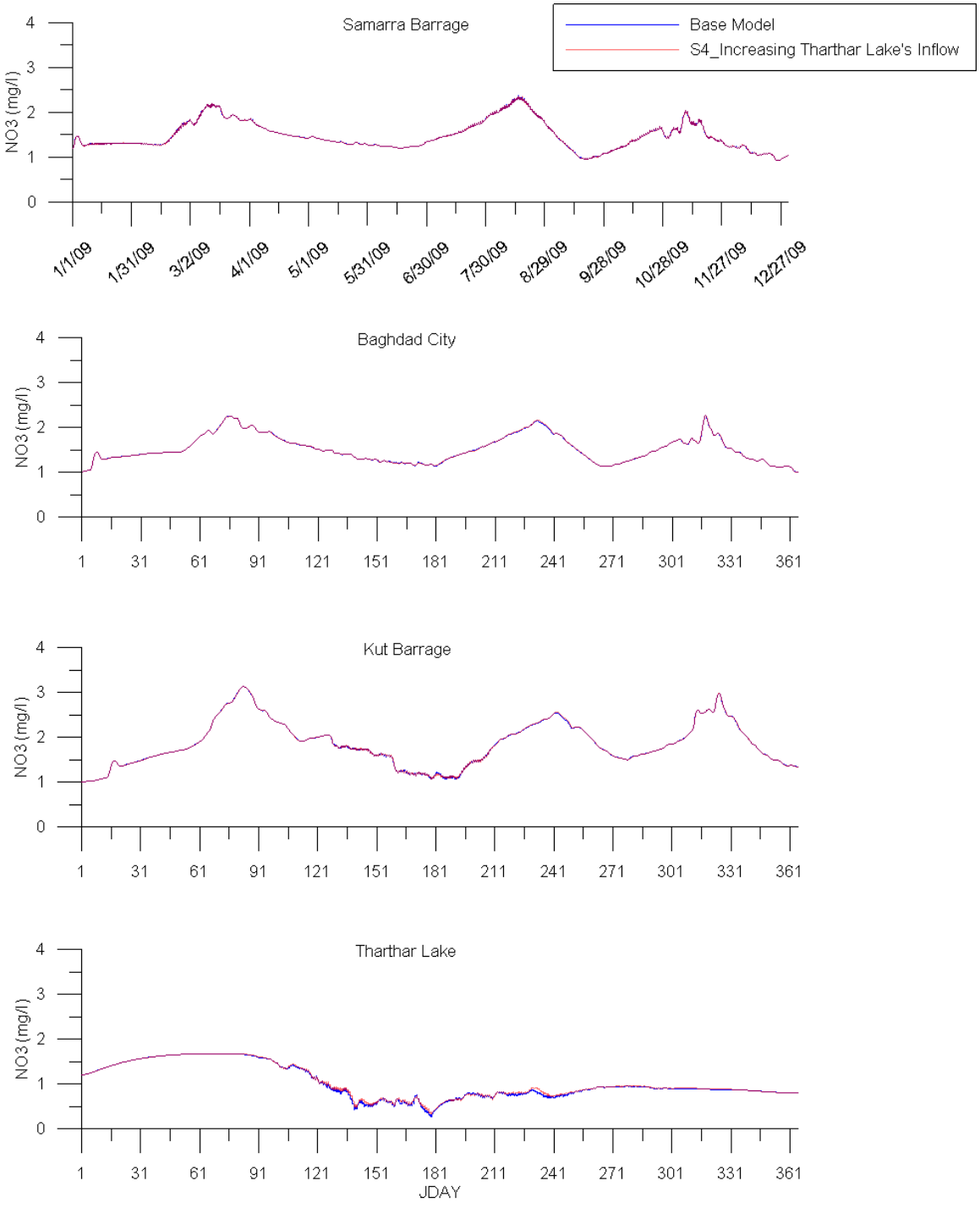

Figure 157: Model nitrate (NO3) predictions for base model and management scenario 4 (increasing Tharthar Lake's inflow) at Samarra Barrage, Baghdad City, Kut Barrage, and Tharthar Lake.

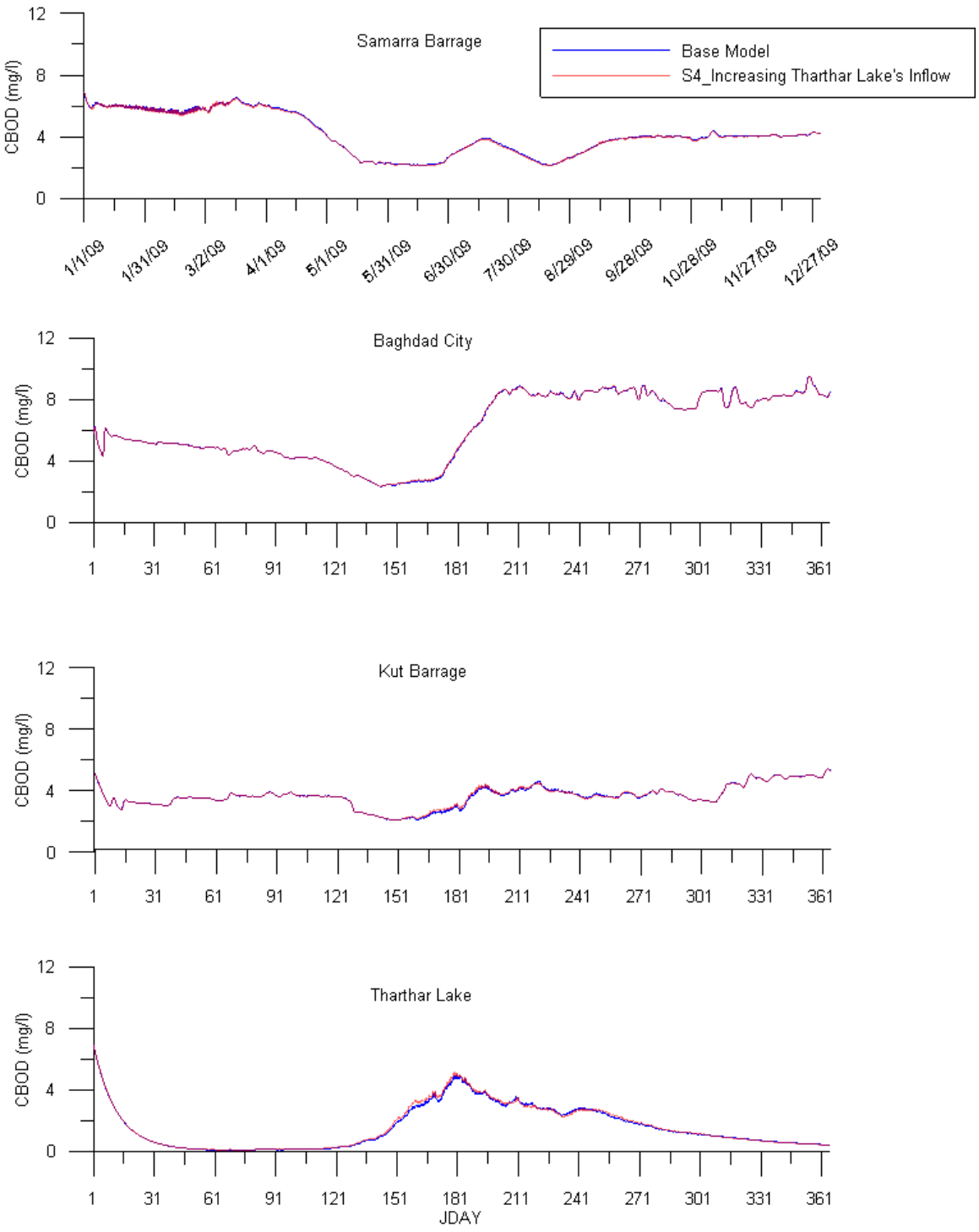

Figure 158: Model carbonaceous biological oxygen demand (CBOD) predictions for base model and management scenario 4 (increasing Tharthar Lake's inflow) at Samarra Barrage, Baghdad City, Kut Barrage, and Tharthar Lake.

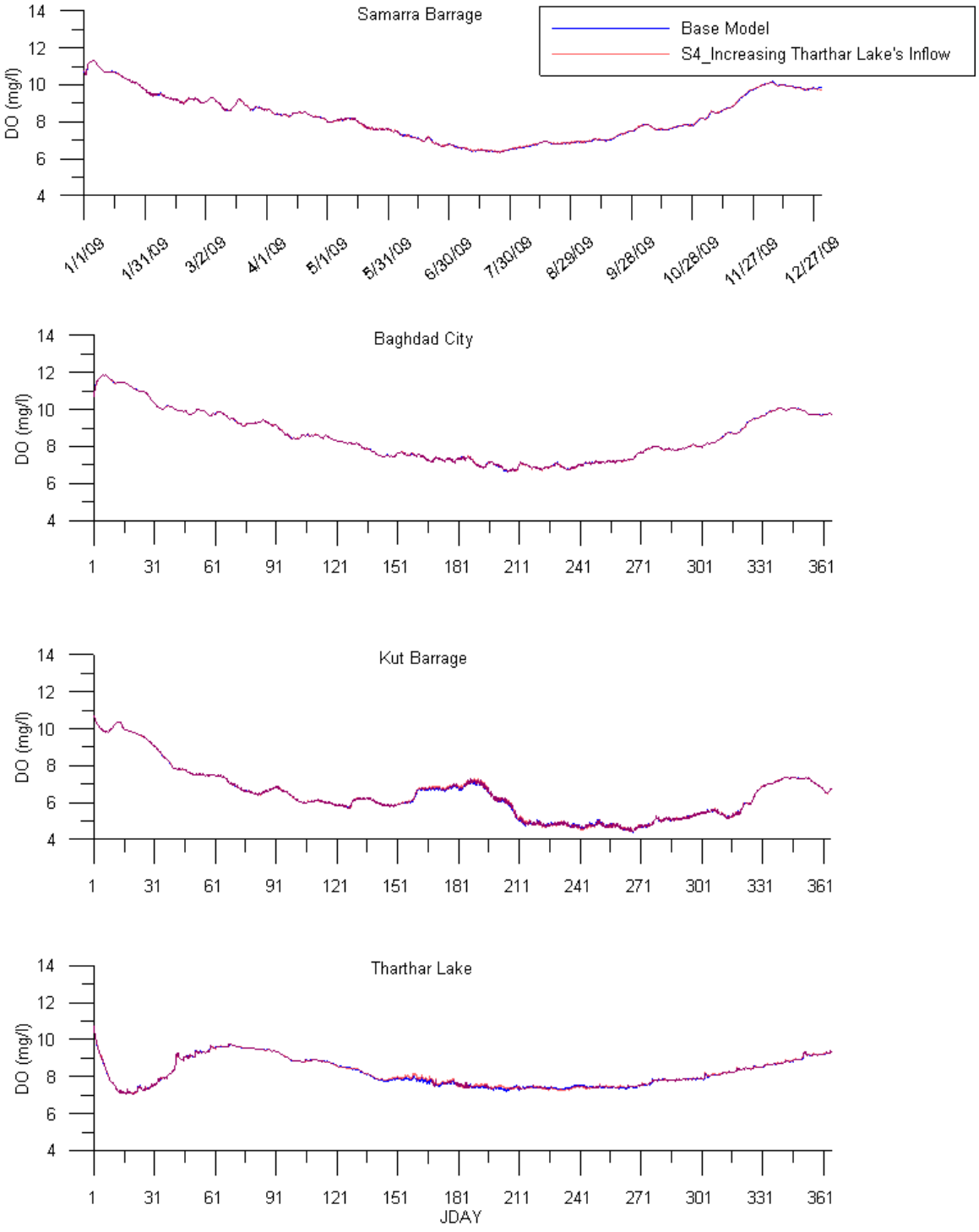

Figure 159: Model dissolved oxygen (DO) predictions for base model and management scenario 4 (increasing Tharthar Lake's inflow) at Samarra Barrage, Baghdad City, Kut Barrage, and Tharthar Lake.

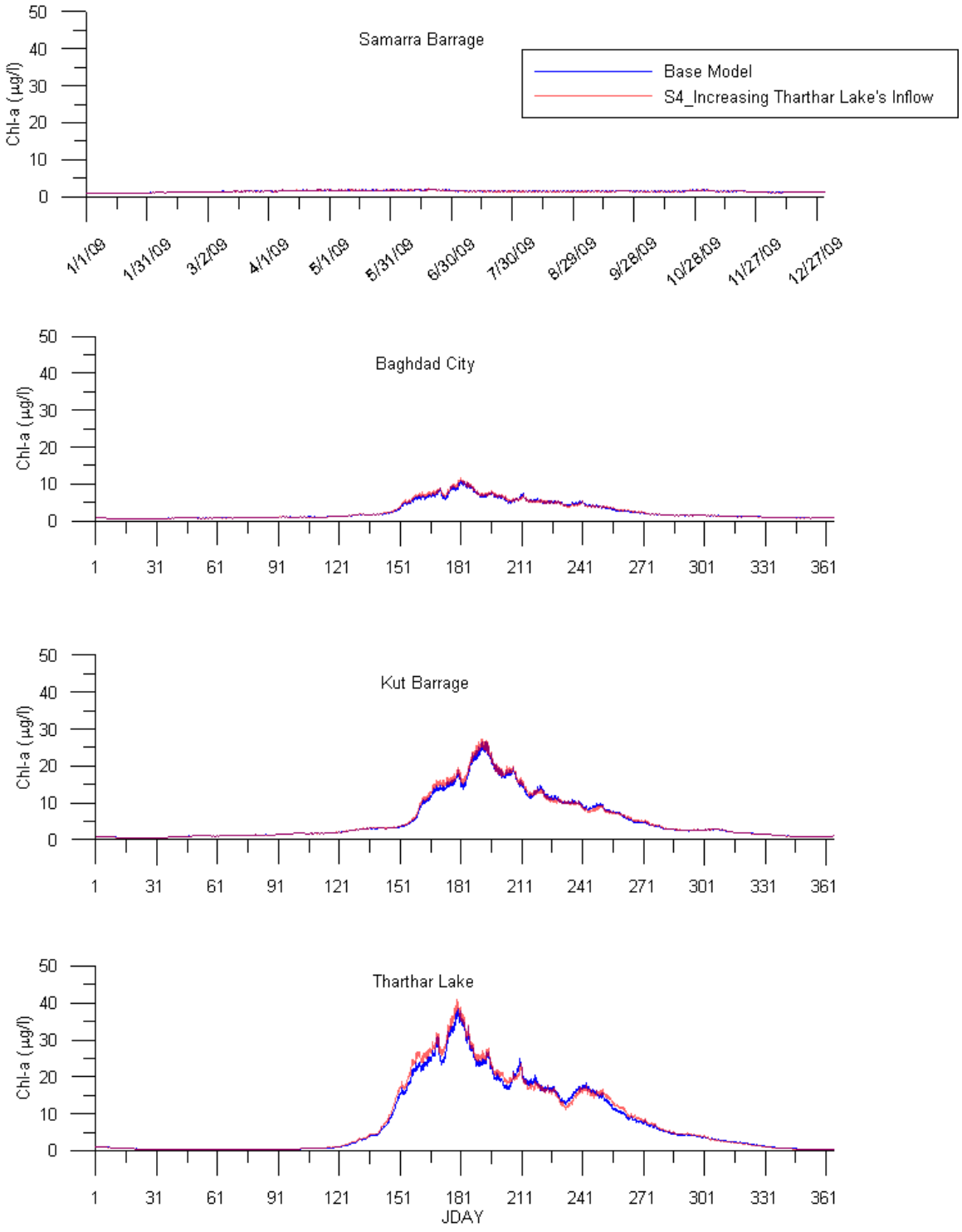

Figure 160: Model chlorophyll-a (Chl-a) predictions for base model and management scenario 4 (increasing Tharthar Lake's inflow) at Samarra Barrage, Baghdad City, Kut Barrage, and Tharthar Lake.

Management Scenario 5: The Effect of Climate Change

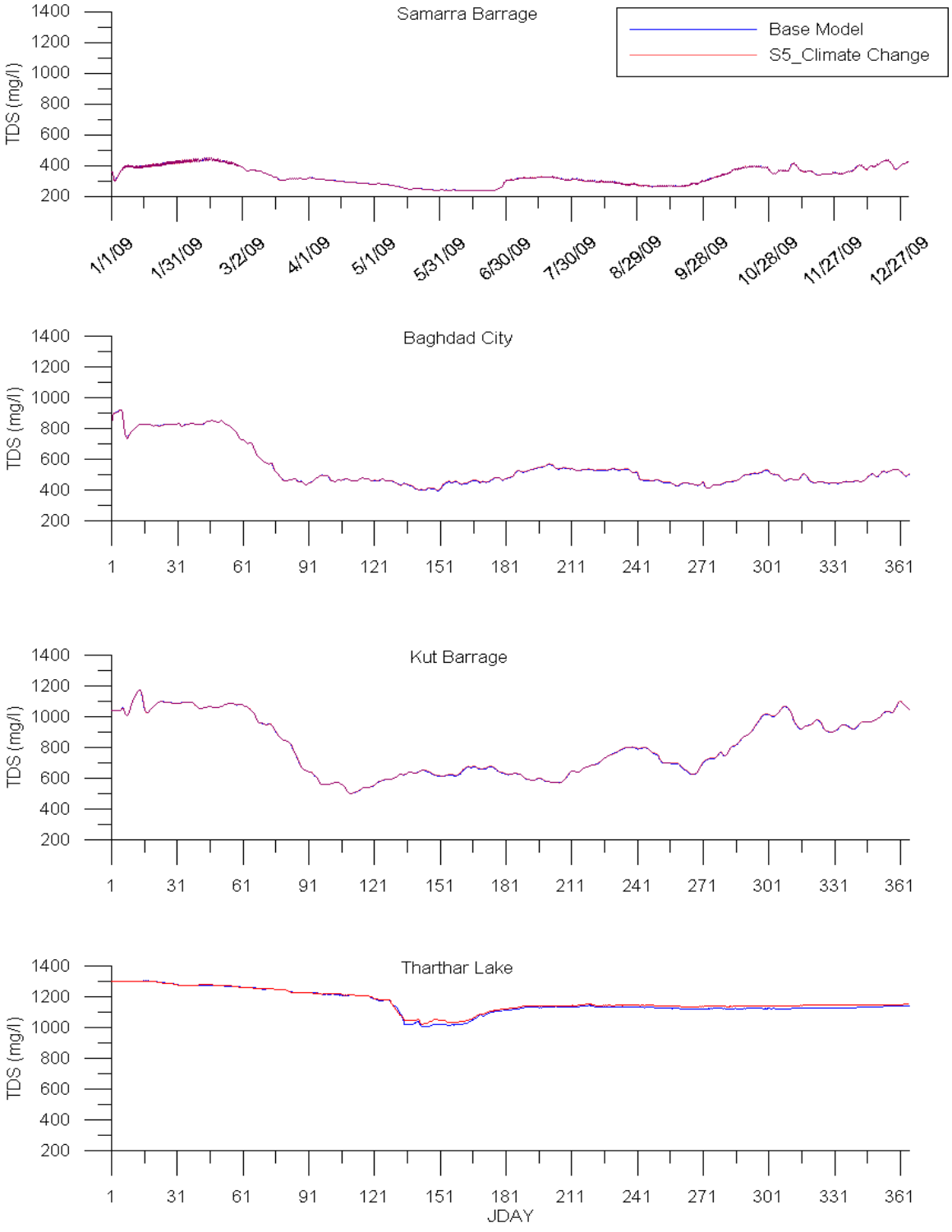

Figure 161: Model total dissolved solids (TDS) predictions for base model and management scenario 5 (climate change) at Samarra Barrage, Baghdad City, Kut Barrage, and Tharthar Lake.

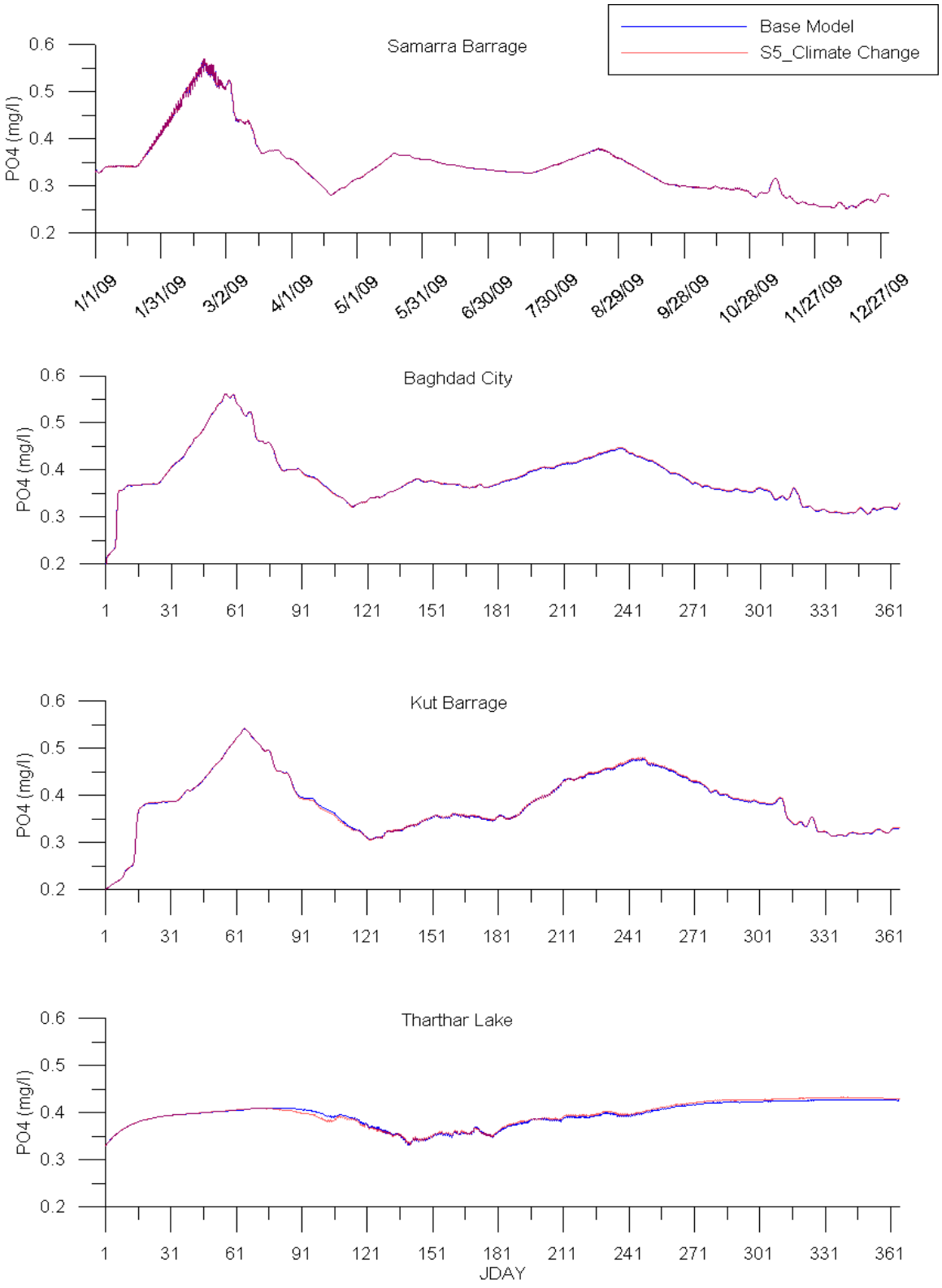

Figure 162: Model phosphate (PO4) predictions for base model and management scenario 5 (climate change) at Samarra Barrage, Baghdad City, Kut Barrage, and Tharthar Lake.

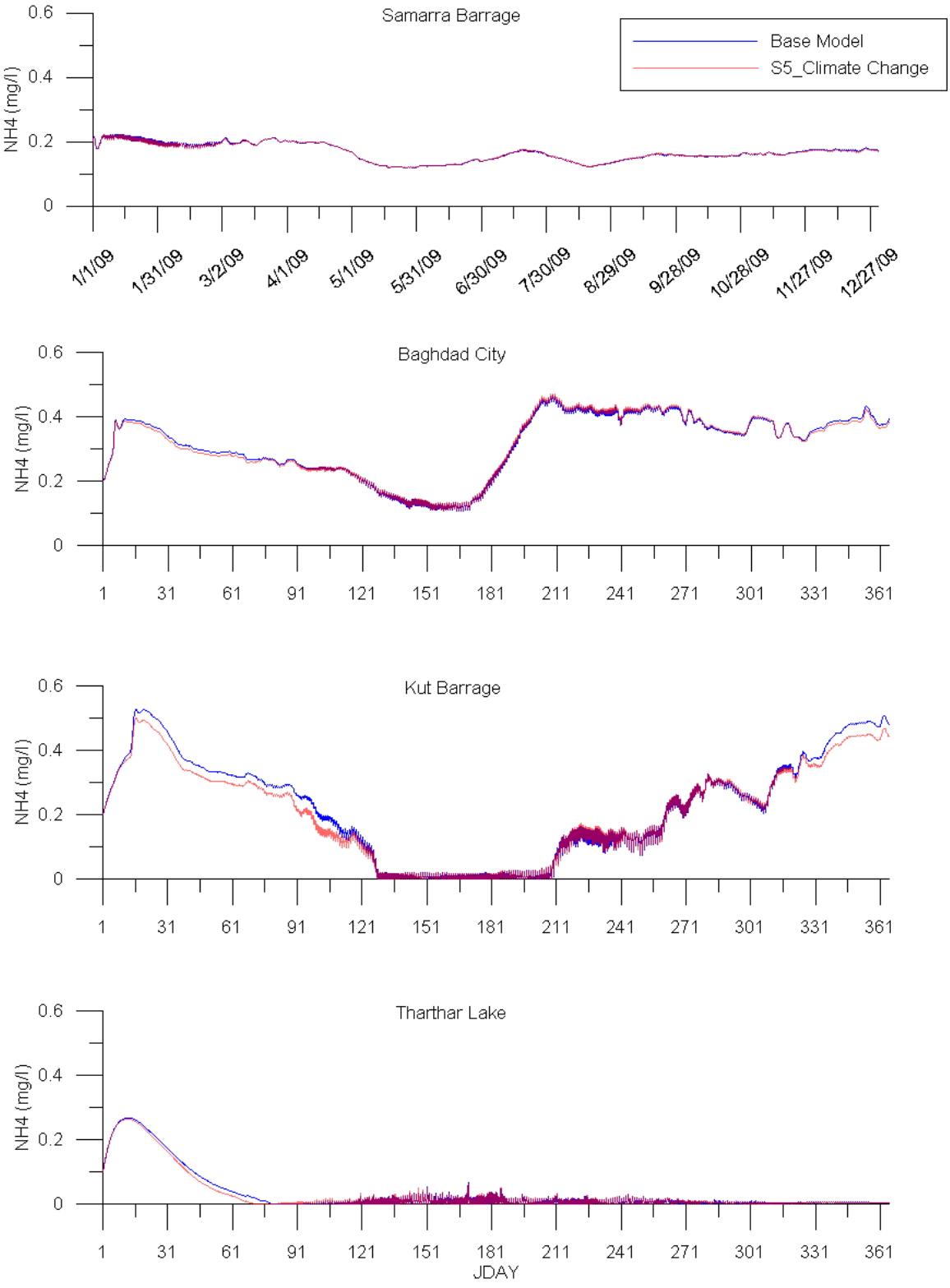

Figure 163: Model ammonia (NH4) predictions for base model and management scenario 5 (climate change) at Samarra Barrage, Baghdad City, Kut Barrage, and Tharthar Lake.

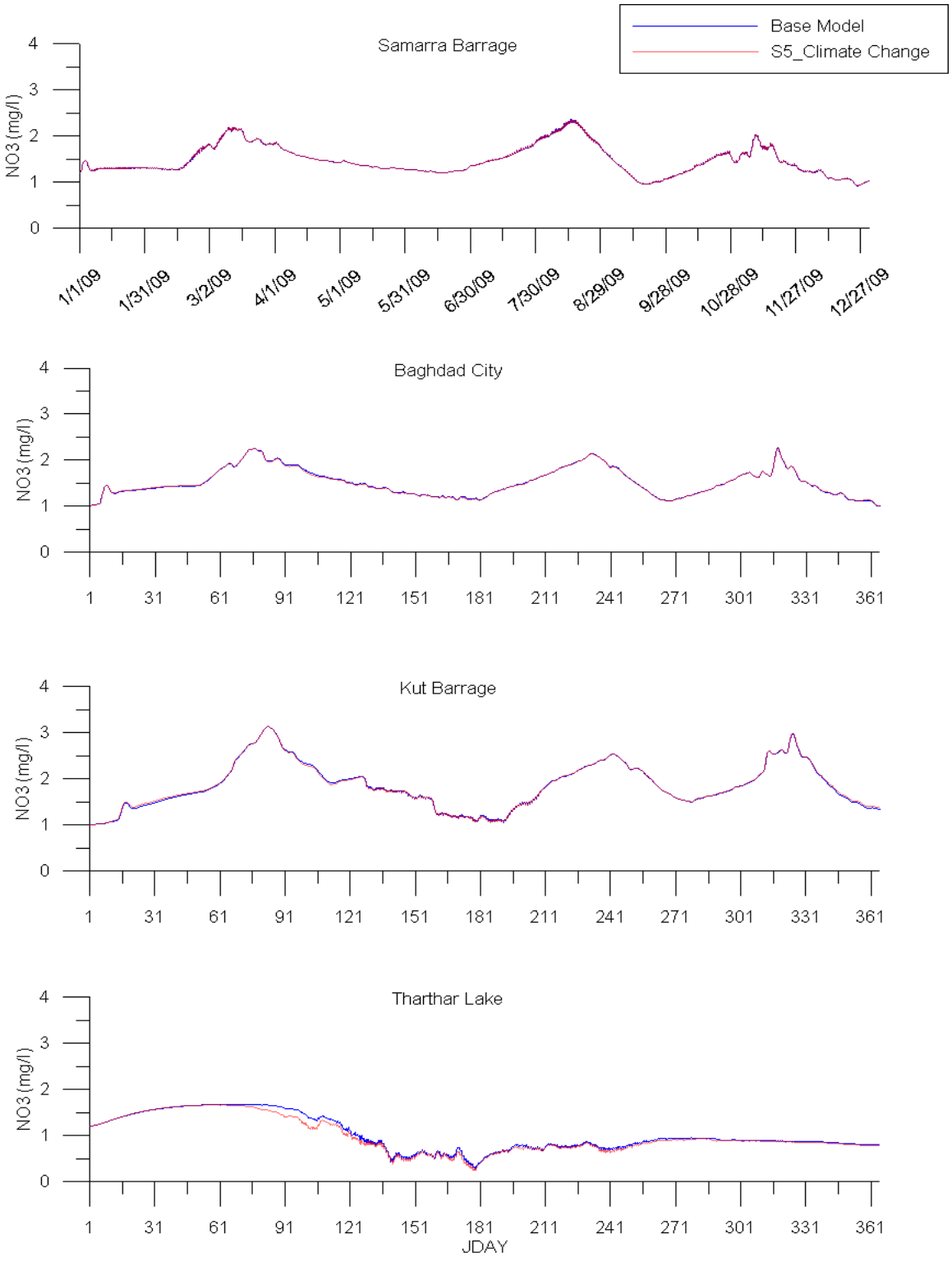

Figure 164: Model nitrate (NO3) predictions for base model and management scenario 5 (climate change) at Samarra Barrage, Baghdad City, Kut Barrage, and Tharthar Lake.

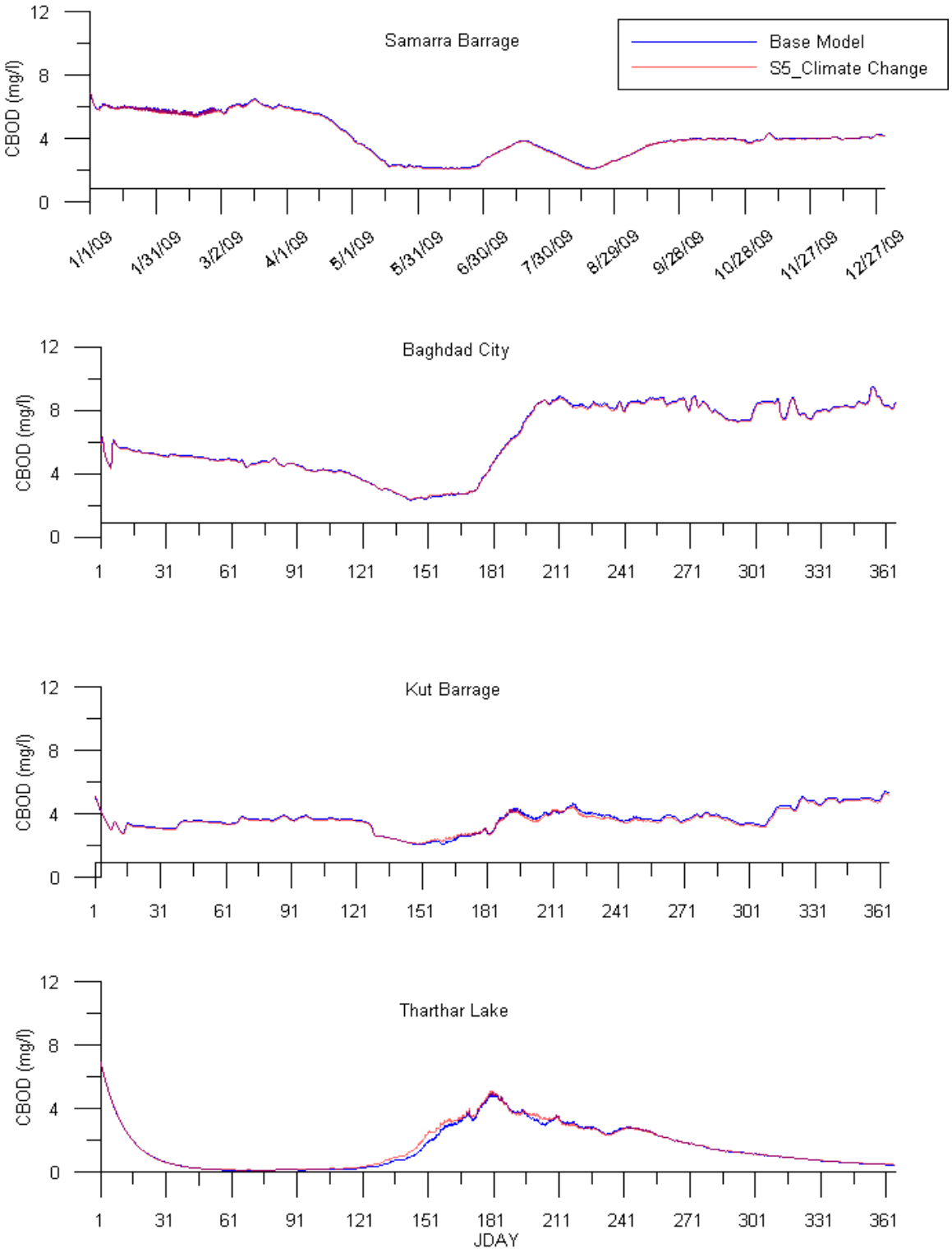

Figure 165: Model carbonaceous biological oxygen demand (CBOD) predictions for base model and management scenario 5 (climate change) at Samarra Barrage, Baghdad City, Kut Barrage, and Tharthar Lake.

Management Scenario 6: The Effect of Climate Change with Decreasing Upstream Flow

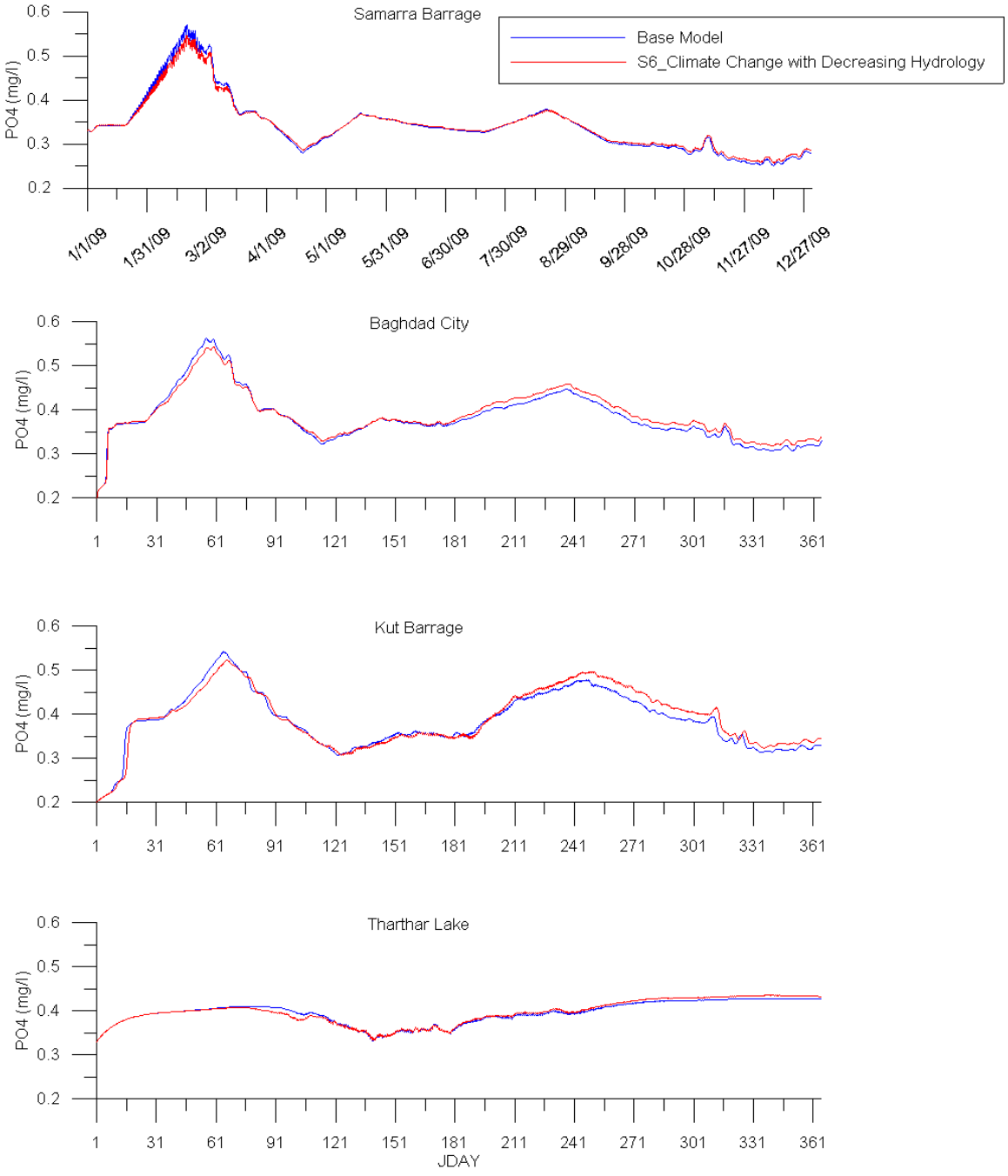

Figure 166: Model phosphate (PO4) predictions for base model and management scenario 6 (climate change with decreasing hydrology) at Samarra Barrage, Baghdad City, Kut Barrage and Tharthar Lake.

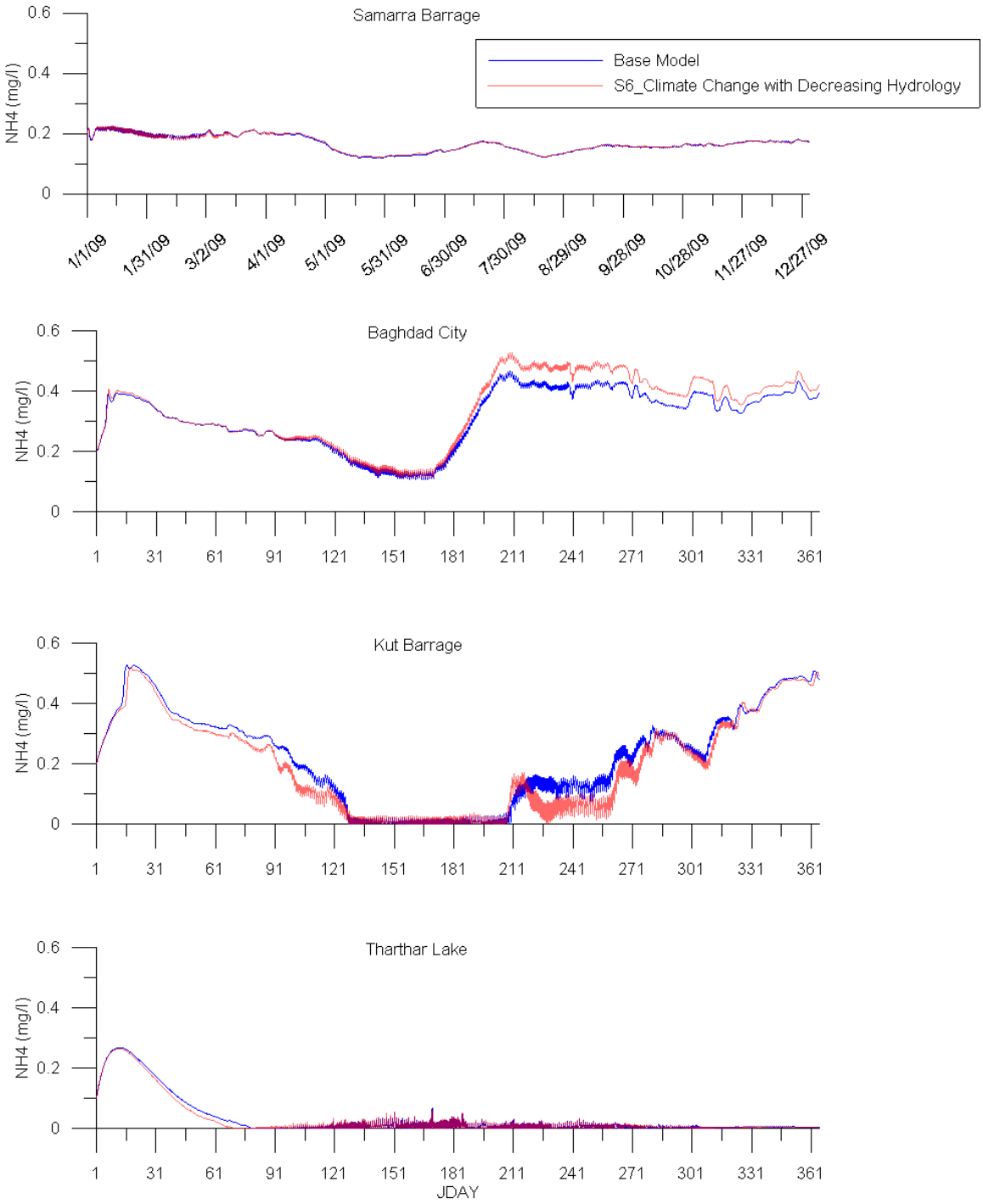

Figure 167: Model ammonia (NH4) predictions for base model and management scenario 6 (climate change with decreasing hydrology) at Samarra Barrage, Baghdad City, Kut Barrage and Tharthar Lake.

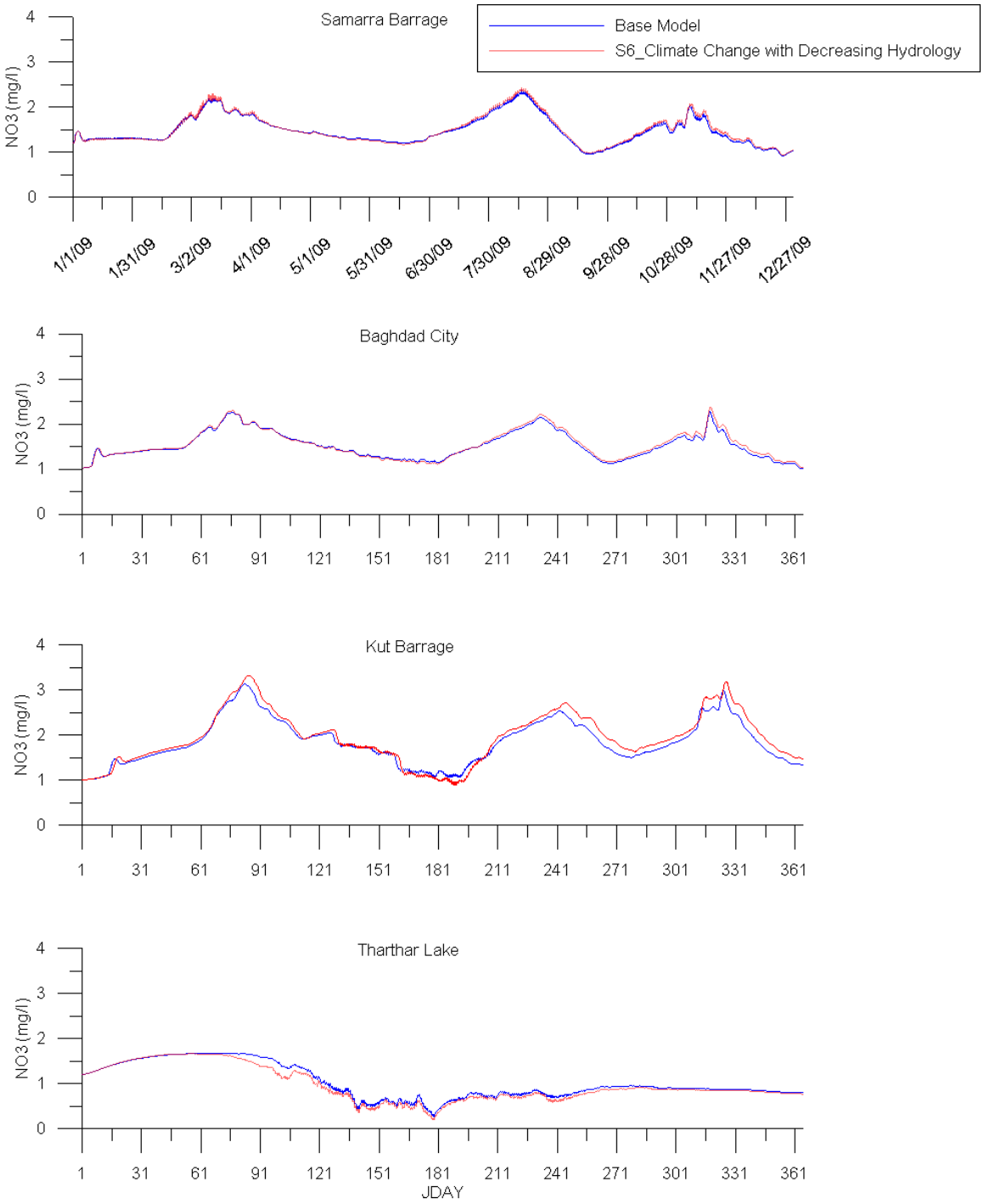

Figure 168: Model nitrate (NO3) predictions for base model and management scenario 6 (climate change with decreasing hydrology) at Samarra Barrage, Baghdad City, Kut Barrage and Tharthar Lake.

Management Scenario 7: Disconnecting Tharthar Lake

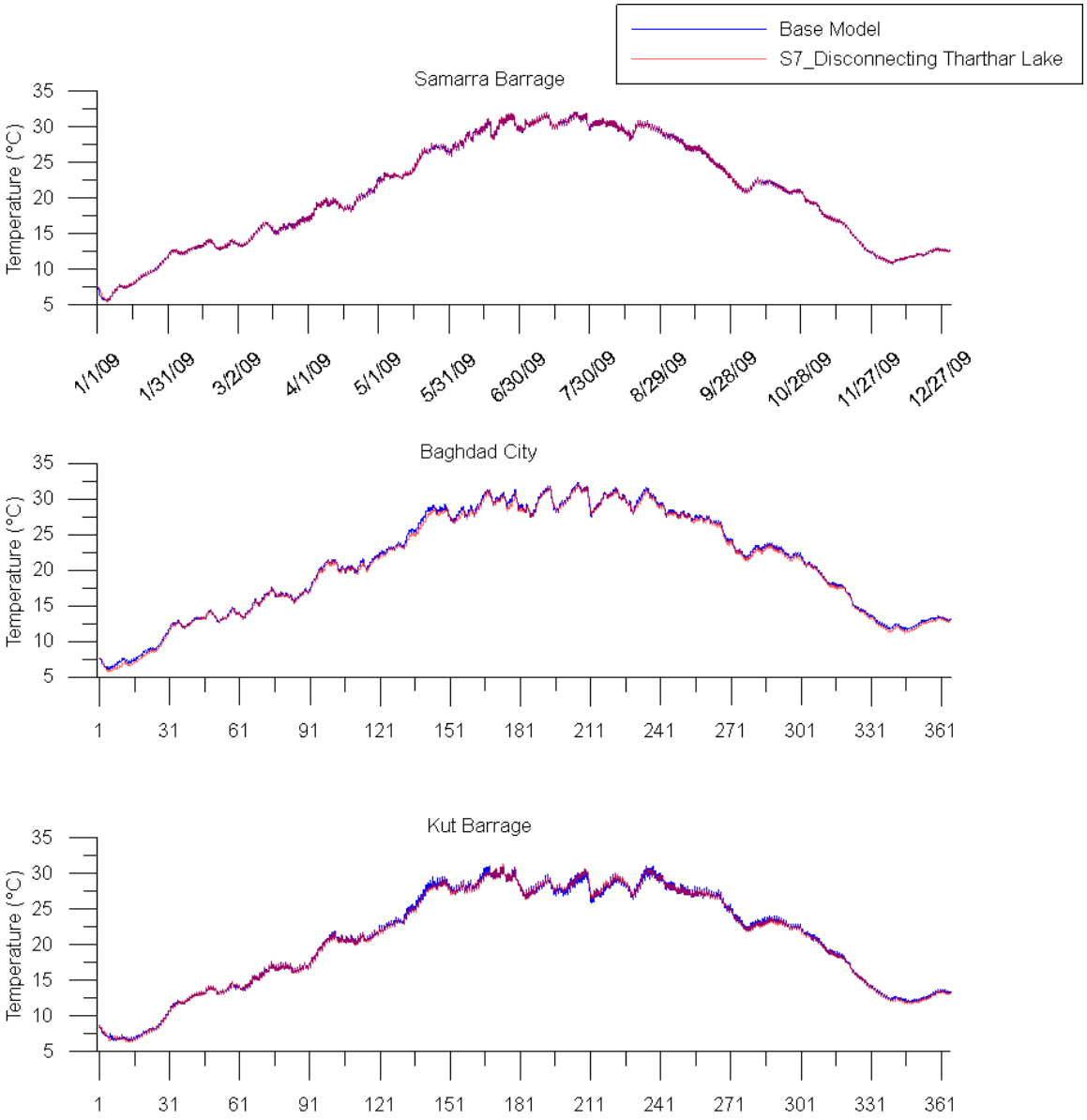

Figure 169: Model water temperature (T_w) predictions for base model and management scenario 7 (disconnecting Tharthar Lake) at Samarra Barrage, Baghdad City, and Kut Barrage.

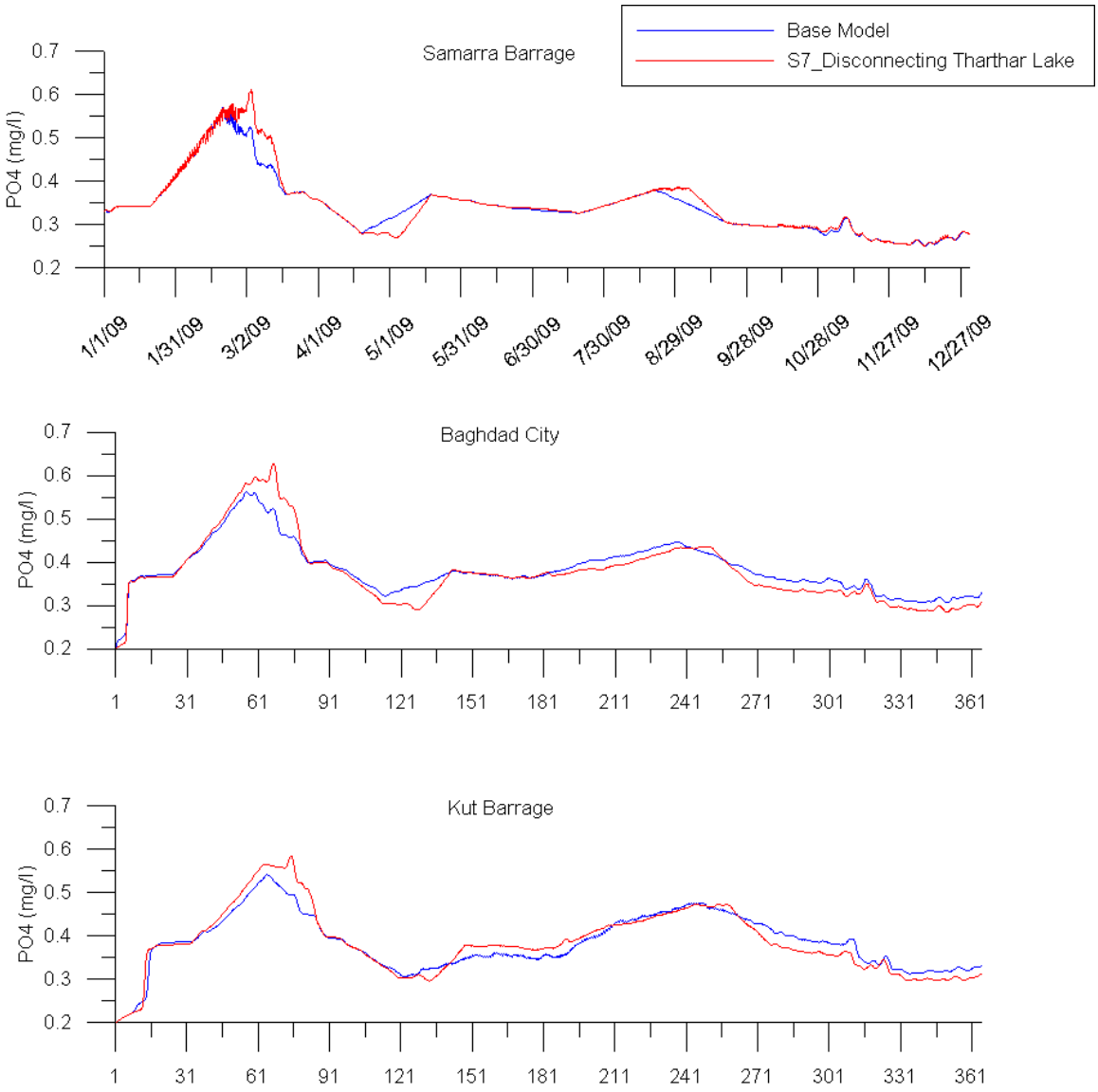

Figure 170: Model phosphate (PO4) predictions for base model and management scenario 7 (disconnecting Tharthar Lake) at Samarra Barrage, Baghdad City, Kut Barrage.

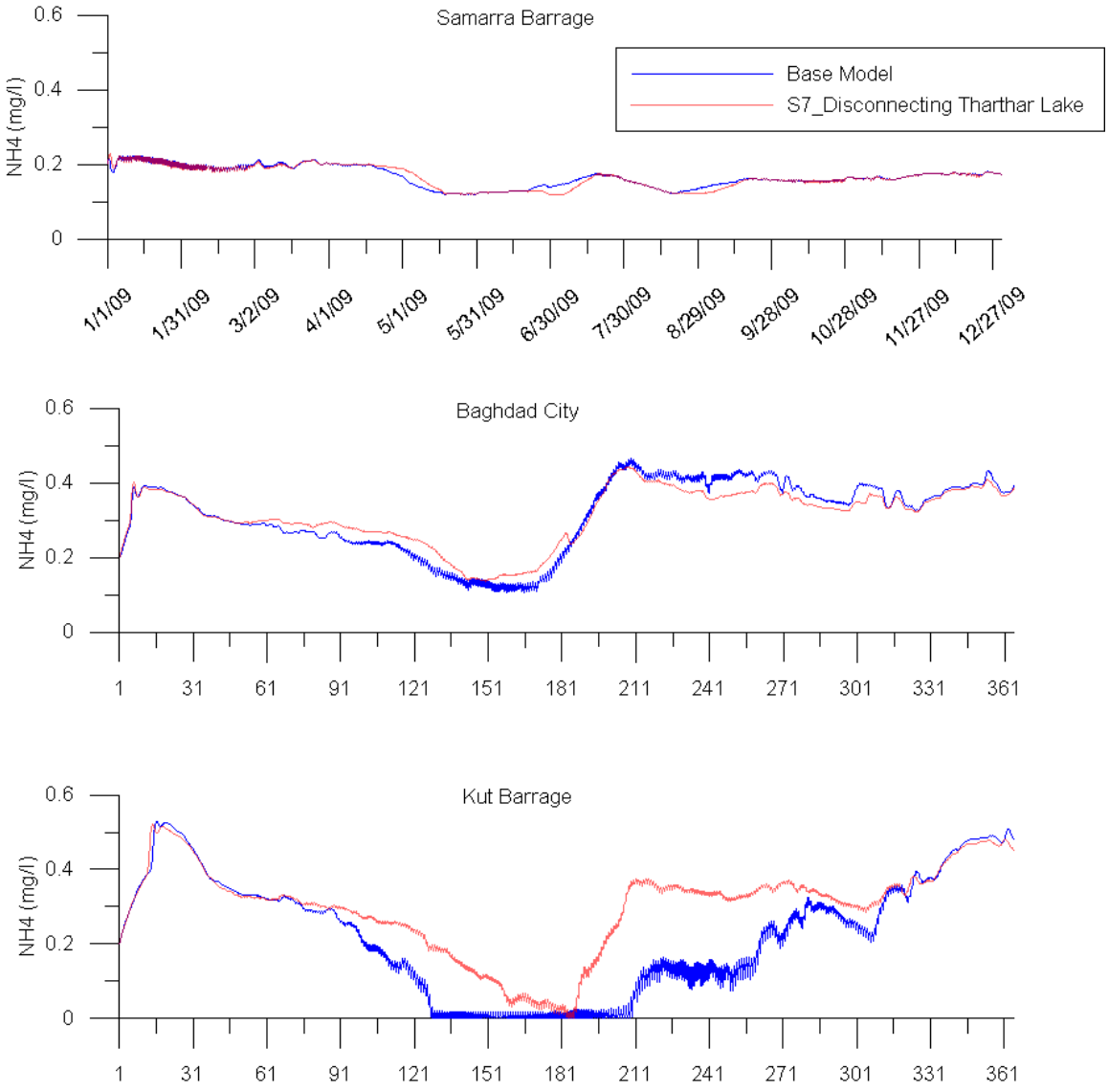

Figure 171: Model ammonia (NH4) predictions for base model and management scenario 7 (disconnecting Tharthar Lake) at Samarra Barrage, Baghdad City, Kut Barrage.

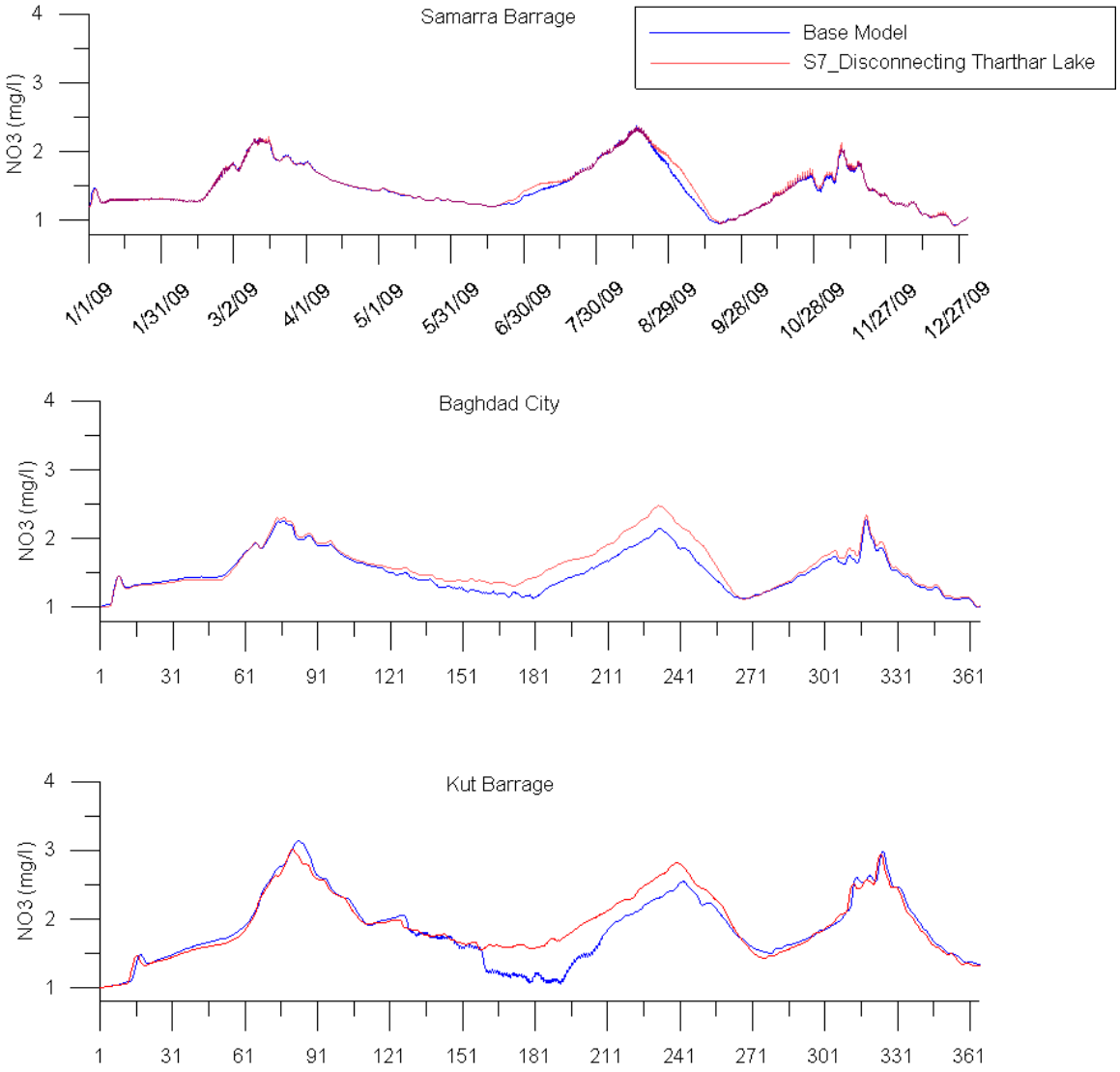

Figure 172: Model nitrate (NO3) predictions for base model and management scenario 7 (disconnecting Tharthar Lake) at Samarra Barrage, Baghdad City, Kut Barrage.

Appendix B: Histograms of Water Quality Constituents in the Tigris River System

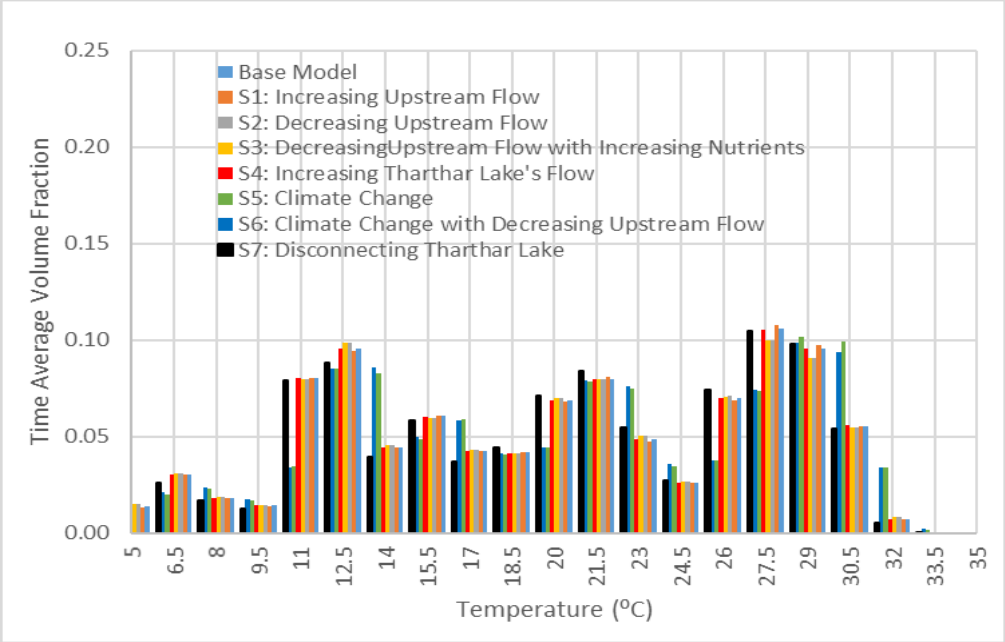

Figure 173: Environmental performance for 7 different scenario runs comparing water temperatures in the mainstem of the Tigris River.

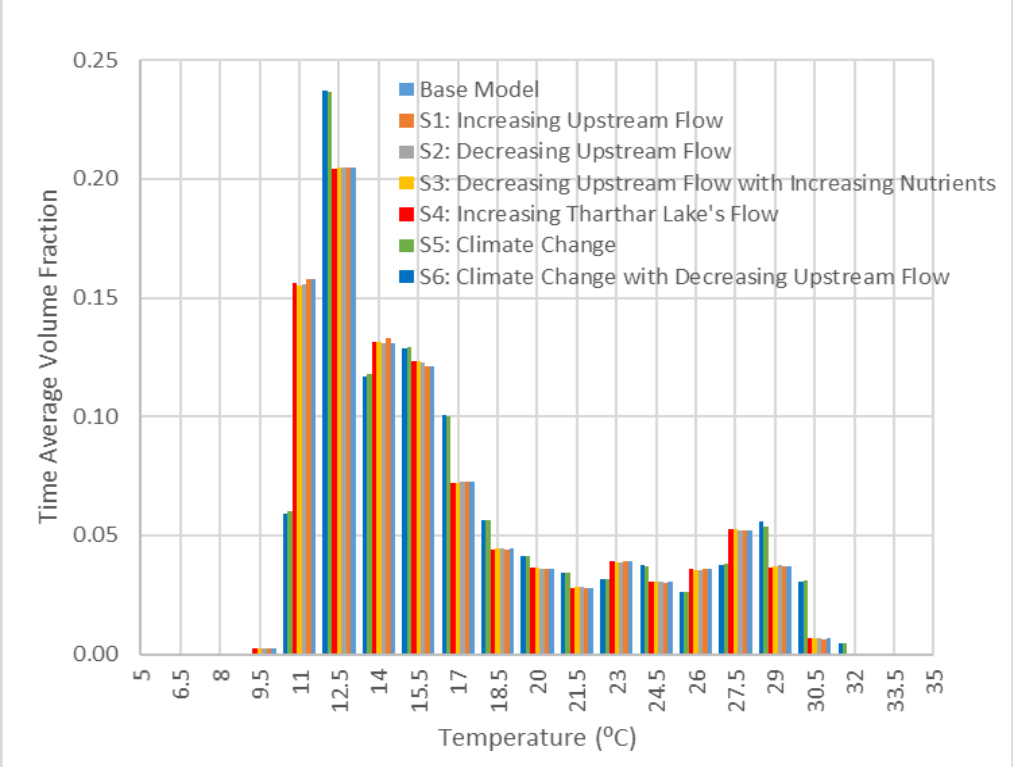

Figure 174: Environmental performance for 6 different scenario runs comparing water temperatures in Tharthar Lake.

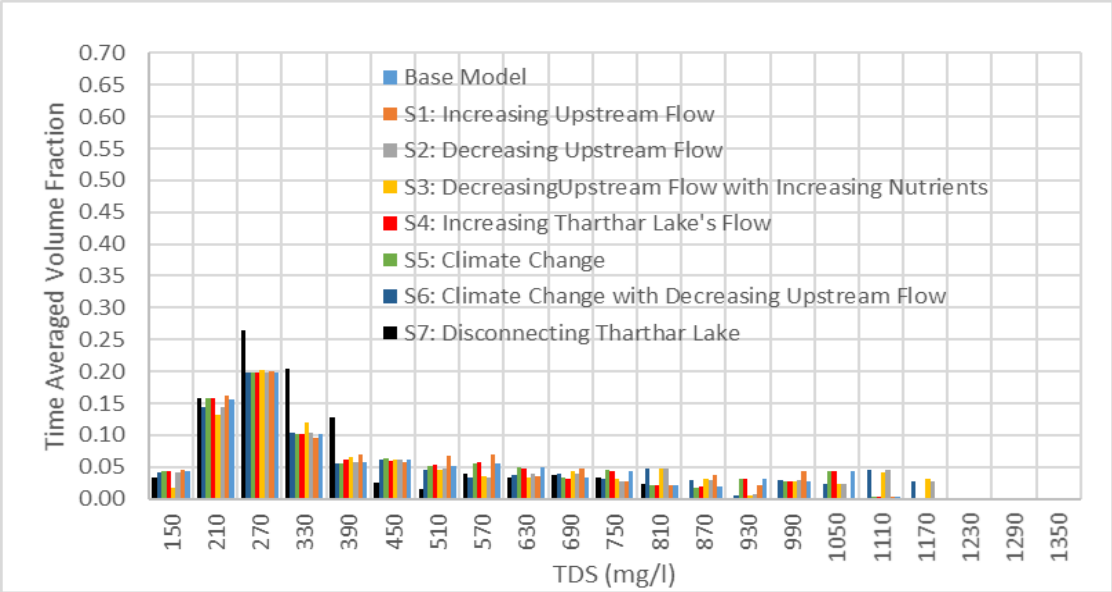

Figure 175: Environmental performance for 7 different scenario runs comparing total dissolved solids in the mainstem of the Tigris River.

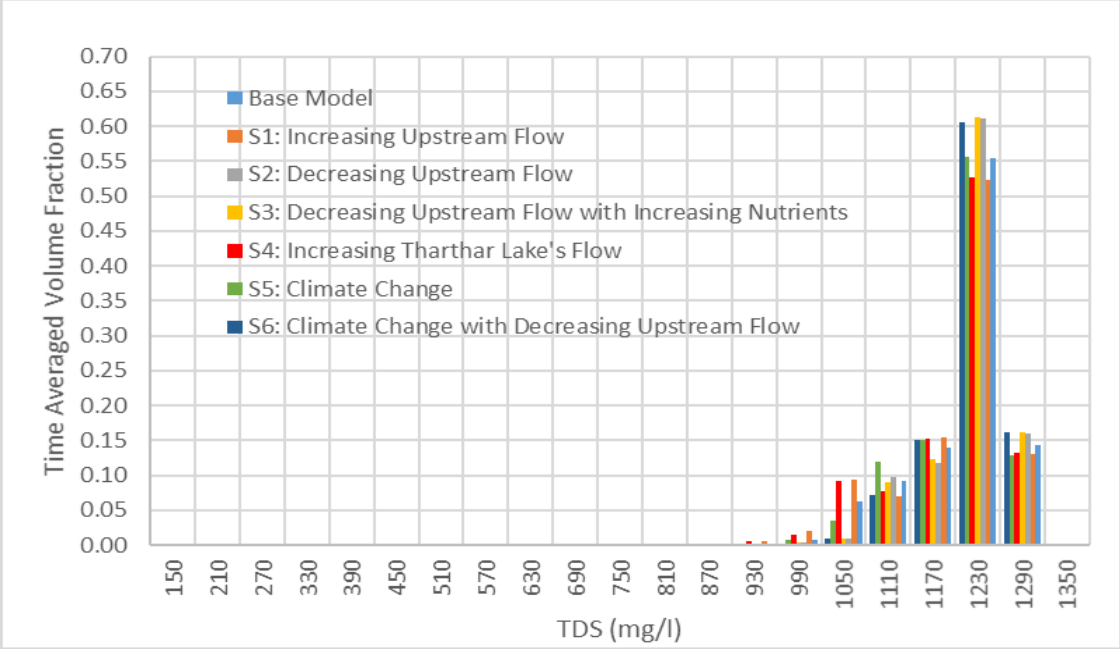

Figure 176: Environmental performance for 6 different scenario runs comparing total dissolved solids in Tharthar Lake.

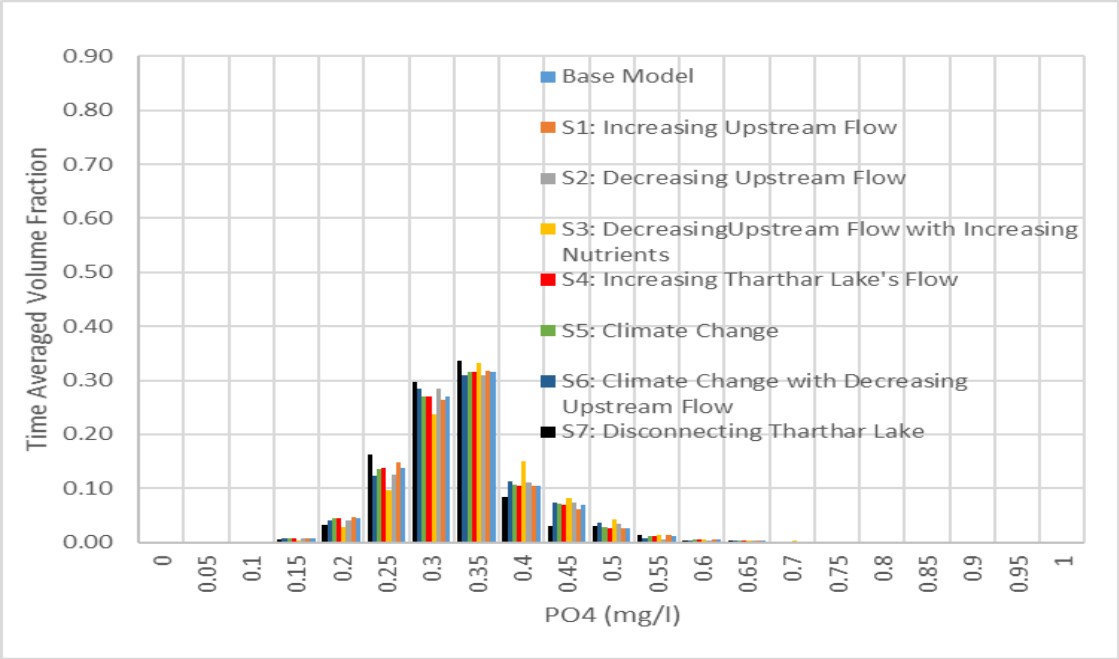

Figure 177: Environmental performance for 7 different scenario runs comparing phosphate in the mainstem of the Tigris River.

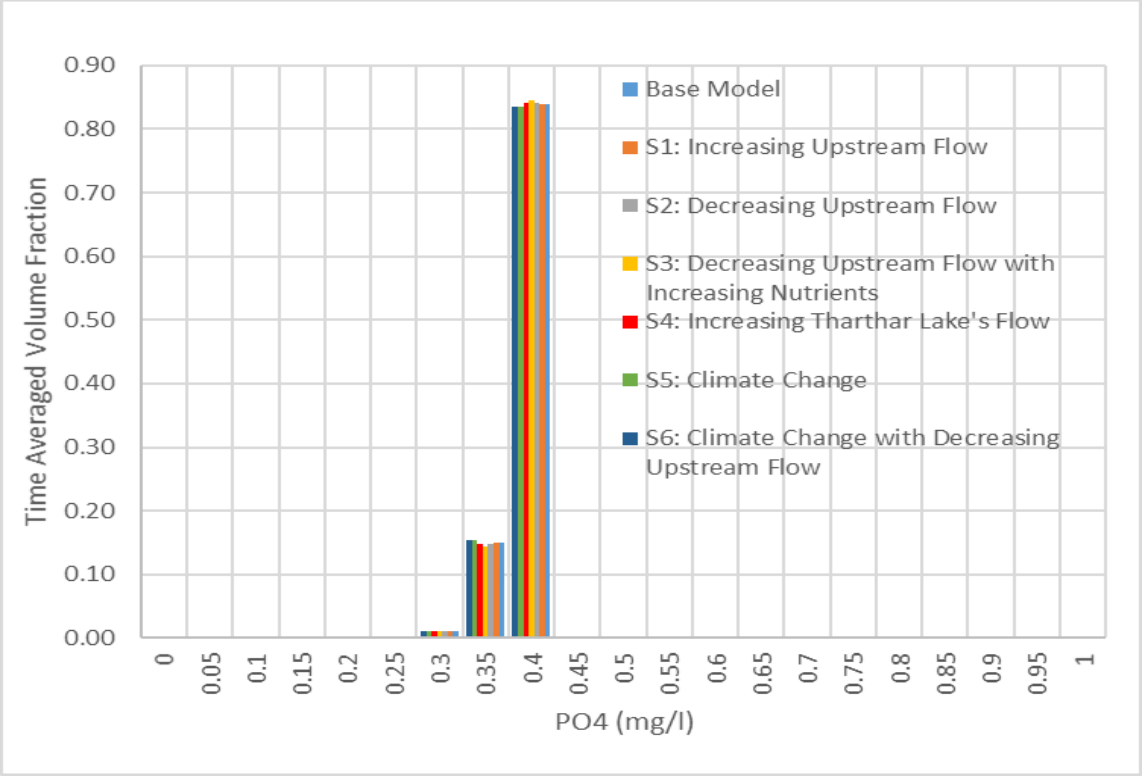

Figure 178: Environmental performance for 6 different scenario runs comparing phosphate in Tharthar Lake.

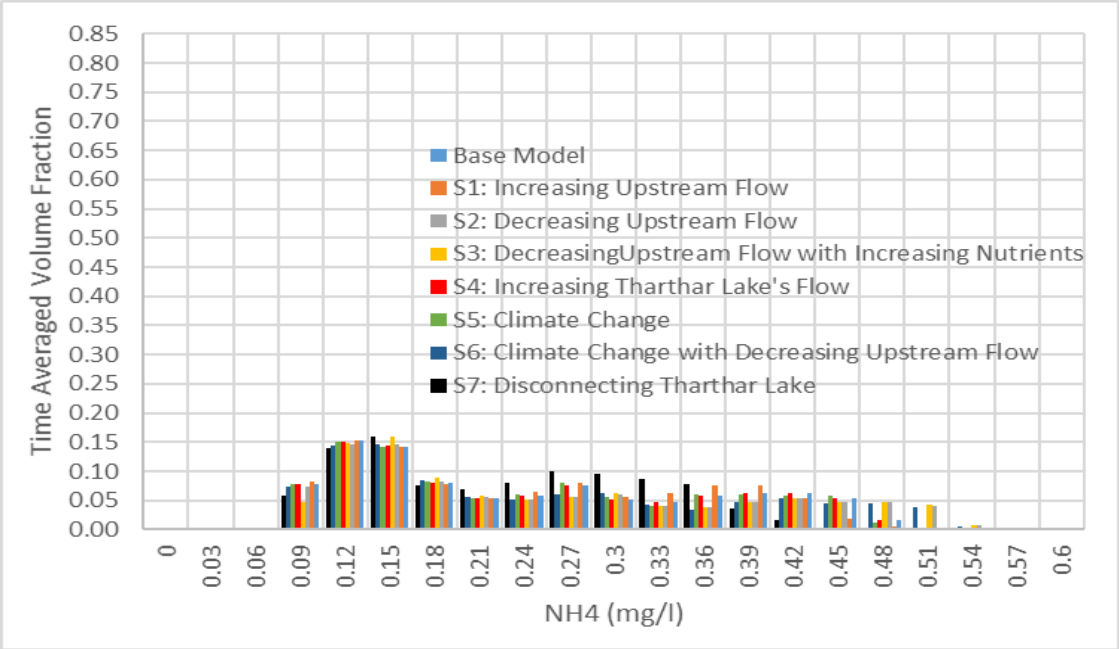

Figure 179: Environmental performance for 7 different scenario runs comparing ammonium in the mainstem of the Tigris River.

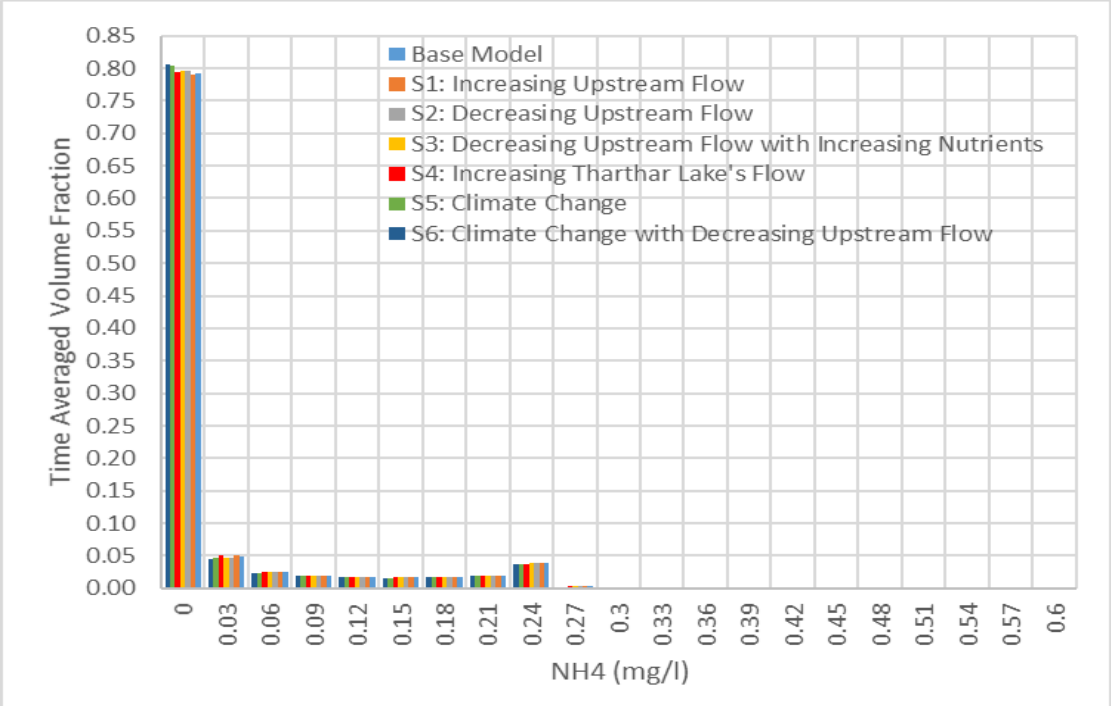

Figure 180: Environmental performance for 6 different scenario runs comparing ammonium in Tharthar Lake.

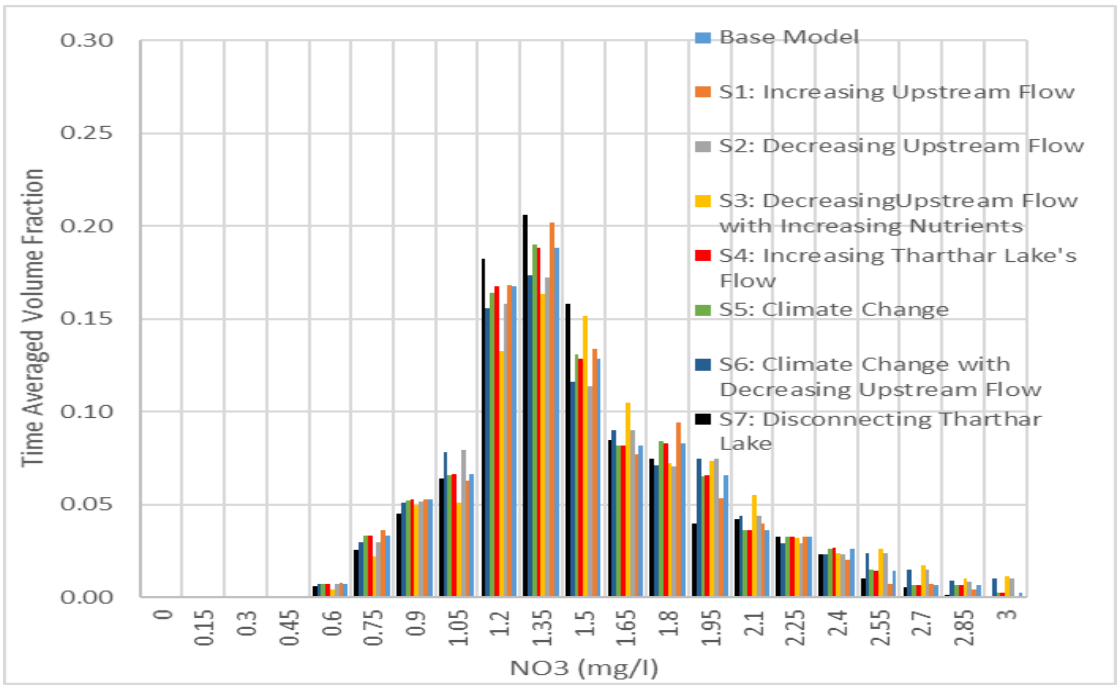

Figure 181: Environmental performance for 7 different scenario runs comparing nitrate in the mainstem of the Tigris River.

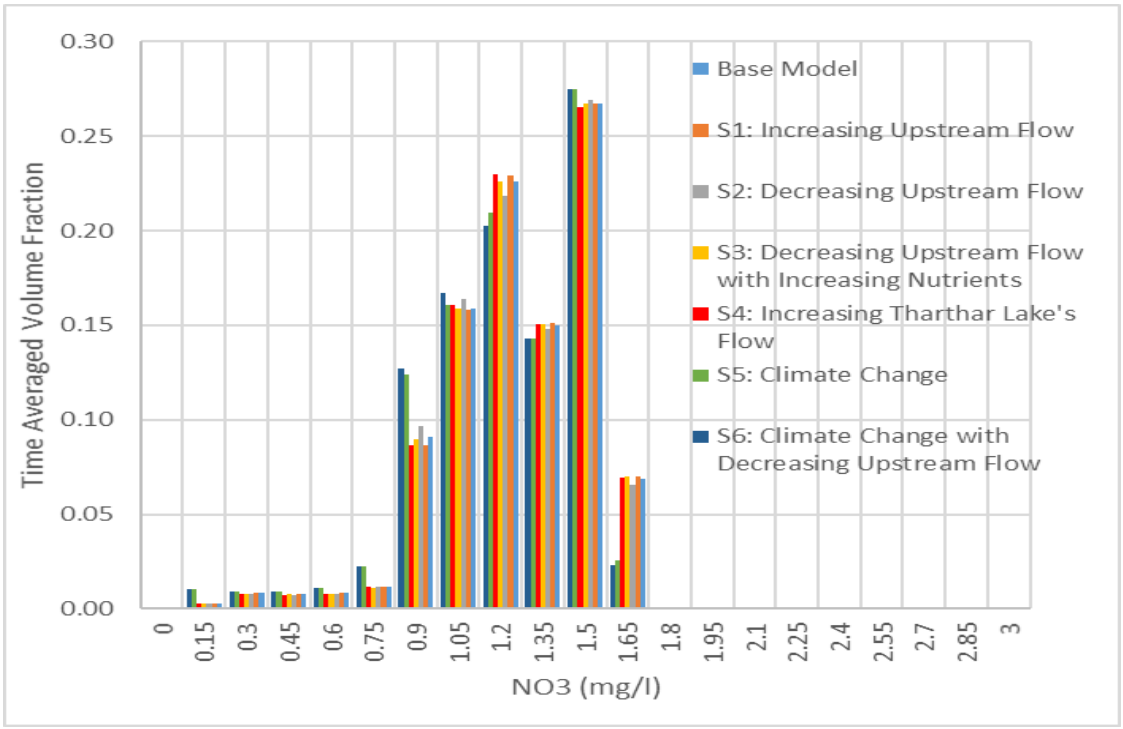

Figure 182: Environmental performance for 6 different scenario runs comparing nitrate in Tharthar Lake.

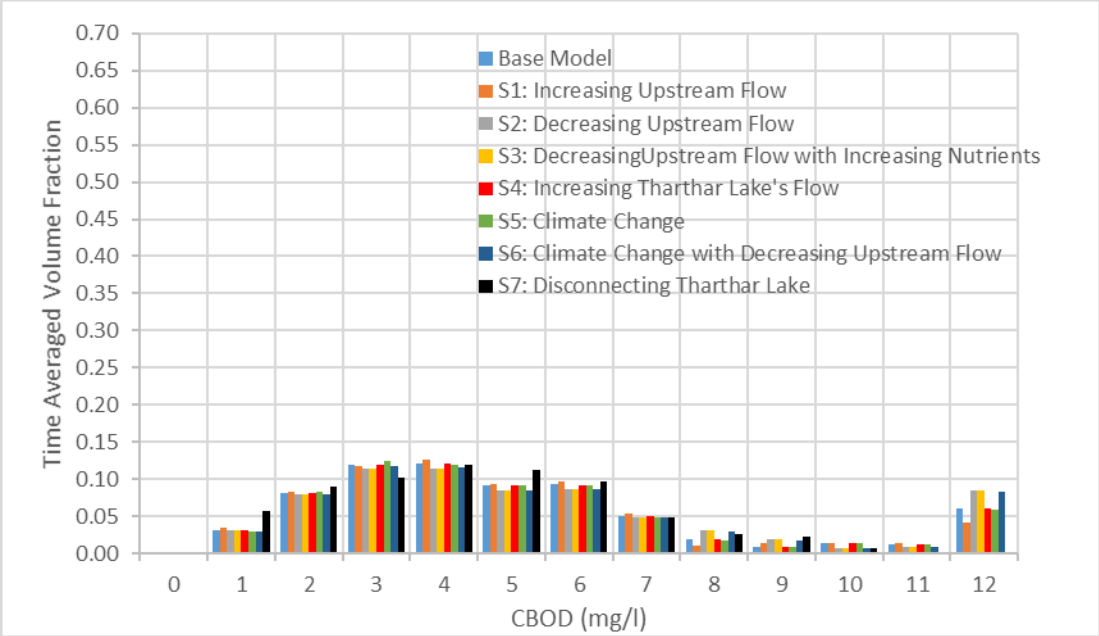

Figure 183: Environmental performance for 7 different scenario runs comparing carbonaceous biological oxygen demand in the mainstem of the Tigris River.

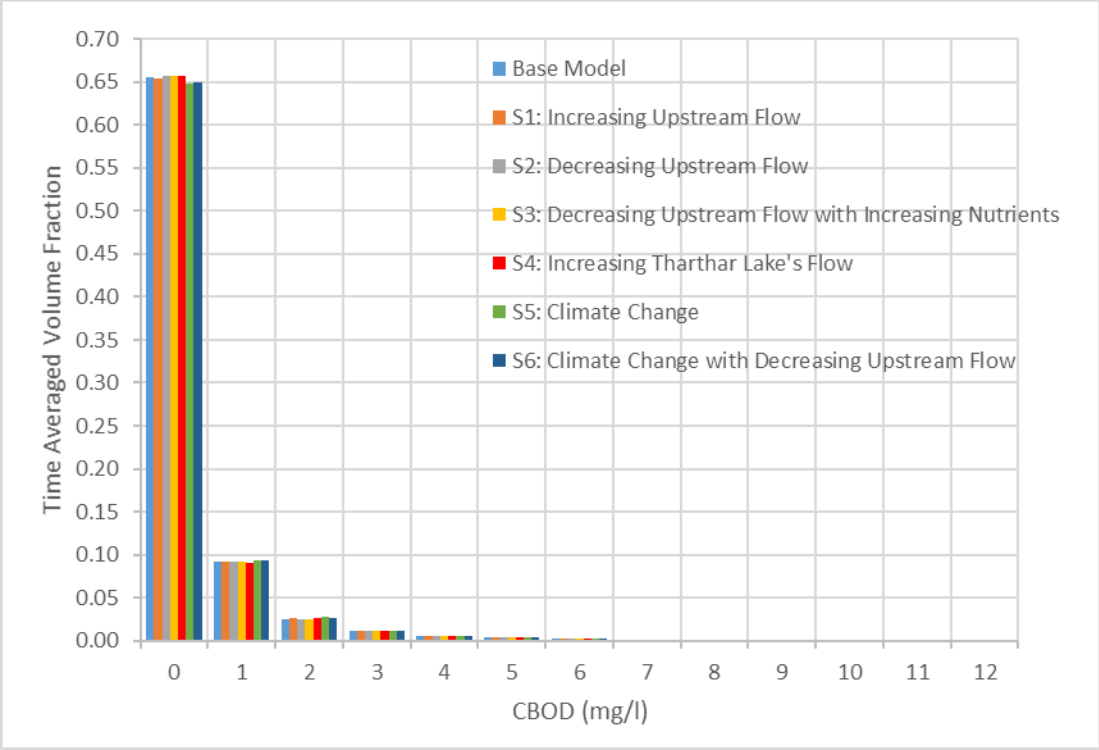

Figure 184: Environmental performance for 6 different scenario runs comparing carbonaceous biological oxygen demand in Tharthar Lake.

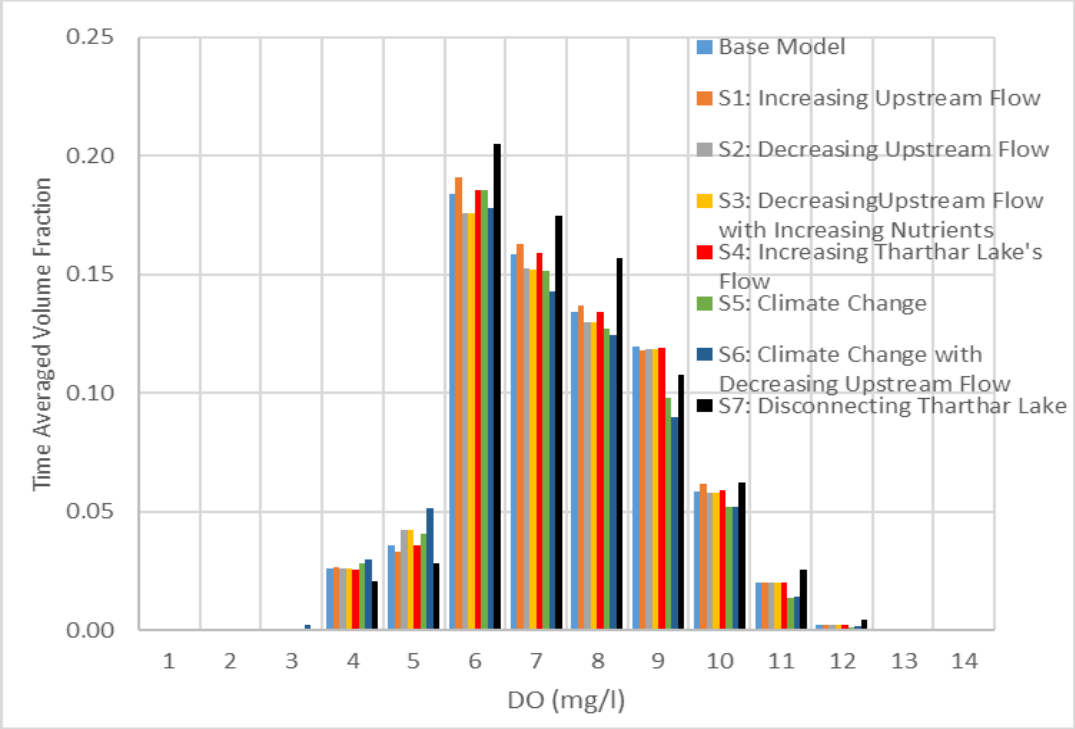

Figure 185: Environmental performance for 7 different scenario runs comparing dissolved oxygen in the mainstem of the Tigris River.

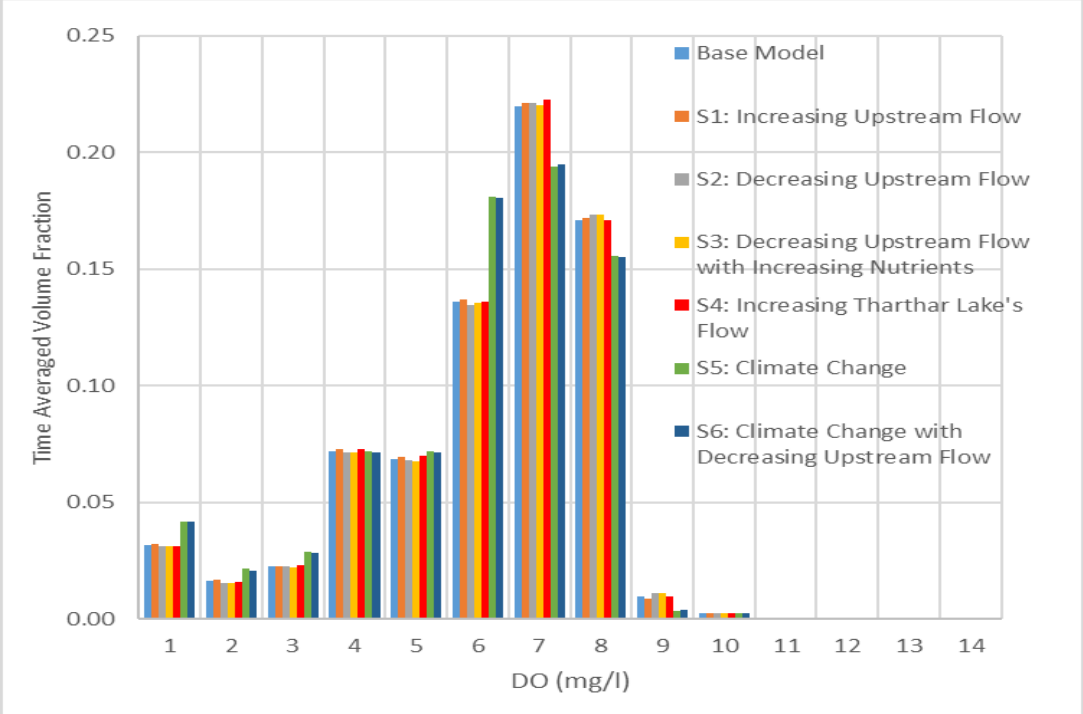

Figure 186: Environmental performance for 6 different scenario runs comparing dissolved oxygen in Tharthar Lake.

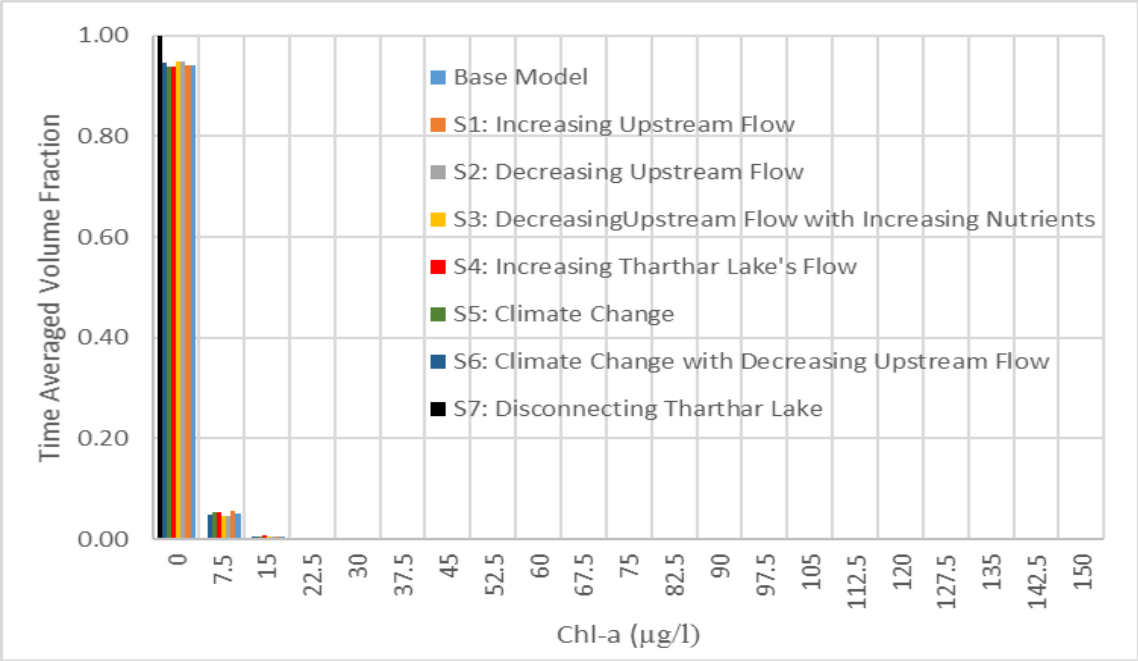

Figure 187: Environmental performance for 7 different scenario runs comparing chlorophyll-a in the mainstem of the Tigris River.

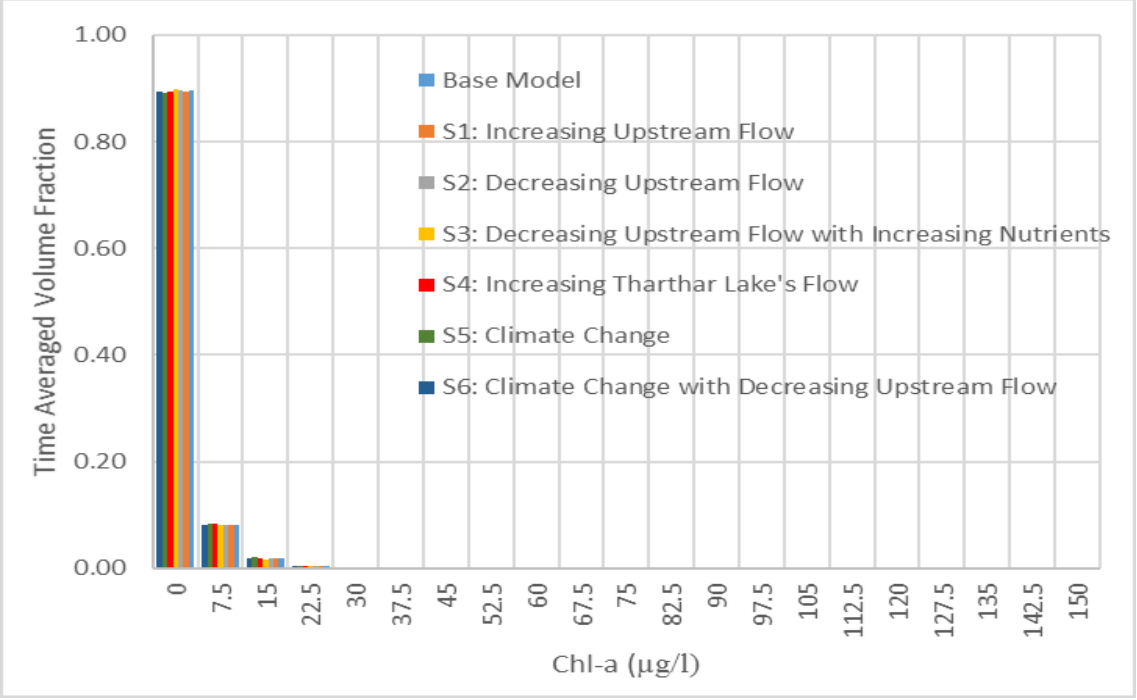

Figure 188: Environmental performance for 6 different scenario runs comparing chlorophyll-a in Tharthar Lake.

Appendix C: The Tigris River Model Control File

```
  PSU W2 Model Version 4.0

TITLE C
...............................TITLE.................................
....
        CE-Qual-W2 Model / Version 4.0
        The Tigris River Model
        Muhanned Al Murib & Scott Wells




GRID          NWB      NBR      IMX      KMX    NPROC  CLOSEC
                9        9      343       84        1     OFF

IN/OUTFL      NTR      NST      NIW      NWD      NGT      NSP      NPI
NPU
                7        2        0        9        2        6        0
0

CONSTITU      NGC      NSS      NAL      NEP     NBOD      NMC      NZP
                2        1        1        0        1        0        0

MISCELL      NDAY SELECTC HABTATC ENVIRPC AERATEC INITUWL
              100     OFF     OFF      ON     OFF     OFF

TIME CON  TMSTRT   TMEND    YEAR
           1.000 365.000    2009

DLT CON       NDT  DLTMIN DLTINTR
                2   0.100      ON

DLT DATE    DLTD    DLTD    DLTD    DLTD    DLTD    DLTD    DLTD
DLTD    DLTD
         1.00000   2.000

DLT MAX   DLTMAX  DLTMAX  DLTMAX  DLTMAX  DLTMAX  DLTMAX  DLTMAX
DLTMAX  DLTMAX
         25.0000  50.000

DLT FRN     DLTF    DLTF    DLTF    DLTF    DLTF    DLTF    DLTF
DLTF    DLTF
         0.90000  0.9000

DLT LIMI    VISC    CELC
WB 1          ON      ON
```

```
WB 2          ON      ON
WB 3          ON      ON
WB 4          ON      ON
WB 5          ON      ON
WB 6          ON      ON
WB 7          ON      ON
WB 8          ON      ON
WB 9          ON      ON

BRANCH G      US      DS     UHS     DHS     UQB     DQB   NLMIN
SLOPE  SLOPEC
BR1            2      70       0      73       0       0       1
0.00054 0.00054
BR2           73      80      70       0       0       0
10.0000010.000001
BR3           83     137     -80     140       0       0
10.0001540.000154
BR4          140     189     137       0       0       0
10.0000010.000001
BR5          192     206       0       0       0       0       1
0.00012 0.00012
BR6          209     297       0       0       0       0       1
0.00000 0.00000
BR7          300     305    -297       0       0       0       1
0.00011 0.00011
BR8          308     320       0       0       0       0       1
0.00020 0.00020
BR9          323     342       0       0       0       0
10.0000010.000001

LOCATION     LAT    LONG    EBOT      BS      BE    JBDN
WB 1     36.3566 -43.164 61.0000       1       1       1
WB 2     34.1600 -43.900 60.0000       2       2       2
WB 3     33.3128 -44.361 11.0000       3       3       3
WB 4     32.5168 -45.847 11.0000       4       4       4
WB 5     34.1600 -43.900 45.0000       5       5       5
WB 6     33.9847 -43.252 -3.0000       6       6       6
WB 7     33.9847 -43.252 38.0000       7       7       7
WB 8     33.9847 -43.252 30.0000       8       8       8
WB 9     34.1600 -43.900 45.0000       9       9       9

INIT CND     T2I    ICEI  WTYPEC   GRIDC
WB 1     6.11000 0.00000   FRESH    RECT
WB 2     7.60000 0.00000   FRESH    RECT
WB 3     7.70000 0.00000   FRESH    RECT
WB 4     8.70000 0.00000   FRESH    RECT
WB 5     6.11000 0.00000   FRESH    RECT
WB 6     14.0000 0.00000   FRESH    RECT
WB 7     8.00000 0.00000   FRESH    RECT
WB 8     8.00000 0.00000   FRESH    RECT
WB 9     6.11000 0.00000   FRESH    RECT

CALCULAT     VBC     EBC     MBC     PQC     EVC     PRC
```

WB 1	ON	ON	ON	OFF	ON	OFF
WB 2	ON	ON	ON	OFF	ON	OFF
WB 3	ON	ON	ON	OFF	ON	OFF
WB 4	ON	ON	ON	OFF	ON	OFF
WB 5	ON	ON	ON	OFF	ON	OFF
WB 6	ON	ON	ON	OFF	ON	OFF
WB 7	ON	ON	ON	OFF	ON	OFF
WB 8	ON	ON	ON	OFF	ON	OFF
WB 9	ON	ON	ON	OFF	ON	OFF

DEAD SEA	WINDC	QINC	QOUTC	HEATC
WB 1	ON	ON	ON	ON
WB 2	ON	ON	ON	ON
WB 3	ON	ON	ON	ON
WB 4	ON	ON	ON	ON
WB 5	ON	ON	ON	ON
WB 6	ON	ON	ON	ON
WB 7	ON	ON	ON	ON
WB 8	ON	ON	ON	ON
WB 9	ON	ON	ON	ON

INTERPOL	QINIC	DTRIC	HDIC
BR1	ON	ON	ON
BR2	ON	ON	ON
BR3	ON	ON	ON
BR4	ON	ON	ON
BR5	ON	OFF	ON
BR6	ON	OFF	ON
BR7	ON	OFF	ON
BR8	ON	OFF	ON
BR9	ON	OFF	ON

HEAT EXCH	SLHTC	SROC	RHEVAP	METIC	FETCHC	AFW	BFW	CFW	WINDH
WB 1	TERM	OFF	OFF	ON	OFF	9.20000	0.46000	2.00000	2.00000
WB 2	TERM	OFF	OFF	ON	OFF	9.20000	0.46000	2.00000	2.00000
WB 3	TERM	OFF	OFF	ON	OFF	9.20000	0.46000	2.00000	2.00000
WB 4	TERM	OFF	OFF	ON	OFF	9.20000	0.46000	2.00000	2.00000
WB 5	TERM	OFF	OFF	ON	OFF	9.20000	0.46000	2.00000	2.00000
WB 6	TERM	OFF	OFF	ON	OFF	9.20000	0.46000	2.00000	2.00000
WB 7	TERM	OFF	OFF	ON	OFF	9.20000	0.46000	2.00000	2.00000
WB 8	TERM	OFF	OFF	ON	OFF	9.20000	0.46000	2.00000	2.00000
WB 9	TERM	OFF	OFF	ON	OFF	9.20000	0.46000	2.00000	2.00000

```
ICE COVE    ICEC  SLICEC  ALBEDO   HWICE    BICE    GICE  ICEMIN
ICET2
WB 1         OFF  DETAIL 0.00000 0.00000 0.00000 0.00000 0.00000
0.00000
WB 2         OFF  DETAIL 0.00000 0.00000 0.00000 0.00000 0.00000
0.00000
WB 3         OFF  DETAIL 0.00000 0.00000 0.00000 0.00000 0.00000
0.00000
WB 4         OFF  DETAIL 0.00000 0.00000 0.00000 0.00000 0.00000
0.00000
WB 5         OFF  DETAIL 0.00000 0.00000 0.00000 0.00000 0.00000
0.00000
WB 6         OFF  DETAIL 0.00000 0.00000 0.00000 0.00000 0.00000
0.00000
WB 7         OFF  DETAIL 0.00000 0.00000 0.00000 0.00000 0.00000
0.00000
WB 8         OFF  DETAIL 0.00000 0.00000 0.00000 0.00000 0.00000
0.00000
WB 9         OFF  DETAIL 0.00000 0.00000 0.00000 0.00000 0.00000
0.00000

TRANSPOR   SLTRC   THETA
WB 1    ULTIMATE 0.55000
WB 2    ULTIMATE 0.55000
WB 3    ULTIMATE 0.55000
WB 4    ULTIMATE 0.55000
WB 5    ULTIMATE 0.55000
WB 6    ULTIMATE 0.55000
WB 7    ULTIMATE 0.55000
WB 8    ULTIMATE 0.55000
WB 9    ULTIMATE 0.55000

HYD COEF      AX      DX    CBHE    TSED      FI   TSEDF   FRICC
Z0
WB 1      1.0000 1.00000 0.30000 20.0000 0.01000 1.00000    MANN
0.00100
WB 2      1.0000 1.00000 0.30000 20.0000 0.01000 1.00000    MANN
0.00100
WB 3      1.0000 1.00000 0.30000 12.0000 0.01000 1.00000    MANN
0.00100
WB 4      1.0000 1.00000 0.30000 12.0000 0.01000 1.00000    MANN
0.00100
WB 5      1.0000 1.00000 0.30000 12.0000 0.01000 1.00000    MANN
0.00100
WB 6      1.0000 1.00000 0.30000 12.0000 0.01000 1.00000    MANN
0.00100
WB 7      1.0000 1.00000 0.30000 12.0000 0.01000 1.00000    MANN
0.00100
WB 8      1.0000 1.00000 0.30000 12.0000 0.01000 1.00000    MANN
0.00100
WB 9      1.0000 1.00000 0.30000 12.0000 0.01000 1.00000    MANN
0.00100
```

```
EDDY VISC    AZC   AZSLC   AZMAX     FBC       E   ARODI STRCKLR
BOUNDFR  TKECAL
WB 1         TKE     IMP 1.00000       3 9.53500 0.43000 24.0000
10.0000     IMP
WB 2         TKE     IMP 1.00000       3 9.53500 0.43100 0.00000
0.00000     IMP
WB 3         TKE     IMP 1.00000       3 9.53500 0.43100 0.00000
0.00000     IMP
WB 4         TKE     IMP 1.00000       3 9.53500 0.43100 0.00000
0.00000     IMP
WB 5         TKE     IMP 1.00000       3 9.53500 0.43100 0.00000
0.00000     IMP
WB 6         TKE     IMP 1.00000       3 9.53500 0.43100 0.00000
0.00000     IMP
WB 7         TKE     IMP 1.00000       3 9.53500 0.43100 0.00000
0.00000     IMP
WB 8         TKE     IMP 1.00000       3 9.53500 0.43100 0.00000
0.00000     IMP
WB 9         TKE     IMP 1.00000       3 9.53500 0.43100 0.00000
0.00000     IMP

N STRUC     NSTR DYNELEV
BR1            0     OFF
BR2            1     OFF
BR3            0     OFF
BR4            0     OFF
BR5            0     OFF
BR6            1     OFF
BR7            0     OFF
BR8            0     OFF
BR9            0     OFF

STR INT    STRIC   STRIC   STRIC   STRIC   STRIC   STRIC   STRIC
STRIC   STRIC
BR 1
BR 2          ON
BR 3
BR 4          ON
BR 5
BR 6          ON
BR 7          ON
BR 8
BR 9

STR TOP    KTSTR   KTSTR   KTSTR   KTSTR   KTSTR   KTSTR   KTSTR
KTSTR   KTSTR
BR1
BR2            2
BR3
BR4            2
BR5
BR6            2
BR7            2
```

```
BR8
BR9

STR BOT    KBSTR   KBSTR   KBSTR   KBSTR   KBSTR   KBSTR   KBSTR
KBSTR   KBSTR
BR1
BR2           81
BR3
BR4           81
BR5
BR6           42
BR7           81
BR8
BR9

STR SINK   SINKC   SINKC   SINKC   SINKC   SINKC   SINKC   SINKC
SINKC   SINKC
BR1
BR2         LINE
BR3
BR4         LINE
BR5
BR6         LINE
BR7         LINE
BR8
BR9

STR ELEV    ESTR    ESTR    ESTR    ESTR    ESTR    ESTR    ESTR
ESTR    ESTR
BR1
BR2      70.0000
BR3
BR4      18.0000
BR5
BR6      46.0000
BR7      56.0000
BR8
BR9

STR WIDT    WSTR    WSTR    WSTR    WSTR    WSTR    WSTR    WSTR
WSTR    WSTR
BR1
BR2     400.000
BR3
BR4      370.000
BR5
BR6      10.0000
BR7      55.0000
BR8
BR9

PIPES       IUPI    IDPI    EUPI    EDPI     WPI   DLXPI     FPI
FMINPI   WTHLC DYNPIPE
```

```
PIPE UP    PUPIC   ETUPI   EBUPI   KTUPI   KBUPI


PIPE DOWN  PDPIC   ETDPI   EBDPI   KTDPI   KBDPI


SPILLWAY    IUSP    IDSP     ESP    A1SP    B1SP    A2SP    B2SP
WTHLC
SP 1         206     278 46.0000  81.000 1.50000 427.180 1.50000
LAT
SP 2         342       0 45.5000  68.200 1.50000 359.700 1.50000
LAT
SP 3         320     119 31.0000  36.140 1.50000 190.650 1.50000
LAT
SP 4         305       0 42.0000 68.2000 1.50000 359.700 1.50000
LAT
SP 5         189       0 17.0000 627.400 1.50000 3309.54 1.50000
LAT
SP 6          80     323 68.5000 2045.78 1.50000 10791.9 1.50000
LAT

SPILL UP   PUSPC   ETUSP   EBUSP   KTUSP   KBUSP
SP 1     DENSITY 0.00000   0.000       2      83
SP 2       DISTR 0.00000 0.00000       2      83
SP 3       DISTR 0.00000 0.00000       2      83
SP 4       DISTR 0.00000 0.00000       2      83
SP 5       DISTR 0.00000 0.00000       2      83
SP 6       DISTR 0.00000 0.00000       2      83

SPILL DOWN PDSPC   ETUSP   EBUSP   KTDSP   KBDSP
SP 1     DENSITY 0.00000 0.00000       2      80
SP 2       DISTR 0.00000 0.00000       2      83
SP 3       DISTR 0.00000 0.00000       2      83
SP 4       DISTR 0.00000 0.00000       2      83
SP 5       DISTR 0.00000 0.00000       2      83
SP 6       DISTR 0.00000 0.00000       2      83

SPILL GAS GASSPC    EQSP  AGASSP  BGASSP  CGASSP
SP 1         OFF       0 0.00000 0.00000 0.00000
SP 2         OFF       0 0.00000 0.00000 0.00000
SP 3         OFF       0 0.00000 0.00000 0.00000
SP 4         OFF       0 0.00000 0.00000 0.00000
SP 5         OFF       0 0.00000 0.00000 0.00000
SP 6         OFF       0 0.00000 0.00000 0.00000

GATES       IUGT    IDGT     EGT    A1GT    B1GT    G1GT    A2GT
B2GT    G2GT   WTHLC
Gate1         80     192 61.0000 1.00000 0.00000 1.00000 0.00000
0.00000 1.00000     LAT
Gate2        305     308 50.0000 1.00000 0.00000 1.00000 0.00000
0.00000 1.00000     LAT
```

```
GATE WEIR   GTA1    GTB1    GTA2    GTB2  DYNVAR    GTIC
Gate1    1.00000 1.00000 1.00000 1.00000    FLOW      ON
Gate2    1.00000 1.00000 1.00000 1.00000    FLOW      ON

GATE UP    PUGTC   ETUGT   EBUGT   KTUGT   KBUGT
Gate1      DISTR 0.00000 0.00000       2      81
Gate2      DISTR 0.00000 0.00000       2      81

GATE DOWN  PDGTC   ETDGT   EBDGT   KTDGT   KBDGT
Gate1      DISTR 0.00000 0.00000       2      81
Gate2      DISTR 0.00000 0.00000       2      81

GATE GAS  GASGTC    EQGT  AGASGT  BGASGT  CGASGT
Gate1        OFF       0 0.00000 0.00000 0.00000
Gate2        OFF       0 0.00000 0.00000 0.00000

PUMPS 1     IUPU    IDPU     EPU  STRTPU   ENDPU   EONPU  EOFFPU
QPU   WTHLC DYNPUMP


PUMPS 2     PPUC    ETPU    EBPU    KTPU    KBPU


WEIR SEG     IWR     IWR     IWR     IWR     IWR     IWR     IWR
IWR     IWR


WEIR TOP    KTWR    KTWR    KTWR    KTWR    KTWR    KTWR    KTWR
KTWR    KTWR


WEIR BOT    KBWR    KBWR    KBWR    KBWR    KBWR    KBWR    KBWR
KBWR    KBWR


WD INT      WDIC    WDIC    WDIC    WDIC    WDIC    WDIC    WDIC
WDIC    WDIC
             OFF     OFF     OFF     OFF     OFF     OFF     OFF
OFF     OFF

WD SEG       IWD     IWD     IWD     IWD     IWD     IWD     IWD
IWD     IWD
             114     120     122     123     125     126     127
128     189

WD ELEV      EWD     EWD     EWD     EWD     EWD     EWD     EWD
EWD     EWD
            34.8    31.6    28.7    27.8    24.3    23.9    23.2
22.0      16

WD TOP      KTWD    KTWD    KTWD    KTWD    KTWD    KTWD    KTWD
KTWD    KTWD
```

```
                2       2       2       2       2       2       2
2       2

WD BOT      KBWD    KBWD    KBWD    KBWD    KBWD    KBWD    KBWD
KBWD    KBWD
               83      83      83      83      83      83      83
83      83

TRIB PLA    PTRC    PTRC    PTRC    PTRC    PTRC    PTRC    PTRC
PTRC    PTRC
            DISTR   DISTR   DISTR   DISTR   DISTR   DISTR   DISTR

TRIB INT    TRIC    TRIC    TRIC    TRIC    TRIC    TRIC    TRIC
TRIC    TRIC
               ON      ON      ON      ON      ON      ON      ON

TRIB SEG     ITR     ITR     ITR     ITR     ITR     ITR     ITR
ITR     ITR
               27      50      97     130      84     140      66

TRIB TOP   ELTRT   ELTRT   ELTRT   ELTRT   ELTRT   ELTRT   ELTRT
ELTRT   ELTRT
          0.00000 0.00000 0.00000 0.00000 0.00000 0.00000 0.00000

TRIB BOT   ELTRB   ELTRB   ELTRB   ELTRB   ELTRB   ELTRB   ELTRB
ELTRB   ELTRB
          0.00000 0.00000 0.00000 0.00000 0.00000 0.00000 0.00000

DST TRIB    DTRC    DTRC    DTRC    DTRC    DTRC    DTRC    DTRC
DTRC    DTRC
BR 1           ON
BR 2           ON
BR 3           ON
BR 4           ON
BR 5          OFF
BR 6          OFF
BR 7          OFF
BR 8          OFF
BR 9          OFF

HYD PRIN  HPRWBC  HPRWBC  HPRWBC  HPRWBC  HPRWBC  HPRWBC  HPRWBC
HPRWBC  HPRWBC
NVIOL         OFF     OFF     OFF     OFF     OFF     OFF     OFF
OFF     OFF
U              ON      ON      ON      ON      ON      ON      ON
ON      ON
W              ON      ON      ON      ON      ON      ON      ON
ON      ON
T              ON      ON      ON      ON      ON      ON      ON
ON      ON
RHO           OFF     OFF     OFF     OFF     OFF     OFF     OFF
OFF     OFF
```

```
AZ            OFF     OFF     OFF     OFF     OFF     OFF     OFF
OFF     OFF
SHEAR         OFF     OFF     OFF     OFF     OFF     OFF     OFF
OFF     OFF
ST            OFF     OFF     OFF     OFF     OFF     OFF     OFF
OFF     OFF
SB            OFF     OFF     OFF     OFF     OFF     OFF     OFF
OFF     OFF
ADMX          OFF     OFF     OFF     OFF     OFF     OFF     OFF
OFF     OFF
DM            OFF     OFF     OFF     OFF     OFF     OFF     OFF
OFF     OFF
HDG           OFF     OFF     OFF     OFF     OFF     OFF     OFF
OFF     OFF
ADMZ          OFF     OFF     OFF     OFF     OFF     OFF     OFF
OFF     OFF
HPG           OFF     OFF     OFF     OFF     OFF     OFF     OFF
OFF     OFF
GRAV          OFF     OFF     OFF     OFF     OFF     OFF     OFF
OFF     OFF

SNP PRINT   SNPC    NSNP   NISNP
WB 1          ON       2       5
WB 2          ON       2       2
WB 3          ON       2       2
WB 4          ON       2       2
WB 5         OFF       2       2
WB 6         OFF       2       2
WB 7         OFF       2       2
WB 8         OFF       2       2
WB 9         OFF       2       2

SNP DATE    SNPD    SNPD    SNPD    SNPD    SNPD    SNPD    SNPD
SNPD    SNPD
WB 1     1.00000 1.60000
WB 2     1.00000 1.60000
WB 3     1.00000 1.60000
WB 4     1.00000 1.60000
WB 5     1.00000 1.60000
WB 6     1.00000 1.60000
WB 7     1.00000 1.60000
WB 8     1.00000 1.60000
WB 9     1.00000 1.60000

SNP FREQ    SNPF    SNPF    SNPF    SNPF    SNPF    SNPF    SNPF
SNPF    SNPF
WB 1     0.10000 7.00000
WB 2     0.10000 7.00000
WB 3     0.10000 7.00000
WB 4     0.10000 7.00000
WB 5     0.10000 7.00000
WB 6     0.10000 7.00000
WB 7     0.10000 7.00000
```

```
WB 8     0.10000 7.00000
WB 9     0.10000 7.00000

SNP SEG     ISNP    ISNP    ISNP    ISNP    ISNP    ISNP    ISNP
ISNP    ISNP
WB 1           2      20      40      60      70
WB 2          73      80
WB 3          83     123
WB 4         140     189
WB 5         192     206
WB 6         209     297
WB 7         300     305
WB 8         308     320
WB 9         323     342

SCR PRINT   SCRC    NSCR
WB 1          ON       1
WB 2         OFF       0
WB 3         OFF       0
WB 4         OFF       0
WB 5         OFF       0
WB 6         OFF       0
WB 7         OFF       0
WB 8         OFF       0
WB 9         OFF       0

SCR DATE    SCRD    SCRD    SCRD    SCRD    SCRD    SCRD    SCRD
SCRD    SCRD
WB 1     1.00000
WB 2
WB 3
WB 4
WB 5
WB 6
WB 7
WB 8
WB 9

SCR FREQ    SCRF    SCRF    SCRF    SCRF    SCRF    SCRF    SCRF
SCRF    SCRF
WB 1     0.25000
WB 2
WB 3
WB 4
WB 5
WB 6
WB 7
WB 8
WB 9

PRF PLOT    PRFC    NPRF   NIPRF
WB 1         OFF       0       0
WB 2         OFF       0       0
```

WB 3	OFF	0	0
WB 4	OFF	0	0
WB 5	OFF	0	0
WB 6	OFF	0	0
WB 7	OFF	0	0
WB 8	OFF	0	0
WB 9	OFF	0	0

PRF DATE	PRFD	PRFD	PRFD	PRFD	PRFD	PRFD	PRFD	PRFD	PRFD
WB 1									
WB 2									
WB 3									
WB 4									
WB 5									
WB 6									
WB 7									
WB 8									
WB 9									

PRF FREQ	PRFF	PRFF	PRFF	PRFF	PRFF	PRFF	PRFF	PRFF	PRFF
WB 1									
WB 2									
WB 3									
WB 4									
WB 5									
WB 6									
WB 7									
WB 8									
WB 9									

PRF SEG	IPRF	IPRF	IPRF	IPRF	IPRF	IPRF	IPRF	IPRF	IPRF
WB 1									
WB 2									
WB 3									
WB 4									
WB 5									
WB 6									
WB 7									
WB 8									
WB 9									

SPR PLOT	SPRC	NSPR	NISPR
WB 1	OFF	12	1
WB 2	OFF	0	0
WB 3	OFF	0	0
WB 4	OFF	0	0
WB 5	OFF	0	0
WB 6	OFF	0	0
WB 7	OFF	0	0
WB 8	OFF	0	0

```
WB 9         OFF       0       0

SPR DATE    SPRD    SPRD    SPRD    SPRD    SPRD    SPRD    SPRD
SPRD    SPRD
WB 1     158.670 179.670 200.670 228.670 229.670 242.670 244.670
245.670 249.670
         257.670 270.670 271.670
WB 2
WB 3
WB 4
WB 5
WB 6
WB 7
WB 8
WB 9

SPR FREQ    SPRF    SPRF    SPRF    SPRF    SPRF    SPRF    SPRF
SPRF    SPRF
WB 1     500.000 500.000 500.000 500.000 500.000 500.000 500.000
500.000 500.000
         500.000 500.000 500.000
WB 2
WB 3
WB 4
WB 5
WB 6
WB 7
WB 8
WB 9

SPR SEG     ISPR    ISPR    ISPR    ISPR    ISPR    ISPR    ISPR
ISPR    ISPR
WB 1          36
WB 2
WB 3
WB 4
WB 5
WB 6
WB 7
WB 8
WB 9

VPL PLOT    VPLC    NVPL
WB 1          ON       1
WB 2         OFF       0
WB 3         OFF       0
WB 4         OFF       0
WB 5         OFF       0
WB 6         OFF       0
WB 7         OFF       0
WB 8         OFF       0
WB 9         OFF       0
```

VPL DATE	VPLD	VPLD	VPLD	VPLD	VPLD	VPLD	VPLD	VPLD	VPLD
WB 1	1.5								
WB 2									
WB 3									
WB 4									
WB 5									
WB 6									
WB 7									
WB 8									
WB 9									

VPL FREQ	VPLF	VPLF	VPLF	VPLF	VPLF	VPLF	VPLF	VPLF	VPLF
WB 1	1.0								
WB 2									
WB 3									
WB 4									
WB 5									
WB 6									
WB 7									
WB 8									
WB 9									

CPL PLOT	CPLC	NCPL	TECPLOT
WB 1	ON	1	OFF
WB 2	ON	1	OFF
WB 3	ON	1	OFF
WB 4	ON	1	OFF
WB 5	OFF	0	OFF
WB 6	ON	1	OFF
WB 7	OFF	0	OFF
WB 8	OFF	0	OFF
WB 9	OFF	0	OFF

CPL DATE	CPLD	CPLD	CPLD	CPLD	CPLD	CPLD	CPLD	CPLD	CPLD
WB 1	1.0	20.0	30.0	40.0	50.0	60.0	70.0		
WB 2	1.0	20.0	30.0	40.0	50.0	60.0	70.0		
WB 3	1.0	20.0	30.0	40.0	50.0	60.0	70.0		
WB 4	1.0	20.0	30.0	40.0	50.0	60.0	70.0		
WB 5									
WB 6	1.0	20.0	30.0	40.0	50.0	60.0	70.0		
WB 7									
WB 8									
WB 9									

CPL FREQ	CPLF	CPLF	CPLF	CPLF	CPLF	CPLF	CPLF	CPLF	CPLF
WB 1	1								
WB 2	1								
WB 3	1								
WB 4	1								

```
WB 5
WB 6           1
WB 7
WB 8
WB 9

FLUXES      FLXC    NFLX
WB 1          ON       1
WB 2          ON       1
WB 3          ON       1
WB 4          ON       1
WB 5         OFF       0
WB 6          ON       1
WB 7         OFF       0
WB 8         OFF       0
WB 9         OFF       0

FLX DATE    FLXD    FLXD    FLXD    FLXD    FLXD    FLXD    FLXD
FLXD    FLXD
WB 1          1.5
WB 2          1.5
WB 3          1.5
WB 4          1.5
WB 5
WB 6          1.5
WB 7
WB 8
WB 9

FLX FREQ    FLXF    FLXF    FLXF    FLXF    FLXF    FLXF    FLXF
FLXF    FLXF
WB 1         10.0
WB 2         10.0
WB 3         10.0
WB 4         10.0
WB 5
WB 6         10.0
WB 7
WB 8
WB 9

TSR PLOT    TSRC    NTSR   NITSR
              ON       1      27

TSR DATE    TSRD    TSRD    TSRD    TSRD    TSRD    TSRD    TSRD
TSRD    TSRD
         1.00000

TSR FREQ    TSRF    TSRF    TSRF    TSRF    TSRF    TSRF    TSRF
TSRF    TSRF
         0.10000
```

```
TSR SEG     ITSR    ITSR    ITSR    ITSR    ITSR    ITSR    ITSR
ITSR    ITSR
              140       2      54     230     250      51     120
80     123
               83     189     297     305     320      28     131
11       5
                4       6      10      12      15      20       9
7       8

TSR LAYE    ETSR    ETSR    ETSR    ETSR    ETSR    ETSR    ETSR
ETSR    ETSR
          0.10000 0.10000 0.10000 0.10000 0.10000 0.10000 0.10000
0.10000 0.10000
          0.10000 0.10000 0.10000 0.10000 0.10000 0.10000 0.10000
0.10000 0.10000
          0.10000 0.10000 0.10000 0.10000 0.10000 0.10000 0.10000
0.10000 0.10000

WITH OUT    WDOC    NWDO   NIWDO
              ON       1       8

WITH DAT    WDOD    WDOD    WDOD    WDOD    WDOD    WDOD    WDOD
WDOD    WDOD
          1.00000

WITH FRE    WDOF    WDOF    WDOF    WDOF    WDOF    WDOF    WDOF
WDOF    WDOF
          0.10000

WITH SEG    IWDO    IWDO    IWDO    IWDO    IWDO    IWDO    IWDO
IWDO    IWDO
               80     189     297     305     206     320     342
114     123

RESTART     RSOC    NRSO    RSIC
             OFF       0     OFF

RSO DATE    RSOD    RSOD    RSOD    RSOD    RSOD    RSOD    RSOD
RSOD    RSOD


RSO FREQ    RSOF    RSOF    RSOF    RSOF    RSOF    RSOF    RSOF
RSOF    RSOF


CST COMP     CCC    LIMC     CUF
              ON     OFF       5

CST ACTIVE   CAC
TDS           ON
Gen1          ON
Gen2          ON
ISS          OFF
```

```
PO4            ON
NH4            ON
NO3            ON
DSI           OFF
PSI           OFF
FE            OFF
LDOM           ON
RDOM           ON
LPOM           ON
RPOM           ON
BOD1           ON
BOD1-P         ON
BOD1-N         ON
ALG1           ON
DO             ON
TIC           OFF
ALK           OFF
LDOM-P        OFF
RDOM-P        OFF
LPOM-P        OFF
RPOM-P        OFF
LDOM-N        OFF
RDOM-N        OFF
LPOM-N        OFF
RPOM-N        OFF

CST DERI   CDWBC   CDWBC   CDWBC   CDWBC   CDWBC   CDWBC   CDWBC
CDWBC   CDWBC
DOC            OFF      OFF      OFF      OFF      OFF      OFF      OFF
OFF      OFF
POC            OFF      OFF      OFF      OFF      OFF      OFF      OFF
OFF      OFF
TOC            OFF      OFF      OFF      OFF      OFF      OFF      OFF
OFF      OFF
DON            OFF      OFF      OFF      OFF      OFF      OFF      OFF
OFF      OFF
PON            OFF      OFF      OFF      OFF      OFF      OFF      OFF
OFF      OFF
TON            OFF      OFF      OFF      OFF      OFF      OFF      OFF
OFF      OFF
TKN            OFF      OFF      OFF      OFF      OFF      OFF      OFF
OFF      OFF
TN              ON       ON       ON       ON       ON       ON       ON
ON       ON
DOP            OFF      OFF      OFF      OFF      OFF      OFF      OFF
OFF      OFF
POP            OFF      OFF      OFF      OFF      OFF      OFF      OFF
OFF      OFF
TOP            OFF      OFF      OFF      OFF      OFF      OFF      OFF
OFF      OFF
TP              ON       ON       ON       ON       ON       ON       ON
ON       ON
```

```
APR          OFF     OFF     OFF     OFF     OFF     OFF     OFF
OFF     OFF
CHLA          ON      ON      ON      ON      ON      ON      ON
ON      ON
ATOT         OFF     OFF     OFF     OFF     OFF     OFF     OFF
OFF     OFF
%DO          OFF     OFF     OFF     OFF     OFF     OFF     OFF
OFF     OFF
TSS          OFF     OFF     OFF     OFF     OFF     OFF     OFF
OFF     OFF
TISS         OFF     OFF     OFF     OFF     OFF     OFF     OFF
OFF     OFF
CBOD          ON      ON      ON      ON      ON      ON      ON
ON      ON
pH           OFF     OFF     OFF     OFF     OFF     OFF     OFF
OFF     OFF
CO2          OFF     OFF     OFF     OFF     OFF     OFF     OFF
OFF     OFF
HCO3         OFF     OFF     OFF     OFF     OFF     OFF     OFF
OFF     OFF
CO3          OFF     OFF     OFF     OFF     OFF     OFF     OFF
OFF     OFF

CST FLUX   CFWBC   CFWBC   CFWBC   CFWBC   CFWBC   CFWBC   CFWBC
CFWBC   CFWBC
TISSIN       OFF     OFF     OFF     OFF     OFF     OFF     OFF
OFF     OFF
TISSOUT      OFF     OFF     OFF     OFF     OFF     OFF     OFF
OFF     OFF
PO4AR         ON      ON      ON      ON      ON      ON      ON
ON      ON
PO4AG         ON      ON      ON      ON      ON      ON      ON
ON      ON
PO4AP         ON      ON      ON      ON      ON      ON      ON
ON      ON
PO4ER         ON      ON      ON      ON      ON      ON      ON
ON      ON
PO4EG         ON      ON      ON      ON      ON      ON      ON
ON      ON
PO4EP         ON      ON      ON      ON      ON      ON      ON
ON      ON
PO4POM       OFF     OFF     OFF     OFF     OFF     OFF     OFF
OFF     OFF
PO4DOM       OFF     OFF     OFF     OFF     OFF     OFF     OFF
OFF     OFF
PO4OM         ON      ON      ON      ON      ON      ON      ON
ON      ON
PO4SED        ON      ON      ON      ON      ON      ON      ON
ON      ON
PO4SOD        ON      ON      ON      ON      ON      ON      ON
ON      ON
PO4SET        ON      ON      ON      ON      ON      ON      ON
ON      ON
```

NH4NITR	ON	ON	ON	ON	ON	ON	ON	ON	ON	ON
NH4AR	ON	ON	ON	ON	ON	ON	ON	ON	ON	ON
NH4AG	ON	ON	ON	ON	ON	ON	ON	ON	ON	ON
NH4AP	ON	ON	ON	ON	ON	ON	ON	ON	ON	ON
NH4ER	ON	ON	ON	ON	ON	ON	ON	ON	ON	ON
NH4EG	ON	ON	ON	ON	ON	ON	ON	ON	ON	ON
NH4EP	ON	ON	ON	ON	ON	ON	ON	ON	ON	ON
NH4POM	OFF	OFF	OFF	OFF	OFF	OFF	OFF	OFF	OFF	OFF
NH4DOM	OFF	OFF	OFF	OFF	OFF	OFF	OFF	OFF	OFF	OFF
NH4OM	ON	ON	ON	ON	ON	ON	ON	ON	ON	ON
NH4SED	ON	ON	ON	ON	ON	ON	ON	ON	ON	ON
NH4SOD	ON	ON	ON	ON	ON	ON	ON	ON	ON	ON
NO3DEN	ON	ON	ON	ON	ON	ON	ON	ON	ON	ON
NO3AG	ON	ON	ON	ON	ON	ON	ON	ON	ON	ON
NO3EG	ON	ON	ON	ON	ON	ON	ON	ON	ON	ON
NO3SED	ON	ON	ON	ON	ON	ON	ON	ON	ON	ON
DSIAG	OFF	OFF	OFF	OFF	OFF	OFF	OFF	OFF	OFF	OFF
DSIEG	OFF	OFF	OFF	OFF	OFF	OFF	OFF	OFF	OFF	OFF
DSIPIS	OFF	OFF	OFF	OFF	OFF	OFF	OFF	OFF	OFF	OFF
DSISED	OFF	OFF	OFF	OFF	OFF	OFF	OFF	OFF	OFF	OFF
DSISOD	OFF	OFF	OFF	OFF	OFF	OFF	OFF	OFF	OFF	OFF
DSISET	OFF	OFF	OFF	OFF	OFF	OFF	OFF	OFF	OFF	OFF
PSIAM	OFF	OFF	OFF	OFF	OFF	OFF	OFF	OFF	OFF	OFF
PSINET	OFF	OFF	OFF	OFF	OFF	OFF	OFF	OFF	OFF	OFF
PSIDK	OFF	OFF	OFF	OFF	OFF	OFF	OFF	OFF	OFF	OFF
FESET	OFF	OFF	OFF	OFF	OFF	OFF	OFF	OFF	OFF	OFF

FESED	OFF	OFF	OFF	OFF	OFF	OFF	OFF	OFF	OFF	OFF
LDOMDK	OFF	OFF	OFF	OFF	OFF	OFF	OFF	OFF	OFF	OFF
LRDOM	OFF	OFF	OFF	OFF	OFF	OFF	OFF	OFF	OFF	OFF
RDOMDK	OFF	OFF	OFF	OFF	OFF	OFF	OFF	OFF	OFF	OFF
LDOMAP	OFF	OFF	OFF	OFF	OFF	OFF	OFF	OFF	OFF	OFF
LDOMEP	OFF	OFF	OFF	OFF	OFF	OFF	OFF	OFF	OFF	OFF
LPOMDK	OFF	OFF	OFF	OFF	OFF	OFF	OFF	OFF	OFF	OFF
LRPOM	OFF	OFF	OFF	OFF	OFF	OFF	OFF	OFF	OFF	OFF
RPOMDK	OFF	OFF	OFF	OFF	OFF	OFF	OFF	OFF	OFF	OFF
LPOMAP	OFF	OFF	OFF	OFF	OFF	OFF	OFF	OFF	OFF	OFF
LPOMEP	OFF	OFF	OFF	OFF	OFF	OFF	OFF	OFF	OFF	OFF
LPOMSET	OFF	OFF	OFF	OFF	OFF	OFF	OFF	OFF	OFF	OFF
RPOMSET	OFF	OFF	OFF	OFF	OFF	OFF	OFF	OFF	OFF	OFF
CBODDK	OFF	OFF	OFF	OFF	OFF	OFF	OFF	OFF	OFF	OFF
DOAP	OON	ON	ON	ON	ON	ON	ON	ON	ON	ON
DOAR	OON	ON	ON	ON	ON	ON	ON	ON	ON	ON
DOEP	OFF	OFF	OFF	OFF	OFF	OFF	OFF	OFF	OFF	OFF
DOER	OFF	OFF	OFF	OFF	OFF	OFF	OFF	OFF	OFF	OFF
DOPOM	OFF	OFF	OFF	OFF	OFF	OFF	OFF	OFF	OFF	OFF
DODOM	OFF	OFF	OFF	OFF	OFF	OFF	OFF	OFF	OFF	OFF
DOOM	ON	ON	ON	ON	ON	ON	ON	ON	ON	ON
DONITR	ON	ON	ON	ON	ON	ON	ON	ON	ON	ON
DOCBOD	OFF	OFF	OFF	OFF	OFF	OFF	OFF	OFF	OFF	OFF
DOREAR	ON	ON	ON	ON	ON	ON	ON	ON	ON	ON
DOSED	ON	ON	ON	ON	ON	ON	ON	ON	ON	ON
DOSOD	ON	ON	ON	ON	ON	ON	ON	ON	ON	ON

```
TICAG         OFF     OFF     OFF     OFF     OFF     OFF     OFF
OFF     OFF
TICEG         OFF     OFF     OFF     OFF     OFF     OFF     OFF
OFF     OFF
SEDDK         OFF     OFF     OFF     OFF     OFF     OFF     OFF
OFF     OFF
SEDAS         OFF     OFF     OFF     OFF     OFF     OFF     OFF
OFF     OFF
SEDLPOM       OFF     OFF     OFF     OFF     OFF     OFF     OFF
OFF     OFF
SEDSET        OFF     OFF     OFF     OFF     OFF     OFF     OFF
OFF     OFF
SODDK         OFF     OFF     OFF     OFF     OFF     OFF     OFF
OFF     OFF

CST ICON    C2IWB   C2IWB   C2IWB   C2IWB   C2IWB   C2IWB   C2IWB
C2IWB   C2IWB
TDS       249.000 360.000  850.00 1040.00  400.00 1300.00 1300.00
1300.00 400.000
Gen1      0.00000 0.00000 0.00000 0.00000 0.00000 0.00000 0.00000
0.00000 0.00000
Gen2      0.00000 0.00000 0.00000 0.00000 0.00000 0.00000 0.00000
0.00000 0.00000
ISS       0.00000 0.00000 0.00000 0.00000 0.00000 0.00000 0.00000
0.00000 0.00000
PO4       0.31500 0.33000 0.20000 0.20000 0.33000 0.33000 0.33000
0.33000 0.33000
NH4       0.10000 0.20000 0.20000 0.20000 0.10000 0.10000 0.10000
0.10000 0.10000
NO3       1.50000 1.20000 1.00000 1.00000 1.20000 1.20000 1.20000
1.20000 1.20000
DSI       0.00000 0.00000 0.00000 0.00000 0.00000 0.00000 0.00000
0.00000 0.00000
PSI       0.00000 0.00000 0.00000 0.00000 0.00000 0.00000 0.00000
0.00000 0.00000
FE        0.00000 0.00000 0.00000 0.00000 0.00000 0.00000 0.00000
0.00000 0.00000
LDOM      0.00000 0.00000 0.00000 0.00000 0.00000 0.00000 0.00000
0.00000 0.00000
RDOM      0.00000 0.00000 0.00000 0.00000 0.00000 0.00000 0.00000
0.00000 0.00000
LPOM      0.00000 0.00000 0.00000 0.00000 0.00000 0.00000 0.00000
0.00000 0.00000
RPOM      0.00000 0.00000 0.00000 0.00000 0.00000 0.00000 0.00000
0.00000 0.00000
BOD1      6.86000 6.85000 5.80000 5.08000 6.85000 6.85000 6.85000
6.85000 6.85000
BOD1-P    0.06900 0.06800 0.05000 0.05000 0.06800 0.06800 0.06800
0.06800 0.06800
BOD1-N    0.55000 0.54800 0.40600 0.40600 0.54800 0.54800 0.54800
0.54800 0.54800
ALG1      0.05000 0.05000 0.05000 0.05000 0.05000 0.05000 0.05000
0.05000 0.05000
```

```
DO      11.20000 10.7600 10.7300 10.7300 10.7600 10.7600 10.7600
10.7600 10.7600
TIC      0.00000 0.00000 0.00000 0.00000 0.00000 0.00000 0.00000
0.00000 0.00000
ALK      0.00000 0.00000 0.00000 0.00000 0.00000 0.00000 0.00000
0.00000 0.00000
LDOM-P   0.00000 0.00000 0.00000 0.00000 0.00000 0.00000 0.00000
0.00000 0.00000
RDOM-P   0.00000 0.00000 0.00000 0.00000 0.00000 0.00000 0.00000
0.00000 0.00000
LPOM-P   0.00000 0.00000 0.00000 0.00000 0.00000 0.00000 0.00000
0.00000 0.00000
RPOM-P   0.00000 0.00000 0.00000 0.00000 0.00000 0.00000 0.00000
0.00000 0.00000
LDOM-N   0.00000 0.00000 0.00000 0.00000 0.00000 0.00000 0.00000
0.00000 0.00000
RDOM-N   0.00000 0.00000 0.00000 0.00000 0.00000 0.00000 0.00000
0.00000 0.00000
LPOM-N   0.00000 0.00000 0.00000 0.00000 0.00000 0.00000 0.00000
0.00000 0.00000
RPOM-N   0.00000 0.00000 0.00000 0.00000 0.00000 0.00000 0.00000
0.00000 0.00000

CST PRIN  CPRWBC  CPRWBC  CPRWBC  CPRWBC  CPRWBC  CPRWBC  CPRWBC
CPRWBC  CPRWBC
TDS           ON      ON      ON      ON      ON      ON      ON
ON      ON
Gen1          ON      ON      ON      ON      ON      ON      ON
ON      ON
Gen2          ON      ON      ON      ON      ON      ON      ON
ON      ON
ISS          OFF     OFF     OFF     OFF     OFF     OFF     OFF
OFF     OFF
PO4           ON      ON      ON      ON      ON      ON      ON
ON      ON
NH4           ON      ON      ON      ON      ON      ON      ON
ON      ON
NO3           ON      ON      ON      ON      ON      ON      ON
ON      ON
DSI          OFF     OFF     OFF     OFF     OFF     OFF     OFF
OFF     OFF
PSI          OFF     OFF     OFF     OFF     OFF     OFF     OFF
OFF     OFF
FE           OFF     OFF     OFF     OFF     OFF     OFF     OFF
OFF     OFF
LDOM          ON      ON      ON      ON      ON      ON      ON
ON      ON
RDOM          ON      ON      ON      ON      ON      ON      ON
ON      ON
LPOM          ON      ON      ON      ON      ON      ON      ON
ON      ON
RPOM          ON      ON      ON      ON      ON      ON      ON
ON      ON
```

```
BOD1          ON      ON      ON      ON      ON      ON      ON
ON      ON
BOD1-P        ON      ON      ON      ON      ON      ON      ON
ON      ON
BOD1-N        ON      ON      ON      ON      ON      ON      ON
ON      ON
ALG1          ON      ON      ON      ON      ON      ON      ON
ON      ON
DO            ON      ON      ON      ON      ON      ON      ON
ON      ON
TIC          OFF     OFF     OFF     OFF     OFF     OFF     OFF
OFF     OFF
ALK          OFF     OFF     OFF     OFF     OFF     OFF     OFF
OFF     OFF
LDOM-P       OFF     OFF     OFF     OFF     OFF     OFF     OFF
OFF     OFF
RDOM-P       OFF     OFF     OFF     OFF     OFF     OFF     OFF
OFF     OFF
LPOM-P       OFF     OFF     OFF     OFF     OFF     OFF     OFF
OFF     OFF
RPOM-P       OFF     OFF     OFF     OFF     OFF     OFF     OFF
OFF     OFF
LDOM-N       OFF     OFF     OFF     OFF     OFF     OFF     OFF
OFF     OFF
RDOM-N       OFF     OFF     OFF     OFF     OFF     OFF     OFF
OFF     OFF
LPOM-N       OFF     OFF     OFF     OFF     OFF     OFF     OFF
OFF     OFF
RPOM-N       OFF     OFF     OFF     OFF     OFF     OFF     OFF
OFF     OFF

CIN CON   CINBRC  CINBRC  CINBRC  CINBRC  CINBRC  CINBRC  CINBRC
CINBRC  CINBRC
TDS           ON      ON      ON      ON      ON      ON      ON
ON      ON
Gen1          ON      ON      ON      ON      ON      ON      ON
ON      ON
Gen2         OFF     OFF     OFF     OFF     OFF     OFF     OFF
OFF     OFF
ISS          OFF     OFF     OFF     OFF     OFF     OFF     OFF
OFF     OFF
PO4           ON      ON      ON      ON      ON      ON      ON
ON      ON
NH4           ON      ON      ON      ON      ON      ON      ON
ON      ON
NO3           ON      ON      ON      ON      ON      ON      ON
ON      ON
DSI          OFF     OFF     OFF     OFF     OFF     OFF     OFF
OFF     OFF
PSI          OFF     OFF     OFF     OFF     OFF     OFF     OFF
OFF     OFF
FE           OFF     OFF     OFF     OFF     OFF     OFF     OFF
OFF     OFF
```

```
LDOM          ON      ON      ON      ON      ON      ON      ON
ON      ON
RDOM          ON      ON      ON      ON      ON      ON      ON
ON      ON
LPOM          ON      ON      ON      ON      ON      ON      ON
ON      ON
RPOM          ON      ON      ON      ON      ON      ON      ON
ON      ON
BOD1          ON      ON      ON      ON      ON      ON      ON
ON      ON
BOD1-P        ON      ON      ON      ON      ON      ON      ON
ON      ON
BOD1-N        ON      ON      ON      ON      ON      ON      ON
ON      ON
ALG1          ON      ON      ON      ON      ON      ON      ON
ON      ON
DO            ON      ON      ON      ON      ON      ON      ON
ON      ON
TIC          OFF     OFF     OFF     OFF     OFF     OFF     OFF
OFF     OFF
ALK          OFF     OFF     OFF     OFF     OFF     OFF     OFF
OFF     OFF
LDOM-P       OFF     OFF     OFF     OFF     OFF     OFF     OFF
OFF     OFF
RDOM-P       OFF     OFF     OFF     OFF     OFF     OFF     OFF
OFF     OFF
LPOM-P       OFF     OFF     OFF     OFF     OFF     OFF     OFF
OFF     OFF
RPOM-P       OFF     OFF     OFF     OFF     OFF     OFF     OFF
OFF     OFF
LDOM-N       OFF     OFF     OFF     OFF     OFF     OFF     OFF
OFF     OFF
RDOM-N       OFF     OFF     OFF     OFF     OFF     OFF     OFF
OFF     OFF
LPOM-N       OFF     OFF     OFF     OFF     OFF     OFF     OFF
OFF     OFF
RPOM-N       OFF     OFF     OFF     OFF     OFF     OFF     OFF
OFF     OFF

CTR CON   CTRTRC  CTRTRC  CTRTRC  CTRTRC  CTRTRC  CTRTRC  CTRTRC
CTRTRC  CTRTRC
TDS           ON      ON      ON      ON      ON      ON      ON
OFF     OFF
Gen1          ON      ON      ON      ON      ON      ON      ON
OFF     OFF
Gen2         OFF     OFF     OFF     OFF     OFF     OFF     OFF
OFF     OFF
ISS          OFF     OFF     OFF     OFF     OFF     OFF     OFF
OFF     OFF
PO4           ON      ON      ON      ON      ON      ON      ON
OFF     OFF
NH4           ON      ON      ON      ON      ON      ON      ON
OFF     OFF
```

```
NO3             ON      ON      ON      ON      ON      ON      ON
OFF     OFF
DSI             OFF     OFF     OFF     OFF     OFF     OFF     OFF
OFF     OFF
PSI             OFF     OFF     OFF     OFF     OFF     OFF     OFF
OFF     OFF
FE              OFF     OFF     OFF     OFF     OFF     OFF     OFF
OFF     OFF
LDOM            ON      ON      ON      ON      ON      ON      ON
OFF     OFF
RDOM            ON      ON      ON      ON      ON      ON      ON
OFF     OFF
LPOM            ON      ON      ON      ON      ON      ON      ON
OFF     OFF
RPOM            ON      ON      ON      ON      ON      ON      ON
OFF     OFF
BOD1            ON      ON      ON      ON      ON      ON      ON
OFF     OFF
BOD1-P          ON      ON      ON      ON      ON      ON      ON
OFF     OFF
BOD1-N          ON      ON      ON      ON      ON      ON      ON
OFF     OFF
ALG1            ON      ON      ON      ON      ON      ON      ON
OFF     OFF
DO              ON      ON      ON      ON      ON      ON      ON
OFF     OFF
TIC             OFF     OFF     OFF     OFF     OFF     OFF     OFF
OFF     OFF
ALK             OFF     OFF     OFF     OFF     OFF     OFF     OFF
OFF     OFF
LDOM-P          OFF     OFF     OFF     OFF     OFF     OFF     OFF
OFF     OFF
RDOM-P          OFF     OFF     OFF     OFF     OFF     OFF     OFF
OFF     OFF
LPOM-P          OFF     OFF     OFF     OFF     OFF     OFF     OFF
OFF     OFF
RPOM-P          OFF     OFF     OFF     OFF     OFF     OFF     OFF
OFF     OFF
LDOM-N          OFF     OFF     OFF     OFF     OFF     OFF     OFF
OFF     OFF
RDOM-N          OFF     OFF     OFF     OFF     OFF     OFF     OFF
OFF     OFF
LPOM-N          OFF     OFF     OFF     OFF     OFF     OFF     OFF
OFF     OFF
RPOM-N          OFF     OFF     OFF     OFF     OFF     OFF     OFF
OFF     OFF

CDT CON    CDTBRC  CDTBRC  CDTBRC  CDTBRC  CDTBRC  CDTBRC  CDTBRC
CDTBRC  CDTBRC
TDS             ON      ON      ON      ON      OFF     OFF     OFF
OFF     OFF
Gen1            ON      ON      ON      ON      OFF     OFF     OFF
OFF     OFF
```

Gen2	OFF	OFF	OFF	OFF	OFF	OFF	OFF	OFF
OFF	OFF							
ISS	OFF	OFF	OFF	OFF	OFF	OFF	OFF	OFF
OFF	OFF							
PO4	ON	ON	ON	ON	OFF	OFF	OFF	OFF
OFF	OFF							
NH4	ON	ON	ON	ON	OFF	OFF	OFF	OFF
OFF	OFF							
NO3	ON	ON	ON	ON	OFF	OFF	OFF	OFF
OFF	OFF							
DSI	OFF	OFF	OFF	OFF	OFF	OFF	OFF	OFF
OFF	OFF							
PSI	OFF	OFF	OFF	OFF	OFF	OFF	OFF	OFF
OFF	OFF							
FE	OFF	OFF	OFF	OFF	OFF	OFF	OFF	OFF
OFF	OFF							
LDOM	ON	ON	ON	ON	OFF	OFF	OFF	OFF
OFF	OFF							
RDOM	ON	ON	ON	ON	OFF	OFF	OFF	OFF
OFF	OFF							
LPOM	ON	ON	ON	ON	OFF	OFF	OFF	OFF
OFF	OFF							
RPOM	ON	ON	ON	ON	OFF	OFF	OFF	OFF
OFF	OFF							
BOD1	ON	ON	ON	ON	OFF	OFF	OFF	OFF
OFF	OFF							
BOD1-P	ON	ON	ON	ON	OFF	OFF	OFF	OFF
OFF	OFF							
BOD1-N	ON	ON	ON	ON	OFF	OFF	OFF	OFF
OFF	OFF							
ALG1	ON	ON	ON	ON	OFF	OFF	OFF	OFF
OFF	OFF							
DO	ON	ON	ON	ON	OFF	OFF	OFF	OFF
OFF	OFF							
TIC	OFF	OFF	OFF	OFF	OFF	OFF	OFF	OFF
OFF	OFF							
ALK	OFF	OFF	OFF	OFF	OFF	OFF	OFF	OFF
OFF	OFF							
LDOM-P	OFF	OFF	OFF	OFF	OFF	OFF	OFF	OFF
OFF	OFF							
RDOM-P	OFF	OFF	OFF	OFF	OFF	OFF	OFF	OFF
OFF	OFF							
LPOM-P	OFF	OFF	OFF	OFF	OFF	OFF	OFF	OFF
OFF	OFF							
RPOM-P	OFF	OFF	OFF	OFF	OFF	OFF	OFF	OFF
OFF	OFF							
LDOM-N	OFF	OFF	OFF	OFF	OFF	OFF	OFF	OFF
OFF	OFF							
RDOM-N	OFF	OFF	OFF	OFF	OFF	OFF	OFF	OFF
OFF	OFF							
LPOM-N	OFF	OFF	OFF	OFF	OFF	OFF	OFF	OFF
OFF	OFF							

```
RPOM-N        OFF     OFF     OFF     OFF     OFF     OFF     OFF
OFF     OFF

CPR CON    CPRBRC  CPRBRC  CPRBRC  CPRBRC  CPRBRC  CPRBRC  CPRBRC
CPRBRC  CPRBRC
TDS           OFF     OFF     OFF     OFF     OFF     OFF     OFF
OFF     OFF
Gen1          OFF     OFF     OFF     OFF     OFF     OFF     OFF
OFF     OFF
Gen2          OFF     OFF     OFF     OFF     OFF     OFF     OFF
OFF     OFF
ISS           OFF     OFF     OFF     OFF     OFF     OFF     OFF
OFF     OFF
PO4           OFF     OFF     OFF     OFF     OFF     OFF     OFF
OFF     OFF
NH4           OFF     OFF     OFF     OFF     OFF     OFF     OFF
OFF     OFF
NO3           OFF     OFF     OFF     OFF     OFF     OFF     OFF
OFF     OFF
DSI           OFF     OFF     OFF     OFF     OFF     OFF     OFF
OFF     OFF
PSI           OFF     OFF     OFF     OFF     OFF     OFF     OFF
OFF     OFF
FE            OFF     OFF     OFF     OFF     OFF     OFF     OFF
OFF     OFF
LDOM          OFF     OFF     OFF     OFF     OFF     OFF     OFF
OFF     OFF
RDOM          OFF     OFF     OFF     OFF     OFF     OFF     OFF
OFF     OFF
LPOM          OFF     OFF     OFF     OFF     OFF     OFF     OFF
OFF     OFF
RPOM          OFF     OFF     OFF     OFF     OFF     OFF     OFF
OFF     OFF
BOD1          OFF     OFF     OFF     OFF     OFF     OFF     OFF
OFF     OFF
BOD1-P        OFF     OFF     OFF     OFF     OFF     OFF     OFF
OFF     OFF
BOD1-N        OFF     OFF     OFF     OFF     OFF     OFF     OFF
OFF     OFF
ALG1          OFF     OFF     OFF     OFF     OFF     OFF     OFF
OFF     OFF
DO            OFF     OFF     OFF     OFF     OFF     OFF     OFF
OFF     OFF
TIC           OFF     OFF     OFF     OFF     OFF     OFF     OFF
OFF     OFF
ALK           OFF     OFF     OFF     OFF     OFF     OFF     OFF
OFF     OFF
LDOM-P        OFF     OFF     OFF     OFF     OFF     OFF     OFF
OFF     OFF
RDOM-P        OFF     OFF     OFF     OFF     OFF     OFF     OFF
OFF     OFF
LPOM-P        OFF     OFF     OFF     OFF     OFF     OFF     OFF
OFF     OFF
```

```
RPOM-P       OFF     OFF     OFF     OFF     OFF     OFF     OFF
OFF     OFF
LDOM-N       OFF     OFF     OFF     OFF     OFF     OFF     OFF
OFF     OFF
RDOM-N       OFF     OFF     OFF     OFF     OFF     OFF     OFF
OFF     OFF
LPOM-N       OFF     OFF     OFF     OFF     OFF     OFF     OFF
OFF     OFF
RPOM-N       OFF     OFF     OFF     OFF     OFF     OFF     OFF
OFF     OFF

EX COEF    EXH2O    EXSS    EXOM    BETA     EXC    EXIC
WB 1     0.45000 0.01000 0.40000 0.45000     OFF     OFF
WB 2     0.45000 0.01000 0.40000 0.45000     OFF     OFF
WB 3     0.45000 0.01000 0.40000 0.45000     OFF     OFF
WB 4     0.45000 0.01000 0.40000 0.45000     OFF     OFF
WB 5     0.45000 0.01000 0.40000 0.45000     OFF     OFF
WB 6     0.45000 0.01000 0.40000 0.45000     OFF     OFF
WB 7     0.45000 0.01000 0.40000 0.45000     OFF     OFF
WB 8     0.45000 0.01000 0.40000 0.45000     OFF     OFF
WB 9     0.45000 0.01000 0.40000 0.45000     OFF     OFF

ALG EX       EXA     EXA     EXA     EXA     EXA     EXA
         0.20000

ZOO EX       EXZ     EXZ     EXZ     EXZ     EXZ     EXZ
         0.20000

MACRO EX     EXM     EXM     EXM     EXM     EXM     EXM
         0.01000

GENERIC    CGQ10   CG0DK   CG1DK     CGS
CG 1     0.00000 -1.0000 0.00000 0.00000
CG 2     0.00000  0.0000 0.00000 0.00000

S SOLIDS     SSS   SEDRC   TAUCR
SS# 1    1.50000     OFF 0.00000

ALGAL RATE    AG      AR      AE      AM      AS    AHSP    AHSN
AHSSI    ASAT
ALG1     0.98000 0.04000 0.04000 0.10000 0.20000 0.00300 0.01400
0.00000 40.0000

ALGAL TEMP   AT1     AT2     AT3     AT4     AK1     AK2     AK3
AK4
ALG1     5.00000 25.0000 35.0000 40.0000 0.10000 0.99000 0.99000
0.10000

ALG STOI    ALGP    ALGN    ALGC   ALGSI   ACHLA   ALPOM   ANEQN
ANPR
ALG1     0.00500 0.08000 0.45000 0.18000 0.05000 0.80000       2
0.00100
```

```
EPIPHYTE    EPIC    EPIC    EPIC    EPIC    EPIC    EPIC    EPIC
EPIC    EPIC
EPI1         OFF     OFF     OFF     OFF     OFF     OFF     OFF
OFF     OFF

EPI PRIN    EPRC    EPRC    EPRC    EPRC    EPRC    EPRC    EPRC
EPRC    EPRC
EPI1         OFF     OFF     OFF     OFF     OFF     OFF     OFF
OFF     OFF

EPI INIT   EPICI   EPICI   EPICI   EPICI   EPICI   EPICI   EPICI
EPICI   EPICI
EPI1     0.00000 0.00000 0.00000 0.00000 0.00000 0.00000 0.00000
0.00000 0.00000

EPI RATE      EG      ER      EE      EM      EB    EHSP    EHSN
EHSSI
EPI1     1.20000 0.04000 0.04000 0.10000 0.00100 0.00300 0.01400
0.00000

EPI HALF    ESAT     EHS   ENEQN    ENPR
EPI1     150.000 25.0000       2 0.00500

EPI TEMP     ET1     ET2     ET3     ET4     EK1     EK2     EK3
EK4
EPI1     1.00000 3.00000 20.0000 30.0000 0.30000 0.99000 0.99000
0.10000

EPI STOI      EP      EN      EC     ESI   ECHLA    EPOM
EPI1     0.00500 0.08000 0.45000 0.00000 0.65000 0.80000

ZOOP RATE     ZG      ZR      ZM    ZEFF   PREFP  ZOOMIN    ZS2P
Zoo1     1.50000 0.10000 0.01000 0.50000 0.50000 0.01000 0.30000

ZOOP ALGP  PREFA   PREFA   PREFA   PREFA   PREFA   PREFA   PREFA
PREFA   PREFA
Zoo1     0.00000

ZOOP ZOOP  PREFZ   PREFZ   PREFZ   PREFZ   PREFZ   PREFZ   PREFZ
PREFZ   PREFZ
Zoo1     0.00000

ZOOP TEMP    ZT1     ZT2     ZT3     ZT4     ZK1     ZK2     ZK3
ZK4
Zoo1     0.00000 15.0000 20.0000 36.0000 0.10000 0.90000 0.98000
0.10000

ZOOP STOI     ZP      ZN      ZC
Zoo1     0.01500 0.08000 0.45000

MACROPHY  MACWBC  MACWBC  MACWBC  MACWBC  MACWBC  MACWBC  MACWBC
MACWBC  MACWBC
Mac1         OFF     OFF     OFF     OFF     OFF     OFF     OFF
```

```
MAC PRIN  MPRWBC  MPRWBC  MPRWBC  MPRWBC  MPRWBC  MPRWBC  MPRWBC
MPRWBC  MPRWBC
Mac1         OFF     OFF     OFF     OFF     OFF     OFF     OFF

MAC INI  MACWBCI MACWBCI MACWBCI MACWBCI MACWBCI MACWBCI MACWBCI
MACWBCI MACWBCI
Mac1     0.00000 0.00000 0.00000 0.00000 0.00000 0.00000 0.00000

MAC RATE      MG      MR      MM    MSAT    MHSP    MHSN    MHSC
MPOM  LRPMAC
Mac1     0.30000 0.05000 0.05000 30.0000 0.00000 0.00000 0.00000
0.90000 0.20000

MAC SED     PSED    NSED
Mac1     0.50000 0.50000

MAC DIST    MBMP    MMAX
Mac1     40.0000 500.000

MAC DRAG  CDDRAG     DMV    DWSA   ANORM
Mac1     3.00000 70000.0 8.00000 0.30000

MAC TEMP     MT1     MT2     MT3     MT4     MK1     MK2     MK3
MK4
Mac1     7.00000 15.0000 24.0000 34.0000 0.10000 0.99000 0.99000
0.01000

MAC STOICH    MP      MN      MC
Mac1     0.00500 0.08000 0.45000

DOM       LDOMDK  RDOMDK   LRDDK
WB 1     0.10000 0.00100 0.01000
WB 2     0.10000 0.00100 0.01000
WB 3     0.10000 0.00100 0.01000
WB 4     0.10000 0.00100 0.01000
WB 5     0.10000 0.00100 0.01000
WB 6     0.10000 0.00100 0.01000
WB 7     0.10000 0.00100 0.01000
WB 8     0.10000 0.00100 0.01000
WB 9     0.10000 0.00100 0.01000

POM       LPOMDK  RPOMDK   LRPDK    POMS
WB 1     0.08000 0.00100 0.01000 0.10000
WB 2     0.08000 0.00100 0.01000 0.10000
WB 3     0.08000 0.00100 0.01000 0.10000
WB 4     0.08000 0.00100 0.01000 0.10000
WB 5     0.08000 0.00100 0.01000 0.10000
WB 6     0.08000 0.00100 0.01000 0.10000
WB 7     0.08000 0.00100 0.01000 0.10000
WB 8     0.08000 0.00100 0.01000 0.10000
WB 9     0.08000 0.00100 0.01000 0.10000
```

```
OM STOIC    ORGP    ORGN    ORGC   ORGSI
WB 1     0.00500 0.08000 0.45000 0.18000
WB 2     0.00500 0.08000 0.45000 0.08000
WB 3     0.00500 0.08000 0.45000 0.08000
WB 4     0.00500 0.08000 0.45000 0.08000
WB 5     0.00500 0.08000 0.45000 0.08000
WB 6     0.00500 0.08000 0.45000 0.08000
WB 7     0.00500 0.08000 0.45000 0.08000
WB 8     0.00500 0.08000 0.45000 0.08000
WB 9     0.00500 0.08000 0.45000 0.08000

OM RATE     OMT1    OMT2    OMK1    OMK2
WB 1     4.00000 25.0000 0.10000 0.99000
WB 2     4.00000 25.0000 0.10000 0.99000
WB 3     4.00000 25.0000 0.10000 0.99000
WB 4     4.00000 25.0000 0.10000 0.99000
WB 5     4.00000 25.0000 0.10000 0.99000
WB 6     4.00000 25.0000 0.10000 0.99000
WB 7     4.00000 25.0000 0.10000 0.99000
WB 8     4.00000 25.0000 0.10000 0.99000
WB 9     4.00000 25.0000 0.10000 0.99000

CBOD        KBOD    TBOD    RBOD   CBODS
BOD 1    0.10000 1.02000 1.00000 0.00000

CBOD STOIC  BODP    BODN    BODC
BOD 1    0.01000 0.08000 0.32000

PHOSPHOR    PO4R   PARTP
WB 1     0.00100 0.00000
WB 2     0.00100 0.00000
WB 3     0.00100 0.00000
WB 4     0.00100 0.00000
WB 5     0.00100 0.00000
WB 6     0.00100 0.00000
WB 7     0.00100 0.00000
WB 8     0.00100 0.00000
WB 9     0.00100 0.00000

AMMONIUM    NH4R   NH4DK
WB 1     0.00100 0.12000
WB 2     0.00100 0.12000
WB 3     0.00100 0.12000
WB 4     0.00100 0.12000
WB 5     0.00100 0.12000
WB 6     0.00100 0.12000
WB 7     0.00100 0.12000
WB 8     0.00100 0.12000
WB 9     0.00100 0.12000

NH4 RATE   NH4T1   NH4T2   NH4K1   NH4K2
WB 1     5.00000 25.0000 0.10000 0.99000
WB 2     5.00000 25.0000 0.10000 0.99000
```

```
WB 3     5.00000 25.0000 0.10000 0.99000
WB 4     5.00000 25.0000 0.10000 0.99000
WB 5     5.00000 25.0000 0.10000 0.99000
WB 6     5.00000 25.0000 0.10000 0.99000
WB 7     5.00000 25.0000 0.10000 0.99000
WB 8     5.00000 25.0000 0.10000 0.99000
WB 9     5.00000 25.0000 0.10000 0.99000

NITRATE    NO3DK    NO3S FNO3SED
WB 1     0.03000 0.00100 0.00000
WB 2     0.03000 0.00100 0.00000
WB 3     0.03000 0.00100 0.00000
WB 4     0.03000 0.00100 0.00000
WB 5     0.03000 0.00100 0.00000
WB 6     0.03000 0.00100 0.00000
WB 7     0.03000 0.00100 0.00000
WB 8     0.03000 0.00100 0.00000
WB 9     0.03000 0.00100 0.00000

NO3 RATE   NO3T1   NO3T2   NO3K1   NO3K2
WB 1     5.00000 25.0000 0.10000 0.99000
WB 2     5.00000 25.0000 0.10000 0.99000
WB 3     5.00000 25.0000 0.10000 0.99000
WB 4     5.00000 25.0000 0.10000 0.99000
WB 5     5.00000 25.0000 0.10000 0.99000
WB 6     5.00000 25.0000 0.10000 0.99000
WB 7     5.00000 25.0000 0.10000 0.99000
WB 8     5.00000 25.0000 0.10000 0.99000
WB 9     5.00000 25.0000 0.10000 0.99000

SILICA      DSIR    PSIS   PSIDK  PARTSI
WB 1     0.10000 0.00000 0.30000 0.20000
WB 2     0.00000 0.00000 0.00000 0.00000
WB 3     0.00000 0.00000 0.00000 0.00000
WB 4     0.00000 0.00000 0.00000 0.00000
WB 5     0.00000 0.00000 0.00000 0.00000
WB 6     0.00000 0.00000 0.00000 0.00000
WB 7     0.00000 0.00000 0.00000 0.00000
WB 8     0.00000 0.00000 0.00000 0.00000
WB 9     0.00000 0.00000 0.00000 0.00000

IRON         FER     FES
WB 1     0.10000 0.00000
WB 2     0.00000 0.00000
WB 3     0.00000 0.00000
WB 4     0.00000 0.00000
WB 5     0.00000 0.00000
WB 6     0.00000 0.00000
WB 7     0.00000 0.00000
WB 8     0.00000 0.00000
WB 9     0.00000 0.00000

SED CO2     CO2R
```

```
WB 1     0.10000
WB 2     0.10000
WB 3     0.10000
WB 4     0.10000
WB 5     0.10000
WB 6     0.10000
WB 7     0.10000
WB 8     0.10000
WB 9     0.10000

STOICH 1   O2NH4    O2OM
WB 1     4.57000 1.40000
WB 2     4.57000 1.40000
WB 3     4.57000 1.40000
WB 4     4.57000 1.40000
WB 5     4.57000 1.40000
WB 6     4.57000 1.40000
WB 7     4.57000 1.40000
WB 8     4.57000 1.40000
WB 9     4.57000 1.40000

STOICH 2    O2AR    O2AG
ALG1     1.10000 1.40000

STOICH 3    O2ER    O2EG
EPI1     1.10000 1.80000

STOICH 4    O2ZR
Zoop1    1.10000

STOICH 5    O2MR    O2MG
Mac1     1.10000 1.40000

O2 LIMIT   O2LIM
         0.70000

SEDIMENT    SEDC  SEDPRC   SEDCI    SEDK    SEDS    FSOD    FSED
SEDBR DYNSEDK
WB 1         OFF     OFF 0.00000 0.08000 0.10000 1.00000 1.00000
0.00000     OFF
WB 2         OFF     OFF 0.00000 0.00000 0.00000 1.00000 1.00000
0.00000     OFF
WB 3         OFF     OFF 0.00000 0.00000 0.00000 1.00000 1.00000
0.00000     OFF
WB 4         OFF     OFF 0.00000 0.00000 0.00000 1.00000 1.00000
0.00000     OFF
WB 5         OFF     OFF 0.00000 0.00000 0.00000 1.00000 1.00000
0.00000     OFF
WB 6          ON      ON 0.00000 0.08000 0.10000 1.00000 1.00000
0.00800     OFF
WB 7         OFF     OFF 0.00000 0.00000 0.00000 1.00000 1.00000
0.00000     OFF
```

```
WB 8         OFF     OFF 0.00000 0.00000 0.00000 1.00000 1.00000
0.00000     OFF
WB 9         OFF     OFF 0.00000 0.00000 0.00000 1.00000 1.00000
0.00000     OFF

SOD RATE   SODT1   SODT2   SODK1   SODK2
WB 1     4.00000 30.0000 0.10000 0.99000
WB 2     4.00000 30.0000 0.10000 0.99000
WB 3     4.00000 30.0000 0.10000 0.99000
WB 4     4.00000 30.0000 0.10000 0.99000
WB 5     4.00000 30.0000 0.10000 0.99000
WB 6     4.00000 30.0000 0.10000 0.99000
WB 7     4.00000 30.0000 0.10000 0.99000
WB 8     4.00000 30.0000 0.10000 0.99000
WB 9     4.00000 30.0000 0.10000 0.99000

S DEMAND     SOD     SOD     SOD     SOD     SOD     SOD     SOD
SOD     SOD
         0.60000 0.60000 0.60000 0.60000 0.60000 0.60000 0.60000
0.60000 0.60000
         0.60000 0.60000 0.60000 0.60000 0.60000 0.60000 0.60000
0.60000 0.60000
         0.60000 0.60000 0.60000 0.60000 0.60000 0.60000 0.60000
0.60000 0.60000
         0.60000 0.60000 0.60000 0.60000 0.60000 0.60000 0.60000
0.60000 0.60000
         0.60000 0.60000 0.60000 0.60000 0.60000 0.60000 0.60000
0.60000 0.60000
         0.60000 0.60000 0.60000 0.60000 0.60000 0.60000 0.60000
0.60000 0.60000
         0.60000 0.60000 0.60000 0.60000 0.60000 0.60000 0.60000
0.60000 0.60000
         0.60000 0.60000 0.60000 0.60000 0.60000 0.60000 0.60000
0.60000 0.60000
         0.60000 0.60000 0.60000 0.60000 0.60000 0.60000 0.60000
0.60000 0.60000
         0.60000 0.60000 0.60000 0.60000 0.60000 0.60000 0.60000
0.60000 0.60000
         0.60000 0.60000 0.60000 0.60000 0.60000 0.60000 0.60000
0.60000 0.60000
         0.60000 0.60000 0.60000 0.60000 0.60000 0.60000 0.60000
0.60000 0.60000
         0.60000 0.60000 0.60000 0.60000 0.60000 0.60000 0.60000
0.60000 0.60000
         0.60000 0.60000 0.60000 0.60000 0.60000 0.60000 0.60000
0.60000 0.60000
         0.60000 0.60000 0.60000 0.60000 0.60000 0.60000 0.60000
0.60000 0.60000
         0.60000 0.60000 0.60000 0.60000 0.60000 0.60000 0.60000
0.60000 0.60000
         0.60000 0.60000 0.60000 0.60000 0.60000 0.60000 0.60000
0.60000 0.60000
```

```
          0.60000 0.60000 0.60000 0.60000 0.60000 0.60000 0.60000
0.60000 0.60000
          0.60000 0.60000 0.60000 0.60000 0.60000 0.60000 0.60000
0.60000 0.60000
          0.60000 0.60000 0.60000 0.60000 0.60000 0.60000 0.60000
0.60000 0.60000
          0.60000 0.60000 0.60000 0.60000 0.60000 0.60000 0.60000
0.60000 0.60000
          0.60000 0.60000 0.60000 0.60000 0.60000 0.60000 0.60000
0.60000 0.60000
          0.60000 0.60000 0.60000 0.60000 0.60000 0.60000 0.60000
0.60000 0.60000
          0.60000 0.60000 0.60000 0.60000 0.60000 0.60000 0.60000
0.60000 0.60000
          0.60000 0.60000 0.60000 0.60000 0.60000 0.60000 0.60000
0.60000 0.60000
          0.60000 0.60000 0.60000 0.60000 0.60000 0.60000 0.60000
0.60000 0.60000
          0.60000 0.60000 0.60000 0.60000 0.60000 0.60000 0.60000
0.60000 0.60000
          0.60000 0.60000 0.60000 0.60000 0.60000 0.60000 0.60000
0.60000 0.60000
          0.60000 0.60000 0.60000 0.60000 0.60000 0.60000 0.60000
0.60000 0.60000
          0.60000 0.60000 0.60000 0.60000 0.60000 0.60000 0.60000
0.60000 0.60000
          0.60000 0.60000 0.60000 0.60000 0.60000 0.60000 0.60000
0.60000 0.60000
          0.60000 0.60000 0.60000 0.60000 0.60000 0.60000 0.60000
0.60000 0.60000
          0.60000 0.60000 0.60000 0.60000 0.60000 0.60000 0.60000
0.60000 0.60000
          0.60000 0.60000 0.60000 0.60000 0.60000 0.60000 0.60000
0.60000 0.60000
          0.60000 0.60000 0.60000 0.60000 0.60000 0.60000 0.60000
0.60000 0.60000
          0.60000 0.60000 0.60000 0.60000 0.60000 0.60000 0.60000
0.60000 0.60000
          0.60000 0.60000 0.60000 0.60000 0.60000 0.60000 0.60000
0.60000 0.60000
          0.60000 0.60000 0.60000 0.60000 0.60000 0.60000 0.60000
0.60000 0.60000
          0.60000 0.60000 0.60000 0.60000 0.60000 0.60000 0.60000
0.60000 0.60000

REAERATION  TYPE    EQN#   COEF1   COEF2   COEF3   COEF4
WB 1       RIVER       7 0.00000 0.00000 0.00000 0.00000
WB 2       RIVER       7 0.00000 0.00000 0.00000 0.00000
WB 3       RIVER       7 0.00000 0.00000 0.00000 0.00000
WB 4       RIVER       7 0.00000 0.00000 0.00000 0.00000
WB 5       RIVER       7 0.00000 0.00000 0.00000 0.00000
WB 6        LAKE       6 0.00000 0.00000 0.00000 0.00000
WB 7       RIVER       7 0.00000 0.00000 0.00000 0.00000
```

```
WB 8       RIVER       7 0.00000 0.00000 0.00000 0.00000
WB 9       RIVER       7 0.00000 0.00000 0.00000 0.00000

RSI
FILE.................................RSIFN.....................
........
        rsi.npt

QWD
FILE.................................QWDFN.....................
........
        qWD.npt

QGT
FILE.................................QGTFN.....................
........
        qgt.npt

WSC
FILE.................................WSCFN.....................
........
        wsc.npt

SHD
FILE.................................SHDFN.....................
........
        shade.npt

BTH
FILE.................................BTHFN.....................
........
WB 1    bth_wb1.csv
WB 2    bth_wb2.csv
WB 3    bth_wb3.csv
WB 4    bth_wb4.csv
WB 5    bth_wb5.csv
WB 6    bth_wb6.csv
WB 7    bth_wb7.csv
WB 8    bth_wb8.csv
WB 9    bth_wb9.csv

MET
FILE.................................METFN.....................
........
WB 1    met_wb1.npt
WB 2    met_wb2.npt
WB 3    met_wb3.npt
WB 4    met_wb4.npt
WB 5    met_wb5.npt
WB 6    met_wb6.npt
WB 7    met_wb7.npt
WB 8    met_wb8.npt
WB 9    met_wb9.npt
```

```
EXT
FILE.................................EXTFN.......................
........
WB 1    ext_1.npt - not used
WB 2    ext_2.npt
WB 3    ext_3.npt
WB 4    ext_4.npt
WB 5    ext_5.npt
WB 6    ext_6.npt
WB 7    ext_7.npt
WB 8    ext_8.npt
WB 9    ext_9.npt

VPR
FILE.................................VPRFN.......................
........
WB 1    vpr_1.npt
WB 2    vpr_2.npt
WB 3    vpr_3.npt
WB 4    vpr_4.npt
WB 5    vpr_5.npt
WB 6    vpr_6.npt
WB 7    vpr_7.npt
WB 8    vpr_8.npt
WB 9    vpr_9.npt

LPR
FILE.................................LPRFN.......................
........
WB 1    lpr_1.npt - not used
WB 2    lpr_2.npt
WB 3    lpr_3.npt
WB 4    lpr_4.npt
WB 5    lpr_5.npt
WB 6    lpr_6.npt
WB 7    lpr_7.npt
WB 8    lpr_8.npt
WB 9    lpr_9.npt

QIN
FILE.................................QINFN.......................
........
BR1     qin_br1.npt
BR2     qin_br2.npt
BR3     qin_br3.npt
BR4     qin_br4.npt
BR5     qin_br5.npt
BR6     qin_br6.npt
BR7     qin_br7.npt
BR8     qin_br8.npt
BR9     qin_br9.npt
```

```
TIN
FILE.................................TINFN.........................
........
BR1     tin_br1.npt
BR2     tin_br2.npt
BR3     tin_br3.npt
BR4     tin_br4.npt
BR5     tin_br5.npt
BR6     tin_br6.npt
BR7     tin_br7.npt
BR8     tin_br8.npt
BR9     tin_br9.npt

CIN
FILE.................................CINFN.........................
........
BR1     cin_br1.csv
BR2     cin_br2.npt
BR3     cin_br3.npt
BR4     cin_br4.npt
BR5     cin_br5.npt
BR6     cin_br6.npt
BR7     cin_br7.npt
BR8     cin_br8.npt
BR9     cin_br9.npt

QOT
FILE.................................QOTFN.........................
........
BR1     qot_br1.npt
BR2     qot_br2.npt
BR3     qot_br3.npt
BR4     qot_br4.npt
BR5     qot_br5.npt
BR6     qot_br6.npt
BR7     qot_br7.npt
BR8     qot_br8.npt
BR9     qot_br9.npt

QTR
FILE.................................QTRFN.........................
........
TR1     qtr_tr1.npt
TR2     qtr_tr2.npt
TR3     qtr_tr3.npt
TR4     qtr_tr4.npt
TR5     qtr_tr5.npt
TR6     qtr_tr6.npt
TR7     qtr_tr7.npt

TTR
FILE.................................TTRFN.........................
........
```

```
TR1     ttr_tr1.npt
TR2     ttr_tr2.npt
TR3     ttr_tr3.npt
TR4     ttr_tr4.npt
TR5     ttr_tr5.npt
TR6     ttr_tr6.npt
TR7     ttr_tr7.npt

CTR
FILE.................................CTRFN.....................
........
TR1     ctr_tr1.csv
TR2     ctr_tr2.csv
TR3     ctr_tr3.csv
TR4     ctr_tr4.csv
TR5     ctr_tr5.csv
TR6     ctr_tr6.csv
TR7     ctr_tr7.csv

QDT
FILE.................................QDTFN.....................
........
BR1     qdt_br1.npt
BR2     qdt_br2.npt
BR3     qdt_br3.npt
BR4     qdt_br4.npt
BR5     qdt_br5.npt
BR6     qdt_br6.npt
BR7     qdt_br7.npt
BR8     qdt_br8.npt
BR9     qdt_br9.npt

TDT
FILE.................................TDTFN.....................
........
BR1     tdt_br1.npt
BR2     tdt_br2.npt
BR3     tdt_br3.npt
BR4     tdt_br4.npt
BR5     tdt_br5.npt
BR6     tdt_br6.npt
BR7     tdt_br7.npt
BR8     tdt_br8.npt
BR9     tdt_br9.npt

CDT
FILE.................................CDTFN.....................
........
BR1     cdt_br1.csv
BR2     cdt_br2.csv
BR3     cdt_br3.csv
BR4     cdt_br4.csv
BR5     cdt_br5.csv
```

```
BR6     cdt_br6.csv
BR7     cdt_br7.csv
BR8     cdt_br8.csv
BR9     cdt_br9.csv

PRE
FILE.....................................PREFN.....................
........
BR1     pre_br1.npt - not used
BR2     pre_br2.npt
BR3     pre_br3.npt
BR4     pre_br4.npt
BR5     pre_br5.npt
BR6     pre_br6.npt
BR7     pre_br7.npt
BR8     pre_br8.npt
BR9     pre_br9.npt

TPR
FILE.....................................TPRFN.....................
........
BR1     tpr_br1.npt - not used
BR2     tpr_br2.npt
BR3     tpr_br3.npt
BR4     tpr_br4.npt
BR5     tpr_br5.npt
BR6     tpr_br6.npt
BR7     tpr_br7.npt
BR8     tpr_br8.npt
BR9     tpr_br9.npt

CPR
FILE.....................................CPRFN.....................
........
BR1     cpr_br1.npt - not used
BR2     cpr_br2.npt
BR3     cpr_br3.npt
BR4     cpr_br4.npt
BR5     cpr_br5.npt
BR6     cpr_br6.npt
BR7     cpr_br7.npt
BR8     cpr_br8.npt
BR9     cpr_br9.npt

EUH
FILE.....................................EUHFN.....................
........
BR1     euh_br1.npt
BR2     euh_br2.npt
BR3     euh_br3.npt
BR4     euh_br4.npt
BR5     euh_br5.npt
BR6     euh_br6.npt
```

```
BR7     euh_br7.npt
BR8     euh_br8.npt
BR9     euh_br9.npt

TUH
FILE.................................TUHFN.....................
........
BR1     tuh_br1.npt
BR2     tuh_br2.npt
BR3     tuh_br3.npt
BR4     tuh_br4.npt
BR5     tuh_br5.npt
BR6     tuh_br6.npt
BR7     tuh_br7.npt
BR8     tuh_br8.npt
BR9     tuh_br9.npt

CUH
FILE.................................CUHFN.....................
........
BR1     cuh_br1.npt
BR2     cuh_br2.npt
BR3     cuh_br3.npt
BR4     cuh_br4.npt
BR5     cuh_br5.npt
BR6     cuh_br6.npt
BR7     cuh_br7.npt
BR8     cuh_br8.npt
BR9     cuh_br9.npt

EDH
FILE.................................EDHFN.....................
........
BR1     edh_br1.npt
BR2     edh_br2.npt
BR3     edh_br3.npt
BR4     edh_br4.npt
BR5     edh_br5.npt
BR6     edh_br6.npt
BR7     edh_br7.npt
BR8     edh_br8.npt
BR9     edh_br9.npt

TDH
FILE.................................TDHFN.....................
........
BR1     tdh_br1.npt
BR2     tdh_br2.npt
BR3     tdh_br3.npt
BR4     tdh_br4.npt
BR5     tdh_br5.npt
BR6     tdh_br6.npt
BR7     tdh_br7.npt
```

```
BR8     tdh_br8.npt
BR9     tdh_br9.npt

CDH
FILE.................................CDHFN.....................
........
BR1     cdh_br1.npt
BR2     cdh_br2.npt
BR3     cdh_br3.npt
BR4     cdh_br4.npt
BR5     cdh_br5.npt
BR6     cdh_br6.npt
BR7     cdh_br7.npt
BR8     cdh_br8.npt
BR9     cdh_br9.npt

SNP
FILE.................................SNPFN.....................
........
WB 1    snp1.opt
WB 2    snp_WB2.opt
WB 3    snp_WB3.opt
WB 4    snp_WB4.opt
WB 5    snp_WB5.opt
WB 6    snp_WB6.opt
WB 7    snp_WB7.opt
WB 8    snp_WB8.opt
WB 9    snp_WB9.opt

PRF
FILE.................................PRFFN.....................
........
WB 1    prf1.opt
WB 2    prf_2.opt
WB 3    prf_3.opt
WB 4    prf_4.opt
WB 5    prf_5.opt
WB 6    prf_6.opt
WB 7    prf_7.opt
WB 8    prf_8.opt
WB 9    prf_9.opt

VPL
FILE.................................VPLFN.....................
........
WB 1   Tigris.w2l
WB 2    vpl_2.opt
WB 3    vpl_3.opt
WB 4    vpl_4.opt
WB 5    vpl_5.opt
WB 6    vpl_6.opt
WB 7    vpl_7.opt
WB 8    vpl_8.opt
```

```
WB 9    vpl_9.opt

CPL
FILE.................................CPLFN.....................
........
WB 1    cpl1.opt
WB 2    cpl_2.opt
WB 3    cpl_3.opt
WB 4    cpl_4.opt
WB 5    cpl_5.opt
WB 6    cpl_6.opt
WB 7    cpl_7.opt
WB 8    cpl_8.opt
WB 9    cpl_9.opt

SPR
FILE.................................SPRFN.....................
........
WB 1    spr1.opt
WB 2    spr_2.opt
WB 3    spr_3.opt
WB 4    spr_4.opt
WB 5    spr_5.opt
WB 6    spr_6.opt
WB 7    spr_7.opt
WB 8    spr_8.opt
WB 9    spr_9.opt

FLX
FILE.................................FLXFN.....................
........
WB 1    kfl1.opt
WB 2    flx_2.opt
WB 3    flx_3.opt
WB 4    flx_4.opt
WB 5    flx_5.opt
WB 6    flx_6.opt
WB 7    flx_7.opt
WB 8    flx_8.opt
WB 9    flx_9.opt

TSR
FILE.................................TSRFN.....................
........
        tsr.csv

WDO
FILE.................................WDOFN.....................
........
        wdo.csv
```